Universidade de Aveiro

Departamento de Química

2019

João Henrique Picado Madalena Santos

Potencial da PEGuilação para o desenvolvimento de proteínas para fins terapêuticos e analíticos

PEGylation strategy to the development of analytical and therapeutic proteins

Universidade de Aveiro Departamento de Química

2019

João Henrique Picado Madalena Santos

Potencial da PEGuilação para o desenvolvimento de proteínas para fins terapêuticos e analíticos

PEGylation strategy to the development of analytical and therapeutic proteins

Tese apresentada à Universidade de Aveiro para cumprimento dos requisitos necessários à obtenção do grau de Doutor em Engenharia Química, na condição de doutoramento duplo com a Universidade de São Paulo, realizada sob a orientação científica da Professora Doutora Sónia Patrícia Marques Ventura do Departamento de Química, CICECO, da Universidade de Aveiro e da Professora Doutora Carlota de Oliveira Rangel Yagui do Departamento de Tecnologia Bioquímico-Farmacêutica da Faculdade de Ciências Farmacêuticas da Universidade de São Paulo, e com a coorientação do Professor Doutor João Manuel da Costa e Araújo Pereira Coutinho, Professor Catedrático do Departamento de Química, CICECO, da Universidade de Aveiro

Apoio financeiro do POCTI no âmbito do III Quadro Comunitário de Apoio.

O doutoramento agradece o apoio financeiro da FCT e do FSE no âmbito do III Quadro Comunitário de Apoio (SFRH/BD/102915/2014).

Este trabalho foi desenvolvido no âmbito do projeto CICECO-Instituto de Materiais de Aveiro, Refª. FCT UID/CTM/50011/2019, financiado por fundos nacionais através da FCT/MCTES.

“A change is gonna come”

O júri

Presidente

Prof. Doutor João Manuel Nunes Torrão
professor catedrático e diretor do Departamento de Línguas e Culturas da Universidade de Aveiro

Prof.ª Doutora Isabel Maria Delgado Jana Marrucho Ferreira
professora associada com agregação no Instituto de Tecnologia Química e Biológica, Universidade Nova de Lisboa

Doutor Óscar Rodríguez Figueiras
investigador da Escola Técnica Superior de Engenharia, Universidade de Santiago de Compostela

Doutora Ana Alexandra Figueiredo Matias
investigadora Auxiliar do Instituto de Biologia Experimental e Tecnológica

Prof.ª Doutora Mara Guadalupe Freire Martins
investigadora coordenadora do Departamento de Química da Universidade de Aveiro

Prof.ª Doutora Sónia Patrícia Marques Ventura
professora auxiliar do Departamento de Química da Universidade de Aveiro

Agradecimentos

Os meus sinceros agradecimentos às minhas orientadoras Prof.ª Dr.ª Sónia Ventura e Prof.ª Dr.ª Carlota Rangel-Yagui e ao meu co-orientador, Prof. Dr. João Coutinho. Reconheço o quanto importante foram no desenvolvimento de todo o trabalho ao longo destes quatro anos. Agradeço-lhes toda a paciência e tempo disponibilizado, a confiança em acreditar nas minhas ideias, dando-me autonomia para me deixar mais preparado para as etapas que estão por vir e também a forma sempre cuidadosa que me transmitiram conhecimentos permitindo desse modo a minha evolução profissional.

Gostaria também de agradecer a todos os colaboradores que directa ou indirectamente me auxiliriam, no desenvolvimento do trabalho compilado neste documento, destacando o Prof. Dr. Adalberto Pessoa Júnior da Universidade de São Paulo, o Dr. Gustavo Carretero e a Dr.ª Camila Areias de Oliveira da mesma Universidade, o Prof. Dr. Attilio Converti da Universidade de Génova e a Prof.ª Dr.ª Mara Freire da Universidade de Aveiro. Gostaria também de agradecer à Fundação para a Ciência e Tecnologia pela bolsa de doutoramento atribuída, que me permitiu a possibilidade de realizar o doutoramento duplo entre duas Universidades de grande prestígio. Obrigado também a todos os professores que já tive, pois contribuiram enormente para hoje poder atingir o título de Doutor. Um bem-haja a todos!

Não posso deixar de agradecer a todos os meus colegas e amigos dos grupos de investigação do PATh e Nanobiolab, que foram verdadeiramente duas famílias em Portugal e no Brasil, respetivamente. Obrigado especial a todos os meus amigos de Ílhavo e São Paulo, que me acompanharam neste processo e se orgulham muito de mim.

Por fim, agradeço especialmente a toda a minha família, em particular aos meus pais, mana e avôs, por todos os valores que me transmitiram e por nunca deixarem de acreditar em mim. Obrigado também a minha estrela-guia, Avó Dina, que sei que está sempre comigo.

Palavras-chave

PEGuilação; asparaginase; citocromo c; sistemas aquosos bifásicos; purificação; plataformas de purificação, cromatografia de partição centrífuga.

Resumo

A PEGuilação de proteínas é a ligação covalente de polímeros de polietilenoglicol (PEG) a resíduos de aminoácidos da proteína e é uma das técnicas mais promissoras para melhorar o efeito terapêutico dos biofármacos e a estabilidade a longo prazo de biossensores proteícos. Esta modificação química traz vantagens aos produtos biofarmacêuticos, como um aumento da meia-vida, maior estabilidade e imunogenicidade reduzida. Além disso, no campo analítico, a PEGuilação melhora as múltiplas propriedades dos biossensores baseados em proteínas, incluindo biocompatibilidade, estabilidade térmica e a longo prazo, e solubilidade em solventes orgânicos. No entanto, o uso de conjugados PEGuilados em campos analíticos e terapêuticos não tem sido amplamente explorado. A aplicação industrial limitada dos bioconjugados PEGuilados pode ser atribuída ao facto de as etapas de reacção e separação serem atualmente um desafio. A seleção correcta do *design* da reacção de PEGuilação e do processo de purificação são importantes desafios no campo da bioconjugação. Neste sentido, a concepção e otimização de reações de PEGuilação sítio-específicas e aplicação de sistemas aquosos bifásicos (ABS) como plataformas de purificação de conjugados PEGuilados são os dois principais objetivos desta tese. No que concerne à etapa de purificação foi estudado o eficiente fracionamento (i) dos conjugados PEGuilados, da proteína nativa e (ii) dos conjugados PEGuilados baseados no seu grau de PEGuilação. A cromatografia por partição centrífuga (CPC) foi aplicada como uma plataforma de regime contínuo baseada na tecnologia de ABS para purificar eficientemente as proteínas PEGuiladas.

As duas proteínas em estudo são a L-asparaginase, importante biofármaco aplicado no tratamento da leucemia linfoblástica aguda e o citocromo c, um potencial biossensor.

A partir dos trabalhos desenvolvidos, é possível confirmar o grande potencial dos ABS no fracionamento de proteínas PEGuiladas, em regime contínuo e descontínuo. Além disso, a recuperação *in situ* dos produtos PEGuilados através da integração em uma única etapa de bioconjugação e purificação por ABS foi comprovada com sucesso para ambas as enzimas estudadas. Embora ainda sejam necessários estudos adicionais sobre a viabilidade destes sistemas em larga escala, os resultados aqui apresentados demonstram a relevância dos ABS para o desenvolvimento de processos de separação de proteínas PEGuiladas.

Keywords

PEGylation; asparaginase; cytochrome c; aqueous biphasic systems; purification; downstream processing, centrifugal partition chromatography.

Abstract

Protein PEGylation is the covalent bonding of polyethylene glycol (PEG) polymers to amino acid residues of the protein and it is one of the most promising techniques for improving the therapeutic effect of biopharmaceuticals and long-term stability of protein-based biosensors. This chemical modification brings advantages to biopharmaceuticals, such as an increased half-life, enhanced stability, and reduced immunogenicity. Moreover, in the analytical field, PEGylation improves the multiple properties of protein-based biosensors including biocompatibility, thermal and long-term stability, and solubility in organic solvents. However, the use of PEGylated conjugates in the analytical and therapeutic fields has not been widely explored. The limited industrial application of PEGylated bioconjugates can be attributed to the fact that the reaction and separation steps are currently a challenge. The correct selection of the PEGylation reaction design and the purification process are important challenges in the field of bioconjugation. In this sense, the design and optimization of site-specific PEGylation reactions and application of aqueous biphasic systems (ABS) as purification platforms for PEGylated conjugates are the two main objectives of this thesis. Regarding the purification step, the efficient fractionation (i) of the PEGylated conjugates from the native protein and (ii) of the PEGylated conjugates based on their degree of PEGylation was studied. Centrifugal partition chromatography (CPC) was applied as a continuous regime platform based on ABS technology to efficiently purify the PEGylated proteins.

The two proteins under study are L-asparaginase, an important biopharmaceutical applied in the treatment of acute lymphoblastic leukemia and cytochrome c, a promising biosensor.

The current work developed in this thesis demonstrates the great potential of ABS in the fractionation of PEGylated proteins, under batch and continuous regime. In addition, *in situ* recovery of the PEGylated products through one-pot bioconjugation and ABS purification was successfully demonstrated for both enzymes studied. Although further research on scale-up is still required, the results presented show the relevance of ABS platforms for the development of separation processes of PEGylated proteins.

List of Abbreviations

ABS - Aqueous biphasic system
ATPS - Aqueous two phase system
AMTPS - Aqueous micellar two phase system
ALL - Acute lymphoblastic leukemia
ASNase - L-asparaginase
APBS - Adaptive Poisson-Boltzmann Solver
ATPE - Aqueous Two-Phase Extraction
ADA - Anti-drug antibodies
ANOVA - Analysis of Variance
ABTS - 2,2'-azino-bis(3-ethylbenzothiazoline-6-sulphonic acid
AEP - Asparaginyl endopeptidase
BSA - Bovine serum albumin
BCA - Bicinchoninic acid
CE - Capillary electrophoresis
CD - Circular dichroism
CCD - Counter current distribution
CMC - Critical micelle concentration
CPC - Centrifugal partition chromatography
Cyt-c - Cytochrome c
CMC - Critical micelle concentration
CCD-ABS - Countercurrent distribution in aqueous biphasic systems
CAT - Catalase
CD - Circular dichroism
CTSB - Cathepsin B
DPPI - Aminopeptidase dipeptidyl peptidase I
DES - Deep eutectic solvents
DTT - Dithiothreitol
DLS - Dynamic light scattering
EMA - European Medicine Agency
EA - Enzymatic activity
E^* - activation energy of enzyme-catalysed reaction
E^*_d - activation energy of irreversible enzyme denaturation
FPLC - Fast protein liquid chromatography
FDA - US Agency for Food and Drug Administration
FCPC - Fast centrifugal partition chromatography
GCT - Glutamine cyclotransferase
GHG - Greenhouse gas
GM-CSF - granulocyte macrophage colony-stimulating factor
HIC - Hydrophobic interaction chromatography
HSCCC - High-speed countercurrent chromatography
HAS - Human serum albumin
HUVEC - Healthy human umbilical vein endothelial cell line

HPLC - High-performance liquid chromatography
IEX - Ion exchange chromatography
IL - Ionic liquid
IMAC - Immobilized Metal ion Affinity Chromatography
IPTG - Isopropylthio-β-D-galactoside
IgG - Immunoglobulin G
K - Partition coefficient
K_P - Partition coefficient of proteins
K_A - Partition coefficient of active enzyme
KH_2PO_4 - Potassium phosphate
K_2HPO_4 - Dipotassium phosphate
K_3PO_4 - Tripotassium phosphate
K_m – Michaelis-Menten constant
k_{cat} - Turnover number
k_d - deactivation rate constant
LB - Luria Bertani
LYS - Lysozyme
MW - Molecular weight
mPEG – Methoxy polyethylene glycol
mPEG-NHS - Methoxy polyethylene glycol succinimidyl NHS ester
MALDI - Matrix-assisted laser desorption/ionization
MOLT-4 - Acute T-cell lymphoblastic leukemia
MB - Mass balance
NIBS - Non-invasive backscatter
n - Degree of PEGylation
NHS - *N*-hydroxysuccinimide
OMB - Overall mass balance
PDB - Protein Data Bank
PARSE - PARameters for Solvation Energy
PEG - Polyethylene glycol
PPG - Polypropylene glycol
PF - Purification factor
P_x - Purity
PEG-NHS - *N*-hydroxylsuccinimide functionalized polyethylene glycol
PAHs - Polycyclic aromatic hydrocarbons
PHPMA - Poly(*N*-(2-hydroxypropyl) methacrylamide
POEGMA - Polyoligoethylene glycol methyl ether methacrylate
PLGA – Poly D,L-lacticco-glycolic acid
PGA – Poly glutamic acid
PNIPAM – Poly *N*-isopropyl acrylamide
PDEAM – Poly *N*,*N*'-diethyl acrylamide
Phe - Phenylalanine
PF - Purification factor
PSA - Ammonium persulphate

PGAP - Pyroglutamyl aminopeptidase
PPG – Poly propylene glycol
PBE - Poisson-Boltzmann equation
REH - B-cell lines
RPMI - Roswell Park Memorial Institute medium
RNase A - Ribonuclease A
SC - Succinimidyl carbonate
S – Selectivity
SA - Specific activity
SDS-PAGE - Sodium dodecyl sulfate polyacrylamide gel electrophoresis
SEC - Size-exclusion chromatography
SASA - Solvent-accessible surface area
SCID - Severe combined immunodeficiency disease
SDS - Sodium dodecyl sulfate
S_0 - Initial substrate concentration
TL - Tie-line
TLL - Tie-line length
TEMED – Tetramethylethylenediamine
TCA - Trichloroacetic acid
Trp – Tryptophan
Tyr - Tyrosine
TOF - Time of flight
TFA - Trifluoracetic acid
$t_{1/2}$ - Enzyme half-life
U - enzyme unit
*V*r - Volume ratio
v_{max} - Maximum reaction rate
Y% - Yields of recovery
wt% - Weight percentage
$[Prot]_T$ - Concentration of protein in the top phase
$[Prot]_B$ - Concentration protein in the bottom phase
$[C_4mim]Cl$ - 1-butyl-3-methylimidazolium chloride
$[C_4mim][CH_3SO_3]$ - 1-butyl-3-methylimidazolium methanesulfonate
$[C_4mim][CF_3SO_3]$ - 1-butyl-3-methylimidazolium triflate
[C_4mim][DMP] - 1-butyl-3-methylimidazolium dimethyl phosphate
%*Rec* P - Recovery yield of total proteins
%*Rec* – Recovery yield percentage
ΔH^*_d – Enthalpy of enzyme irreversible denaturation
ΔS^*_d - Entropy of enzyme irreversible denaturation
ΔG^*_d - Gibbs free energy of enzyme irreversible denaturation
ΔH^o_U - Standard enthalpy variation of enzyme unfolding
Ψ - residual activity coefficient

List of Tables

Table 3.3. Kinetic parameters of Cyt-c-catalysed reaction for the native cytochrome c (Cyt-c) or PEGylated conjugates, the Cyt-c-PEG-4 and Cyt-c-PEG-8. The catalytic oxidation of ABTS was performed in the presence of 0.5 mM of H_2O_2, at 25±1°C and pH 7.4.

Table 3.4. Thermodynamic parameters of Cyt-c-catalyzed reaction and reversible unfolding of native Cyt-c, Cyt-c-PEG-4 and Cyt-c-PEG-8 estimated according to the Arrhenius equation. The concentration of non-PEGylated and PEGylated Cyt-c was 10 µM in 0.01 M of potassium phosphate buffer (0.14 M of NaCl, pH 7.4). The catalytic oxidation of the substrate ABTS was performed in the range of T = 30 – 100 °C (ΔT = 10 °C).

Table 3.5. Thermodynamic and kinetic parameters of the irreversible thermal deactivation (denaturation) of native Cyt-c, Cyt-c-PEG-4 and Cyt-c-PEG-8

Table 4.1. Recoveries towards top and bottom phases, log (K), purities and mass balances (MB) obtained for the unreacted Cyt-c and for the PEGylated conjugates, respectively Cyt-c-PEG-4 and Cyt-c-PEG-8, in the integrated multistep process using polymer-based ABS as purification platforms, for the system using PEG (8000 and 1500) + potassium phosphate buffer (pH = 7). The overall mass balance (OMB) is also depicted in this table for unreacted and Cyt-c PEGylated forms.

Table 4.2. Effect of molecular weight (MW) of mPEG-NHS upon the volume ratio (V_R) and partitioning behaviour, represented as the partition coefficient (K), top and bottom-phase recoveries (%*RecT* and %*RecB*), and selectivity (S) of native and PEGylated Cyt-c in Cyt-c-PEG + potassium citrate buffer-based ABS.

Table 4.3. Effect of PEGylation reaction time on the volume ratio (V_R) and partition behaviour, represented as the partition coefficient (K), top and bottom-phase recoveries (%*RecT* and %*RecB*), and selectivity (S) of native and PEGylated Cyt-c in ABS composed of 1.0 wt% Cyt-c + 12.5 wt% Cyt-c-PEG/PEG + 12.5 wt% potassium citrate buffer, at pH 7.0.

Table 4.4. Partition parameters for Cyt-c, LYS, ASNase, and CAT for the *in-situ* approach under development: Volume ratio (V_R), partition coefficient (K), top and bottom-phase

List of Figures

cells were pre inoculated in LB media overnight at a 37°C and 250 rpm. The inoculum was initially diluted to OD_{600nm} 0.2 in fresh culture media, grown at the same conditions until OD_{600nm} 0.4 when 0.1mM of IPTG was added and culture temperature was changed to 12°C. This *Sc*_ASNaseII induction was performed for 24 hours. In this expression vector construction, the protein starts at the amino-acid residue number 32, without the predicted yeast periplasmic signal. - Lane 1: BenchMark™ Protein Ladder; Lane 2: insoluble fraction pelleted after clarification of the cell lysate by centrifugation. Lane 3: supernatant of cell lysate, representing the protein soluble fraction.

Fig. 2.6. SDS-PAGE stained with Comassie-blue representing the expression of *Sc*_ASNaseII in the soluble fraction of the *E. coli* cell lysate and the specific activity of this protein. Fractions of nickel affinity purification. Lane 1: Total supernatant after cell lysis; Lane 2: BenchMark™ Protein Ladder; Lanes 3 and 4: Fractions from column elution with 500 mM of imidazole.

Fig. 2.7. Recovery yield of total proteins (%Rec P) and ASNase (%Rec A) and purification factor of ASNase (PF) for the ATPS composed of PEG + citrate buffer (15 wt%/15 wt%) at pH 7. Errors bars correspond to standard deviations obtained from three replicates.

Fig. 2.8. Recovery yield of total proteins (%Rec P) and ASNase (%Rec A), and purification factor of ASNase (PF) for the ATPS composed of PEG 6000 + citrate buffer (15wt%/15 wt%) at different pHs. Error bars correspond to standard deviations obtained from three replicates.

Fig. 2.9. 3D structure of ASNase (PDB: 3ECA) **(A)** hydrophobicity surface using Eisenberg amino acid scale[39] and solvent-accessible surface area (SASA), calculated for pHs 5, 6, 7 and 8. Red-scale refers to less hydrophobic (white) to more hydrophobic (red) parts of ASNase; **(B)** electrostatic charge at the ASNase surface and solvent-accessible surface area (SASA) calculated for pHs 5 to 8. Red-white-blue scale refers to minimum (-5 kT/e, red) and maximum (5 kT/e, blue) surface potential.

Fig. 2.10. (A) Ternary phase diagram of PEG 6000 + citrate buffer system at pH = 7 with representation of tie-lines (TL) for the following mixture points: PEG 6000 wt%/citrate buffer wt% = 15.0/15.0; 17.5/17.5; 20.0/20.0; 22.5/22.5. **(B)** Recovery yields of total

proteins (%Rec P) and ASNase (%Rec A) and purification factor (PF) for the PEG 6000 + citrate buffer ATPS at pH = 7, considering four distinct mixture points. Error bars correspond to standard deviations obtained from three replicates.

Fig. 2.11. Recovery yield of total proteins (%Rec P) and ASNase (%Rec A), and purification factor (PF) in the ATPS composed of PEG 6000 + citrate buffer (15wt%/15 wt%) at pH = 7 and with 1 wt% of [C_4mim]-based ILs as adjuvants. Error bars correspond to standard deviations obtained from three replicates.

Fig. 2.12. Recovery yield of total proteins (%Rec P) and ASNase (%Rec A) and purification factor (PF) in the ATPS composed PEG of 6000 + citrate buffer (15wt%/15 wt%) at pH = 7 and with [C_4mim][CH_3SO_3] as adjuvant. Errors bars correspond to standard deviations obtained from three replicates.

Fig. 2.13. Comparison between pre-purification step, IL-free ATPS, ATPS with IL, IL-free ATPS integrated with pre-purification step and ATPS with IL integrated with pre-purification step for the extraction and purification of periplasmatic L-asparaginase from *E.coli* cell paste.

Fig. 2.14. SDS-PAGE of commercial ASNase from *E.coli* (1) Precipitated proteins from fermentation broth (2) Fermentation broth (3) Top-phase of the optimized ATPS, the PEG 6000/citrate with 5 wt% [C_4mim][CH_3SO_3] (as adjuvant) with pre-purification (4) Top-phase of the optimized ATPS, the PEG 6000/citrate with 5 wt% [C_4mim][CH_3SO_3] (as adjuvant) without pre-purification (5). Molar masses reference Precision Plus Protein (BIORAD, CA, US) (M).

Fig. 2.15. Schematic representation of the *in situ* purification process of periplasmatic ASNase by using polymer-based ATPS with [C_4mim][CH_3SO_3] as adjuvant. The isolation of ASNase and the recycling of both aqueous phases are also represented.

Fig. 2.16. Phase diagrams of the copolymer Pluronic L-35 and inorganic salts - **(♦)** K_2HPO_4; (●) KH_2PO_4; (▲); K_3PO_4 and (■) K_2HPO_4/ KH_2PO; at 25ºC. The lines represent the Merchuk fit through **Eq. 1.**

Fig. 2.17. Phase diagrams of the copolymer Pluronic L-35 + potassium phosphate buffer (pH = 6.6), without the addition of surfactant (—); and with the addition of 1 wt% of Triton X-100 (■); and Triton X-114 (♦), at 25ºC. The lines represent the Merchuk fit through **Eq.1**.

Fig. 2.18. Phase diagrams obtained for the copolymers: Pluronic 17R4 (●); Pluronic 10R5 (▲); and Pluronic L-35 (■) + potassium phosphate buffer (pH = 6.6), at 25ºC. The lines represent the Merchuk fit through **Eq.1**.

Fig. 2.19. Coexistence curves for the ternary systems with potassium phosphate buffer + water + Pluronic 17R4 (♦); Pluronic 10R5 (●); and Pluronic L-35 (▲); and for the quaternary system composed of potassium phosphate buffer + Pluronic L-35 + water + 1 wt% of Triton X-114 (--■--).

Fig. 2.20. Recovery data obtained for the three proteins regarding top/copolymer-rich phase (%*Rec Top*) and bottom/salt-rich phase (%*Rec Bottom*) and respective standard deviations (σ) by using the different ATPS: cytochrome c, Cyt c (■); azocasein, Azo (■); and ovalbumin, Ova (■). For each system studied the selectivity results are reported.

Fig. 2.21. Recovery values obtained for the surfactant-rich phase (%*Rec Top*) and surfactant-poor phase (%*Rec Bottom*), with the respective standard deviations (σ) by applying AMTPS to separate azocasein (■); and ovalbumin (■). For each system studied the selectivity results are presented.

Fig. 2.22. Diagram of the integrated process to selectively separate cytochrome c (Cyt c), ovalbumin (Ova) and azoasein (Azo). The proposed strategy includes two steps of purification using, respectively, ATPS and AMTPS based on Pluronic L-35 and potassium phosphate buffer - PB (pH = 6.6). The purity (P_x) and recovery (R_x) of each step is provided in the present diagram. An ultrafiltration was applied to improve the separation of Cyt c and Ova and an acid precipitation was applied to isolate the Azo from Pluronic L35. The potassium phosphate buffer was maintained in the Azo-rich phase as a stabilizing solution.

Fig. 3.1. Reaction conditions to produce monoPEGylated L-asparaginase (monoPEG-ASNase). (**A**) Electrophoresis (SDS-PAGE) showing the influence of PBS buffer ionic strength on N-terminal PEGylation with pH 7.5 (PEG:ASNase ratio of 25:1, 2 kDa mPEG-NHS): Column 1- ASNase (control), column 2- reaction in 10 mM PBS, column 3- reaction in 100 mM of PBS, column 4- reaction in 200 mM PBS, and column 5- Molecular weight (BioRad). (**B**) Percentage of PEGylation at different PEG:ASNase ratios, 25:1 and 50:1, in 100 mM of PBS pH 7.5, 30 min of time reaction. (**C**) Percentage of PEGylation at different pH values (6.0, 6.5, 7.0, 7.5 or 8.0) in 100 mM of PBS, PEG:ASNase ratio of 25:1 and 30 min of reaction time. (**D**) Percentage of PEGylation on different reaction times (15 to 90 minutes) in 100 mM of PBS, pH 7.5, PEG:ASNase ratio of 25:1. Grey bars - polypegylated ASNase, white bars - monoPEGylated ASNase, dotted bars - free ASNase. Percentage of PEGylation was based on gel analysis by band intensity.

Fig. 3.2. Enzymatic behavior of monoPEG-ASNase compared to ASNase (control) and polyPEGylated form. (**A**) Enzymatic kinetics of ASNase. (**B**) Enzymatic kinetics of monoPEG-ASNase. (**C**) Enzymatic kinetics of polyPEG-ASNase. Data analysis and statistical analysis (F-test) were done using GraphPad Prism 5.0 software. All trials were in triplicates and error bars represent the standard deviation

Fig. 3.3. PEG attachment influence on native enzyme. (**A**) Enzymatic activity *versus* storage time at 4 °C for ASNase control, monoPEG-ASNase and polyPEG-ASNase. (**B**) Dynamic light scattering profiles of unreacted ASNase, mono and polyPEGylated ASNase. The hydrodynamic radius were 7.53 nm, 9.85 nm and 11.75 nm, respectively.

Fig. 3.4. MALDI-TOF of free ASNAse and monoPEG-ASNase (with 2 kDa and 10 kDa PEG). **(A)** N-terminal peptide LPNITILATGGTIAGGGDSATK.(S) at m/z 2028.1809 and **(B)** lysine peptide SVNYGPLGYIHNGK.(I), at m/z 1518.7. Samples were acquired in duplicate. ASNase; blue line (spectrum 4), monoPEG-ASNase 2 kDa light and dark green line (spectrum 6 and 2), and monoPEG-ASNase 10 kDa; light blue line and orange (spectrum 5 and 1).

Fig. 3.5. Electrophoresis gel (native-PAGE) showing the proteolytic degradation /resistance of native ASNase and PEGylated forms. ASNase, monoPEG-ASNase and polyPEG-ASNase in presence of asparagine endopeptidase (AEP) and cathepsin B (CTSB)

after 84 h at 37 °C, stained with CBB (top gel) and stained with ferric chloride (bottom gel). Column 1- Protease-free ASNase, column 2- ASNase with CTSB, column 3- ASNase with AEP, column 4- protease-free monoPEG-ASNase, column 5- monoPEG-ASNase with CTSB, column 6- monoPEG-ASNase with AEP, 7- protease-free polyPEG-ASNase, column 8- polyPEG-ASNase with CTSB and column 9- polyPEG-ASNase with AEP.

Fig. 3.6. Cytotoxicity of monoPEG-ASNase in MOLT-4 and REH cells. Assays performed at 48 h and 72 h, with cells alone (control), without enzyme (PBS) and at different concentrations of enzymatic activity (0.01, 0.05, 0.1, 0.3 or 0.6 $U.mL^{-1}$). Grey bars - free ASNase and white bars - monoPEGylated ASNase. Error bars represent the standard deviation. Likelihood of significance less than 0.05 (*), less than 0.01 (**) and less than 0.001 (***) when compared with the control.

Fig. 3.7. Schematic overview of PEGylation reaction.

Fig. 3.8. Molecular visualization of theoretical lysine residues (LYS) of cytochrome c (Cyt-c, PDB code 1HRC) PEGylated, using the Software PyMOL. **(A)** Four residues of conjugation are highlighted: LYS - 22, 25, 27 and 39, resulting in Cyt-c-PEG-4. **(B)** Eight residues of conjugation are defined i.e. LYS - 22, 25, 27, 39, 55, 79, 86 and 87 resulting in Cyt-c-PEG-8.

Fig. 3.9. Effect of pH on Cyt-c PEGylation yields. The PEGylation reaction was performed in 0.1 M phosphate buffer (at different pHs), 1:25 molar proportion (protein:mPEG-NHS, 5 KDa), at room temperature, for 30 minutes, and with a constant stirring of 400 rpm. Different letters indicate significant differences ($P < 0.05$) between conditions (A-E).

Fig. 3.10. SDS-PAGE for the mixture obtained after PEGylation of Cyt-c with mPEG-NHS, at different pH values. Lane 1: molecular weight marker, Lane 2: Cyt-c. The protein mixtures obtained after PEGylation of Cyt-c were: Lane 3: pH = 7, Lane 4: pH = 8, Lane 5: pH = 9; Lane 6: pH = 10, Lane 7: pH = 11, Lane 8: pH = 12.

Fig. 3.11. Effect of molar ratio (protein:mPEG-NHS) on Cyt-c PEGylation yields. The PEGylation reaction was performed in 0.1 M phosphate buffer (pH = 7), at room

temperature, for 30 minutes, and with a constant stirring of 400 rpm. Different letters indicate significant differences ($P < 0.05$) between conditions (A-C).

Fig. 3.12. SDS-PAGE for the mixture obtained after PEGylation of Cyt-c at different molar proportions (protein:mPEG-NHS). Lane 1: molecular weight marker, Lane 2: 1:5, Lane 3: 1:10, Lane 4: 1:25, Lane 5: 1:35.

Fig. 3.13. Effect of reaction time on Cyt-c PEGylation yields. Effect of molar ratio (protein:mPEG-NHS) on Cyt-c PEGylation yields. The PEGylation reaction was performed in 0.1 M phosphate buffer (pH = 7), 1:25 molar proportion (protein:mPEG-NHS, 5 KDa), at room temperature, and with a constant stirring of 400 rpm. Different letters indicate significant differences ($P < 0.05$) between conditions (A-C).

Fig. 3.14. SDS-PAGE for the mixture obtained after PEGylation of Cyt-c with mPEG-NHS at different reaction times. Lane 1: molecular weight marker, Lane 2: 15 min, Lane 3: 30 min, Lane 4: 45 min.

Fig. 3.15. Near-UV CD spectra of Cyt-c (—), Cyt-c-PEG-4 (—) and Cyt-c-PEG-8 (—) in 0.01 M sodium phosphate buffer (0.14 M NaCl, pH = 7.4) in the region reflecting the protein tertiary structure.

Fig. 3.16. Far-UV CD spectra of Cyt-c (—), Cyt-c-PEG-4 (—) and Cyt-c-PEG-8 (—) in 0.01 M sodium phosphate buffer (0.14 M NaCl, pH = 7.4) in the region reflecting the protein secondary structure.

Fig. 3.17. Plot of the residual activity of Cyt-c and PEGylated protein forms (Cyt-c-PEG-4 and Cyt-c-PEG-8) determined during 60 days at 4°C **(A)** and room temperature of 25°C **(B)**.

Fig. 3.18. (A) Far-UV and **(B)** Near-UV circular dichroism spectra of equine heart cytochrome c either in native form (Cyt-c, —) or PEGylated with 4 (Cyt-c-PEG-4, —) or 8 (Cyt-c-PEG-8, —) PEGs. Experiments were carried out with 13-15 µM of Cyt-c/Cyt-c-PEG-4/Cyt-c-PEG-8 in 0.01 M phosphate buffer (0.14 M NaCl, pH = 7.4) at room temperature (25±1°C). **(C)** Thermal stability curves of unfolding (■) and refolding (—) processes of the same enzyme preparations.

Fig. 3.19. Arrhenius-type plots of initial activity of Cyt-c and PEGylated conjugates with 4 (Cyt-c-PEG-4) or 8 (Cyt-c-PEG-8) PEGs attached, using 0.300 mM ABTS as a substrate.

Fig. 3.20. Semi-log plots of the first-order denaturation constant (k_d) vs. the reciprocal temperature (1/*T*). The slopes of the resulting straight lines used were used to estimate the activation energies (E^*_d) of irreversible inactivation (denaturation) of native cytochrome c (Cyt-c) and PEGylated conjugated with 4 (Cyt-c-PEG-4) or 8 (Cyt-c-PEG-8) PEGs attached.

Fig. 4.1. Effect of polymer MW on log(*K*) of Cyt-c and PEGylated forms (Cyt-c-PEG-4 and Cyt-c-PEG-8) in PEG-phosphate buffer ABS (pH = 7). The PEG MW 300, 600, 1000, 1500, 2000, 4000, 6000 and 8000 $g.mol^{-1}$ were studied in a fixed mixture point 15 wt% PEG + 20 wt% phosphate buffer.

Fig. 4.2. Phase diagram (●) and respective tie-lines; *TLs* defined for the ABS composed of PEG 1500 + potassium phosphate buffer (pH = 7). The TLs were calculated considering the following mixture points (potassium phosphate buffer; PEG 1500 wt%): ■ (15; 15 wt%), ▪ (17.5; 15 wt%), ◆ (20; 15 wt%), ● (22.5; 15 wt%), ▲ (25; 15 wt%).

Fig. 4.3. Effect of water content in the top-phase on log(*K*) of Cyt-c and PEGylated forms (Cyt-c-PEG-4 and Cyt-c-PEG-8) in PEG 1500 + phosphate buffer ABS (pH = 7). The studied mixture points were: (15; 15 wt%), (17.5; 15 wt%), (20; 15 wt%), (22.5; 15 wt%) (25; 15 wt%) phosphate buffer; PEG 1500 wt%.

Fig. 4.4. Diagram of multistep process to fractionate selectively the unreacted cytochrome c and each one of the PEGylated conjugates (Cyt-c-PEG-4 and Cyt-c-PEG-8). The proposed strategy includes three steps of purification using ABS, namely considering the ABS I and ABS II composed of PEG 8000 + potassium phosphate buffer (pH = 7) to separate Cyt-c-PEG-8 and ABS III using PEG 1500 + potassium phosphate buffer (pH = 7) to fractionate the unreacted Cyt-c from the Cyt-c-PEG-4 conjugate. The recovery yield of each step is also provided in the present diagram. The recycle and reuse of the unreacted Cyt-c in a new PEGylation cycle after recovery in the last step is also demonstrated.

Fig. 4.5. SEC-FPLC chromatogram of **(A)** unreacted Cyt-c concentrated in the bottom-phase used directly in a new cycle of PEGylation; **(B)** unreacted Cyt-c used in a new cycle of PEGylation but after its isolation from the bottom phase through precipitation with cold acetone. **(C)** SDS-PAGE showing the successful use of the recycled Cyt-c in a new cycle of PEGylation: Lane M – Molecular Marker, Lane 1 – commercial equine heart Cyt-c, Lane 2 – PEGylation mixture obtained after a new cycle of PEGylation using the purified Cyt-c.

Fig. 4.6. Far-UV CD spectra of Cyt-c control (—) and Cyt-c purified through aqueous biphasic system (—). Cyt-c concentrations used are 15 and 13 µM for the control and purified forms, respectively.

Fig. 4.7. Logarithm of *K* of both native (light grey bars) and PEGylated proteins (dark grey bars) in the one-step approach under development PEG-Prot + citrate (pH = 7) ABS [*1.0 wt% Protein (condition 2) + 12.5 wt% Prot-PEG/PEG + 12.5 wt% citrate buffer*]. The selectivity of each system (*S*) is presented in red. Pictures of each ABS prepared are depicted for each system.

Fig. 4.8. FTIR-ATR spectrum of ABS (1.0 wt% Protein + 12.5 wt% Prot-PEG/PEG + 12.5 wt% citrate buffer) top-phase (---) bottom-phase (•••), pure Cyt-c (—) and PEG (—).

Fig. 4.9. Schematic diagram of the integrated process combining bioconjugation reaction and separation with the polishing step and solvent recycling process for a complete PEGylation reaction. The dashed line represents steps that were not experimentally developed.

Fig. 4.10. Schematic diagram of the integrated process combining bioconjugation reaction and separation with the polishing step and solvent recycling process for an incomplete PEGylation reaction. The dashed line represents steps that were not experimentally developed.

Fig. 5.1. Chromatogram of FCPC purification of Cyt-c and Cyt-c-PEG performed employing ABS comprising 15 wt% of PEG (1000, 1500 and 2000) + 20 wt% of potassium phosphate buffer, at pH 7.0.

Index

Chapter 1. General Introduction

Chapter 2. Production and purification of ASNase and Cyt-c

Chapter 3. PEGylation reaction

1. General Introduction

Chapter 1. General Introduction[1]

1.1. Protein PEGylation technology

Proteins are considered one of the most versatile biotechnological materials due to their ubiquitous nature allied with their wide range of applications. In this context, great technological and scientific efforts have been made to find ways to exploit the potential of biological functions that proteins exert *in vivo*. These efforts have culminated in an extensive diversity of products that include biopharmaceuticals, detergents, industrial biocatalysts, biosensors, among others. Albeit, the biological origin of the proteins gives them specific limitations, which must be taken into account to not compromise their properties and final application. In this sense, the development of novel techniques that seek to preserve, ensure, and even enhance the protein functionality are desired. These techniques include protein engineering,[1,2] and chemical modifications of the protein.[3–8] The first technique takes advantage of the DNA technology and consists in the changing of specific amino-acid or sequences from the original protein structure in order to design a protein with improved characteristics.[2] The chemical modifications of the protein can be achieved through protein crosslinking[8] or by chemical binding of specific polymers to the protein.[3] These proteins are modified intentionally for structure-function relationship studies or for development of new and improved products. PEGylation is a technique in which at least one chain of polyethylene glycol (PEG) is grafted onto the structure of the protein.[9] PEGylation technology was first reported in 1977 by Abuchowski *et al*.[10] for the modification of albumin and catalase. Depending on the number, molecular weight and location of the attached PEG chains, this covalent modification can enhance the physicochemical properties of the protein, without compromising the secondary structure.[11]

1.1.1. PEGylation reaction design

Selecting the appropriate chemistry in the design of PEGylated conjugates is the first step to a successful process.[5,6] PEGylation reactions have been extensively reviewed in

[1] This chapter is based on the following article: **Santos, J. H. P. M**., Torres-Obreque, K. M., Pastore, G. M., Amaro, B. P. & Rangel-Yagui, C. O. Protein PEGylation for the design of biobetters: from reaction to purification processes. Brazilian J. Pharm. Sci. **54**, (2018).

literature.[3,5,6,12,13] The selection of the PEG derivative (the reactive PEG used in the PEGylation reaction) is fundamental, since it depends strongly on the location and number of amino-acids that are able to be PEGylated.[14,15] Generally, the reactive groups in proteins involved in covalent binding to PEG molecules are nucleophiles,[14,16] with the following moieties ranked in decreasing order of reactivity: thiol, α-amino, ε-amino, carboxyl, and hydroxyl.[11] Moreover, the number and local reactivity of the available PEGylation sites (nucleophilic groups of the amino-acids), the experimental conditions of PEGylation reaction (*i.e.* pH, temperature, reaction time and molar ratio between PEG derivative and protein), and reactivity of the PEG derivative will have a noticeable influence on the composition of the PEGylated products.[11] Thus, PEG coupling may result in heterogeneous mixtures, formed by different PEGylated conjugates with several degrees of PEGylation. Nevertheless, by the optimization of experimental reaction conditions, it is possible to direct the PEGylation reaction towards the formation of site-specific PEGylated conjugates and enhance the efficiency of PEGylation.[15–17] It should be noticed that the PEGylation reactions are preferably conducted in single-step unidirectional batch system to guarantee the batch-to-batch control and the formation of all products in equal conditions. In this sense, validation, reproducibility, and optimization of the reaction are easier. Additionally, it allows to easily trace the potential formation of undesirable products (*i.e.* PEGylation adducts).[11] The maximization of the PEGylation yield and specificity of every reaction is required, whereas minimizing the costs. Therefore, some challenges in the PEGylation reaction still need to be addressed, namely (i) the design of site-specific PEGylation reactions to avoid a heterogeneity of PEGylated conjugates; (ii) to enhance the PEGylation reaction yield, through the use of liquid biocompatible solvents that guarantee the structure integrity of the proteins in alternative to aqueous buffer solutions; (iii) to allow shortened-time reactions to increase the PEGylation productivity; (iv) to decrease the amount of reactive PEG used in PEGylation reactions and the overall cost of the process. PEGylation of therapeutic proteins is commonly performed using reactive mono-methoxy PEG (mPEG), approved for the use in pharmaceutical preparations by FDA and EMA. It has one of the hydroxyl groups methylated and the other linked to a specific group to react with the protein. This strategy avoids the formation of undesirable

byproducts, *e.g.* crossed linked products.[3,18] One of the most used mPEG is the N-hydroxylsuccinimide (NHS) functionalized polyethylene glycol (PEG-NHS). This amino (-NH_2) reactive PEG derivative can be used to modify proteins, peptides or any other surface by covalent bond to available amino groups; NHS esters react with primary amine groups at pH 7-8.5 to form stable amide bonds.[19] Compared to other PEG NHS ester derivatives, the succinimidyl carbonate (SC) functionalized mPEG-NHS offers superior reactivity and higher stability in aqueous solution.

1.2. Current advances in the purification of PEGylated conjugates

PEGylation reactions commonly result in heterogeneous mixtures of unreacted protein, PEGylated conjugates and undesired PEGamers.[20,21] Furthermore, the PEGylated conjugates formed are dissimilar among themselves, varying in the number of grafted chains and attaching sites. Therefore, efficient downstream strategies are needed to purify these complex mixtures for commercial approval.[21] The purification of PEGylated conjugates consists in removing from the obtained mixture all species that do not present adequate characteristics. This implies three main challenges: (i) isolation and recycling of the unreacted protein from the PEGylated conjugates, (ii) isolation of each PEGylated protein form from the reaction media (*e.g.* PEG derivate, undesired PEGamers and hydroxylamine), and (iii) fractionation of PEGylated conjugates according to their degree of PEGylation. These multifaceted challenges are not easy to overcome, due to the fact that the hybrid PEG-protein conjugate is structurally similar to the originator protein.[11] Therefore, a combination of chromatographic[20] and/or non-chromatographic[22] techniques can be used and designed for each PEGylation process, exploiting the physicochemical properties of the target biomolecules present in the mixture. In the last years, chromatographic fractionation platforms have been commonly used in downstream processes of protein PEGylation, as shown in **Fig. 1.1.** However, this tendency to prefer chromatographic techniques is related to the vast empirical knowledge obtained from several studies with a large spectrum of proteins.[20,23–26] Non-chromatographic techniques have been used as alternatives to chromatographic strategies in the recent years, however, these are not fully characterized for the fractionation and analysis of PEGylated conjugates.[22]

Nevertheless, these later techniques are considered attractive downstream processes, since they exhibit several advantages: high versatility, ease of scale-up, biocompatible character, and low overall cost and time of processing.[27] Non-chromatographic techniques are believed to offer the characteristics needed for higher selectivity and purity in the fractionation of PEGylated conjugates at low operating costs. Currently, efforts are being made to fully characterize those purification platforms and optimize them for a larger spectrum of PEGylated proteins.[22,28]

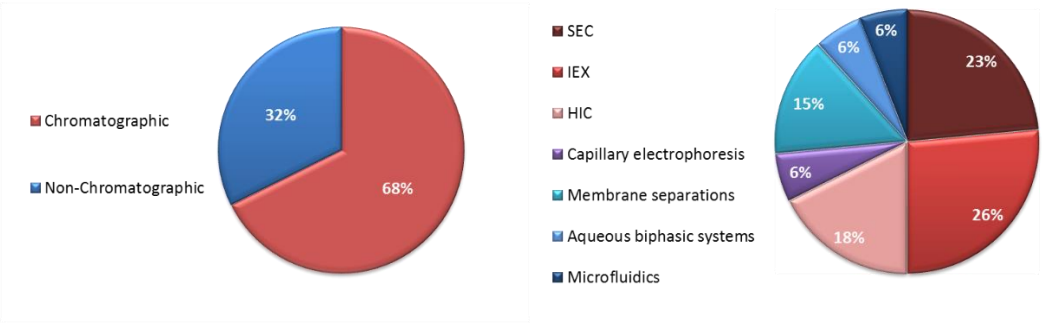

Fig. 1.1. Distribution of the publications/papers reported in the last years (> 2010) dealing with the chromatographic and non-chromatographic techniques for the separation of PEGylated proteins. **SEC – size exclusion chromatography, IEX – ion exchange chromatography, HIC – hydrophobic interaction chromatography.**

1.2.1. Chromatographic fractionation processes

Currently, most purification processes for PEGylated proteins are based on chromatographic techniques, especially size exclusion chromatography (SEC)[29–32] and ion exchange chromatography (IEX).[17,26,33,34] SEC is a chromatographic method in which molecules in solution are separated by their molecular weight (MW). It is well recognized that SEC can be used to separate PEGylated species from unreacted protein and other components, but the effectiveness will greatly depend upon the molecular size of the species involved.[29] For instance, the conjugation of a single PEG polymer with a protein with the same MW increases the protein molecular radius more than doubling, due to the conformation and high degree of hydration of PEG chains.[35] Therefore, native and mono-PEGylated proteins should be readily separable by SEC.[29–32] For protein conjugates with MW significantly different than the originator protein, SEC will be an effective purification platform, but the resolution among chromatographic peaks will be expected to diminish as PEGylation extent increases, due to the presence of more

PEGylated conjugates.[31,32] However, SEC is not able to purify with great selectivity the positional isomers of PEGylated conjugates, due to the minimal differences among these protein species.[35] For its part, IEX is capable of separating these proteins, because for each PEG molecule attached to an amino group, for example, a PEGylated protein has one less positive charge and this chromatographic technique separates the protein depending on net surface charge.[35] By choosing the optimal ion exchanger and separation conditions, higher resolution can be obtained. This step must be achieved case-by-case depending on the specific protein and type of PEGylation.[35] In the recent years, IEX has been the most used downstream technique for the separation of PEGylated conjugates[17,26,33,34] (**Fig. 1.1.**). However, some drawbacks are observed due to the fact that PEG chains sterically interfere in the interaction of the charged residues of the protein and the ionic exchange support, producing a masking effect of the charges.[35] Hydrophobic interaction chromatography (HIC) is also being applied in the fractionation of PEGylated proteins,[20,24,25] although not so extensively as IEX and SEC. HIC takes advantage of the hydrophobicity changes through PEGylation process, separating PEGylated conjugates based on the relatively hydrophobicity/hydrophilicity of these protein species.[35] Nonetheless, HIC has low capacity and poor resolution between adjacent peaks. To date it is not possible to conclude which type of chromatographic technique is the best option to fractionate PEGylated conjugates. Furthermore, there is no generalized chromatographic protocols to purify PEGylated conjugates among themselves, making it necessary to describe empirically the separation strategies on a case-by-case basis.[22,35]

1.2.2. Non-chromatographic fractionation processes

The non-chromatographic fractionation platforms applied in the purification of the PEGylated conjugates are: capillary electrophoresis (CE), membrane separation techniques (ultrafiltration, diafiltration and dialysis), aqueous biphasic systems (ABS) and microfluidics devices.[22] Membrane separation processes are the simplest among all non-chromatographic platforms currently used and are based on the molecular weight and hydrodynamic radius. The main results show that PEGylated species can be fractionated and recovered efficiently using ultrafiltration and diafiltration, thus

achieving high yields and purification factors.[36,37] Albeit, ultrafiltration methods may generate high product losses, particularly when using membranes with pores considerably smaller than the PEGylated protein hydrodynamic radius.[38] Even though membrane separation techniques are not able to separate conjugates according to their positional isomerism, these unit operations seem to present certain advantages over SEC and IEX, where proteins of the same molecular size but different polymer lengths and number of attaching sites cannot be separated or fully resolved.[39] Capillary electrophoresis (CE) has been used in the analysis and small-scale purification of PEGylated proteins.[40–42] CE proved to be a powerful tool for the high resolution separation of different PEGylated products. The major advantages of this technique are automation capability, low sample consumption and short-time of the downstream process.[42–44] CE is not adequate for industrial implementation due to technique scale-up incapability.

The design of novel microfluidic devices for rapid separation, concentration, and recovery of PEGylated proteins in a one-step operation is a current trend in the non-chromatographic downstream processes.[21,45,46] The application of aqueous biphasic systems, due to their great importance and advantages in the purification of PEGylated proteins are well-described in the **Section 1.2.2.1.** Moreover, it is important to highlight that those aqueous downstream platforms are focus of interest in the experimental work of this thesis, due to their versatile character and boundless potentiality in this field.

1.2.2.1. Aqueous biphasic systems (ABS)

Aqueous biphasic systems (ABS) were originally proposed by Albertsson[47] as cleaner liquid-liquid extraction processes that could be used as potential substitutes for the conventional ones. This is mainly due to the fact that ABS are not based on hazardous volatile organic solvents and present abundant water content, providing milder and more biocompatible conditions for bioseparation/downstream processes.[48,49] In fact, ABS are able to maintain the native conformation and biological activity of diverse biomolecules, while allowing high yields and purity levels. Evidences of their successful application are well-documented for a wide array of compounds, namely proteins[50–52]

including enzymes,[53–55] cells,[56,57] and antibiotics.[58,59] Apart from their environmentally benign status, ABS are full of flexibility related with the countless types of chemical compounds that can be combined to create them, *e.g.* polymer + polymer,[60–62] polymer + salt,[63–65] or salt + salt.[66–68] More recently, the use of ionic liquids (ILs) as either phase forming agents,[54,69–71] electrolytes[72,73] or adjuvants[74–76] emerged. Remarkably, the introduction of such ionic compounds in polymer-based ABS significantly increases the polarity differences between the phases.[67] ILs are salts in the liquid state below a stated temperature of 100ºC, conventionally composed of a large organic cation and an anion of either inorganic or organic nature.[77] They present unique characteristics such as insignificant vapour pressure and flammability, being these the main reasons why ILs are labelled as greener solvents. Moreover, they possess high chemical[78] and thermal[79] stabilities and outstanding capability of solvating compounds from a wide spectrum of polarities.[80,81] These characteristics have contributed for the recognition of ILs as important phase forming agents in ABS. Furthermore, the ILs' status of designer solvents,[82] *i.e.* (almost) immeasurable cation/anion possible combinations, brings the possibility to manipulate ABS phases' polarities and to develop tailor-made systems with specific affinities for certain biomolecules and applications.

Several works addressed the application of ABS as purification tools to be used in the separation of PEGylated proteins.[28,83–86] **Table 1.1.** presents information regarding the reports about the fractionation, recovery and partial purification of the PEGylated conjugates using ABS. Delgado et al.[85,86] used PEG/dextran ABS as a feasible technique to characterize the degree of PEGylation (n) in PEGylated bovine serum albumin and PEGylated granulocyte-macrophage colony stimulating factor in mixtures of PEG-protein conjugates. These authors determined the relationship between the increase in partition coefficient (*K*) of the PEGylated conjugate, considering the ratio of the concentration of the target protein in both top and bottom phases, with the degree of PEGylation of the protein species present in the resulting mixtures. González-Valdez et al.[83] studied other type of ABS, in this case, PEG/salt-based ABS and evaluated the effect of PEG MW, tie-line length (*TLL*) and volume ratio (*V*r) on the partition of native RNase A and lactoalbumin and their respective PEGylated conjugates. The results presented by the authors showed the potential of ABS for the fractionation of PEGylated proteins

from their unreacted proteins, however the sub-fractionation of PEGylated proteins among themselves (depending on their degree of PEGylation) was not achieved. The extended application of ABS was achieved by other authors, with the combination of this technique with continuous scale-up platforms, such as the counter current distribution ABS (CCD-ABS). This technique uses ABS to purify in continuous regime, as described in detail in **Section 1.2.2.2**. The application of CCD-ABS was already performed for the fractionation of PEGylated forms of lysozyme and RNase.[28,87] From the reported results using ABS as purification platforms, it is necessary to fully characterize the behaviour of protein-polymer conjugates in ABS based operations, either for batch or continuous processing.

Table 1.1. ABS applied in the separation of PEGylated proteins.

Protein	PEGylation degree (n)	Polymer ABS used	Goal	Reference
GM-CSF	0-2.5	4.75% PEG + 4.75% Dextran T-500 + 0.15 M NaCl buffered with sodium phosphate, pH 6.8	Correlation between log K vs *n* and purification of protein-conjugates from unreacted protein and PEG	85,86
BSA	0-46	NaCl-enriched ABS containing Dextran T-500 and PEG 8000 or 6000	Use of NaCl enriched ABS to purify protein-conjugates	86
IgG	0-43	NaCl-enriched ABS containing Dextran T-500 and PEG 8000 or 6000	Separation of conjugates from the unreacted protein	86
α-Lactalbumin	0-2	PEG 400/1000/3350/8000 + potassium phosphate	Use of countercurrent distribution (CCD) with ABS for the separation of PEGylated conjugates with different degrees of PEGylation (*i.e.* mono- and di-PEGylated RNase A)	83
RNase A	0-2	PEG 400/1000/3350/8000 + potassium phosphate		28,83,84
Lysozyme	0-2	19.36% PEG 3400 + 14.68% potassium phosphate (pH=7)	Fractionation of unmodified lysozyme,(PEG)1-lysozyme and (PEG)2-lysozyme using countercurrent distribution (CCD) and ABS	87

GM-CSF, granulocyte macrophage colony-stimulating factor; BSA, bovine serum albumin; IgG, immunoglobulin G; RNase A, ribonuclease A.

Despite the advances reported, there is still much that needs to be address regarding the improvement of the purification of PEGylated conjugates with different degrees of PEGylation. Actually, it seems urgent the application of other types of ABS, such as PEG/polyacrylate (with or without electrolytes present), PEG/IL, copolymer/salt, just to

mention a few. *In situ* product recovery through use of ABS in continuous regime and the application of other approaches regarding the continuous flow purification, namely the centrifugal partition chromatography (CPC), should also be focused in the near future.[22]

1.2.2.2. Use of ABS to separate PEGylated proteins and their application in Centrifugal Partition Chromatography (CPC)

Centrifugal Partition Chromatography (CPC) is a type of liquid-liquid chromatography requiring two immiscible liquid phases, one of which remaining stationary in the machine while the other acts as the mobile phase.[88] The lack of a solid support distinguishes this technique from commonly used chromatographic methods, like high-performance liquid chromatography (HPLC), where a column with an adsorbent material is usually utilized.[89] While the basis of this technique is indeed common to other liquid-liquid chromatographic methods - the partition of solutes between the two phases formed, the notable difference between them and CPC is the use of a centrifugal force by the later, in order to hold the stationary liquid phase in place.[88] The concept of CPC was introduced in 1982 by Murayama et al.,[90] stemming from an already established technique developed in 1944 by Lyman Craig,[91] the counter current distribution (CCD), with the first functional CPC instrument being manufactured by Sanki Engineering.[92] The main advantage of using CPC comes from the liquid-liquid nature of this process, making it unnecessary to use solid chromatographic supports, guaranteeing therefore almost 100 % of compound recovery and an easy recyclability of the solvents, thus minimizing environmental problems and process costs,[88] while also avoiding the need to buy, maintain and clean high-cost solid columns.[93] The high volume of the stationary phase that can be loaded into the CPC is also a significant advantage, making this technique suitable for industrial application.[94] While this adaptability is seen as an advantage in terms of potential applications, a careful choice of the solvents/phases is needed and defined according to the following criteria: easy phase separation; high capacity to be retained by the CPC; and separation/purification effectiveness.[94] Even though the selection of a solvent system for use in CPC can be in many ways similar to other chromatographic methods, when it comes to criteria such as polarity, charge and

complexation, one also has to take into account the partition coefficients of the sample in that particular system.[88] While classical chloroform/methanol/water or n-hexane/ethyl acetate/methanol systems can be a good starting point, allowing for some manipulation of the system's polarity to achieve the required sample distribution,[88] there has been a major interest in utilizing ABS in CPC. This increase in interest is not only due to ABSs already outlined advantages in terms of tunability,[64] an essential characteristic for the development of a worthy CPC separation protocols, but also because of the highly biocompatible environment that ABS can provide, especially when compared to common organic solvents that, in many cases, induce significant conformational changes in proteins.[49,95]

1.3. Applications of protein PEGylation

1.3.1. Design of novel biobetters: PEGylation in biopharmaceutical field

Therapies based on biopharmaceuticals were a revolutionary innovation in the pharmaceutical field due to the success to reach medical needs previously unmet, such as haemophilia, diabetes, arthritis and diseases of the immune system. Because of patent protections and the high market price of biopharmaceuticals, the holding companies of innovative molecules generated considerable revenue. Only six companies were responsible for the marketing of the ten best-selling biopharmaceuticals in 2011, about 37.6 % of total sales and reached a value of US $ 142 billion.[96] However, some drawbacks upsurge, which are mainly related to the immunogenicity and low plasma half-life of these molecules. The immunogenicity is a concern in the production of anti-drug antibodies (ADA – Anti-drug Antibodies) that may reduce the clinical efficacy by neutralization of the biological activity, the responses of hypersensitivity, anaphylactic reactions, among others.[97,98] The lower biological half-life of biopharmaceuticals leads to more recurrent administrations to achieve the desired clinical effect in patients.[99] Another concern related to biopharmaceuticals available in the pharmaceutical market is of economic nature and is called "*Patent Cliff*", a market phenomenon well described and known to the chemical drugs, that is approaching for biopharmaceuticals.[96] This term refers to a sharp drop in sales of blockbusters when approaching the end of their patent protection. This drop in sales can impact negatively or positively the main

participants in the biological drug industry depending on the marketing strategies adopted.[96]

Taking into account the economic need to remain competitive in the market and the necessity to solve the inherent problems of biopharmaceuticals, a new generation of protein-based medicines emerge: the follow-on biologics. This new generation of biopharmaceuticals is divided in two main groups: the biosimilars[96,98] and biobetters.[98–100] Both are variants of an original protein-based medicine. However biosimilars, as the term suggests, aim to establish similarity to a known biological, while biobetters seek superiority in one or various aspects of their clinical profile.[18] In this sense, biosimilars are close copies of marketed originator biotherapeutics, which must have the same safety, purity and efficacy profile as the originator compound.[101] On the other hand, by definition, a biobetter is a biopharmaceutical changed through chemical or molecular modifications from an originator protein-based medicine, with functional changes that include increased half-life, reduced toxicity, reduced immunogenicity, and enhanced pharmacodynamic effects.[18,101]

The biobetters represent an opportunity for innovation with reduced risk and increased sales for manufacturers, since the mechanism of action of the starting material molecule is already known. At the same time, these promote an improved treatment for patients and the reduction of the costs for health systems. One of the principal tools used for the development of biobetters is the PEGylation technique. After the first report of protein PEGylation in the 1970s,[9] many proteins and peptides have been covalently conjugated with PEG.

To date, 14 biobetters (PEGylated proteins, peptides, antibody fragments, and oligonucleotides) have been approved by FDA and are currently on the market (**Table 1.2.**). From these 14 biobetters, 12 are PEGylated proteins, presented in biopharmaceutical market with a total market value of over US $ 8 billion per year and many others are in clinical trials.[13]

Table 1.2. FDA-approved PEGylated drugs in United and States and/or Europe.

Brand name	Company	PEG size (Da)	Indication(s)	Year of approval
Adagen®	Enzon	5000	Severe combined immunodeficiency diseases (SCID)	1990
Oncaspar®	Enzon	5000	Acute lymphoblastic leukemia (ALL)	1994
PEG-INTRON®	Schering-Plough	12,000	Hepatitis C	2000
PEGASYS®	Hoffman-La Roche	40,000	Hepatitis C	2001
Neulasta®	Amgen	20,000	Neutropenia	2002
Somavert®	Pfizer	5000	Acromegaly	2003
Macugen®	Pfizer	40,000	Age-related macular degeneration	2004
Mircera®	Hoffman-La Roche	30,000	Anemia associated with chronic renal failure	2007
Cimzia®	UCB	40,000	Chronic, moderate to severe RA, Crohn's disease, axial spondyloarthritis and psoriatic arthritis	2008
Puricase1®	Savient	10,000	Chronic gout	2010
Sylatron®	Merck	12,000	Melanoma	2011
Omontys®	Affymax/Takeda	40,000	Anemia associated with chronic kidney disease	2012
Plegridy®	Biogen	20,000	Multiple sclerosis	2014
Adynovate®	Baxalta	20,000	Hemophilia A	2015

1.3.2. Design of novel biosensors: PEGylation in the biosensing field

A biosensor is an analytical device, used for the detection of an analyte, which combines a biological component with a physicochemical detector.[102,103] The sensitive element is a biologically derived material or biomimetic component that interacts (binds or recognizes) with the analyte under study (*e.g.* tissues, microorganisms, organelles, cell receptors, enzymes, antibodies, nucleic acids, etc).[103,104] Biocatalysts can be widely applied in the biosensing field.[105–108] However, enzyme-based biosensors suffer from the fact that proteins have a fragile conformation, being affected by several exogenous conditions (*i.e.* pH, salt concentration, presence of proteases, temperature, among

others).[105,109] Moreover, the exposure of redox enzymes to electrode materials often leads to unfolding and, subsequently, to irreversible inactivation.[110] In general, long-term stability and thermal stability are the two main drawbacks related to the potential application of enzyme-based biosensors. In order to overcome those drawbacks, chemical modification of the enzyme is frequently employed.[8,111] As mentioned before, the chemical modification of proteins with polyethylene glycol (PEG) improves multiple properties: biocompatibility, long-term stability, enhanced thermal stability, and solubility in organic solvents.[12] It is therefore not surprising that PEGylation has been employed to stabilize several biocatalysts with peroxidase-like activity, such as: cytochrome c,[14,105,111,112] hemoglobin,[113] myoglobin,[114] and horseradish peroxidase.[115]

1.4. Scopes and objectives

This thesis has as main objective the development of PEGylation strategies to the creation of novel analytical and therapeutic proteins. The biopharmaceutical chosen for this purpose was the L-asparaginase (ASNase), an enzyme used in the treatment of Acute Lymphoblastic Leukemia (ALL). The PEGylation of this biopharmaceutical increases the half-life time of the enzyme in the human blood, protects the biopharmaceutical against proteolytic attack, and reduces the immunological reactions and protein aggregation. For the analytical part, a protein-based biosensor, namely the cytochrome c (Cyt-c), was selected to be studied in this thesis. This biocatalyst has peroxidase-like activity and can be applied as biosensor, however due to its problems related to long-term and thermal stability, the PEGylation will also be applied to overcome those drawbacks. This thesis is divided in the following Chapters:

Chapter 2 shows the development and implementation of ABS as new purification platforms for the recovery of L-asparaginase (ASNase) from fermentation medium and cytochrome-c (Cyt-c) from a complex protein mixture. **Chapter 3** reports a new strategy regarding the development of site-specific PEGylation reactions for the two studied proteins: ASNase (therapeutic enzyme) and Cyt-c (biosensor).

After identifying the more efficient PEGylation reactions for Cyt-c and ASNase, **Chapter 4** shows the use of ABS to optimize an efficient downstream process to purify and obtain pure PEGylated forms of each protein under study.

Considering the necessity of exploring the purification strategies in continuous flow, in **Chapter 5**, the development of continuous purification processes, capable of contributing to purify different site-specific PEGylated proteins between each other and these form the unreacted proteins.

References

1. Baker, M. Protein engineering: navigating between chance and reason. *Nat. Methods* **8,** 623–626 (2011).
2. Brannigan, J. a & Wilkinson, A. J. Protein engineering 20 years on. *Nat. Rev. Mol. Cell Biol.* **3,** 964–70 (2002).
3. Jevševar, S., Kunstelj, M. & Porekar, V. G. PEGylation of therapeutic proteins. *Biotechnol. J.* **5,** 113–128 (2010).
4. Roberts, M. J., Bentley, M. D. & Harris, J. M. Chemistry for peptide and protein PEGylation. *Advanced Drug Delivery Reviews* **64,** 116–127 (2012).
5. Pasut, G. & Veronese, F. M. State of the art in PEGylation: The great versatility achieved after forty years of research. *Journal of Controlled Release* **161,** 461–472 (2012).
6. Pfister, D. & Morbidelli, M. Process for protein PEGylation. *Journal of Controlled Release* **180,** 134–149 (2014).
7. Schwarz, F. & Aebi, M. Mechanisms and principles of N-linked protein glycosylation. *Current Opinion in Structural Biology* **21,** 576–582 (2011).
8. Boutureira, O. & Bernardes, G. J. L. Advances in chemical protein modification. *Chemical Reviews* **115,** 2174–2195 (2015).
9. Hoffman, A. S. The early days of PEG and PEGylation (1970s-1990s). *Acta Biomater.* **40,** 1–5 (2016).
10. Abuchowski, A., van Es, T., Palczuk, N. C. & Davis, F. F. Alteration of immunological properties of bovine serum albumin by covalent attachment of polyethylene glycol. *J. Biol. Chem.* **252,** 3578–81 (1977).
11. González-Valdez, J., Rito-Palomares, M. & Benavides, J. Advances and trends in the design, analysis, and characterization of polymer-protein conjugates for 'PEGylaided' bioprocesses. *Analytical and Bioanalytical Chemistry* **403,** 2225–

2235 (2012).

12. Palm, T., Esfandiary, R. & Gandhi, R. The effect of PEGylation on the stability of small therapeutic proteins. *Pharm. Dev. Technol.* **16,** 441–448 (2011).
13. Ginn, C., Khalili, H., Lever, R. & Brocchini, S. PEGylation and its impact on the design of new protein-based medicines. *Future Med. Chem.* **6,** 1829–46 (2014).
14. Zhou, J. Q., He, T. & Wang, J. W. PEGylation of cytochrome c at the level of lysine residues mediated by a microbial transglutaminase. *Biotechnol. Lett.* **38,** 1121–1129 (2016).
15. Veronese, F. M. Peptide and protein PEGylation: a review of problems and solutions. *Biomaterials* **22,** 405–417 (2001).
16. Da Silva Freitas, D., Mero, A. & Pasut, G. Chemical and enzymatic site specific pegylation of hGH. *Bioconjug. Chem.* **24,** 456–463 (2013).
17. Zhao, T. *et al.* N-terminal PEGylation of human serum albumin and investigation of its pharmacokinetics and pulmonary microvascular retention. *Biosci. Trends* **6,** 81–88 (2012).
18. Sassi, A. B., Nagarkar, R. & Hamblin, P. in *Novel Approaches and Strategies for Biologics, Vaccines and Cancer Therapies* 199–217 (2015). doi:10.1016/B978-0-12-416603-5.00009-2
19. Nanocs. Succinimidyl PEG NHS, mPEG-NHS(SC). (2017). Available at: http://www.nanocs.net/mPEG-SC-5k-1g.htm.
20. Moosmann, A., Müller, E. & Böttinger, H. Purification of PEGylated Proteins, with the example of PEGylated lysozyme and PEGylated scFv. *Methods Mol. Biol.* **1129,** 527–538 (2014).
21. Yoshimoto, N. & Yamamoto, S. PEGylated protein separations: Challenges and opportunities. *Biotechnology Journal* **7,** 592–593 (2012).
22. Mayolo-Deloisa, K. *et al.* Current advances in the non-chromatographic fractionation and characterization of PEGylated proteins. *J. Chem. Technol. Biotechnol.* **86,** 18–25 (2011).
23. Fee, C. J. Size-exclusion reaction chromatography (SERC): A new technique for protein PEGylation. *Biotechnol. Bioeng.* **82,** 200–206 (2003).
24. Mayolo-Deloisa, K., Lienqueo, M. E., Andrews, B., Rito-Palomares, M. & Asenjo, J.

A. Hydrophobic interaction chromatography for purification of monoPEGylated RNase A. *J. Chromatogr. A* **1242,** 11–16 (2012).

25. Müller, E., Josic, D., Schröder, T. & Moosmann, A. Solubility and binding properties of PEGylated lysozyme derivatives with increasing molecular weight on hydrophobic-interaction chromatographic resins. *J. Chromatogr. A* **1217,** 4696–4703 (2010).
26. Moosmann, A., Christel, J., Boettinger, H. & Mueller, E. Analytical and preparative separation of PEGylated lysozyme for the characterization of chromatography media. *J. Chromatogr. A* **1217,** 209–215 (2010).
27. Cramer, S. M. & Holstein, M. A. Downstream bioprocessing: Recent advances and future promise. *Curr. Opin. Chem. Eng.* **1,** 27–37 (2011).
28. Galindo-López, M. & Rito-Palomares, M. Practical non-chromatography strategies for the potential separation of PEGylated RNase A conjugates. *J. Chem. Technol. Biotechnol.* **88,** 49–54 (2013).
29. Silva Freitas, D. da & Abrahao-Neto, J. Batch purification of high-purity lysozyme from egg white and characterization of the enzyme modified by PEGylation. *Pharm. Biol.* **48,** 554–562 (2010).
30. Pai, S. S., Hammouda, B., Hong, K., Pozzo, D. C., Przybycien, T. M. & Tilton, R. D. The conformation of the poly(ethylene glycol) chain in mono-PEGylated Lysozyme and mono-PEGylated human growth hormone. *Bioconjug. Chem.* **22,** 2317–2323 (2011).
31. Fahrländer, E., Schelhaas, S., Jacobs, A. H. & Langer, K. PEGylated human serum albumin (HSA) nanoparticles: preparation, characterization and quantification of the PEGylation extent. *Nanotechnology* **26,** 145103 (2015).
32. Maiser, B., Baumgartner, K., Dismer, F. & Hubbuch, J. Effect of lysozyme solid-phase PEGylation on reaction kinetics and isoform distribution. *J. Chromatogr. B Anal. Technol. Biomed. Life Sci.* **1002,** 313–318 (2015).
33. Morgenstern, J., Baumann, P., Brunner, C. & Hubbuch, J. Effect of PEG molecular weight and PEGylation degree on the physical stability of PEGylated lysozyme. *Int. J. Pharm.* **519,** 408–417 (2017).
34. Abe, M., Akbarzaderaleh, P., Hamachi, M., Yoshimoto, N. & Yamamoto, S.

Interaction mechanism of mono-PEGylated proteins in electrostatic interaction chromatography. *Biotechnol. J.* **5,** 477–483 (2010).

35. Fee, C. J. & Van Alstine, J. M. in *Protein Purification: Principles, High Resolution Methods, and Applications: Third Edition* 339–362 (2011). doi:10.1002/9780470939932.ch14
36. Ruanjaikaen, K. & Zydney, A. L. Purification of singly PEGylated α-lactalbumin using charged ultrafiltration membranes. *Biotechnol. Bioeng.* **108,** 822–829 (2011).
37. Cheang, B. & Zydney, A. L. Separation of alpha-lactalbumin and beta-lactoglobulin using membrane ultrafiltration. *Biotechnol. Bioeng.* **83,** 201–209 (2003).
38. Kwon, B., Molek, J. & Zydney, A. L. Ultrafiltration of PEGylated proteins: Fouling and concentration polarization effects. *J. Memb. Sci.* **319,** 206–213 (2008).
39. Latulippe, D. R., Molek, J. R. & Zydney, A. L. Importance of biopolymer molecular flexibility in ultrafiltration processes. *Ind. Eng. Chem. Res.* **48,** 2395–2403 (2009).
40. Li, W., Zhong, Y., Lin, B. & Su, Z. Characterization of polyethylene glycol-modified proteins by semi-aqueous capillary electrophoresis. *J. Chromatogr. A* **905,** 299–307 (2001).
41. Lee, K. S. & Na, D. H. Capillary electrophoretic separation of poly(ethylene glycol)-modified granulocyte-colony stimulating factor. *Arch. Pharm. Res.* **33,** 491–495 (2010).
42. Na, D. H., Park, E. J., Jo, Y. W. & Lee, K. C. Capillary electrophoretic separation of high-molecular-weight poly(ethylene glycol)-modified proteins. *Anal. Biochem.* **373,** 207–212 (2008).
43. Caslavska, J. & Thormann, W. Monitoring of drugs and metabolites in body fluids by capillary electrophoresis with XeHg lamp-based and laser-induced fluorescence detection. *Electrophoresis* **25,** 1623–1631 (2004).
44. Levêque, D., Gailion-Renault, C., Monteil, H. & Jehl, F. Capillary electrophoresis for pharmacokinetic studies. *J. Chromatogr. B. Biomed. Sci. Appl.* **697,** 67–75 (1997).
45. Seyfried, B. K. *et al.* Microchip capillary gel electrophoresis of multiply PEGylated high-molecular-mass glycoproteins. *Biotechnol. J.* **7,** 635–641 (2012).

46. Mata-Gómez, M. A., Gallo-Villanueva, R. C., González-Valdez, J., Mart??nez-Chapa, S. O. & Rito-Palomares, M. Dielectrophoretic behavior of PEGylated RNase A inside a microchannel with diamond-shaped insulating posts. *Electrophoresis* **37,** 519–528 (2016).
47. Albertsson, P. A. Partition of cell particles and macromolecules in polymer two-phase systems. *Adv. Protein Chem.* **24,** 309–341 (1970).
48. Rosa, P. A. J., Azevedo, A. M., Sommerfeld, S., Bäcker, W. & Aires-Barros, M. R. Aqueous two-phase extraction as a platform in the biomanufacturing industry: Economical and environmental sustainability. *Biotechnology Advances* **29,** 559–567 (2011).
49. Hatti-Kaul, R. Aqueous two-phase systems. *Mol. Biotechnol.* **19,** 269–277 (2001).
50. Asenjo, J. A. & Andrews, B. A. Aqueous two-phase systems for protein separation: A perspective. *Journal of Chromatography A* **1218,** 8826–8835 (2011).
51. Alcântara, L. A. P. *et al.* Partitioning of α-lactalbumin and β-lactoglobulin from cheese whey in aqueous two-phase systems containing poly (ethylene glycol) and sodium polyacrylate. *Food Bioprod. Process.* **92,** 409–415 (2014).
52. Lopes, A. M. *et al.* LPS-protein aggregation influences protein partitioning in aqueous two-phase micellar systems. *Applied Microbiology and Biotechnology* **97,** 6201–6209 (2013).
53. Dembczyński, R., Białas, W., Regulski, K. & Jankowski, T. Lysozyme extraction from hen egg white in an aqueous two-phase system composed of ethylene oxide-propylene oxide thermoseparating copolymer and potassium phosphate. *Process Biochem.* **45,** 369–374 (2010).
54. Ventura, S. P. M. *et al.* Production and purification of an extracellular lipolytic enzyme using ionic liquid-based aqueous two-phase systems. *Green Chemistry* **14,** 734 (2012).
55. Ventura, S. P. M. *et al.* Design of ionic liquids for lipase purification. *J. Chromatogr. B Anal. Technol. Biomed. Life Sci.* **879,** 2679–2687 (2011).
56. Peters, T. J. Partition of cell particles and macromolecules: Separation and purification of biomolecules, cell organelles, membranes and cells in aqueous polymer two phase systems and their use in biochemical analysis and

biotechnology. P-A. Albertsson. Third Edition,. *Cell Biochem. Funct.* **5,** 233–234 (1987).

57. Cabral, J. M. S. Cell partitioning in aqueous two-phase polymer systems. in *Advances in Biochemical Engineering/Biotechnology* **106,** 151–171 (2007).
58. Hernandez-Justiz, O., Fernandez-Lafuente, R., Terreni, M. & Guisan, J. M. Use of aqueous two-phase systems for in situ extraction of water soluble antibiotics during their synthesis by enzymes immobilized on porous supports. *Biotechnol. Bioeng.* **59,** 73–79 (1998).
59. Haga, R. B., Santos-Ebinuma, V. C., De Siqueira Cardoso Silva, M., Pessoa, A. & Rangel-Yagui, C. O. Clavulanic acid partitioning in charged aqueous two-phase micellar systems. *Sep. Purif. Technol.* **103,** 273–278 (2013).
60. Karakatsanis, A. & Liakopoulou-Kyriakides, M. Comparison of PEG/fractionated dextran and PEG/industrial grade dextran aqueous two-phase systems for the enzymic hydrolysis of starch. *J. Food Eng.* **80,** 1213–1217 (2007).
61. Da Silva, L. M. & Meirelles, A. A. Phase equilibrium in polyethylene glycol/maltodextrin aqueous two-phase systems. *Carbohydr. Polym.* **42,** 273–278 (2000).
62. Johansson, H.-O., Magaldi, F. M., Feitosa, E., Pessoa Jr, A. & Pessoa, A. Protein partitioning in poly(ethylene glycol)/sodium polyacrylate aqueous two-phase systems. *J. Chromatogr. A* **1178,** 145–53 (2008).
63. Hirata, D. B., Badino, A. C. J. & Hokka, C. O. Utilization of PEG-phosphate aqueous two-phase system for clavulanic acid extraction from fermentation broth. in *2nd Mercosur Congress on Chemical Engineering and 4th Mercosur Congress on Process Systems Engineering* 1–6 (2005).
64. Azevedo, A. M., Rosa, P. A. J., Ferreira, I. F. & Aires-Barros, M. R. Optimisation of aqueous two-phase extraction of human antibodies. *J. Biotechnol.* **132,** 209–217 (2007).
65. Zafarani-Moattar, M. T. & Sadeghi, R. Phase diagram data for several PPG + salt aqueous biphasic systems at 25 ^{o}C. *J. Chem. Eng. Data* **50,** 947–950 (2005).
66. Bridges, N. J., Gutowski, K. E. & Rogers, R. D. Investigation of aqueous biphasic systems formed from solutions of chaotropic salts with kosmotropic salts

(salt/salt ABS). *Green Chemistry* **9,** 177 (2007).

67. Freire, M. G. *et al.* Aqueous biphasic systems: a boost brought about by using ionic liquids. *Chemical Society Reviews* **41,** 4966 (2012).
68. Sintra, T. E., Cruz, R., Ventura, S. P. M. & Coutinho, J. A. P. Phase diagrams of ionic liquids-based aqueous biphasic systems as a platform for extraction processes. *Journal of Chemical Thermodynamics* **77**, 206–213 (2014).
69. Pereira, J. F. B. *et al.* Aqueous biphasic systems composed of ionic liquids and polymers: A platform for the purification of biomolecules. *Sep. Purif. Technol.* **113,** 83–89 (2013).
70. Tomé, L. I. N. *et al.* Evidence for the interactions occurring between ionic liquids and tetraethylene glycol in binary mixtures and aqueous biphasic systems. *J. Phys. Chem. B* **118,** 4615–4629 (2014).
71. Domínguez-Pérez, M. *et al.* (Extraction of biomolecules using) aqueous biphasic systems formed by ionic liquids and aminoacids. *Sep. Purif. Technol.* **72,** 85–91 (2010).
72. Santos, J. H. P. M., e Silva, F. A., Coutinho, J. A. P., Ventura, S. P. M. & Pessoa, A. Ionic liquids as a novel class of electrolytes in polymeric aqueous biphasic systems. *Process Biochem.* **50**, 661–668 (2015).
73. Santos, J. H. P. M., Martins, M., Silvestre, A. J. D., Coutinho, J. A. P. & Ventura, S. P. M. Fractionation of phenolic compounds from lignin depolymerisation using polymeric aqueous biphasic systems with ionic surfactants as electrolytes. *Green Chem.* **18**, 5569-5579 (2016).
74. Pereira, J. F. B., Lima, Á. S., Freire, M. G. & Coutinho, J. A. P. Ionic liquids as adjuvants for the tailored extraction of biomolecules in aqueous biphasic systems. *Green Chem.* **12,** 1661 (2010).
75. Souza, R. L., Ventura, S. P. M., Soares, C. M. F., Coutinho, J. A. P. & Lima, Á. S. Lipase purification using ionic liquids as adjuvants in aqueous two-phase systems. *Green Chem.* **17,** 3026–3034 (2015).
76. Ferreira, A. M., Faustino, V. F. M., Mondal, D., Coutinho, J. A. P. & Freire, M. G. Improving the extraction and purification of immunoglobulin G by the use of ionic liquids as adjuvants in aqueous biphasic systems. *J. Biotechnol.* **236,** 166–175

(2016).

77. Bhattacharjee, A. *et al.* Thermophysical properties of sulfonium- and ammonium-based ionic liquids. *Fluid Phase Equilib.* **381,** 36–45 (2014).
78. Hapiot, P. & Lagrost, C. Electrochemical reactivity in room-temperature ionic liquids. *Chemical Reviews* **108,** 2238–2264 (2008).
79. Meine, N., Benedito, F. & Rinaldi, R. Thermal stability of ionic liquids assessed by potentiometric titration. *Green Chem.* **12,** 1711 (2010).
80. Brandt, A., Gräsvik, J., Hallett, J. P. & Welton, T. Deconstruction of lignocellulosic biomass with ionic liquids. *Green Chem.* **15,** 550–583 (2013).
81. Cláudio, A. F. M. *et al.* Extended scale for the hydrogen-bond basicity of ionic liquids. *Phys. Chem. Chem. Phys.* **16,** 6593–6601 (2014).
82. Freemantle, M. Designer Solvents. *Chem. Eng. News Arch.* **76,** 32–37 (1998).
83. González-Valdez, J., Cueto, L. F., Benavides, J. & Rito-Palomares, M. Potential application of aqueous two-phase systems for the fractionation of RNase A and α-Lactalbumin from their PEGylated conjugates. *J. Chem. Technol. Biotechnol.* **86,** 26–33 (2011).
84. González-Valdez, J., Rito-Palomares, M. & Benavides, J. Effects of chemical modifications in the partition behavior of proteins in aqueous two-phase systems: A case study with RNase A. *Biotechnol. Prog.* **29,** 378–385 (2013).
85. Delgado, C., Malik, F., Selisko, B., Fisher, D. & Francis, G. E. Quantitative analysis of polyethylene glycol (PEG) in PEG-modified proteins/cytokines by aqueous two-phase systems. *J. Biochem. Biophys. Methods* **29,** 237–50 (1994).
86. Delgado, C., Malmsten, M. & Van Alstine, J. M. Analytical partitioning of poly(ethylene glycol)-modified proteins. *J. Chromatogr. B Biomed. Appl.* **692,** 263–272 (1997).
87. Sookkumnerd, T. & Hsu, J. T. Purification og PEG-protein conjugates by countercurrent disturbution in aqueous two-phase systems. *J. Liq. Chromatogr. Relat. Technol.* **23,** 497–503 (2000).
88. Wanasundara, U. & Fedec, P. Centrifugal partition chromatography (CPC): Emerging separation and purification technique for lipid and related compounds. *Inf. - Int. News Fats, Oils Relat. Mater.* **13,** 726–730 (2002).

89. Baczek, T., Kaliszan, R., Novotná, K. & Jandera, P. Comparative characteristics of HPLC columns based on quantitative structure-retention relationships (QSRR) and hydrophobic-subtraction model. *J. Chromatogr. A* **1075,** 109–115 (2005).

90. Murayama, W. *et al.* A new centrifugal counter-current chromatograph and its application. *J. Chromatogr. A* **239,** 643–649 (1982).

91. Craig, L. C. Identification of small amounts of organic compounds by distribution studies: ii. Separation by counter-current distribution. *J. Biol. Chem.* **155,** 519–534 (1944).

92. Marchal, L., Legrand, J. & Foucault, A. Centrifugal partition chromatography: A survey of its history, and our recent advances in the field. *Chem. Rec.* **3,** 133–143 (2003).

93. Melorose, J., Perroy, R. & Careas, S. Introduction to Centrifugal Partition Chromatography CPC/CCC. *Statew. Agric. L. Use Baseline 2015* **1,** (2015).

94. Berthod, A., Maryutina, T., Spivakov, B., Shpigun, O. & Sutherland, I. a. Countercurrent chromatography in analytical chemistry (IUPAC Technical Report). *Pure Appl. Chem.* **81,** 355–387 (2009).

95. Schwienheer, C., Merz, J. & Schembecker, G. Selection and Use of Poly Ethylene Glycol and Phosphate Based Aqueous Two-Phase Systems for the Separation of Proteins by Centrifugal Partition Chromatography. *J. Liq. Chromatogr. Relat. Technol.* **38,** 929–941 (2015).

96. Calo-Fernández, B. & Martínez-Hurtado, J. L. Biosimilars: Company strategies to capture value from the biologics market. *Pharmaceuticals* **5,** 1393–1408 (2012).

97. Kuriakose, A., Chirmule, N. & Nair, P. Immunogenicity of Biotherapeutics: Causes and Association with Posttranslational Modifications. *Journal of Immunology Research* **2016,** (2016).

98. Barbosa, M. D. F. S., Kumar, S., Loughrey, H. & Singh, S. K. Biosimilars and biobetters as tools for understanding and mitigating the immunogenicity of biotherapeutics. *Drug Discovery Today* **17,** 1282–1288 (2012).

99. Ryu, J. K., Kim, H. S. & Nam, D. H. Current status and perspectives of biopharmaceutical drugs. *Biotechnology and Bioprocess Engineering* **17,** 900–911 (2012).

100. Gorham, H. The Value of Biobetters. *PRA Heal. Sci.* **62,** 471–489 (2015).
101. Beck, A., Sanglier-Cianférani, S. & Van Dorsselaer, A. Biosimilar, biobetter, and next generation antibody characterization by mass spectrometry. *Anal. Chem.* **84,** 4637–4646 (2012).
102. Tothill, I. E. Biosensors developments and potential applications in the agricultural diagnosis sector. *Comput. Electron. Agric.* **30,** 205–218 (2001).
103. Luong, J. H. T., Male, K. B. & Glennon, J. D. Biosensor technology: Technology push versus market pull. *Biotechnology Advances* **26,** 492–500 (2008).
104. Velasco-Garcia, M. N. & Mottram, T. Biosensor technology addressing agricultural problems. *Biosystems Engineering* **84,** 1–12 (2003).
105. Santiago-Rodríguez, L. *et al.* Enhanced stability of a nanostructured cytochrome c biosensor by PEGylation. *J. Electroanal. Chem.* **663,** 1–7 (2011).
106. Liu, G., Lin, Y., Ostatná, V. & Wang, J. Enzyme nanoparticles-based electronic biosensor. *Chem. Commun.* 3481 (2005). doi:10.1039/b504943a
107. Lenigk, R. *et al.* Enzyme biosensor for studying therapeutics of Alzheimer's disease. *Biosens. Bioelectron.* **15,** 541–547 (2000).
108. Yang, Z. & Zhang, C. Single-enzyme nanoparticles based urea biosensor. *Sensors Actuators, B Chem.* **188,** 313–317 (2013).
109. Gouda, M. D., Kumar, M. A., Thakur, M. S. & Karanth, N. G. Enhancement of operational stability of an enzyme biosensor for glucose and sucrose using protein based stabilizing agents. *Biosens. Bioelectron.* **17,** 503–507 (2002).
110. Zull, J. E. *et al.* Problems and approaches in covalent attachment of peptides and proteins to inorganic surfaces for biosensor applications. *Journal of Industrial Microbiology* **13,** 137–143 (1994).
111. García-Arellano, H., Buenrostro-Gonzalez, E. & Vazquez-Duhalt, R. Biocatalytic Transformation of Petroporphyrins by Chemical Modified Cytochrome C. *Biotechnol. Bioeng.* **85,** 790–798 (2004).
112. Mabrouk, P. A. Effect of pegylation on the structure and function of horse cytochrome c. *Bioconjug. Chem.* **5,** 236–241 (1994).
113. Ohno, H. & Yamaguchi, N. Redox reaction of poly(ethylene oxide)-modified hemoglobin in poly(ethylene oxide) oligomers at 120 degrees C. *Bioconjug. Chem.*

5, 379–381 (1994).

114. Kawahara, N. Y., Ohkubo, W. & Ohno, H. Effect of cast solvent on the electron transfer reaction for poly(ethylene oxide)-modified myoglobin on the electrode in poly(ethylene oxide) oligomers. *Bioconjug. Chem.* **8,** 244–248 (1997).

115. Kawahara, N.Y., Muneyasu, K., Ohno, H. Conformation and redox reaction of poly(ethylene oxide)-modified horseradish peroxidase in poly(ethylene oxide) oligomers. *Chem. Lett.* 381–382 (1997).

2. PRODUCTION AND PURIFICATION OF ASNASE AND CYT-C

2.1. Heterologous expression and purification of active L-asparaginase I of *Saccharomyces cerevisiae* in *Escherichia coli* host

Santos, J. H. P. M., Costa, I. M., Molino, J. V. D., Leite, M. S. M., Pimenta, M. V., Coutinho, J. A. P., Pessoa. A. J., Ventura, S. P. M., Lopes, A. M. & Monteiro, G. *Biotechnology Progress*, 2017, **33**, 416-424.[2]

Abstract

L-asparaginase (ASNase) is a biopharmaceutical widely used to treat child leukemia. However, it presents some side effects, and in order to provide an alternative biopharmaceutical, in this work, the genes encoding ASNase from *Saccharomyces cerevisiae* (*Sc*_ASNaseI and *Sc*_ASNaseII) were cloned in the prokaryotic expression system *Escherichia coli.* In the 93 different expression conditions tested, the *Sc*_ASNaseII protein was always obtained as an insoluble and inactive form. However, the *Sc*_ASNaseI $(His)_6$-tagged recombinant protein was produced in large amounts in the soluble fraction of the protein extract. Affinity chromatography was performed on a Fast Protein Liquid Chromatography (FPLC) system using Ni^{2+}-charged, HiTrap Immobilized Metal ion Affinity Chromatography (IMAC) FF in order to purify active *Sc*_ASNaseI recombinant protein. The results suggest that the strategy for the expression and purification of this potential new biopharmaceutical protein with lower side effects was efficient since high amounts of soluble *Sc*_ASNaseI with high specific activity (110.1 ± 0.3 $U.mg^{-1}$) were obtained. In addition, the use of FPLC-IMAC proved to be an efficient tool in the purification of this enzyme, since a good recovery (40.50 ± 0.01%) was achieved with a purification factor of 17-fold.

Keywords: Biopharmaceutical; Fast Protein Liquid Chromatography (FPLC); Purification; Recombinant DNA; Enzyme technology.

[2] Contributions: JS, IC, ML and MP constructed vectors and expressed ASNase, carried out enzyme activity assay and purification process, and wrote the manuscript drafting, JM participated in data analysis and carried out the computational analysis of recombinant enzyme, JC, PJ and SV participated in the design of the study analysed data, and wrote the manuscript, AL and GM conceived the study and participated in its design and coordination and helped to draft the manuscript. All authors read and approved the final manuscript.

1. Introduction

The L-asparaginase (ASNase), L-asparagine amidohydrolase [EC 3.5.1.1] is an enzyme which catalyzes the hydrolysis of the amino group of L-asparagine, forming L-aspartic acid and ammonia. The discovery of this enzyme started with Kidd's[1] remarkable observation that Guinea pig serum had anti-tumor activity against several types of lymphoma in mice. Broome[2] elucidated this anti-leukemic activity attributing it to ASNase action. Nevertheless, only in 1967, the ASNase was isolated in enough quantity to prove its anti-tumoral activity in clinical trials.[3] Since then, the demand for the proper and efficient isolation and purification techniques for ASNase has increased, due to its pharmacological importance and proved application.

ASNase was shown to be very useful in treating acute lymphocytic leukemia (ALL),[4–6] acute myeloid leukemia[7] and lymphomas.[8] ALL is a blood and bone marrow-related cancer whose prevalence is higher in childhood[9,10]. Nowadays, ASNase based drugs are available in different preparations/formulations as described in **Table 2.1**..[11–16]

Table 2.1. Commercially approved ASNase.[11–16]

Drug Name	Production Source	Type	Manufacteur
Elspar®	*Escherichia coli*	Native enzyme	Lundbeck Inc
Kidrolase®	*Escherichia coli*	Native enzyme	EUSA Pharma S.A.
Oncaspar® (PEG-asparaginase)	*Escherichia coli*	PEGylated native enzyme	Sigma Tau Pharmaceuticals
Graspa®	*Escherichia coli*	Native enzyme encapsulated in erythrocytes	ERYTECH Pharma
Leunase®	*Escherichia coli*	Modified *E.coli* HAP strain	Kyowa Hakko Kirin Co. Ltd.
Spectrila®	*Escherichia coli*	Recombinant Enzyme	Medac Gesellschaft fuer klinische Spezialpraeparate mbH
Erwinase®	*Erwinia chrysanthemi*	Native enzyme	EUSA Pharma
Crisantaspase®	*Erwinia chrysanthemi*	Native enzyme	Ohara Pharmaceutical

However, there are some factors limiting its use as a chemotherapeutic agent, namely i) the daily dose demand (10-200 $U.kg^{-1}$ *per* day), for different periods of time, which may last for 21 days, and ii) the toxic side effects that can occur during therapy, *i.e.*

hyperglycemia, decreased serum albumin, lipoproteins and fibrinogen, increased liver fat and some mild brain dysfunctions[6,11,17–20] and iii) the development of hypersensitivity to treatment. The hypersensitivity reactions ranging from a small allergy in the drug injection area, bronchospasm and even anaphylactic shock, occurs in 5 to 50% of the treated patients. Nowadays, the researchers are focused in the partial or total elimination of these problems, regarding some protein structural modification approaches, through genetic engineering, gene enhancement and/or by ASNase conjugation with biopolymers (*e.g.* polyethylene glycol (PEG), dextran, albumin and heparin)[5,11,21–23] or by changing the expression host systems.[24]

In this work, the genes codifying ASNase were isolated from the *Saccharomyces cerevisiae* BY4741 (Invitrogen), a microorganism able to synthesize two distinct forms of ASNase: *Sc*_ASNaseI, an intracellular constitutive enzyme and *Sc*_ASNaseII, a periplasmic enzyme which is secreted when the microorganism is exposed to some stress conditions, in particular to nitrogen starvation. Both enzymes are poorly characterized; Ferrara et al.[25] obtained a better endogenous amount of *Sc*_ASNaseII using the double mutant strain *Δure2Δdal80.* However, the posterior yield of *Sc*_ASNaseII heterologous expression in *Pichia pastoris* was 7-fold higher than in the mutant *S. cerevisiae*[26] and the protein has been successfully expressed and purified in its active form, using this host cell.[27] In this work, the intention was to analyze the expression of the *Sc*_ASNases, eukaryotic forms of the biopharmaceutical ASNase, by applying the well-characterized, simple, fast and cheap host heterologous *E. coli* expression system. In order to access this system capacity, a bioinformatics analysis was conducted to evaluate both enzymes requirements as for its post-translational modifications in the native host, followed by the expression of the enzymes and evaluation of their activities. Moreover, the Fast Protein Liquid Chromatography (FPLC) purification of *Sc*_ASNaseI was applied as a downstream methodology platform. Actually, the use of the FPLC purification in proteins has been previously explored,[28–30] thus being considered a well-established technique in different biotechnological industries.

2. Materials and methods

2.1. *E. coli* expression vector construction

In order to amplify the *ASP1* and *ASP3* genes, the genomic DNA of *S. cerevisiae* extracted with PureLink® Genomic DNA Purification Kit (Invitrogen®, Carlsbad, CA, USA) was used. Also, the *ASP3* synthetic gene with optimized codons to express protein in *E. coli* was purchased from GenScript Corporation. Primers to amplify the target yeast genes were commissioned to the company *Exxtend* (Paulínea, SP, Brazil) (sequences described in **Table 2.2.**). *Sc_ASNase* genes were cloned into expression vectors described in **Table 2.3..** Restriction enzymes *NdeI, BamHI* and *XhoI* were purchased from New England Biolabs (NEB, Ipswich, UK). T4 DNA ligase was obtained from Promega (Madison, WI, USA). The bacteria transformation was carried out by electroporation in a MicroPulser Electroporator (BioRad®, Hercules, CA, USA). Luria Bertani – L.B. (0.5% NaCl, 0.5% yeast extract, and 1% triptone) solid medium (2% agar added) with added carbenicillin (50 $\mu g.\mu L^{-1}$) was used to select transformants which contain pET15b or pET22b vectors or added of kanamycin (15 $\mu g.\mu L^{-1}$) to select transformants with pET28a+SUMO construction. The recovery of the plasmids from bacteria was performed using a QIAprep Spin Miniprep Kit (Qiagen®, Hilden, Germany), according to the manufacturer's instructions. The correct insert of *Sc_ASNase* genes into the pET vectors were confirmed by DNA sequencing, for all expression vectors described in **Table 2.3.**

Table 2.2. Sequence of primers used to carry out the constructions of the *Sc*_ASNases overexpression vectors.

Primer name	***Sequence (5'→3')***	***Restriction enzyme site***
ASP1-fw	GGGAATTCCATATGAAAAGCGATTCAGTTGAAATCA	*NdeI*
ASP1-rv	CGCGGATCCTCACCACCATAGAC	*BamHI*
ASP3-1-fw	GGGAATTCCATATGAGATCTTTAAATACCC	*NdeI*
ASP3-26-fw	CGGGATCCGAAGAGAAGAATTCTTC	*BamHI*
ASP3-32-fw	GGGAATTCCATATGTTGCCATCAATCAAAATTTTTGG	*NdeI*
ASP3-26opt-fw	GGGAATTCCATATGGAAGAAAAAAATAGCTC	*NdeI*
ASP3-BamHI-rv	CGGGATCCTTAACCACCGTAGACG	*BamHI*
ASP3-XhoI –rv	CCGCTCGAGACCACCGTAG	*XhoI*
ASP3-opt-rv	CATTGGATCCTCAACCGCC	*BamHI*

Table 2.3. Description of the primers combination, type of DNA templates and expression vectors used in this work.

Forward primer	***Reverse Primer***	***DNA template***	***Vector***	***Final construction***
ASP1-fw	ASP1-rv	*S. cerevisiae* genomic DNA	pET15b	ASP1+pET15b
ASP3-1-fw	ASP3-BamHI-rv	*S. cerevisiae* genomic DNA	pET15b	ASP3_1-362+pET15b[A]
ASP3-32-fw	ASP3-BamHI-rv	*S. cerevisiae* genomic DNA	pET15b	ASP3_32-362+pET15b[B]
ASP3-26-fw	ASP3-XhoI –rv	*S. cerevisiae* genomic DNA	pET22b	ASP3_26-362+pET22b[C]
ASP3-26opt-fw	ASP3-opt-rv	*ASP3* optimized gene	pET15b	ASP3opt_26-362_pET15b[D]
ASP3-26-fw	ASP3-XhoI –rv	*S. cerevisiae* genomic DNA	pET28b+SUMO	ASP3_26-362+ pET28b+SUMO[E]

[A] Complete *Sc*_ASNaseII fused with N-terminal His_6-tag and expressed in cytoplasm in *E. coli.*

[B] *Sc*_ASNaseII without the first 32 amino acids – sequence of protein that aligns with bacterial *Ec*_ASNaseII- fused with N-terminal His_6-tag and expressed in cytoplasm in *E. coli.*

[C] Mature *Sc*_ASNaseII without the 26 first amino acids involved in the intermembrane signalling secretion in yeast *S. cerevisiae.* Protein fused with C-terminal His_6-tag and expressed in periplasmic space in *E. coli.*

[D] Mature *Sc*_ASNaseII without the 26 first amino acids involved in the intermembrane signalling secretion in yeast *S. cerevisiae.* The gene was synthesised with optimal codons to express in *E. coli;* expressed with N-terminal His_6-tag and in cytoplasm.

[E] Mature *Sc*_ASNaseII without the 26 first amino acids involved in the intermembrane signalling secretion in yeast *S. cerevisiae* fused with N-terminal high solubilizing protein SUMO, expressed in cytoplasm.

2.2. Heterologous expression of *Sc*_ASNaseI

The *E. coli* BL21 (DE3) strain was grown in LB liquid media, supplemented with the appropriate antibiotics, at 37°C until OD_{600nm} = 0.6-0.7. When the bacteria were in the log-phase, 1 mM of isopropylthio-β-D-galactoside (IPTG) was added, and the solution was incubated for 3 h at 37°C to induce the transcription and, consequently, to allow the production of *Sc*_ASNaseI. The sample pre-treatment was conducted by a chemical lysis procedure; herein cell pellets from genetically transformed *E. coli* BL21 (DE3) were suspended in 10 mL of BugBuster Master Mix (Merck-Millipore™, Billerica, MA, USA) *per* g of cell, mixed gently for 20 min and centrifuged at 16,000 x *g* for 20 min at 4°C; the pellet was discarded and the supernatant was subjected to vacuum filter membrane (0.45 µm, Merck-Millipore); to the filtered sample, the final concentration of 20 mM imidazole was added.

The affinity chromatography was performed on a FPLC™ System (ÄKTA purifier, GE Healthcare) using a Ni^{2+}-charged, 5 mL HiTrap IMAC FF column (GE Healthcare). A linear gradient, running from 0-500 mM of imidazole at 5.0 $mL.min^{-1}$ was carried in order to be possible to identify the lowest imidazole concentration of the elution buffer required to extract the highest amount of the purified *Sc*_ASNaseI. This concentration range was further used in an imidazole gradient step, in which two-step concentrations of imidazole (160 and 272 mM) were applied. The initial sample volume applied was 5.0 mL. A binding buffer (20 mM sodium phosphate buffer at pH 8.0 and 500 mM NaCl) and an elution buffer (20 mM sodium phosphate buffer at pH 8.0, 500 mM NaCl and 500 mM imidazole) were used in the purification process. The samples were previously centrifuged 4,000 x *g* for 20 min at 4°C and desalted through an exclusion chromatography step in a PD-10 column (GE Healthcare Life Sciences) with Tris-HCl buffer (20 mM) at pH 8.6.

2.3. Screening of conditions for *Sc*_ASNaseII expression

The *E. coli* strains (**Table A.1 at Appendix A**) were genetically transformed with the chosen construction containing the *ASP3* gene (**Table 2.3**). The screening of conditions for *Sc*_ASNaseII protein expression was carried out in 10 mL of LB medium plus the selective antibiotic medium, starting with a cell optical density of OD_{600nm} = 0.2, at 37°C and 180 rpm until a cell density of OD_{600nm} = 0.6-0.7. At this point, an IPTG solution was added at the described concentrations (0.01, 0.1, 0.5 and 1.0 mM) and incubated for 3 h at 37°C or overnight at 20°C to induce the production of *Sc*_ASNaseII using the conditions, vectors and gene combinations described in **Table A.2 at Appendix A**. At the end of this procedure, the cells were pelleted, the supernatant discarded and 1.5 mL of BugBuster Master Mix (Merck-Millipore) was added, gently mixed for 20 min and centrifuged at 16,000 x *g* for 20 min. The pellet containing the cellular debris and inclusion bodies (containing insoluble proteins), was separated from the supernatant (with the soluble proteins) and both were analyzed by SDS-PAGE 12%, under reducing conditions, in accordance with the Laemmli' method[31]. The electrophoresis was performed at 120 V using a vertical BioRad® system. The protein markers of different molecular weights were acquired from BioRad®. The volume of the samples added to the gel was 10 µL with a protein concentration ranging from 0.01 to 3 $mg.mL^{-1}$. The gels

were silver stained for the protein bands detection, using the Silver Staining Kit (Amersham Pharmacia Biotech®) and following the manufacturer's instructions.

2.4. Nessler activity assay and purification parameters calculation

The determination of the enzymatic activity was performed by the Nessler activity assay (expressed in $U.mL^{-1}$).[32] The sample volume of 0.1 mL was incubated at 37°C for 30 min in Tris-HCl buffer (50 mM, pH 8.6) with L-asparagine (9 mM). Then, the reaction was stopped with the addition of trichloroacetic acid (TCA). The Nessler reagent (Merck) was mixed by inversion for 1 min and then the reactions were measured in a microplate reader at λ_{436nm} (Spectramax Plus384, Molecular Devices). A standard curve was prepared using ammonium sulfate. In order to remove the possible interferences of quantification, two blanks composed by Tris buffer + L-asparagine + TCA were made for each sample. Moreover, at least three samples of each enzymatic activity measurement were prepared, being the results described, the average of the three replicas.

The total protein concentration was measured through absorbance assay, measuring the absorbance at λ_{280nm}, by UV-Vis spectroscopy. A calibration curve with bovine serum albumin (BSA) (lyophilized powder, ≥ 96 wt%, Sigma-Aldrich, St. Louis, MO, USA) was used to determine the protein concentration in each sample.

2.5. Computational analysis of recombinant *Sc*_ASNases

The possible N-glycosylation sites were predicted using NetNGlyc 1.0 program.[33] The presence and location of signal peptide cleavage sites in the amino acid sequence was determined using the SignalP 4.1 program.[34] The method incorporates a prediction of cleavage sites and a signal peptide/non-signal peptide prediction based on a combination of several artificial neural networks and hidden Markov models.

3. Results and discussion

3.1. Bioinformatics analysis of *Sc*_ASNases

A computational analysis of the *Sc*_ASNases using bioinformatics tools was carried out. This analysis included the prediction of glycosylation sites using sequence information (NetNGlyc 1.0) and the presence, prediction and location of signal peptide cleavage sites in the ASNase amino acid sequences (SignalP 4.1).

The bioinformatics results obtained predicted that the *Sc*_ASNaseI could be expressed in its active form in *E. coli*, despite its prokaryotic expression nature. These data (NetNGlyc 1.0 and SignalP 4.1) resulted in three possible glycosylation sites (**Fig. 2.1.A**), even in the absence of a signal peptide (**Fig. 2.2.A**). This observation suggests that the glycosylation, if present in its native host, is not essential for the enzyme activity, which is supported by the high value of the enzyme specific activity (*SA*) found for the purified *Sc*_ASNaseI (see below). This is an important result, since *E. coli* is a robust expression system, largely adopted by biopharmaceutical companies due its high titers outcomes.

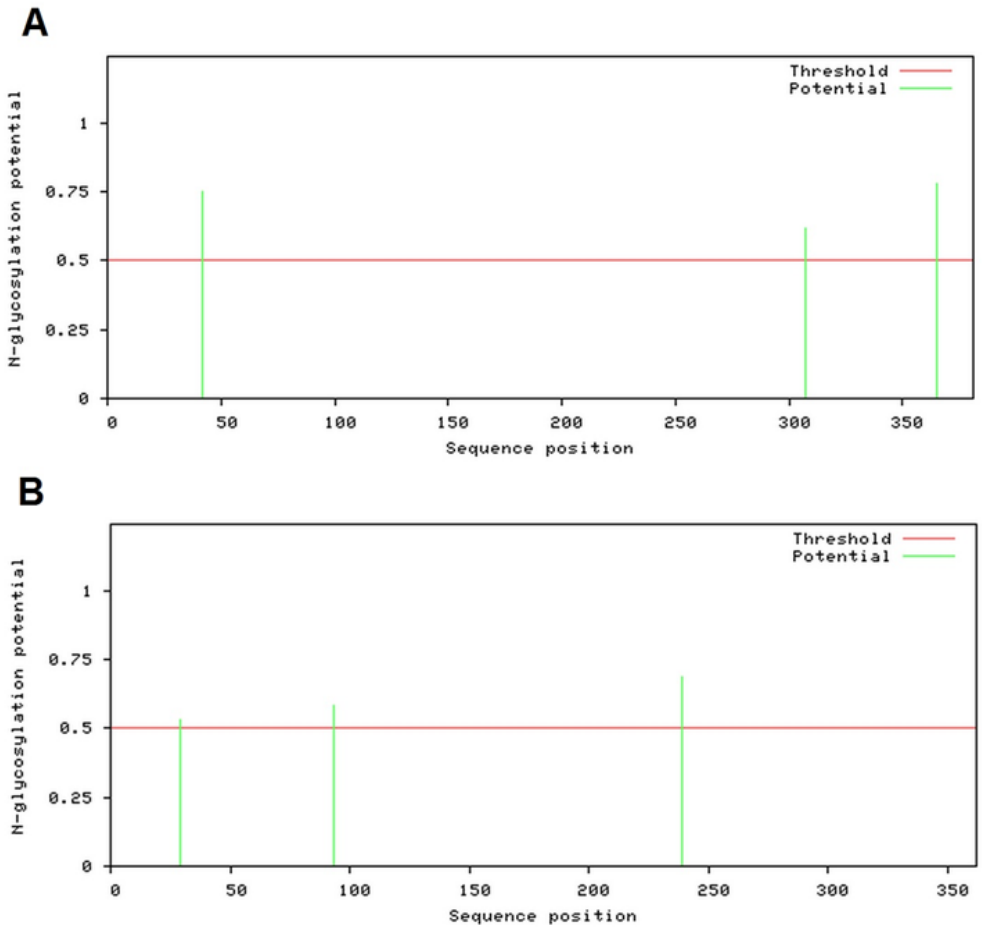

Fig. 2.1. Prediction results of N-glycosylation in the *Sc*_ASNaseI **(A)** and *Sc*_ASNaseII **(B)**, using the NetNGlyc 1.0 software. The sequence position represents the protein amino-acids position. The graph depicts the possible sites of N-glycosylation in the *Sc*_ASNases sequence (- blue lines), represented by the blue bars that rise vertically and pass the program threshold (- red line).

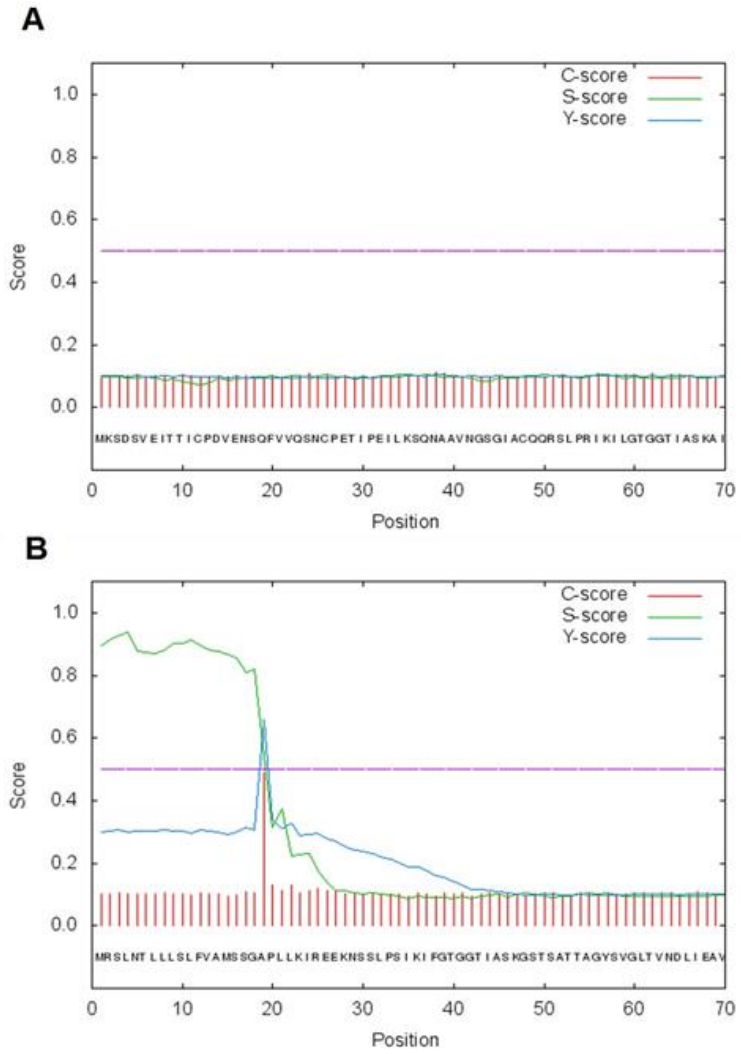

Fig. 2.2. Presence and location predictions of signal peptide and signal peptide cleavage sites in the *Sc*_ASNaseI **(A)** and *Sc*_ASNaseII **(B)** sequences by the SignalP-4.1 software. C-score represents the raw cleavage site score generated by the software. S-score: signal peptide score generated by the software. Y-score: combined cleavage site score generated by the software. If a signal peptide cleavage site is predicted, a C-score above the threshold (dashed purple line) would be present for some of the amino-acids. In our specific case, a signal peptide cleavage site and signal peptide itself is not predicted.

In contrast, *Sc*_ASNaseII presents 3 possible glycosylation sites (**Fig. 2.1.B**) and a signal peptide to direct this protein to the endoplasmic reticulum (**Fig. 2.2.B**); therefore, it is highly probable that this protein undergoes glycosylation. In fact, endogenously produced *Sc*_ASNaseII was observed with a high molecular weight due to hypermannosylation.[35] Moreover, Castro-Girão et al.[27] have described that heterologous produced *Sc*_ASNaseII produced by *P. pastoris* undergoes glycosylation, since after the purification process, two bands were observed by electrophoresis, which were then turned into one, just after treatment of *Sc*_ASNaseII with PNGase F (a

deglycosylation protein). In addition, as previously discussed, these authors observed the specific activity of *Sc*_ASNaseII produced by *P. pastoris* in the soluble fraction. Summing up, glycosylation seems to play an essential role for this enzyme activity and a prokaryotic system might be inappropriate to produce *Sc*_ASNaseII.

3.2. Expression and purification of *Sc*_ASNaseI

Recombinant protein expression in industrial scale demands careful evaluation of all process production steps. The choice of an appropriate host lies as a major step to this goal, moreover in the production of biopharmaceuticals. The proper protein folding, activity, purity and yield are dependent on the host ability to translate, fold and keep high amounts of the desirable protein in its soluble form. Sajitha et al.[24] successfully expressed the ASNase from *E. coli* into the eukaryotic host *P. pastoris*. The authors obtained a soluble and active ASNase in the supernatant and speculate that this protein might undergo eukaryotic glycosylation conferring more stability to the protein and fewer side effects. In an attempt to obtain a cost effective, fast and efficient *Sc*_ASNase expression system, the gene *ASP1* was cloned into pET15b between *NdeI* and *BamHI* restriction sites, which results in a *Sc*_ASNaseI N-terminal His-tag fusion protein. The native protein is predicted to present a molecular weight of 41,385.6 Da, but the recombinant protein with His-tag and thrombin recognition site, presents a molecular weight of 43,139.0 Da. As depicted in **Fig. 2.3**., the prokaryotic *E. coli* cell was able to express high amounts of soluble *Sc*_ASNaseI. However, the protein obtained in this first test presented a considerable number of contaminant proteins, especially in the fraction of higher *Sc*_ASNaseI concentration (**Fig. 2.3**., lane 6).

Taking into account that the administration of this biopharmaceutical (ASNase) will be potentially carried by its direct injection into the human blood, the high purity of ASNase is certainly a crucial demand for it to be considered as a promising therapeutic alternative. In this sense, an FPLC purification was performed considering two main tasks; the first one using a linear gradient of imidazole in order to identify the lowest imidazole concentration able to elute the highest amount of Sc_ASNaseI, and the second one using the optimized imidazole concentration to develop a purification protocol in which the same buffer was used to perform a two-step purification procedure.

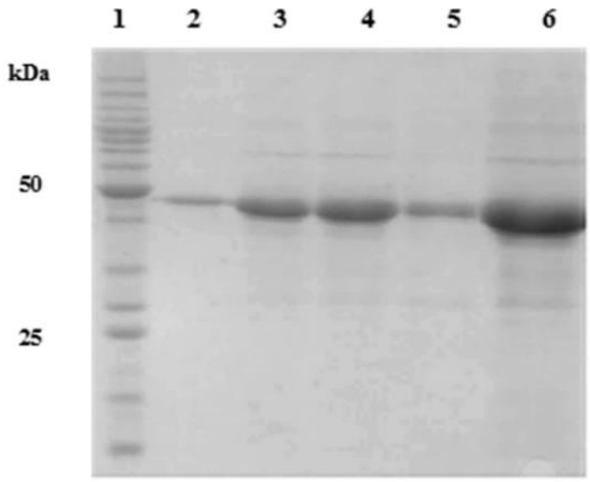

Fig. 2.3. SDS-PAGE stained with Comassie-Blue representing the first attempt of *Sc*_ASNaseI purification by IMAC. In the left are indicated the molecular protein weights of the highlight bands of the BenchMark protein ladder (lane 1). Lanes 2-6: sequential eluted *Sc*_ASNaseI from a nickel column purification.

Both approaches were applied and from the general results (**Table 2.4.**), it was concluded that, while fractions 4-5 contain the expression of host contaminant proteins resulting in a very low specific *Sc*_ASNaseI activity (0.02 ± 0.01 $U.mg^{-1}$), the purified fractions 20-31 exhibited the highest specific activity (6.61 ± 0.08 $U.mg^{-1}$). Considering the results obtained, the imidazole concentrations chosen for the stepwise purification were 160 and 272 mM, which correspond to fractions 23 and 30, respectively. **Table 2.5.** summarizes the results obtained, correlating the fractions collected with the respective *Sc*_ASNaseI activity results, along with the protein concentration, enzymatic activity (*EA*), specific activity (*SA*), purification factor (*PF*), and recovery (%*Rec*) parameters. From the set of results obtained (**Fig. 2.4.** and **Table 2.5**.), we conclude that the most pure fraction exhibited a *SA* of 110.1 $U.mg^{-1}$ comparable to the commercially available ASNase formulations, like Erwinaze® (from *E. chrysanthemi*) and Elspar® (from recombinant *E. coli*) containing 225 $U.mg^{-1}$ (information displayed in the Product Datasheet - Active Asparaginase full-length protein ab73439). In what concerns the application of the purification step (FPLC purification), even higher specific activities would be reached, these similar to the values described for the commercial ASNase. Moreover, not only the enzyme activity is maintained but also the yields of purification of ASNase obtained were considerable (enzyme yield *circa* 1,001 $U.g\ cell^{-1}$). It should be highlighted that *Sc*_ASNaseI was remarkably purified at 15 wt% of total cell dry weight,

which is a sizable piece of total cellular protein. Taking into account the results obtained and the demands of future applications, further optimization studies should be performed to the FPLC purification protocol, namely evaluating the effect of the fraction volume, pump pressure, initial volume injected, elution and binding buffer formulations in order to further improve the purifying yields. Other authors have reported some attempts to purify *Sc*_ASNaseI in the same line of work, namely Dunlop and collaborators.[35] These authors used several steps of purification to obtain the endogenous *Sc*_ASNaseI from *S. cerevisiae*; being the best specific activity found around 5 $U.mg^{-1}$, which is almost 20-fold lower than the obtained in the present work. In addition, the same authors commented on the difficulty to separate both isoforms endogenously expressed *Sc*_ASNaseI from *Sc*_ASNaseII,[35] a difficulty surpassed in this work by the use of an heterologous strategy and just one chromatographic purification step, which allowed the purification of *Sc*_ASNaseI resulting in a much higher specific activity than that obtained from endogenous expression. For a method/process to be of industrial relevance, the polishing of the target macromolecule being produced and purified is a crucial step. In this case, and considering the potential application of the biopharmaceutical in the ALL treatment, the elimination of the $(His)_6$-tag from the biopharmaceutical[36] can be achieved through the use of the aminopeptidase dipeptidyl peptidase I (DPPI), either alone or in combination with glutamine cyclotransferase (GCT) and pyroglutamyl aminopeptidase (PGAP). In both cases, the $(His)_6$-tag is cleaved off by DPPI, which catalyses a stepwise excision of a wide range of dipeptides from the N-terminus of a peptide chain.[37] Other major concern considering the potential use of the biopharmaceutical in the ALL treatment is related to metal leaching from the column during purification.[38] Although additional costs may be inserted for validation, new technologies have been developed in a lab scale in this context, in particular the treatment of the final sample with EDTA (GE Healthcare's excel[39] and Roche's cOmplete[40]). Albeit, large-scale application of this system still needs to be fully evaluated.

Table 2.4. FPLC purification with an imidazole linear gradient (0-500 mM) step at 5.0 mL.min^{-1}. Fractions eluted with *Sc*_ASNaseI activity are shown, along with the protein concentration (mg.mL^{-1}), enzymatic activity (U.mL^{-1}) and specific activity (U.mg^{-1}) values.

Sample	***Protein concentration*** (mg.mL^{-1})	***EA*** (U.mL^{-1})	***SA*** (U.mg^{-1})
Fractions 4-5	3.52 ± 0.03	0.06 ± 0.01	0.02 ± 0.01
Fractions 14-18	0.05 ± 0.01	0.03 ± 0.01	0.49 ± 0.01
Fractions 20-31	0.02 ± 0.01	0.11 ± 0.01	6.61 ± 0.08

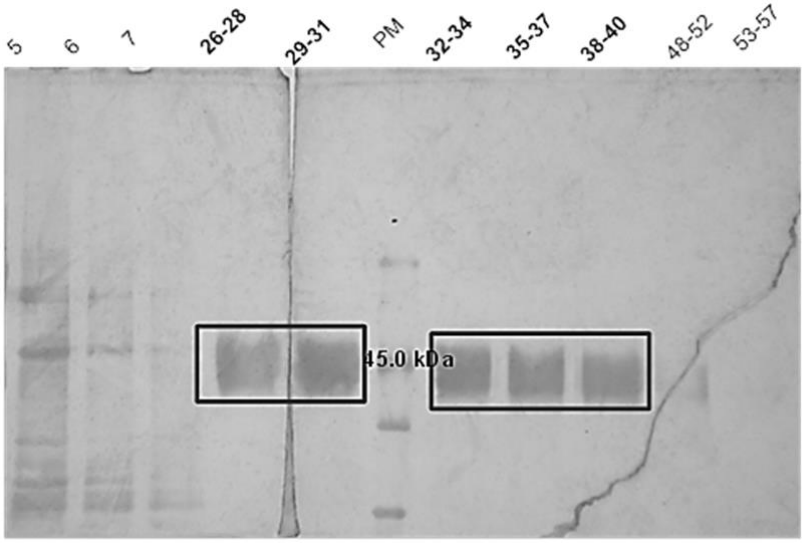

Fig. 2.4. Polyacrylamide gel electrophoresis combined with silver staining, showing the purified samples from the two-step FPLC purification. The brown box stresses the (His)6-tagged ASNase bands (~45.0 kDa). The different lanes represented the eluted fractions (5, 6 and 7: washout unbound proteins; 26-40: purified Sc_ASNase I and 48-57: non-purified Sc_ASNase I) and PM means Unstained Protein Molecular weight marker.

Table 2.5. FPLC purification with the two-step concentration methodology of the initial imidazole concentration (160 and 272 mM), applied at 5.0 mL.min^{-1}. Fractions eluted with *Sc*_ASNaseI activity are shown, along with protein concentration (mg.mL^{-1}), enzymatic activity (U.mL^{-1}), specific activity (U.mg^{-1}), purification factor (fold) and recovery (%) parameters.

Sample	*Protein concentration* (mg.mL^{-1})	*EA* (U.mL^{-1})	*SA* (U.mg^{-1})	*PF (fold)*	*Recovery activity (%)*
Cell extract	0.38 ± 0.01	2.50 ± 0.01	6.52 ± 0.01	1.00	100.00
Stepwise FPLC purification (Fractions 38-42)	0.02 ± 0.01	2.017 ± 0.01	110.06 ± 0.34	16.88	40.50

3.3. Expression and purification of *Sc*_ASNaseII

Initially, the same expression and purification procedures described for *Sc*_ASNaseI were applied to express *Sc*_ASNaseII. **Fig. 2.5.** depicts the high level of *Sc*_ASNaseII expression in the *E. coli* host cells. However, the protein was completely concentrated in the insoluble fraction of the cell lysate (**Fig. 2.5.**, lane 2). From the results of the lower growth temperature test, the conclusion was that this test was not improving the insoluble fraction presence as suggested elsewhere.[41] In this context, several growth conditions including temperature of induction, concentration of (the inductor) IPTG and the time of induction were tested, since the optimization of these parameters is being recognized as a good strategy to overexpress soluble recombinant proteins in bacterial cells (as reviewed by Papaneophytou and Kontopidis[42]). None of these conditions were able to produce soluble *Sc*_ASNaseII in the *E. coli* host cell. It was hypothesized that the native gene from the amino-acids 1 to 362, *i.e.* with the yeast periplasmic signal, should enhance the solubility of the protein; however, this expression also resulted in an insoluble protein. Then, several genetic attempts to obtain soluble *Sc*_ASNaseII were carried out, namely (i) the synthetic *ASP3* gene was expressed with optimized codons to the *E. coli* host, (ii) by changing the expression vector modifying the position of His-tag from the N- to C-terminal, and (iii) constructing a vector that expresses *Sc*_ASNaseII in fusion with the SUMO protein (a highly soluble protein). Moreover, eight different types of *E. coli* strains were also tested (**Table A.1 in Appendix A**). In conclusion, 93 different

expression conditions (described in **Table A.2 in Appendix A**) were tested without any success in the production of soluble *Sc*_ASNaseII. The only condition that resulted in low amounts of soluble *Sc*_ASNaseII (described briefly in **Fig. 2.6.**) produced a protein with a low specific activity (3.8 $U.mg^{-1}$ of protein) after the Immobilized Metal ion Affinity Chromatography (IMAC) purification step. These results are in accordance with the bioinformatics analysis, since *Sc*_ASNaseII was predicted to be glycosylated in the native host. The absence of glycosylation, caused by *E. coli* lack of glycosylation machinery, seems to be a key factor in the *Sc*_ASNaseII activity. Dunlop et al.[35] also purified *Sc*_ASNaseII endogenously produced in *S. cerevisiae;* the authors obtained a maximum *SA* of 60 $U.mg^{-1}$ of protein. However, this protein was characterized as hypermannosylated, which means that endogenous obtained *Sc*_ASNaseII is highly immunogenic and cannot be used as a biopharmaceutical from this source, because human immune system cells possess a receptor for mannose.[43] In addition, *Sc*_ASNaseII has been described as possessing 204 $U.mg^{-1}$ of protein, when expressed in *P. pastoris* host, a 3-fold higher activity than the endogenous source.[27] From the main results, it is suggested that, in contrast with *Sc*_ASNaseI, which is soluble and active when expressed in *E. coli* host cells, the *Sc*_ASNaseII cannot be properly produced in this host cell, independent of the growth conditions used.

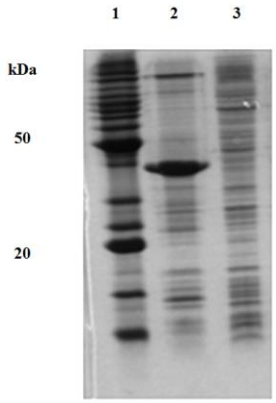

Fig. 2.5. SDS-PAGE stained with Comassie-blue representing the expression of *Sc*_ASNaseII in the insoluble fraction of the *E. coli* cell lysateThe construction pET15b+ASP3_32-362 expressed in the bacterial host strain CodonPlus (DE3) (Merck™); cells were pre inoculated in LB media overnight at a 37ºC and 250 rpm. The inoculum was initially diluted to OD_{600nm} 0.2 in fresh culture media, grown at the same conditions until OD_{600nm} 0.4 when 0.1mM of IPTG was added and culture temperature was changed to 12ºC. This *Sc*_ASNaseII induction was performed for 24 hours. In this expression vector construction, the protein starts at the amino-acid residue number 32, without the predicted yeast periplasmic signal. - Lane 1: BenchMark™ Protein Ladder; Lane 2: insoluble fraction pelleted after clarification of the cell lysate by centrifugation. Lane 3: supernatant of cell lysate, representing the protein soluble fraction.

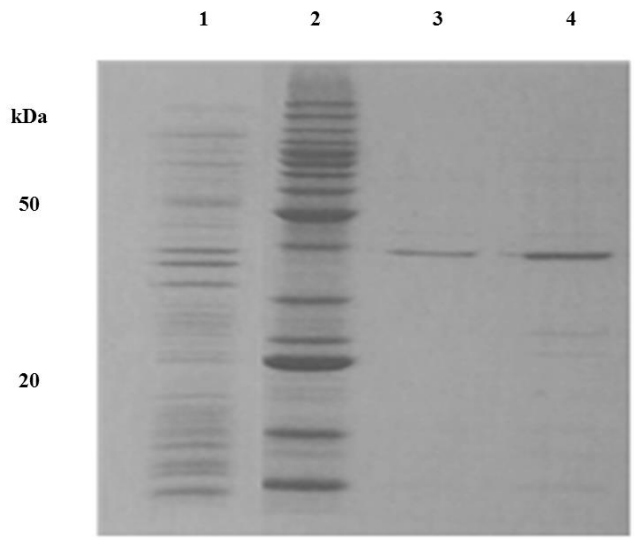

Fig. 2.6. SDS-PAGE stained with Comassie-blue representing the expression of *Sc*_ASNaseII in the soluble fraction of the *E. coli* cell lysate and the specific activity of this protein. Fractions of nickel affinity purification. Lane 1: Total supernatant after cell lysis; Lane 2: BenchMark™ Protein Ladder; Lanes 3 and 4: Fractions from column elution with 500 mM of imidazole.

4. Conclusions

The optimized two-step FPLC purification method allowed the successful purification of *Sc*_ASNaseI from *S. cerevisiae* expressed in *E. coli* BL21 (DE3). Moreover, the bioinformatics analysis together with the enzyme activity results obtained suggested that N-glycosylation is not essential for *Sc*_ASNaseI activity. Antitumor activity and biochemical characterization of *Sc*_ASNaseI are being now conducted to evaluate the potential of this enzyme in acute lymphocytic leukemia treatment. By contrast, the results suggest that *Sc*_ASNaseII requires glycosylation, and therefore a eukaryotic expression host system to produce soluble and active enzyme.

References

1. Kidd, J. G. Regression of transplanted lymphomas induced in vivo by means of normal guinea pig serum, I: course of transplanted cancers of various kinds in mice and rats given guinea pig serum, horse serum, or rabbit serum. *J Exp Med.* **98**,565–582 (1953).
2. Broome, J. D. Studies on the mechanism of tumor inhibition by L-asparaginase. *J Exp Med*. **127**, 1055–1072 (1968).
3. Wade, H. E., Robinson, H. K. & Phillips, B. W. Asparaginase and glutaminase activities of bacteria. *J Gen Microbiol.*; **69**, 299–312 (1971).
4. Piatkowska-Jakubas, B., Krawczyk-Kuliś, M., Giebel, S., Adamczyk-Cioch, M., Czyz, A., Lech Marańda, E., Paluszewska, M., Pałynyczko, G., Piszcz, J., Hołowiecki, J. & Polish Adult Leukemia Group. Use of L-asparaginase in acute lymphoblastic leukemia: recommendations of the Polish Adult Leukemia Group. *Pol Arch Med Wewn.* **118**, 664–669 (2008).
5. Pieters, R., Hunger, S. P., Boos, J., Rizzari, C., Silverman, L., Baruchel, A., Goekbuget, N., Schrappe, M. & Pui, C. H. L-asparaginase treatment in acute lymphoblastic leukemia: a focus on *Erwinia* asparaginase. *Cancer*. **117**, 238–249 (2011).
6. Rizzari, C., Conter, V., Starý, J., Colombini, A., Moericke, A. & Schrappe, M. Optimizing asparaginase therapy for acute lymphoblastic leukemia. *Curr Opin Oncol*. **25**, S1–S9 (2013).
7. Takahashi, H., Koh, K., Kato, M., Kishimoto, H., Oguma, E. & Hanada, R. Acute myeloid leukemia with mediastinal myeloid sarcoma refractory to acute myeloid leukemia therapy but responsive to L-asparaginase. *Int J Hematol*. **96**, 136–140 (2012).
8. Beard, M. E., Crowther, D., Galton, D. A., Guyer, R. J., Fairley, G. H., Kay, H. E., Knapton, P. J., Malpas, J. S. & Scott R. B. L-asparaginase in treatment of acute leukaemia and lymphosarcoma. *Br Med J*. **1**, 191–195 (1970).
9. Pui, C. H., Relling, M. V. & Downing, J. R. Acute lymphoblastic leukemia. *N Eng J Med*. **350**, 1535–1548 (2004).
10. Pui, C. H., Robison, L. L. & Look, A. T. Acute lymphoblastic leukemia. *Lancet*. **371**, 1030–1043 (2008).

11. Narta, U. K., Kanwar, S. S. & Azmi, W. Pharmacological and clinical evaluation of L-asparaginase in the treatment of leukemia. *Cr Rev Oncol-Hem*. **61**, 208–221 (2007).
12. Guo, Q. L., Wu, M. S. & Chen, Z. Comparison of antitumor effect of recombinant L-asparaginase with wild type one *in vitro* and *in vivo*. *Acta Pharm Sinic*. **23**, 946–951 (2002).
13. Soares, A. L., Guimarães, G. M., Polakiewicz, B., Pitombo, R. N. D. M. & Abrahão-Neto, J. Effects of polyethylene glycol attachment on physicochemical and biological stability of *E. coli* L-asparaginase. *Int J Pharm*. **237**, 163–170 (2002).
14. EMA, European Medicines Agency; 2016. http://www.ema.europa.eu/ema/index.jsp?curl=pages/medicines/human/medicines/002661/human_med_001954.jsp&mid=WC0b01ac058001d124
15. Cortijo-Cascajares, S., Jimínez-Cerezo, M. J. & Tejada, A. H. D. Revisión de las reacciones de hipersensibilidad a antineoplásicos. *Farm Hosp.*, **36**,148–158 (2012).
16. Pieters, R., Appel, I., Kuehnel, H. J., Tetzlaff-Fohr, I., Pichlmeier, U., van der Vaart, I., Visser, E. & Stigter, R. Pharmacokinetics, pharmacodynamics, efficacy, and safety of a new recombinant asparaginase preparation in children with previously untreated acute lymphoblastic leukemia: a randomized phase 2 clinical trial. *Blood*. **112**, 4832–4838 (2008).
17. Billett, A. L., Carls, A., Gelber, R. D. & Sallan, S. E. Allergic reactions to *Erwinia* asparaginase in children with acute lymphoblastic leukemia who had previous allergic reactions to *Escherichia coli* asparaginase. *Cancer*. **70**, 201–206 (1992).
18. Knoderer, H. M., Robarge, J. & Flockhart, D. A. Predicting asparaginase-associated pancreatitis. *Pediatr Blood Cancer*. **49**, 634–639 (2007).
19. Raja, R. A., Schmiegelow, K. & Frandsen, T. L. Asparaginase-associated pancreatitis in children. *Brit J Haematol*. **159**, 18–27 (2012).
20. Schleis, S. E., Rizzo, S. A, Phillips, J. C. & LeBlanc, A. K. Asparaginase-associated pancreatitis in a dog. *Can Vet J*. **52**, 1009–1012 (2011).
21. Van den Berg, H. Asparaginase revisited. *Leukemia Lymphoma*. **52**, 168–178 (2011).
22. Fu, C. H. & Sakamoto, K. M. PEG-asparaginase. *Expert Opin Pharmaco*. **8**, 1977–1984 (2007).

23. Keating, M. J., Holmes, R., Lerner, S. & Ho, D. H. L-asparaginase and PEG asparaginase - past, present, and future. *Leukemia Lymphoma*. **10**, 153–157 (1993).

24. Sajitha, S., Vidya, J., Varsha, K., Binod, P. & Pandey, A. Cloning and expression of l-asparaginase from *E. coli* in eukaryotic expression system. *Biochem Eng J*. **102**,14-17 (2015).

25. Ferrara, M. A., Mattoso, J. M. V., Bon, E. P. S. & Pereira Jr, N. Kinetics of Asparaginase II fermentation in *Saccharomyces cerevisiae ure2dal80* mutant - Effect of nitrogen nutrition and pH. *Appl Biochem Biotech*. **113–116**,299–305 (2004).

26. Ferrara, M. A., Severino, N. M. B., Mansure, J. J., Martins, A. S., Oliveira, E. M. M., Siani, A. C., Pereira, N., Torres, F. A. G. & Bon, E. P. S. Asparaginase production by a recombinant *Pichia pastoris* strain harbouring *Saccharomyces cerevisiae* ASP3 gene. *Enzyme Microb Tech*. **39**, 1457–1463 (2006).

27. Castro-Girão, L. F., Rocha, S. L. G., Teixeira, R. S., Ferrara, M. A., Perales, J. & Bon, E. P. S. Purification and characterization of asparaginase II from *Saccharomyces cerevisiae* cloned in *Pichia pastoris*: a study on a possible anti-leukemic drug, *BMC Proceedings*. **8**, 78 (2014).

28. Dorrestein, E., Ferreira, R. B., Laureano, O. & Teixeira, A. R. Electrophoretic and FPLC analysis of soluble proteins in four Portuguese wines. *Am J Enol Vitic*. **46**, 235–242 (1995).

29. Sharma, A., Ng, T. B., Wong, J. H. & Lin, P. Purification and characterization of a lectin from *Phaseolus vulgaris cv*. (Anasazi beans). *J Biomed Biotechnol*. 2009; doi:10.1155/2009/929568.

30. Pattenden, L. K. & Thomas, W. G. Amylose affinity chromatography of maltose-binding protein: purification by both native and novel matrix-assisted dialysis refolding methods. *Methods Mol Biol*. **421**, 169–189 (2008).

31. Laemmli, U. K. Cleavage of structural proteins during the assembly of the head of bacteriophage T4, *Nature*. **227**, 680–685 (1970).

32. Imada, A., Igarasi, S., Nakahama, K. & Isono, M. Asparaginase and glutaminase activities of micro-organisms. *J Gen Microbiol*. **76**, 85–89 (1973).

33. Zielinska, D. F., Gnad, F., Schropp, K., Wiśniewski, J. R. & Mann, M. Mapping N-glycosylation sites across seven evolutionarily distant species reveals a divergent

substrate proteome despite a common core machinery. *Mol Cell*. **46**, 542–548 (2012).

34. Petersen, T. N., Brunak, S., von Heijne, G. & Nielsen, H. SignalP 4.0: discriminating signal peptides from transmembrane regions. *Nat Methods*. **8**,785–786 (2011).
35. Dunlop, P. C., Meyer, G. M., Ban, D. & Roon, R. J. Characterization of two forms of asparaginase in *Saccharomyces cerevisiae*. *J BiolChem.* **253**, 1297–1304 (1978).
36. Kinna, A., Tolner, B., Rota, E. M., Titchener-Hooker, N., Nesbeth, D. & Chester, K. IMAC capture of recombinant protein from unclarified mammalian cell feed streams. *Biotechnol Bioeng*. **113**, 130-140 (2016).
37. Pedersen, J., Lauritzen, C., Madsen, M. T. & Weis Dahl, S. Removal of N-terminal polyhistidine tags from recombinant proteins using engineered aminopeptidases. *Protein Expr. Purif.* **15**, 389–400 (1999).
38. Crowe, J., Döbeli, H., Gentz, R., Hochuli, E., Stüber, D. & Henco, K. 6xHis-Ni-NTA chromatography as a superior technique in recombinant protein expression/purification. *Methods Mol Biol.* **31**, 371–387 (1994).
39. Ni Sepharose excel - GE Healthcare Life Sciences; 2016 http://www.gelifesciences.com/webapp/wcs/stores/servlet/productById/en/GELifeSciences-br/17371202.
40. cOmplete His-Tag Purification Resin - Roche Life Sciences; 2016 www.sigmaaldrich.com/catalog/product/roche/cohisrro.
41. Vasina, J. A. & Baneyx, F. Expression of aggregation-prone recombinant proteins at low temperatures: a comparative study of the *Escherichia coli* cspA and tac Promoter systems. *Protein Expr Purif*. **9**, 211–218 (1997).
42. Papaneophytou, C. P. & Kontopidis, G. Statistical approaches to maximize recombinant protein expression in *Escherichia coli*: A general review. *Protein Expr Purif*. **94**, 22–32 (2014).
43. Lee, S. J., Evers, S., Roeder, D., Parlow, A. F., Risteli, J., Risteli, L., Lee, Y. C., Feizi, T., Langen, H. & Nussenzweig, M. C. Mannose receptor-mediated regulation of serum glycoprotein homeostasis. *Science*. **295**, 1898–1901 (2002).

2.2. *In situ* purification of periplasmatic L-asparaginase by aqueous two phase systems with ionic liquids (ILs) as adjuvants

Santos, J. H. P. M., Santos, J. C. F., Meneguetti, G. P., Rangel-Yagui, C. O., Coutinho, J. A. P., Vitolo, M., Ventura, S. P. M. & Pessoa, A. J. *Journal of Chemical Technology & Biotechnology*, 2018, **93**, 1871-1880.[3]

Abstract

Bacterial L-asparaginase is an important biopharmaceutical used in the treatment of acute lymphoblastic leukemia (ALL) and lymphosarcoma. Taking into account its main application in cancer therapy, the most important request for the L-asparaginase production is the need for a highly pure biopharmaceutical obtained in the final of the downstream process, which is considered as the crucial step in the production of this enzyme. In this ambit, this work proposes the use of polymer-salt aqueous two phase systems (ATPS) based on polyethylene glycol and citrate buffer, with ionic liquids (ILs) as adjuvants, combined with the permeabilization of cell membrane using n-dodecane and glycine for the *in-situ* purification of periplasmatic L-asparaginase from *Escherichia coli* (*E. coli*) cells. The process proposed was optimized in terms of polymer molecular weight, pH, tie-line length/mixture point, presence and nature of the adjuvant and its concentration. The results show that L-asparaginase preferentially partitions to the polymer-rich phase, due to hydrophobic interactions between both the PEG and enzyme. Remarkably, the addition of 5 wt% of 1-butyl-3-methylimidazolium methanesulfonate, $[C_4mim][CH_3SO_3]$ as adjuvant lead to high recoveries and purification factors, *i.e.* %*Rec*Top = 87.94 ± 0.03 (%) and *PF* = 20.09 ± 0.35, and a final specific activity *SA* = 3.61 ± 0.38 $U.mg^{-1}$ protein, from a crude enzyme extract with a *SA* = 0.18 ± 0.05 $U.mg^{-1}$ protein. Moreover, better results were achieved when a pre-purification step consisting of an ammonium sulfate precipitation was combined with the optimized ABS. It is here shown that the integration of pre-purification step with the ATPS further increased the specific activity and purification factor of this biopharmaceutical to *SA* = 22.01 ± 1.36 $U.mg^{-1}$ protein and *PF* = 173.8 ± 10.7, without compromising the enzyme structural integrity. Summing up, a novel integrated downstream process was successfully implemented for the *in-situ* purification of a high-cost biopharmaceutical from fermentation broth.

Keywords: Therapeutic enzyme; L-asparaginase, aqueous two-phase systems; ionic liquids as adjuvants; integrated *in-situ* purification process.

[3] Contributions: JHS acquired the experimental data regarding the purification assays, while JFS worked in the production of the enzyme. GM performed the *in silico* assays. JHS, JFS, GM, CY, JC, SV, MV, and AP interpreted the experimental data. SV and AP conceived and directed this work. The manuscript was mainly written by JS with significant contributions from the remaining authors.

1. Introduction

L-asparaginase, L-asparagine amidohydrolase, EC.3.5.1.1 (ASNase) is a biopharmaceutical produced mostly by *E.coli*[1,2] that has been widely studied as a therapeutic agent in the treatment of specific tumour types, including acute lymphoblastic leukemia (ALL)[3–5] in humans and canine lymphosarcoma.[6,7] ASNase was approved for medical use in the United States in 1978[8] and, since then it is on the World Health Organization's List of Essential Medicines.[9] The underlying principle behind the ASNase anti-cancer mechanism of action is the deprivation of the essential amino acid L-asparagine for leukemic cells, which require exogenous sources of this amino acid for their survival.[10] ASNase catalyses the conversion of L-asparagine to aspartic acid and ammonia.[2] Its commercial manufacture conventionally uses downstream processes such as unit chemical lysis,[11] protein precipitation,[12–15] centrifugation,[16] filtration,[13,17] fluidised bed chromatography,[11] and other chromatographic techniques[12,15,16,18–20] (*e.g.* ion-exchange, gel filtration and immobilized metal affinity chromatography - IMAC). Recently, new strategies were developed regarding the purification of ASNase, namely those based in Aqueous Two-Phase Extraction (ATPE) *via* Aqueous Two-Phase Systems (ATPS) and Aqueous Micellar Two-Phase Systems (AMTPS).[17,21] The *in situ* ATPE strategies are combining different cell disruption approaches with the use of ATPS, resulting in higher product yields and lower costs associated to the enzyme purification. Moreover, it can also increase the productivity of the downstream process[22–26] by the elimination of antagonists (including proteases or other product-degrading agents). Actually, through the differential partition behaviour of the target product and antagonists, or the so-called contaminants also present in the bulk after the cell disruption, the product hydrolysis/denaturation is also reduced.[17,27] Furthermore, the industrial scale-up in continuous flow of these integrated processes based in the combination of efficient cell disruption and ATPS is simpler and faster and more productive than the batch operations.[17,26,28]

In this ambit, the first AMTPS described for ASNase purification was composed of Triton X-100 and potassium phosphate (K_2HPO_4).[21] However, this system leads to enzyme inactivation by antagonists (*e.g.* proteases and carbohydrases), high ionic strength, and protein interactions with cell debris, resulting in product loss. Moreover, one of the

major drawbacks of AMTPS is the difficulty to remove the surfactant (approximately 15 w/v%) from the enzyme solution. In the same line, Zhu *et al.*[17] proposed ATPS and AMTPS composed by phosphate buffer (KH_2PO_4/K_2HPO_4) and polyethylene glycol (PEG) or poloxamers (poly(propylene glycol) block with poly(ethylene glycol), PEG-PPG-PEG). The purification factors obtained with these systems were quite low, from 0.75-3.37, probably due to the high salting-out ability of phosphate salts resulting in the proteins (target and contaminants) preferential partition to the polymer-rich phase. Moreover, this work was mainly focused in the application of AMTPS being the PEG/salt-based ATPS poorly optimized. Conditions, like PEG molecular weight (MW), tie-line length (*TLL*), pH and mixture point, normally resulting in big effects were completely neglected in this work. In addition, the phosphate buffer has great interference with the methods of ASNase quantification (Nessler[29] and aspartate hydroxamate[30] assays) used in this work, which is another factor explaining the lower values of purification obtained. Due to the low purification data obtained and the higher purity required to apply ASNase as a biopharmaceutical, it would be important to develop novel and more efficient *in situ* downstream integrated processes.

Ionic liquids (ILs) are salts in which the ions are poorly coordinated, which results in these compounds being liquid below 100°C.[31] Moreover, these liquid salts exhibit tunable physicochemical properties related to their *designer solvent* character, through the manipulation of a large range of cations and anions. Most ILs are soluble in water and have been used as phase forming compounds in ATPS.[32] Recently, ILs have been applied as additives in the ATPS formation, as adjuvants[33–35] and electrolytes[36,37] in polymer-based ATPS, showing outstanding results in the purification of biomolecules. In this way, the presence of ILs in small amounts was proved to potentiate significantly the purification performance of ATPS, when compared to the systems with no adjuvant.[33–35]

In this work, novel polymer-salt ATPS based on polyethylene glycol (PEG) and the biodegradable and nontoxic organic salt citrate buffer with ILs as adjuvants for the *in-situ* purification of periplasmatic ASNase from *Escherichia coli*, were investigated. The conditions, polymer molecular weight, pH, *TLL*/mixture point, presence and nature of adjuvant and its concentration, were extensively investigated to optimize the ATPS purification performance. For the most promising *in situ* ATPS, an additional step of pre-

purification consisting in the enzyme precipitation with ammonium sulfate was applied in order to further enhance the productivity and purification of ASNase. The integrated process of purification and isolation of ASNase will be proposed.

2. Materials and methods

2.1. Materials

The polyethylene oxide polymers, PEG 2000, 4000, 6000, 8000, as well as the potassium citrate, citric acid and ammonium sulphate (> 95 wt%) were purchased from Sigma-Aldrich (St. Louis, MO, USA). The ILs used in this work as adjuvants were 1-butyl-3-methylimidazolium chloride ([C_4mim]Cl), 1-butyl-3-methylimidazolium dimethyl phosphate ([C_4mim][DMP]), 1-butyl-3-methylimidazolium methanesulfonate ([C_4mim][CH_3SO_3]) and 1-butyl-3-methylimidazolium triflate [C_4mim][CF_3SO_3]. The ILs were purchased from Iolitec (Heilbronn, Deutschland), with purity > 97 wt%. The water content of ILs was measured and taken into account in the preparation of the ATPS. Ultrapure water by reverse-osmosis (Millipore Co. Ltd.) was used in all experiments. All chemicals used in upstream process of ASNase, and protein and activity assays were purchased from Sigma-Aldrich (St. Louis, MO, USA).

2.2. Preparation of crude enzyme extract

E. coli BL21 (DE3) (Novagen, WI, USA) harbouring vector (pET15b+ansB) and ampicillin resistance gene as selection marker was grown in Luria Bertani (LB) agar plate containing: tryptone (10 $g.L^{-1}$), yeast extract (5 $g.L^{-1}$), NaCl (10 $g.L^{-1}$), agar 15% w/v and ampicillin (100 $\mu g.mL^{-1}$) at pH 7.0; 37 °C for 24 h. Five isolated colonies were inoculated in 8 mL of LB (Difco, Detroit MI, USA) containing tryptone (10 $g.L^{-1}$), yeast extract (5 $g.L^{-1}$), NaCl (10 $g.L^{-1}$) and ampicillin (100 $\mu g.L^{-1}$); which was incubated in a shaker Excella® E24 (New Brunswick, New Jersey, USA), at 37 °C and 250 rpm for 8 h. For stock cultures, samples were withdrawn and glycerol was added to a final concentration of 15% (v/v) under sterile conditions and stored at - 80 °C. The inoculum was prepared from 0.25 mL of the stock culture in 25 mL of LB (1:10, medium volume:flask volume ratio), at 37 °C and 250 rpm for 12 h. Culture for periplasmatic ASNase production was prepared from 0.5 mL of the inoculum in 25 mL (1:10, medium volume:flask volume ratio) of modified LB (addition of 0.1 M of potassium phosphate buffer pH 7.0; 5.0 $g.L^{-1}$ of glucose; 0.5 $g.L^{-}$

^{1} of $MgSO_4.7H_2O$; 0.05 g.L^{-1} of $CaCl_2.2H_2O$; 0.1 mg.L^{-1} of H_3BO_4; 0.1 mg.L^{-1} of $CoCl_2.6H_2O$; 25 mg.L^{-1} of $ZnSO_4.7H_2O$; 4 mg.L^{-1} of $MnCl_2.4H_2O$; 0.1 mg.L^{-1} of $NaMoO_4.2H_2O$; 1.8 mg.L^{-1} of $CuSO_4.5H_2O$; 20 mg.L^{-1} of $FeSO_4.7H_2O$; 0.1 mg.L^{-1} of $NiSO_4.6H_2O$; 0.8% w/v of glycine and 6% v/v of n-dodecane) in shaker at 37 °C and 250 rpm. After 4 h of growth, culture was induced for 24 h by 0.1 mM of isopropyl β-D-thiogalactopyranoside (IPTG). A crude enzyme extract (cell-free supernatant) was obtained by centrifugation (10000 x*g*, 4 °C and 5 min) and stored at -20°C for further purification experiments. The crude enzyme extract presented protein concentrations of 4.3 ± 1.5 mg.mL^{-1} and specific activity of 0.18 ± 0.05 U.mg^{-1} protein.

2.3. Pre-purification step: enzyme precipitation by ammonium sulfate

A crude enzyme extract volume of 0.3 mL and 0.7 mL of saturated ammonium sulfate (70 wt%) was mixed for 2 min in a vortex mixer. Precipitated proteins were then removed by centrifugation (15000 xg, 15 min, 4°C); the supernatant was discarded and the protein pellet was dissolved in 0.3 mL of distilled water.

2.4. Tie-lines *(TLs)* determined for the polymer-salt ATPS

Before the purification assays, tie-lines (TLs) for the polymer-salt ATPS were determined. The ternary phase diagram of PEG 6000/citrate system at pH = 7 was obtained from literature,[34] and it was correlated using the Merchuk equation[38] (Eq. 1):

$$w_{PEG} = A \exp[(B[w_{Cit}]^{0.5}) - (C[w_{Cit}]^{3})] \quad \textbf{(1)}$$

where w_{PEG} and w_{Cit} are, respectively, the polymer and inorganic salt weight percentages (wt%), and *A*, *B* and *C* are the Merchuk parameters.

The TLs were determined by a gravimetric method originally proposed by Merchuk *et al.*[38] to calculate the composition of the two-phases in equilibrium. The *TLs* were calculated for the system based in PEG 6000/citrate buffer at pH = 7, and considering the following extraction points (PEG/salt – wt%): 15/15; 17.5/17.5; 20/20 and 22.5/22.5. The weight compositions of both phase formers (PEG and citrate) in the top and bottom phases (w_{PEG}^{Top}, w_{CIt}^{Top}, w_{PEG}^{Bot}, w_{Cit}^{Bot}) were obtained by solving the following system of four equations and four unknown variables:

$$w_{PEG}^{Top} = A\exp[\left(B.\ w_{Cit}^{Top^{0.5}}\right) - (C.\ w_{Cit}^{Top^{3}}) \quad \textbf{(2)}$$

$$w_{PEG}^{Bot} = A\exp[\left(B.\ w_{Cit}^{Bot^{0.5}}\right) - (C.\ w_{Cit}^{Top^{3}}) \quad \textbf{(3)}$$

$$w_{PEG}^{Top} = \frac{100\ w_{PEG}^{M}}{\alpha} - \frac{1-\alpha}{\alpha}\ w_{PEG}^{Bot} \quad \textbf{(4)}$$

$$w_{Cit}^{Top} = \frac{100\ w_{Cit}^{M}}{\alpha} - \frac{1-\alpha}{\alpha}\ w_{Cit}^{Bot} \quad \textbf{(5)}$$

The superscripts *Top* and *Bot* designate the PEG 6000-rich and citrate-rich phases, respectively, and *M* represents the initial mixture point composition. The parameter *α* is the ratio between the top weight and total weight of the mixture. The solution of the referred system gives the concentration of the polymer and salt in the top and bottom phases. The tie-line length (*TLL*) is defined as:

$$TLL = \sqrt{\left(w_{Cit}^{Top} - w_{Cit}^{Bot}\right)^2 + \left(w_{PEG}^{Top} - w_{PEG}^{Bot}\right)^2} \quad \textbf{(6)}$$

2.5. ASNase partition in ATPS

Polymer-salt ATPS composed of PEG and citrate, with and without the addition of ILs as adjuvants were prepared. In the studied ATPS, the top phase corresponds to the PEG-rich phase, while the bottom phase is mainly composed of the buffered salt. The ternary mixture compositions for ASNase purification were chosen based on the phase diagrams[34] constituted by PEGs with different molecular weights (2000, 4000, 6000 and 8000 g.mol^{-1}) and the citrate buffer at different pHs (5, 6, 7 and 8). All phase formers were added into an Eppendorf flask as a dry powder or stock solution, along with 0.4 mL of crude extract of ASNase, resulting in a 2.0 g system. Each mixture was then stirred in a vortex mixer and left to equilibrate for 120 minutes (a period of time established in previous optimization experiments) at 4°C in order to achieve the complete partition of ASNase between both phases. The volume of each phase, as well as ASNase activity and total protein concentration, were the parameters to determine. All experiments were carried out in triplicate and the interference of the buffer and PEG ascertained with the use of blank control samples, these prepared without the addition of ASNase crude extract. The partition coefficient of total proteins (K_P) was calculated as the ratio

between the protein concentration in top and bottom phases, respectively, $[P]_t$ and $[P]_b$ according to Eq 7:

$$Kp = \frac{[P]t}{[P]b} \quad \textbf{(7)}$$

The partition coefficient of ASNase (K_A) was calculated as the ratio between the volumetric activity of ASNase ($U.mL^{-1}$) in the top (*A*t) and bottom phases (*A*b), according to Eq 8:

$$K_A = \frac{At}{Ab} \quad \textbf{(8)}$$

The recovery yields of total proteins (%*Rec* P) and ASNase (%*Rec* A) into to PEG-rich phase were defined based on the partition coefficients of total proteins and ASNase, respectively, and the volume ratio (*V*r), according to Eq. 9:

$$\%RecP \text{ or } A = \frac{100}{(1+\left(\frac{1}{Vr \times Kp \text{ or } A}\right))} \quad \textbf{(9)}$$

The purification factor (*PF*) is given by the ratio between the specific activity of the top phase (SA_t) and the specific activity of the initial crude enzyme extract (*SA*i), according to Eq. 10:

$$PF = \frac{SAt}{SAi} \quad \textbf{(10)}$$

2.6. *In situ* extraction of ASNase: pre-purification and purification steps

The *in situ* extraction of ASNase from *E. coli* was performed through cell permeabilization by glycine and *n*-dodecane, followed by the contaminant proteins' precipitation with ammonium sulfate. After the precipitation step, ATPS (with and without ILs as adjuvants) were integrated as a final step of purification. The ATPS used in this downstream process were the PEG 6000/citrate buffer (15/15 wt%) at pH = 7 without IL and PEG 6000/citrate buffer (15/15 wt%) with 5 wt% of $[C_4mim][CH_3SO_3]$ as adjuvant at pH = 7 for the ATPS supplemented with IL.

2.7. Determination of ASNase activity

The ASNase activity was based on the protocol of Drainas and co-workers[30] and expressed as $U.mL^{-1}$. Briefly, 0.1 mL of sample, 0.7 mL of of Tris-HCl buffer (50 mM, pH 8.6), 0.1 mL of L-asparagine (0.1 M) and 0.1 mL of hydroxylamine (1.0 M, pH 7.0) were incubated at 37°C for 30 min. The reaction was interrupted by adding 0.5 mL of 0.31 M of iron chloride reagent (dissolved in HCl 0.33 M and trichloroacetic acid 0.3 M solution). The reaction solution was centrifuged at 3220x*g* for 15 min and the iron chloride–hydroxamic acid complex produced was quantified at 500 nm. The calibration curve was prepared from a β-aspartohydroxamic solution (Sigma-Aldrich, MO, USA). In this work, one unit of ASNase activity is defined as the amount of enzyme that produces 1 μmol of β-aspartohydroxamic acid *per* minute under the experiment conditions defined. The specific activity ($U.mg^{-1}$) represents the ratio between the volumetric activity of ASNase ($U.mL^{-1}$) and the total protein concentration ($mg.mL^{-1}$).

2.8. Determination of total protein concentration

The protein concentration was determined with the Pierce BCA Protein Assay and Micro BCA Protein Assay (Thermo Scientific, Schwerte, Germany) according to the manufacture's recommendations. Bovine serum albumin was used as standard protein.

2.9. *In silico* analysis

E. coli ASNase structure (code 3ECA)[39] was retrieved from the Protein Data Bank (PDB) and converted into PQR files according to Dolinsky *et al.*[40] using PARameters for Solvation Energy (PARSE) force field at different pH values (5, 6, 7 and 8). A PQR file is a PDB file with the temperature and occupancy columns replaced by columns containing the per-atom charge (Q) and radius (R). Electrostatic properties were calculated using automatically-configured sequential focusing multigrid calculation on Adaptive Poisson-Boltzmann Solver (APBS). These systems can module the biomolecular solvation by solving the Poisson-Boltzmann equation (PBE). Moreover, these will also provide implicit solvent models of nonpolar solvation, which accurately account for both repulsive and attractive solute-solvent interactions. Hydrophobicity was estimated by the software ExPasy[41] (adapted to red scale), which is based on amino acid scale from Eisenberg *et al.*.[42] All results were performed using PyMOL Molecular Graphics System, Version 1.8 Schrödinger, LLC.

3. Results and discussion

3.1. Preparation of the ASNase crude extract

After the *E. coli* cultivation (see Materials and Methods Section) and ASNase expression, the cell disruption was promoted by using glycine and *n*-dodecane. From this procedure, the complete secretion of periplasmatic ASNase was achieved, however, other proteins were also released. Chemical permeabilization of outer cell membrane with detergents and salts, such as Triton X-100 and K_2HPO_4, is reported in literature for ASNase secretion from *E. coli.*[21] However, this is the first time that glycine (for the disruption of the peptidoglycan layer)[43] and *n*-dodecane (for the disruption of the outer cell membrane)[44] are employed together in an integrated purification process using ATPS. This permeabilization approach was previously studied and proved to be effective on the enzyme release, with 89% of ASNase secreted to fermentation broth.[45] The final crude enzyme extract obtained has a protein concentration of 4.3 ± 1.5 $mg.mL^{-1}$ and specific activity of 0.18 ± 0.05 $U.mg^{-1}$ protein.

3.2. ASNase partition in polymer-salt ATPS

Polymer-salt ATPS were studied in the purification of ASNase from the crude enzyme extract. The ternary phase diagrams described in literature[34] were used to determine the extraction mixture compositions. Commonly, polymer/phosphate buffer-based ATPS are focused, however in this work, a citrate buffer-based salt was used, since this is more biocompatible and biodegradable. Additionally, this buffer is able to maintain the pH stable in a wider range and to create a larger biphasic region to work on, due to its stronger salting-out ability. **Table 1** summarizes all ASNase partition results obtained by applying *in situ* polymer-salt ATPS, considering the study of several conditions. It should be stressed that no protein precipitation was observed in any experimental condition and the protein mass balance was acceptably in the range of 80-120%. Given the high number of systems and conditions tested, this work will be mainly discussed considering each one of the conditions individually.

3.2.1. ASNase partition in PEG + citrate buffer-based ATPS

Usually, the partition coefficient of proteins (K_P) depends on several factors, such as the characteristics of the phase-forming polymer, the hydrophobic effect, charge and size

of proteins. The partition coefficient of the target protein (K_A) is mostly dependent on the specific characteristics of the enzyme that could lead to interactions with the phase formers, *e.g.* hydrophobicity, hydrophilicity, charge or π-interacting groups.

The recovery yields, %*Rec* A and %*Rec* P, and purification factors of ASNase in ATPS composed of PEGs with different molecular weight + citrate buffer (at pH = 7) are presented in **Fig. 2.7.**. All mixtures compositions used in this set of experiments correspond to the same extraction point composed of 15 wt% of polymer + 15 wt% of citrate buffer + 70 wt% of water. As can be seen, the ASNase partitions preferentially to the polymer-rich phase and this tendency increases with the polymer molecular weight. From the partition coefficient data, it is concluded that the ASNase partition is suffering the highest variations when different polymers molecular weights are tested, which is demonstrated by the greatest variation of K_A (from 3.09 ± 0.15 to 25.59 ± 0.15) when compared with K_P range (from 1.99 ± 0.03 to 2.96 ± 0.32). The ASNase partition results from the combined citrate salting-out effect and hydrophobic interactions between PEG and the hydrophobic parts of ASNase, already reported in literature by Sanches and collaborators.[46] Additionally, recent studies identified the same partition trend for ASNase in PEG 1000, 3000, 6000/potassium dihydrogen phosphate ATPS.[17] This can justify the increase of %*Rec* A (from 67.27 ± 1.05 to 93.86 ± 0.31 %) and K_A (from 3.09 ± 0.15 to 25.59 ± 0.15) by increasing the polymer molecular weight. In terms of total proteins, a different partition behaviour was observed, since PEGs of intermediate molecular mass (4000 and 6000) presented a lower tendency to concentrate contaminant proteins in PEG-top rich phase (**Fig. 2.7.** and **Table 2.6.**). Nevertheless, the higher *PF* was observed for PEG 6000, resulting from the high K_A (25.59 ± 0.15) and %*Rec* A (similar to PEG 8000-based ATPS) and one of the lowest K_P (2.36 ± 0.14) and %*Rec* P values (%*Rec* P = 58.72 ± 0.16%). Taking into consideration the overall set of results obtained for the purification parameters of ASNase, the PEG 6000-based ATPS was selected for further studies.

Table 2.6. Effect of polymer molecular mass, pH, phase composition and adjuvant concentration on the partition behaviour of ASNase through the use of *in situ* polymer-citrate buffer ATPS.

No.	Polymer	pH	Phase composition (wt %)			Adjuvant; Concentration (wt%)	*K*p	*K*a	*%Rec* P	*%Rec* A	*PF*
			PEG	Citrate	Water						
1	PEG 2000	7	15	15	70		2.40 ± 0.26	3.09 ± 0.15	61.37 ± 0.16	67.27 ± 1.05	2.14 ± 0.13
2	PEG 4000	7	15	15	70		1.99 ± 0.03	7.91 ± 0.15	54.60 ± 0.16	82.35 ± 2.07	4.76 ± 0.53
3	PEG 6000	7	15	15	70		2.36 ± 0.14	25.59 ± 0.15	58.72 ± 0.16	93.71 ± 1.05	13.45 ± 1.61
4	PEG 8000	7	15	15	70		2.96 ± 0.32	25.57 ± 3.15	63.80 ± 3.16	93.86 ± 0.31	8.73 ± 0.10
5	PEG 6000	5	15	15	70		2.28 ± 0.71	20.47 ± 1.32	59.24 ± 1.27	91.56 ± 1.25	12.55 ± 1.12
6	PEG 6000	6	15	15	70		2.24 ± 0.45	18.75 ± 0.45	58.26 ± 2.03	90.81 ± 0.32	12.68 ± 1.20
7	PEG 6000	8	15	15	70		4.09 ± 1.16	5.66 ± 1.16	70.19 ± 6.01	92.04 ± 2.64	6.42 ± 2.15
8	PEG 6000	7	17.5	17.5	65		2.36 ± 0.34	7.01 ± 1.00	56.27 ± 2.51	80.51 ± 2.25	7.37 ± 0.18
9	PEG 6000	7	20	20	60		6.56 ± 1.13	17.25 ± 5.60	81.51 ± 0.28	90.35 ± 2.86	6.87 ± 1.36
10	PEG 6000	7	22.5	22.5	55		9.74 ± 0.51	30.22 ± 9.92	85.36 ± 0.80	97.73 ± 0.30	9.67 ± 0.07
11	PEG 6000	7	15	15	69	$[C_4mim]Cl$; 1 wt%	2.43 ± 0.55	26.36 ± 0.25	60.95 ± 1.67	94.05 ± 0.24	13.86 ± 0.41
12	PEG 6000	7	15	15	69	$[C_4mim][DMP]$; 1 wt%	3.91 ± 0.49	18.37 ± 1.30	69.32 ± 3.26	91.65 ± 0.54	9.66 ± 0.68
13	PEG 6000	7	15	15	69	$[C_4mim][CH_3SO_3]$; 1 wt%	2.09 ± 0.18	32.06 ± 0.76	55.19 ± 0.43	95.06 ± 0.11	16.85 ± 0.40
14	PEG 6000	7	15	15	69	$[C_4mim][CF_3SO_3]$; 1 wt%	2.42 ± 0.01	31.02 ± 0.15	59.19 ± 0.16	94.90 ± 0.02	16.30 ± 0.08
15	PEG 6000	7	15	15	67.5	$[C_4mim][CH_3SO_3]$; 2.5 wt%	2.21 ± 0.43	24.78 ± 1.32	57.01 ± 1.39	91.94 ± 0.02	18.85 ± 1.02
16	PEG 6000	7	15	15	65	$[C_4mim][CH_3SO_3]$; 5 wt%	1.21 ± 0.12	22.08 ± 3.02	40.37 ± 1.14	87.94 ± 0.03	20.09 ± 0.35

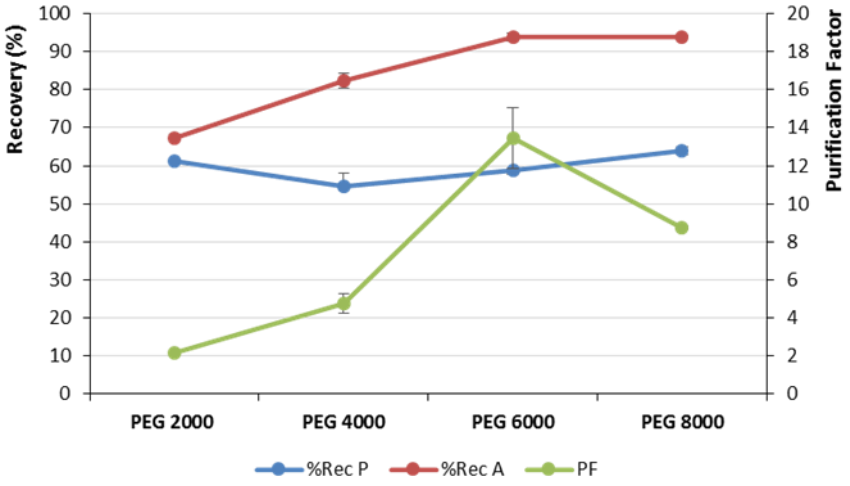

Fig. 2.7. Recovery yield of total proteins (%*Rec* P) and ASNase (%*Rec* A) and purification factor of ASNase (*PF*) for the ATPS composed of PEG + citrate buffer (15 wt%/15 wt%) at pH 7. Errors bars correspond to standard deviations obtained from three replicates.

The recovery yields, %*Rec* A and %*Rec* P and purification factors of ASNase in ATPS composed of PEG 6000/citrate buffer at different pH values are presented in **Fig. 2.8**.. It is observed that through the change of pH, the partition of ASNase continues to be mostly dominated by hydrophobic interactions, since high %*Rec* A are obtained towards the polymer-rich phase.[17] In this sense, *in silico* studies performed to characterize the hydrophobic regions of ASNase, at different pH values, are presented in **Fig. 2.9.A.** The analysis of the solvent-accessible surface area (SASA) shows a significant hydrophobic region on ASNase surface that does not change significantly with pH. Compared with conventional hydrophilic proteins with a size similar to ASNase, human serum albumin (1BM0, HSA)[47] - 57412.180 A^2 and bovine serum albumin (4F5S, BSA)[48] - 58218.199 A^2, it is found that the low SASA values of ASNase confirm its hydrophobic character. Previous results[17] reported an increase of the ASNase partition towards the PEG-rich phase at pH close to the p*I* (pI = 4.9)[17-18] by the application of ABS based on PEG/phosphate-based ATPS, as a result of the electrostatic interactions reduction between cell debris and the product molecules. From the gather data, it was inferred that pH does not affect significantly the ASNase SASA values, nor its partition behaviour in PEG/citrate-based ATPS, reinforcing the hypothesis that hydrophobic interactions are the important driving-force in polymer/salt-based ATPS. However, in aqueous solution pH affects the electric charges of both ASNase (**Fig. 2.9.B**) and periplasmatic

(contaminant) proteins, thus influencing the protein partition between both phases. The recovery of total proteins (%*Rec* P) in the PEG-rich phase increased in alkaline pH values (pH = 8), therefore, leading to a decrease in *PF*. After the optimization of the pH, the system PEG 6000/citrate buffer at pH = 7 was considered as the most efficient and further used in the next studies, comprising the effect of the mixture point/*TLL* and the use of ILs as adjuvants.

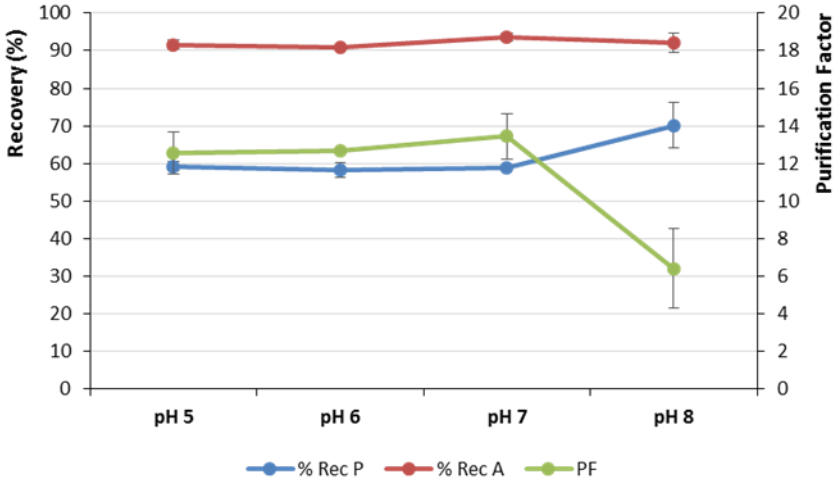

Fig. 2.8. Recovery yield of total proteins (%*Rec* P) and ASNase (%*Rec* A), and purification factor of ASNase (*PF*) for the ATPS composed of PEG 6000 + citrate buffer (15 wt%/15 wt%) at different pHs. Error bars correspond to standard deviations obtained from three replicates.

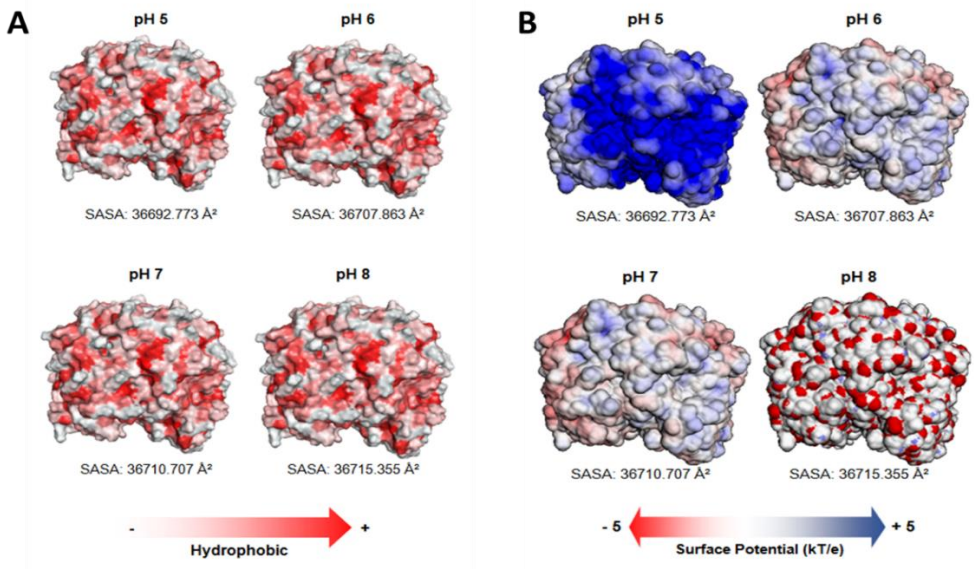

Fig. 2.9. 3D structure of ASNase (PDB: 3ECA) **(A)** hydrophobicity surface using Eisenberg amino acid scale[39] and solvent-accessible surface area (SASA), calculated for pHs 5, 6, 7 and 8. Red-scale refers to less hydrophobic (white) to more hydrophobic (red) parts of ASNase; **(B)** electrostatic charge at the ASNase surface and solvent-accessible surface area (SASA) calculated for pHs 5 to 8. Red-white-blue scale refers to minimum (-5 kT/e, red) and maximum (5 kT/e, blue) surface potential.

Fig. 2.10. shows the results of four mixture points (15.0/15.0; 17.5/17.5; 20.0/20.0; 22.5/22.5 wt% of polymer/salt) studied for the PEG 6000/citrate buffer system at pH 7. The composition of the top polymer-rich phase and bottom salt-rich phase, along with the parameter α and tie-line length (*TLL*) for each studied ATPS are presented in **Table 2.7.**. From the results obtained, it is concluded that higher *TLL* were obtained for the systems with upper amounts of both phase formers. Moreover, the partition of the total proteins seems to be dependent on the *TLL* since there is an increase of K_P (*circa* 4.1-fold) and %*Rec* P (*circa* 20% higher) with the increase of *TLL* (**Fig. 2.10.B** and **Tables 2.6-2.7.**). The citrate content present in the bottom rich-phase ranged from 20.26 to 33.50 wt% (**Table 2.7.**), resulting in a stronger salting-out effect for higher *TLL*. These results show that while hydrophobic interactions are again dominating the partition of ASNase, for the more hydrophilic contaminant periplasmatic proteins, their partition is being dominated by the salting-out effects. It is thus possible to use these distinct driving-force mechanisms of partition of both ASNase and periplasmatic contaminant proteins to manipulate the purification of ASNase. After the optimization of the *TLL* effect, it was defined as the best condition the lowest *TLL* (*TLL* = 38.33), represented by the mixture point composed of 15 wt% of PEG 6000/15 wt% of citrate buffer at pH 7.0, with %*Rec* A > 80 %, K_A > 7, and *PF* = 13.45 ± 1.61. This extraction point was then adopted to investigate the effect of ILs as adjuvants on the ASNase purification.

A

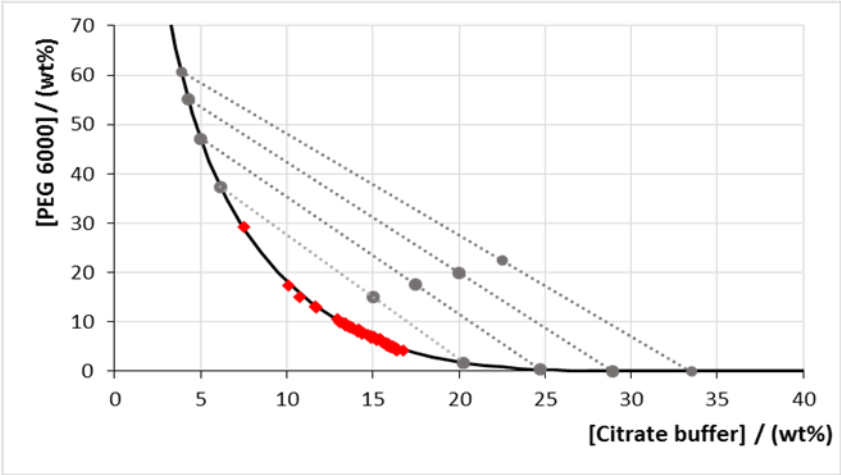

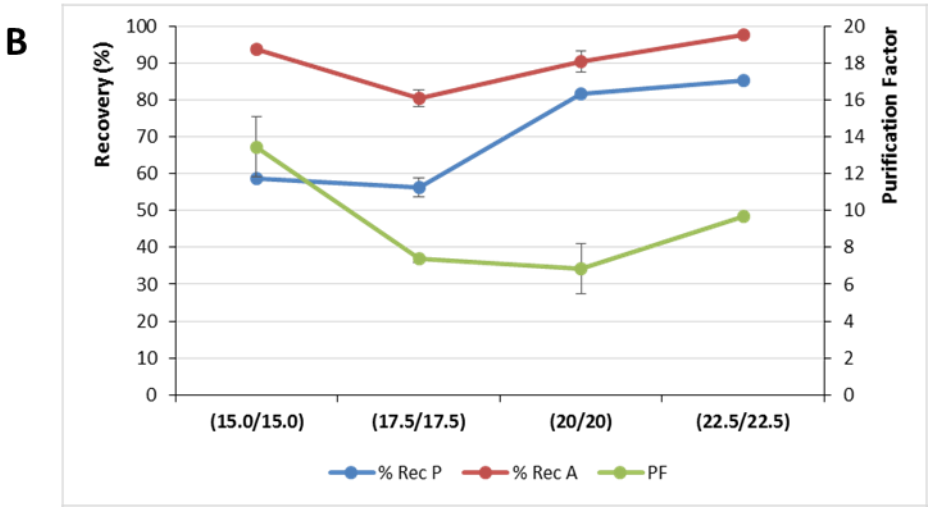

Fig. 2.10. (A) Ternary phase diagram of PEG 6000 + citrate buffer system at pH = 7 with representation of tie-lines (TL) for the following mixture points: PEG 6000 wt%/citrate buffer wt% = 15.0/15.0; 17.5/17.5; 20.0/20.0; 22.5/22.5. **(B)** Recovery yields of total proteins (%*Rec* P) and ASNase (%*Rec* A) and purification factor (*PF*) for the PEG 6000 + citrate buffer ATPS at pH = 7, considering four distinct mixture points. Error bars correspond to standard deviations obtained from three replicates.

Table 2.7. Composition of the initial mixture point (M), polymer-rich phase (Top) and salt-rich phase (Bot), along with the parameter α and the tie-line length (*TLL*).

$[PEG]^{M}$	$[Cit]^{M}$	$[PEG]^{Top}$	$[Cit]^{Top}$	$[PEG]^{Bot}$	$[Cit]^{Bot}$	*α*	*TLL*
15.0	15.0	37.36	6.15	1.72	20.26	0.373	38.33
17.5	17.5	47.10	4.99	0.37	24.74	0.366	50.72
20.0	20.0	55.25	4.24	0.061	28.91	0.361	60.45
22.5	22.5	60.70	3.88	0.0042	33.50	0.371	66.94

3.2.2. ASNase partition in PEG + citrate buffer + IL (as adjuvant)-based ATPS

The study of the effect of the ILs as adjuvants in the purification of enzymes produced via fermentation was recently reported as being one of the most promising approaches of purification[49], which was also adopted in this work. Herein, four ILs were tested as adjuvants, on the ASNase partition, in concentrations of 1 wt% of the overall system weight. Four imidazolium-based ILs presenting the same cation ($[C_4mim]^+$) combined with the anions Cl^-, $[DMP]^-$, $[CH_3SO_3]^-$ and $[CF_3SO_3]^-$ were selected to evaluate the effect of their polarity on the partition of both ASNase and contaminant proteins. Firstly, all imidazolium-based ILs investigated have a preferential partition towards the top phase, as reported elsewhere,[34] affecting the chemical and physical properties of the polymer-

rich phase. According to the results reported in **Fig. 2.11.**, no significant differences were observed in %*Rec* A, independently of the IL used. However, the data suggest that the ILs have an influence on the partition of the periplasmatic proteins, thus resulting in %*Rec* P ranging from 55.19 ± 0.43 to 69.32 ± 3.26 %. The less polar anions, $[C_4mim][CH_3SO_3]$ and $[C_4mim][CF_3SO_3]$, by enhancing the hydrophobicity of the top phase, were found to effectively decrease the amount of contaminant proteins in the PEG 6000-rich phase, increasing the *PF* in approximately 20%. Moreover, the polar anions Cl^- and $[DMP]^-$ seem to reduce the hydrophobicity of the polymer-rich phase enhancing the partition of the periplasmatic proteins to this phase, thus reducing the *PF*. Summing up, ILs with higher polarity decreased the *PF*, meaning that specific polar interactions between the periplasmatic proteins and ILs are promoted in the top phase, enhancing the partition of the contaminant proteins towards the polymer-rich phase. Contrastingly, both $[C_4mim][CH_3SO_3]$ and $[C_4mim][CF_3SO_3]$ display a lower hydrogen-bond basicity and were better at enhancing the ASNase *PF*, through the decrease of IL-contaminant proteins interactions. These results corroborate the importance of the IL anion in the partition of proteins, in this case, the contaminant periplasmatic proteins, thus allowing the increase of the purification performance of the polymeric ATPS. At this stage, the maximum purification achieved was around *PF* = 16.85 ± 0.40 for the $[C_4mim][CH_3SO_3]$. In order to endorse this statement, and aiming at to increase even more the *PF* of ASNase, the effect of IL concentration was studied, specifically for the $[C_4mim][CH_3SO_3]$ (best system). The results (**Fig. 2.12.**) corroborated the tendency previously discussed; the increased concentration of this less polar IL is significantly suppressing the partition of contaminant proteins towards the PEG-rich phase, culminating in the highest *PF* = 20.09 ± 0.35 obtained for the ATPS with 5 wt% of IL. In summary, small IL amounts' could enhance the ASNase partition and improve the purification performance of ATPS, which obviously brings additional advantages regarding the enzyme purity and the cost of the overall process of downstream.

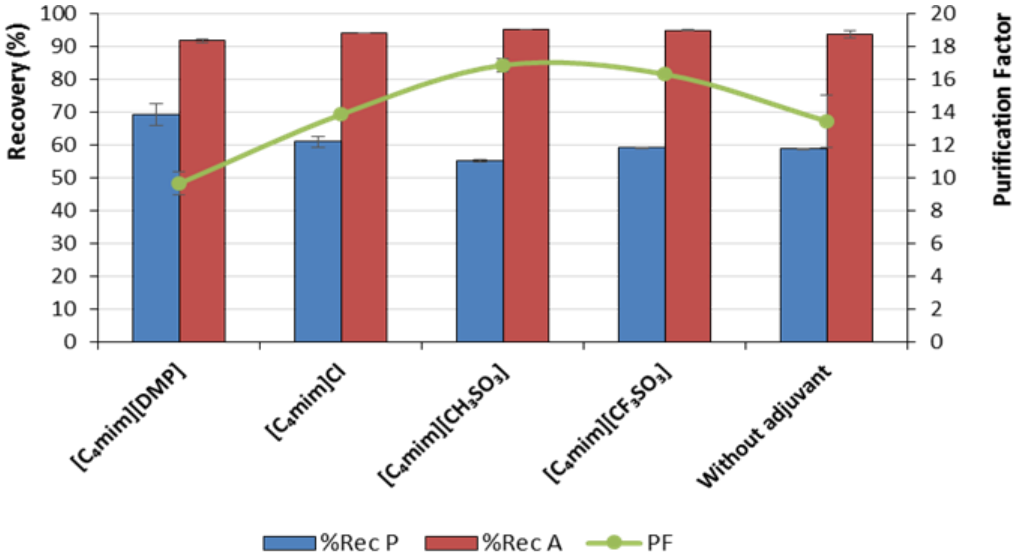

Fig. 2.11. Recovery yield of total proteins (%*Rec* P) and ASNase (%*Rec* A), and purification factor (*PF*) in the ATPS composed of PEG 6000 + citrate buffer (15 wt%/15 wt%) at pH = 7 and with 1 wt% of [C_4mim]-based ILs as adjuvants. Error bars correspond to standard deviations obtained from three replicates.

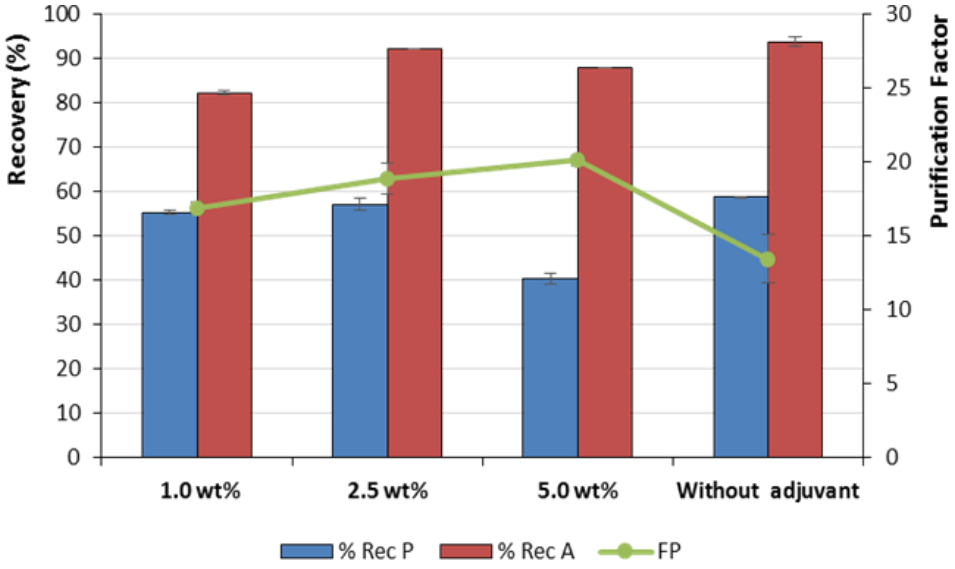

Fig. 2.12. Recovery yield of total proteins (%*Rec* P) and ASNase (%*Rec* A) and purification factor (*PF*) in the ATPS composed PEG of 6000 + citrate buffer (15 wt%/15 wt%) at pH = 7 and with [C_4mim][CH_3SO_3] as adjuvant. Errors bars correspond to standard deviations obtained from three replicates.

3.3. *In situ* extraction of ASNase by ATPS integrated with pre-purification step

Despite the good results of *PF* obtained, these are not sufficient for the use of ASNase as a biopharmaceutical. In this sense, a new strategy of purification was defined, which consists in the integration of two steps of purification. In this ambit, a pre-purification step was included between the stages of production and purification using the most

performant ATPS (15 wt% of PEG 6000 + 15 wt% of citrate buffer + 65 wt% of water + 5 wt% of $[C_4mim][CH_3SO_3]$ at pH = 7). The pre-purification was thus defined by using an ammonium sulfate solution to precipitate as much as possible the contaminant proteins, a strategy recurrently applied in the purification of enzymes.[49] The inclusion of a pre-purification step can help eliminating: (i) the contaminant proteins partitioned to the same aqueous phase as ASNase; and (ii) the antagonists and cell debris that may affect the ASNase activity. Moreover, some other advantages could be defined, like the fact that the ammonium sulfate precipitation is a cost-effective and scalable purification approach that could increase the overall purity of ASNase. Taking these advantages into account, the different strategies/platforms were compared for the purification of ASNase (**Fig. 2.13.**). Analysing the results of **Fig. 2.13.**, it is clear the advantage of using the integration of both pre-purification and purification processes (ammonium sulfate precipitation + $[C_4mim][CH_3SO_3]$-based ATPS, respectively), an approach resulting in the highest purification performance. This integrated downstream process proved to be much more efficient with higher ASNase specific activity (22.0 ± 1.36 $U.mg^{-1}$ protein) and purification factor (*PF* = 174 ± 11) than the isolated purification step by itself (ATPS or protein precipitation). **Fig. 2.14.** depicted the SDS-PAGE profile of the different steps of purification (Lane 5) and of the integrated downstream process (Lane 4) developed in this work. Through the main results it is concluded that a clear band of the ASNase subunit is obtained (≈ 35 kDa) for the integrated process (Lane 4), with the absence of contaminant proteins. Actually, with the pre-purification step, the elimination of a diversified plethora and high content of contaminant periplasmatic proteins,[50] *e.g.* nucleotidases, β-lactamase, alkaline phosphatase, ribonuclease, endonuclease I, caboxypeptidase II, cytochrome c, hydrogenase and nitrite reductase, was possible, while maintaining the ASNase structural integrity and activity for further purification using ATPS.

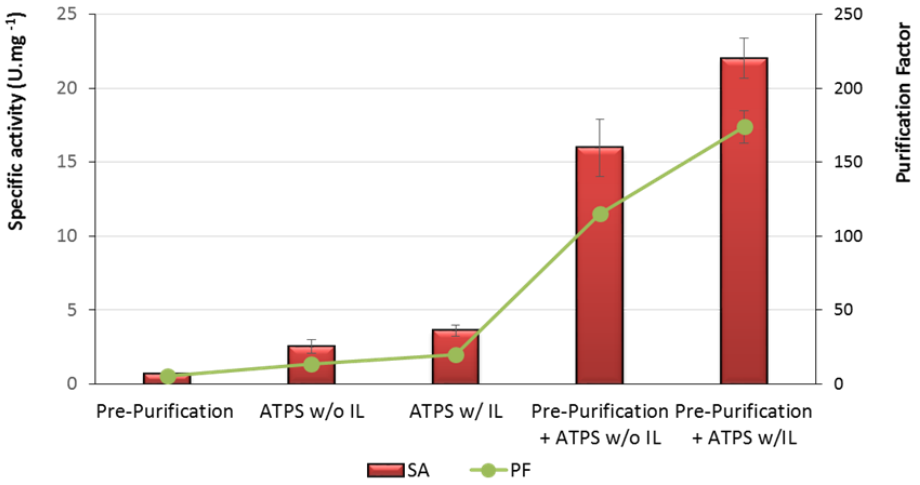

Fig. 2.13. Comparison between pre-purification step, IL-free ATPS, ATPS with IL, IL-free ATPS integrated with pre-purification step and ATPS with IL integrated with pre-purification step for the extraction and purification of periplasmatic L-asparaginase from *E.coli* cell paste.

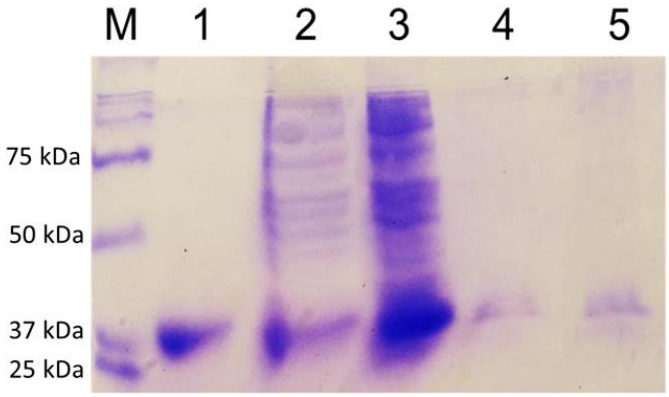

Fig. 2.14. SDS-PAGE of commercial ASNase from *E.coli* (1) Precipitated proteins from fermentation broth (2) Fermentation broth (3) Top-phase of the optimized ATPS, the PEG 6000/citrate with 5 wt% [C_4mim][CH_3SO_3] (as adjuvant) with pre-purification (4) Top-phase of the optimized ATPS, the PEG 6000/citrate with 5 wt% [C_4mim][CH_3SO_3] (as adjuvant) without pre-purification (5). Molar masses reference Precision Plus Protein (BIORAD, CA, US) (M).

Since the main aim of this work is the optimization of the ASNase purification from the fermentation broth, the integrated downstream process envisaged was schematically represented as **Fig. 2.15.**. This comprises the purification step, the cell disruption to release the ASNase, the pre-purification step to eliminate part of the contaminant proteins, the IL-ATPS to refine the purification of the biopharmaceutical, and the isolation of ASNase. As depicted, the best ATPS and conditions selected are represented, as well as the isolation methods defined for the polishing of ASNase and contaminant proteins from both phases by using an ultrafiltration, culminating in the sequent reuse of the phases in new cycles of purification.

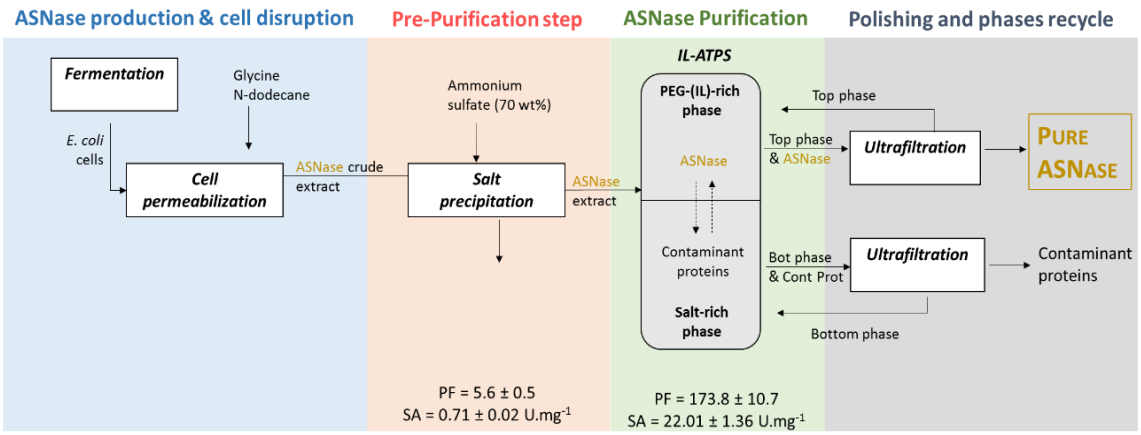

Fig. 2.15. Schematic representation of the *in situ* purification process of periplasmatic ASNase by using polymer-based ATPS with [C_4mim][CH_3SO_3] as adjuvant. The isolation of ASNase and the recycling of both aqueous phases are also represented.

4. Conclusions

In this work, an efficient integrated downstream process combining cell permeabilization (applying glycine and n-dodecane) with the purification of ASNase by using IL-ATPS was here demonstrated. In this ambit, polymer-based ATPS using ILs as adjuvants showed, one more time, to be efficient in the purification of enzymes, *i.e.* ASNase. Actually, our results reveal a high affinity of ASNase for the polymer rich-phase of the ATPS, justified by the hydrophobic interactions established between the enzyme and the polymer. Moreover, it was demonstrated the high purification performance of the ATPS using 5 wt% of a [C_4mim][CH_3SO_3] as adjuvant (when compared with the common polymeric system), attaining a *PF* = 20.09 ± 0.35 and *SA* = 3.33 ± 0.38 U/mg protein. Moreover, and taking into account other purification schemes, an ammonium precipitation pre-purification step was tested, demonstrating again clear advantages in terms of downstream process efficiency over discrete and sequential operations, attaining a purification factor of 173.8 ± 10.7. Actually, it was proven that low amounts of ILs in the formulation of ATPS are shown to be enough to achieve complete extractions of ASNase (%*Rec* ASNase ≈ 90%) with high purity. The system with high purification performance was then used in the design of an integrated process comprising the steps of production, cell disruption, and purification with an ammonium sulfate precipitation followed by the application of ATPS with IL as adjuvant, and culminating in the ASNase isolation and phases reuse.

References

1. Soares, A. L, Guimarães, G. M., Polakiewicz, B., Pitombo, R. N. D. M & Abrahão-Neto J. Effects of polyethylene glycol attachment on physicochemical and biological stability of *E. coli* L-asparaginase. *Int J Pharm* **237**, 163–170 (2002).
2. van den Berg, H. Asparaginase revisited. *Leuk Lymphoma* **52**, 168–178 (2011).
3. Piatkowska-Jakubas, B., Krawczyk-Kuliś, M., Giebel, S., Adamczyk-Cioch, M., Czyz, A., Lech Marańda, E., Paluszewska, M., Pałynyczko, G., Piszcz, J. & Hołowiecki, J. Use of L-asparaginase in acute lymphoblastic leukemia: recommendations of the Polish Adult Leukemia Group. *Pol Arch Med Wewn* **118**, 664–669 (2008).
4. Rizzari, C., Conter, V., Starý, J., Colombini, A., Moericke, A. & Schrappe, M. Optimizing asparaginase therapy for acute lymphoblastic leukemia. *Curr Opin Oncol* **25 Suppl 1**, S1–S9 (2013).
5. Pui, C. H., Robison, L. L. & Look, A. T. Acute lymphoblastic leukaemia. *Lancet* **371**, 1030–1043 (2008).
6. Schleis, S. E., Rizzo, S. A., Phillips, J. C. & LeBlanc, A. K. Asparaginase-associated pancreatitis in a dog. *Can Vet J* **52**, 1009–1012 (2011).
7. Beard, M. E., Crowther, D., Galton, D. A., Guyer, R. J., Fairley, G. H., Kay, H. E., Knapton, P. J., Malpas, J. S. & Scott, R. B. L-asparaginase in treatment of acute leukaemia and lymphosarcoma. *Br Med J* **1**, 191–195 (1970).
8. DeVita, V. T. & Chu, E. A history of cancer chemotherapy. *Cancer Research* **68**, 8643–8653 (2008).
9. WHO, WHO | WHO Model Lists of Essential Medicines. *World Heal Organ* **19**, 55 (2015).
10. Narta, U. K., Kanwar, S. S. & Azmi, W. Pharmacological and clinical evaluation of l-asparaginase in the treatment of leukemia. *Critical Reviews in Oncology/Hematology* **61**, 208–221 (2007).
11. Bierau, H., Hinton, R. J. & Lyddiatt, A. Direct process integration of cell disruption and fluidised bed adsorption in the recovery of labile microbial enzymes. *Bioseparation* **10**, 73–85 (2001).
12. Krasotkina, J., Borisova, A. A., Gervaziev, Y. V. & Sokolov, N. N. One-step purification and kinetic properties of the recombinant L-asparaginase from *Erwinia carotovora*. *Biotechnol Appl Biochem* **39**, 215–221 (2004).

13. Kumar, S., Venkata Dasu, V. & Pakshirajan, K. Purification and characterization of glutaminase-free l-asparaginase from Pectobacterium carotovorum MTCC 1428. *Bioresour Technol* **102**, 2077–2082 (2011).
14. Badoei-Dalfard, A. Purification and characterization of l-asparaginase from *Pseudomonas aeruginosa* strain SN004: Production optimization by statistical methods. *Biocatal Agric Biotechnol* **4**, 388–397 (2015).
15. Dharmaraj, S. Study of L-asparaginase production by *Streptomyces noursei* MTCC 10469, isolated from marine sponge *Callyspongia diffusa*. *Iran J Biotechnol* **9**,102–108 (2011).
16. Upadhyay AK, Singh A, Mukherjee KJ and Panda AK, Refolding and purification of recombinant L-asparaginase from inclusion bodies of *E. coli* into active tetrameric protein. *Front Microbiol* **5***:*486 (2014).
17. Zhu, J. H., Yan, X. L., Chen, H. J. & Wang, Z. H. *In situ* extraction of intracellular l-asparaginase using thermoseparating aqueous two-phase systems. *J Chromatogr A* **1147**, 127–134 (2007).
18. Khushoo, A., Pal, Y., Singh, B. N. & Mukherjee, K. J. Extracellular expression and single step purification of recombinant *Escherichia coli* L-asparaginase II. *Protein Expr Purif* **38**, 29–36 (2004).
19. Kim, S. K., Min, W. K., Park, Y. C. & Seo, J. H. Application of repeated aspartate tags to improving extracellular production of *Escherichia coli* l-asparaginase isozyme II. *Enzyme Microb Technol* **79-80**, 49–54 (2015).
20. Khushoo, A., Pal, Y. & Mukherjee, K. J. Optimization of extracellular production of recombinant asparaginase in *Escherichia coli* in shake-flask and bioreactor. *Appl Microbiol Biotechnol* **68**, 189–197 (2005).
21. Qin, M. & Zhao, F. L-asparaginase release from *Escherichia coli* cells with aqueous two-phase micellar systems. *Appl Biochem Biotechnol* **110**, 11–21 (2003).
22. Hernandez-Justiz, O., Fernandez-Lafuente, R., Terreni, M. & Guisan, J. M. Use of aqueous two-phase systems for *in situ* extraction of water soluble antibiotics during their synthesis by enzymes immobilized on porous supports. *Biotechnol Bioeng* **59**, 73–79 (1998).
23. Azevedo, A. M., Rosa, P. A. J., Ferreira, I .F. & Aires-Barros, M. R. Optimisation of aqueous two-phase extraction of human antibodies. *J Biotechnol* **132**, 209–217

(2007).

24. Viana Marques, D. A., Pessoa-Júnior, A., Lima-Filho, J. L., Converti, A., Perego, P. & Porto, A. L. F. Extractive fermentation of clavulanic acid by *Streptomyces* DAUFPE 3060 using aqueous two-phase system. *Biotechnol Prog* **27**, 95–103 (2011).
25. Rito-Palomares, M., Nuez, L. & Amador, D. Practical application of aqueous two-phase systems for the development of a prototype process for c-phycocyanin recovery from *Spirulina maxima*. *J Chem Technol Biotechnol* **76**, 1273–1280 (2001).
26. Rito-Palomares, M. & Middelberg, A. P. Aqueous two-phase systems for the recovery of a recombinant viral coat protein from *Escherichia coli*. *J Chem Technol Biotechnol* **77**,1025–1029 (2002).
27. Liu, X., Mu, T., Sun, H., Zhang, M. & Chen, J. Optimisation of aqueous two-phase extraction of anthocyanins from purple sweet potatoes by response surface methodology. *Food Chem* **141**, 3034–3041 (2013).
28. Rito-Palomares, M., Negrete, A., Miranda, L., Flores, C., Galindo, E. & Serrano-Carreón, L. The potential application of aqueous two-phase systems for *in situ* recovery of 6-pentyl-infinity-pyrone produced by *Trichoderma harzianum*. *Enzyme Microb Technol* **28**, 625–631 (2001).
29. Imada, A., Igarasi, S. & Nakahama, K. Asparaginase and Glutaminase Activities of Micro-organisms. *Microbiology* **76**,85–89 (1973).
30. Drainas, C. & Pateman, J. A. L-Asparaginase activity in the fungus *Aspergillus nidulans*. *Biochem Soc Trans* **5**, 259–261 (1977).
31. Hapiot, P. & Lagrost, C. Electrochemical reactivity in room-temperature ionic liquids. *Chemical Reviews* **108**, 2238–2264 (2008).
32. Freire, M. G., Cláudio, A. F. M., Araújo, J. M.M. , Coutinho, J. A. P., Marrucho, I. M., Lopes, J. N. C. & Rebelo, L. P. N. Aqueous biphasic systems: a boost brought about by using ionic liquids. *Chemical Society Reviews* **41**, 4966 (2012).
33. Pereira, J. F. B., Lima, Á. S., Freire, M. G. & Coutinho, J. A. P. Ionic liquids as adjuvants for the tailored extraction of biomolecules in aqueous biphasic systems. *Green Chem* **12**, 1661 (2010).
34. Ferreira, A. M., Faustino, V. F. M., Mondal, D., Coutinho, J. A. P. & Freire, M. G.

Improving the extraction and purification of immunoglobulin G by the use of ionic liquids as adjuvants in aqueous biphasic systems. *J. Biotechnol* **236**, 166–175 (2016).

35. de Souza, R. L., Campos, V. C., Ventura, S. P. M., Soares, C. M. F., Coutinho, J. A. P. & Lima, Á. S. Effect of ionic liquids as adjuvants on PEG-based ABS formation and the extraction of two probe dyes. *Fluid Phase Equilib* **375**, 30–36 (2014).
36. Santos, J. H. P. M., e Silva, F. A., Coutinho, J. A. P., Ventura, S. P. M. & Pessoa, A. Ionic liquids as a novel class of electrolytes in polymeric aqueous biphasic systems. *Process Biochem* **50**, 661-668 (2015).
37. Santos, J. H. P. M., Martins, M., Silvestre, A. J. D., Coutinho, J. A. P. & Ventura, S. P. M. Fractionation of phenolic compounds from lignin depolymerisation using polymeric aqueous biphasic systems with ionic surfactants as electrolytes. *Green Chem* **18**, 5569–5579 (2016).
38. Merchuk, J. C., Andrews, B. A. & Asenjo, J. A. Aqueous two-phase systems for protein separation. Studies on phase inversion. *J Chromatogr B Biomed Sci Appl* **711**:285–293 (1998).
39. Swain, A. L., Jaskólski, M., Housset, D., Mohana Rao, J. K. & Wlodawert, A. Crystal structure of *Escherichia coli* L-asparaginase, an enzyme used in cancer therapy. *Biochem. Commun. by David R. Davies* **90**, 1474–1478 (1993).
40. Dolinsky, T. J., Nielsen, J. E., McCammon, J. A. & Baker, N. A., PDB2PQR: An automated pipeline for the setup of Poisson-Boltzmann electrostatics calculations. *Nucleic Acids Res* 32, DOI: 10.1093/nar/gkh381.(2004).
41. ExPasy. Amino acid scale: Normalized consensus hydrophobicity scale [Internet]. (2017) Available from: http://us.expasy.org/tools/pscale/Hphob.Eisenberg.html.
42. Eisenberg, D., Schwarz, E., Komaromy, M. & Wall, R. Analysis of membrane and surface protein sequences with the hydrophobic moment plot. *J Mol Biol* **179**,125–142 (1984).
43. Hammes, W., Schleifer, K. H. & Kandler, O. Mode of action of glycine on the biosynthesis of peptidoglycan. *J. Bacteriol* **116**,1029–1053 (1973).
44. Sikkema, J., de Bont, J. A. & Poolman, B. Mechanisms of membrane toxicity of hydrocarbons. *Microbiol Rev* **59**, 201–222 (1995).
45. Santos, J. C. F., Moguel, I. S., Monteiro, G., Pessoa-Jr, A. & Vitolo, M. Extracellular

secretion improvement of recombinant l-asparaginase II in *Escherichia coli* BL21 (DE3) using glycine and n-dodecane. submitted to *Appl Microbiol Biotechnol* 2017.

46. Sanches, M., Barbosa, J. A. R. G., De Oliveira, R. T., Neto, J. A. & Polikarpov, I. Structural comparison of *Escherichia coli* L-asparaginase in two monoclinic space groups. *Acta Crystallogr - Sect D Biol Crystallogr* **59**, 416–422 (2003).
47. Sugio, S., Kashima, A., Mochizuki, S., Noda, M. & Kobayashi, K. Crystal structure of human serum albumin at 2.5 A resolution. *Protein Eng.* **12**, 439–46 (1999).
48. Bujacz, A. Structures of bovine, equine and leporine serum albumin. *Acta Crystallogr. Sect. D Biol. Crystallogr.* **68**,1278–1289 (2012).
49. Souza, R. L., Ventura, S. P. M., Soares, C. M. F., Coutinho, J. A. P. & Lima, Á. S., Lipase purification using ionic liquids as adjuvants in aqueous two-phase systems. *Green Chem* **17**, 3026–3034 (2015).
50. Beacham, I. R. Periplasmic enzymes in gram-negative bacteria. *International Journal of Biochemistry* **10**, 877–883 (1979).

2.3. Integration of Aqueous (Micellar) Two-Phase Systems on the proteins separation

Vicente, F. A.,* **Santos, J. H. P. M.**,* Pereira, I. M. M., Gonçalves, C. V. M., Dias, A. C. R. V., Coutinho, J. A. P. & Ventura, S. P. M., *BMC Chemical Engineering*, 2019, https://doi.org/10.1186/s42480-019-0004-x.[4]

* Both authors contributed equally to this work.

Abstract

A two-step approach combining an aqueous two-phase system (ATPS) and an aqueous micellar two-phase system (AMTPS), both based on the thermo-responsive copolymer Pluronic L-35, is here proposed for the purification of proteins and tested on the sequential separation of three model proteins, cytochrome c, ovalbumin and azocasein. Phase diagrams were established for the ATPS, as well as co-existence curves for the AMTPS. Then, by scanning and choosing the most promising systems, the separation of the three model proteins was performed. The aqueous systems based on Pluronic L-35 and potassium phosphate buffer (pH = 6.6) proved to be the most selective platform to separate the proteins ($S_{Azo/Cyt}$ = 1667; $S_{Ova/Cyt}$ = 5.33 e $S_{Azo/Ova}$ = 1676). The consecutive fractionation of these proteins as well as their isolation from the aqueous phases was proposed, envisaging the industrial application of this downstream strategy. The environmental impact of this downstream process was studied, considering the carbon footprint as the final output. The main contribution to the total carbon footprint comes from the ultrafiltration (~49%) and the acid precipitation (~33%) due to the energy consumption in the centrifugation. The ATPS step contributes to ~17% while the AMTPS only accounts for 0.30% of the total carbon footprint.

Keywords: aqueous (micellar) two-phase systems; downstream process; thermo-responsive copolymers; proteins; carbon footprint.

[4] Contributions: JS, IP and FV acquired the experimental data. The environmental data was acquired by IG and CD. JS, FV, SV and JC interpreted the experimental data. SV and JC conceived and directed this work. The manuscript was mainly written by JS and FV with significant contributions from the remaining authors.

1. Introduction

In the past few years, there has been an increased interest and effort focused the extraction and separation of proteins, not only those produced via fermentation, but also proteins recovered from different raw materials and biomass matrices. Most fermentative processes result in a product that is a complex combination of proteins and other metabolites or cell debris. However, in this protein rich-pool, it is quite difficult to achieve a good separation and purification of the target protein from all the other contaminants. Bioprocesses require efficient purification platforms for the isolation of the desired components and the elimination of the by-products. These are still the main challenge for the industrial applications,[1] and responsible for up to 80% of the production costs.[2] Recently, with the increased attention given to the valorisation of new products from emergent raw materials and biomass, such as algae[3] and cyanobacteria,[4] the development of improved downstream approaches is of high interest and value.

Conventional downstream processes to purify proteins are based on chromatographic techniques, namely size exclusion chromatography, ion exchange chromatography and hydrophobic chromatography.[5,6] These methods are easy to validate and implement in batch and larger scale, however they are quite expensive. Among the non-chromatographic methods, ultrafiltration [7,8] and precipitation [9,10] appear as the main approaches used in protein separation, though, these methods are ineffective in the separation of similar proteins, since they only act based on protein size and hydrophilicity, respectively. Over the last years, aqueous two-phase systems (ATPS) emerged as an alternative platform for protein separation, considering their intrinsic versatility, in some cases leading to an enhanced purification performance.[11]

ATPS are a particular type of biphasic system used in liquid-liquid extraction as a primary recovery step for the product isolation and purification by partially separating it from impurities or substrates, hence reducing the subsequent downstream processing volume. One of the most important advantages of ATPS is the high-water content in both phases, which turns the microenvironment of the system more biocompatible for proteins and other biomolecules. This downstream platform is interesting since it can

combine several steps into a single operation, namely clarification, extraction, isolation, purification and concentration of the compound.[12] In chemical industry, two-phase systems are employed due to its simplicity, low costs, low viscosity, short phase separation time and easier scale-up.[11,12] ATPS have been widely applied on the purification and recovery of biological products, such as proteins, genetic material, organelles and bionanoparticles.[12] For that purpose there are some physicochemical properties of the biomolecules (isoelectric point, surface hydrophobicity and molar mass) as well as of the ATPS components [11] ((co)polymers, salts, surfactants and ionic liquids [13]) and process conditions selected (such as the system temperature, or pH [6,14]) that must be taken into account and optimized.

Pluronic triblock copolymers are non-ionic surfactants from the polyoxyethylene alkyl ether family being composed by units of polyethylene glycol (PEG) and polypropylene glycol (PPG). By changing the number of PEG units in the copolymer, its hydrophilicity can be controlled. The copolymers critical micelle concentration (CMC) and surface activity are much more sensitive to temperature than those for the conventional surfactants due to their composition,[15] making them more versatile. Among others they are thermo-responsive, being able to form two macroscopic phases when submitted to a temperature above their cloud point, and are commonly known as aqueous micellar two-phase systems (AMTPS).[11] In 2000, Persson *et.al.*[16] proposed a copolymer-starch ATPS as part of an integrated process, in which they managed to purify apolipoprotein A-1 from an *E. coli* fermentation broth and from human plasma.

An integrated platform for the purification of a model protein mixture, composed of cytochrome c, ovalbumin and azocasein, is here proposed. Besides the need to improve the processes efficiency and reduce their cost, there is a growing concern to evaluate their environmental impact. Here, an environmental evaluation of the new two-step approach proposed was carried using the carbon footprint as indicator.

2. Material and Methods

2.1. Materials

Three phosphate-based salts were used, namely monopotassium phosphate (K_2HPO_4) acquired on Panreac (99 wt% purity), dipotassium phosphate (KH_2PO_4) obtained from Sigma (99.5 wt% purity) and tripotassium phosphate (K_3PO_4) attained from Acros Organic (97 wt% purify). A phosphate-buffer solution (K_2HPO_4/KH_2PO_4) was also used at pH = 6.6. The copolymers employed in this work were Pluronic L-35, Pluronic 10R5 and Pluronic 17R4, all acquired at Sigma-Aldrich. As co-surfactants, Triton X-114 and Triton X-100 (purity > 95 wt%) purchased from Acros Organic, were tested. Cytochrome c (purity > 95 wt%) from equine heart and azocasein (99 wt% purity) were acquired from Sigma-Aldrich, whereas albumin from hen egg white (97 wt% purity) was supplied by Fluka, BioChemika.

2.2. Measurement of phase diagrams and tie-lines for ATPS

The binodal curves of the ATPS with different compositions were determined using the cloud-point titration method[17] at 25 (±1)ºC, at atmospheric pressure. This technology is based on the dropwise addition of a salt solution to a polymer aqueous solution, both with known concentrations, until the mixture becomes turbid (representing the biphasic system). Then, a known mass of water was added to clear the solution (corresponding to the monophasic system). This procedure was repeated to obtain enough data for the design of the respective binodal curves. The phase diagram data were correlated using the Merchuk equation,[18] as described in **Eq.1**:

$$[Copolymer] = A \times \exp[(B[Salt]^{0.5}) - (CX^3)] \quad \textbf{(1)}$$

where [*Copolymer*] and [*Salt*] are respectively the copolymer and inorganic salt weight percentages (wt%). Three different studies were attained for the phase diagrams design: the inorganic salt type, the copolymer type and the presence of adjuvants (Triton X-100 and Triton X-114). In this sense, for the inorganic salt type study, four salts were used: K_2HPO_4, KH_2PO_4, K_3PO_4 and K_2HPO_4/KH_2PO_4, being the Pluronic L-35 and Triton X-100 maintained constant. For the second study, different copolymers (Pluronic L-35, Pluronic 10R5, and Pluronic 17R4) were studied while the potassium phosphate buffer (K_2HPO_4/KH_2PO_4, pH = 6.6) was kept constant. Finally, the impact of small amounts of

Triton X-114 (1 wt%) was studied for the system constituted by Pluronic L-35 and the potassium phosphate buffer (pH = 6.6).

The *TLs* were determined by the gravimetric method originally proposed by Merchuk *et al*.[18], for the extraction points presented in **Table A.9 at Appendix A**, to calculate the composition of the two-phases in equilibrium. The compositions of copolymer and salt in the top and bottom phases were obtained as well as the *TLL*,[19] being the data presented in **Figure A.8** and **Table A.7 at Appendix A**

2.3. Measurement of the AMTPS cloud point curves

The AMTPS cloud point curves were carried out by the cloud point method.[20] Herein, the AMTPS corresponds to the ATPS top phase, which was composed of potassium phosphate buffer (K_2HPO_4 /KH_2PO_4) at pH = 6.6 or water and a different copolymer (Pluronic L-35, Pluronic 10R5 or Pluronic 17R4). For the AMTPS using Triton X-114 as adjuvant, the ATPS top phase also displayed this component. Basically, this procedure consists on a visual identification, while raising the temperature, of the point at which a mixture with known compositions becomes turbid (biphasic system), indicating the system cloud point. The experimental curves were obtained by plotting the cloud point *versus* the copolymer mass concentration. These curves represent the boundary between the conditions at which the system presents a single phase (below/outside the curve) or two macroscopic phases (above/inside the curve). Once the cloud point curves were measured, a mixture point for each system in the biphasic region on both the ATPS and AMTPS was selected, at the lowest possible polymer concentration and temperature. The experimental mixture in the ATPS was selected with 23 wt% of copolymer and 6 wt% of potassium phosphate buffer (pH = 6.6), for a final volume of 5 mL. It should be noted that the copolymers concentration in the cloud point curves are not identical for all the studied systems since for Pluronics 10R5 and L-35, there is not a biphasic region for concentrations lower than 22 wt%.

2.4. ATPS coupled with AMTPS to separate model proteins – single protein purification

Two pseudo-ternary systems composed of 23 wt% of Pluronic 10R5 or L-35 + 6 wt% of potassium phosphate buffer + 71 wt% of proteins solution and one quaternary system composed of 23 wt% of Pluronic L-35 + 6 wt% of potassium phosphate buffer + 1 wt% of Triton X-114 + 70 wt% of proteins solution were studied as the purification platforms for three model proteins: cytochrome c (0.5 $g.L^{-1}$), azocasein (0.3 $g.L^{-1}$) and ovalbumin (1.59 $g.L^{-1}$).

On the first step of purification (ATPS), the systems were homogenised for 2 h at 25ºC and then these were centrifuged for 10 min, at 25 ºC, and 251.55 *g*. These conditions allow the two phases formation and equilibrium, after which both phases were collected, their volumes and weights determined, and the proteins quantified by UV-Vis spectroscopy, as described below. For the second step of purification, the top/copolymer-rich-phase was used to the AMTPS formation, being the systems composed of Pluronic 10R5, Pluronic L-35 and Pluronic L-35 + Triton X-114 left at 39ºC, 44ºC and 40ºC overnight, respectively. Both phases were then collected, their volumes and weights determined, and the proteins quantified by UV-Vis spectroscopy, at a wavelength of 280 nm for ovalbumin, and 409 nm for cytochrome c. Azocasein has three characteristic peaks, namely at 215 nm, 342 nm, and 440 nm. However, in this work the wavelength of 342 nm was selected since it represents the maximum absorbance experimentally found. Calibration curves were performed for each model protein. The analytical quantification was performed at least in triplicate, and to prevent possible interferences, blanks were routinely applied. For both steps of purification (ATPS and AMTPS), several parameters were determined. The partition coefficient (*K*) for each model protein was calculated as the ratio between the equilibrium concentrations of the protein in the top phase ($[Prot]_T$) and the protein in the bottom phase ($[Prot]_B$). To facilitate the analysis, the K results were normalized through their logarithmic function, as described by **Eq.2:**

$$\log(K) = \log\left(\frac{[\mathrm{Prot}]_\mathrm{T}}{[\mathrm{Prot}]_\mathrm{B}}\right) \quad \textbf{(2)}$$

The recovery parameter of each protein towards the top (*%Rec Top*) and the bottom

(*%Rec Bottom*) phases was determined by the ratio among the protein mass on top or bottom phases, respectively, and the initial protein mass applied in the system (**Eqs. 3** and **4**):

$$\%Rec\ Top = \frac{V_T[Prot]_T}{V_T[Prot]_T + V_B[Prot]_B} \times 100 \quad \textbf{(3)}$$

$$\%Rec\ Bottom = \frac{V_B[Prot]_B}{V_T[Prot]_T + V_B[Prot]_B} \times 100 \quad \textbf{(4)}$$

Since the main intention was to measure the selective partition of the proteins (*e.g.* protein A and protein B), the selectivity (*S*) parameter was analysed through **Eq. 5**:

$$S = \frac{K_{Prot\ A}}{K_{Prot\ B}} \quad \textbf{(5)}$$

2.5. Integrated ATPS and AMTPS - complex purification mixture

In order to mimic a real system, the three model proteins were simultaneously separated. The most selective integrated system identified, *i.e*. 23 wt% Pluronic L 35 + 6 wt% potassium phosphate buffer (pH = 6.6) ATPS + AMTPS, was applied for the separation of the proteins from the complex mixture.

The quantification of the proteins was performed using size exclusion chromatography (SEC-FPLC). The top and bottom phases upon separation were injected into an AKTA™ purifier system (GE Healthcare) size exclusion chromatographer equipped with a Superdex 200 Increase 10/300 GL chromatographic column prepacked with crosslinked agarose-dextran high resolution resin (GE Healthcare) to quantify the three model proteins. Moreover, through these measurements, the purity and purification yield (%) were also calculated. The column was equilibrated with 0.01 M of potassium phosphate buffer (0.14 M NaCl, pH = 7.4) and eluted with the same buffer at the flow of 0.75 mL.min^{-1}. The quantification of each proteins was carried out at 280 nm by FPLC/UV size-exclusion method. The purification performance of the integrated process was evaluated based on the recovery yield (R_x %) and purity (P_x %) for the three proteins as it can be seen at **Eqs. 6** and **7**.

$$R_x\ (\%) = \frac{m\left(Protein_{purified\ fraction}\right)}{m(Protein_{initial})} x100 \quad \textbf{(6)}$$

$$P_x\ (\%) = \text{wt\%}\ Protein_x \quad \textbf{(7)}$$

The recovery yield was calculated by dividing the protein weight in the purified fraction by the initial protein weight (before purification). The purity was calculated by the weight percentage of the desirable protein (either Ova, Cyt c, or Azo) present in the purified fraction.

2.6. Isolation of model proteins

The polishing step was performed for the purified protein phases envisioning the industrial applicability of this integrated approach. The acid precipitation of azocasein was performed from the top phase of AMTPS, using 0.1 M of trichloroacetic acid (TCA), being the pellet dissolved in 0.1 M of NaOH (**Fig. A5** of **Appendix A**). The copolymer recovery through azocasein precipitation was also confirmed by ^{1}H NMR and ATR-FTIR. The recovery of both cytochrome c and ovalbumin in the bottom phase of ATPS was achieved through ultrafiltration using a 30 kDa cut-off membrane, through Amicon Ultra-15 Centrifugal Filter Units.

2.7. Environmental assessment

The environmental evaluation of the downstream process developed in this work, was carried by the estimation of its carbon footprint for the most performant separation system [Pluronic L-35 triblock + potassium phosphate buffer (K_2HPO_4/KH_2PO_4)]. The analysis of the carbon footprint was done considering the application of both (i) ATPS and (ii) AMTPS platforms, the proteins fractionation using ultrafiltration (iii) as well as for the polishing step using acid precipitation (iv). The carbon footprint is the sum of greenhouse gas (GHG) emissions, associated with the system tested, expressed as mass of carbon dioxide equivalent ($CO_{2\ eq.}$) from a life cycle perspective.

The production of all the solvents (potassium phosphate buffer, Pluronic L-35 triblock copolymer, TCA, NaOH, distilled water), and the electricity consumed during the operation of the equipment was included in this assessment. Data on the amounts of solvents, distilled water and equipment operating time were obtained during the

experiment, while equipment power was taken from equipment catalogues (**Table A.10 at Appendix A**). Data on GHG emissions from the production of all solvents and electricity were sourced from Ecoinvent database version 3.4, being presented in **Table A.11 at Appendix A**.[21] The GHG emissions for the production of distilled water were calculated based on GHG emissions from tap water production[22] and GHG emissions from electricity consumption during the distillation process. The carbon footprint was calculated for 1 kg of the aqueous system.

3. Results and Discussion

3.1. Design and characterization of the separation process

The present work reports a novel approach for the separation of proteins. This is divided into two sequential liquid-liquid extraction steps, a first step based in ATPS and a second step based in AMTPS.

3.1.1. Measurement of the ATPS phase diagrams and *tie-lines*

The ATPS were characterized through the measurement of the phase diagrams and tie-lines (*TL*s), aiming at understanding the effect of different inorganic salts and the copolymer nature along with the influence of surfactants used as adjuvants on their formation. The phase diagrams were determined for all the ATPS studied, as depicted in **Figs 2.16**, **2.17**, and **2.18**. All curves were determined using the cloud-point titration method at 25 ± 1ºC and atmospheric pressure. The experimental points were correlated using the Merchuk equation.[18] Its parameters (A, B and C) used on the description of the experimental binodal data as well as the experimental data for the phase diagrams are reported in **Tables A.3-6 at Appendix A**. The experimental *TL*s, along with their respective length (tie-line length, *TLL*s), are reported in **Table A.7 at Appendix A**. The *TLL* is a numerical indicator of the difference between the compositions of the two phases and it is generally used to correlate trends in the partition of solutes between both phases. The mixtures with total compositions along a specific *TL* have different mass or volume ratios from those of the two coexisting phases, though the composition of each phase is maintained.[23]

Regarding the effect of inorganic salts in the ATPS formation, their aptitude to promote the phase separation was studied for potassium phosphate salts, namely K_2HPO_4, KH_2PO_4, K_3PO_4 and K_2HPO_4/KH_2PO_4. The study of inorganic salt nature has been performed on ATPS composed of Pluronic L-35 as the phase former in presence of small amounts of Triton X-100 (*circa* of 1 wt%) – **Fig. 2.16**. Herein, the ability to promote the two-phase formation follows the order: $K_3PO_4 > K_2HPO_4/KH_2PO_4 \approx K_2HPO_4 > KH_2PO_4$. In general, the potassium phosphate salts with higher *salting-out* strength exhibit a wider biphasic region. This observation corroborates the qualitative trend on the salt cations ability to induce the *salting-out* nature of the copolymer, which follows closely the Hofmeister series[24] with KH_2PO_4 and K_3PO_4 being the weakest and strongest *salting-out* agents, respectively. Considering the buffer capacity of the potassium phosphate buffer (K_2HPO_4/KH_2PO_4), a very attractive aspect for the proteins separation, along with its larger biphasic region, this system was adopted in the following studies.

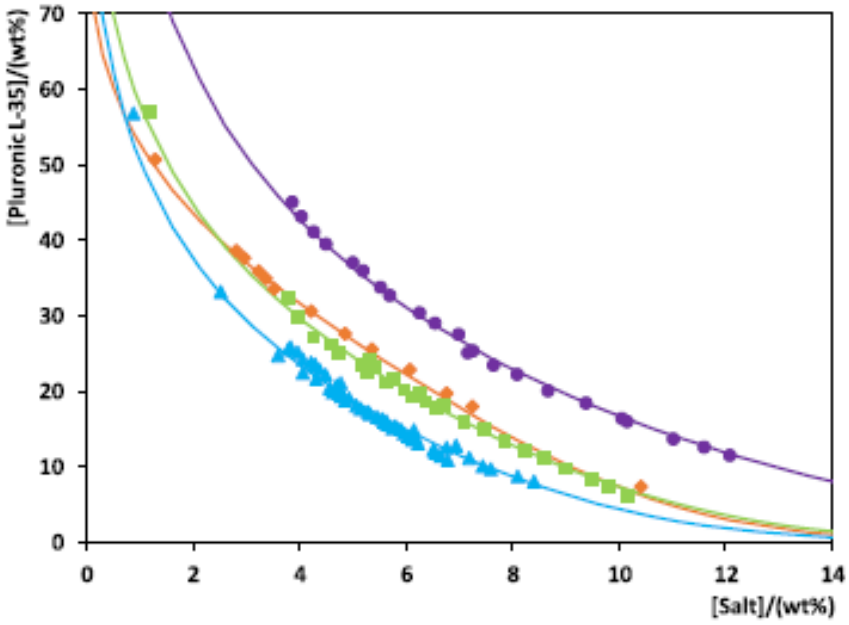

Fig. 2.16. Phase diagrams of the copolymer Pluronic L-35 and inorganic salts - **(♦)** K_2HPO_4; (●) KH_2PO_4; (▲); K_3PO_4 and (■) K_2HPO_4/ KH_2PO; at 25ºC. The lines represent the Merchuk fit through **Eq. 1.**

The presence of a surfactant as adjuvant was evaluated in terms of its ability to promote the two-phase formation by using small amounts (*circa* of 1 wt%) of two non-ionic surfactants, namely Triton X-114 and Triton X-100. These surfactants possess a similar chemical structure, varying only in the number of ethoxylate groups forming the surfactant's crown and thus, its hydrophilicity (*cf*. the hydrophilic-lipophilic balance

(HLB) of the surfactants is presented in **Table A.12 at Appendix A**). The surfactants' influence was analysed in a Pluronic L-35 + potassium phosphate buffer-based ATPS and compared with the conventional system (without any adjuvant present) – **Fig. 2.17.**. The results show that the use of these co-surfactants does not significantly affects the binodal curves, and thus the phases separation in this system.

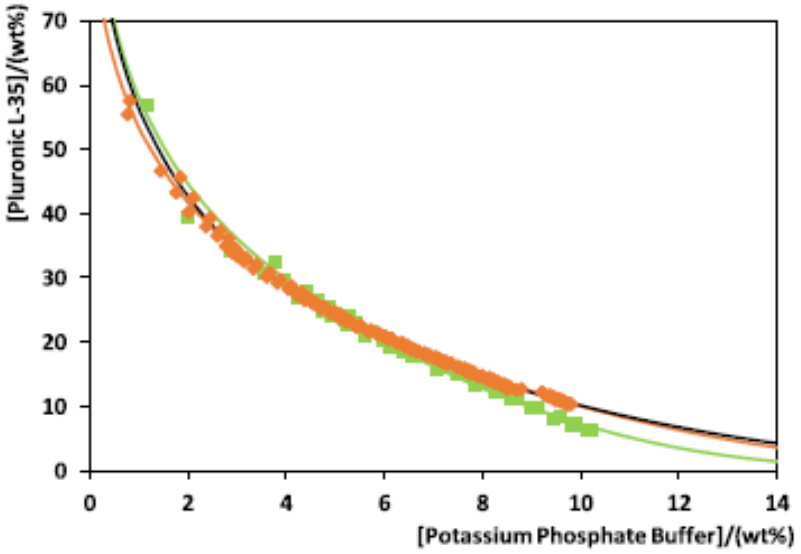

Fig. 2.17. Phase diagrams of the copolymer Pluronic L-35 + potassium phosphate buffer (pH = 6.6), without the addition of surfactant (—); and with the addition of 1 wt% of Triton X-100 (■); and Triton X-114 (♦), at 25ºC. The lines represent the Merchuk fit through **Eq.1**.

The copolymer nature (normal *versus* reverse) and composition (weight percentage of PEG units, *cf*. **Table A.7 at Appendix A**) were two other aspects explored on the phase diagrams. Three different copolymers were selected, namely Pluronics 17R4, 10R5 and L-35 and studied using a pseudo-ternary system composed of potassium phosphate buffer (pH = 6.6). The respective phase diagrams are present in **Fig. 2.18.**, where a tendency can clearly be established, considering their capacity to form two phases, as Pluronic 17R4 > Pluronic 10R5 > Pluronic L-35. Herein, Pluronic 17R4 holds the wider biphasic region, due to its more hydrophobic nature, considering the 60 wt% of PPG in its composition compared with the 50 wt% in the remaining copolymers. In contrast, Pluronic L-35 displays the narrowest biphasic region, though with only a small difference for Pluronic 10R5. This difference is a result of the copolymer structural rearrangement, *i.e.* Pluronic L-35 is composed of repetitive units of PEG-PPG-PEG, while Pluronic 10R5 presents sequences of PPG-PEG-PPG. Therefore, the normal copolymer evidences a

higher hydrophilicity owing to the two PEG units, resulting in a lower ability to form the two-phases.

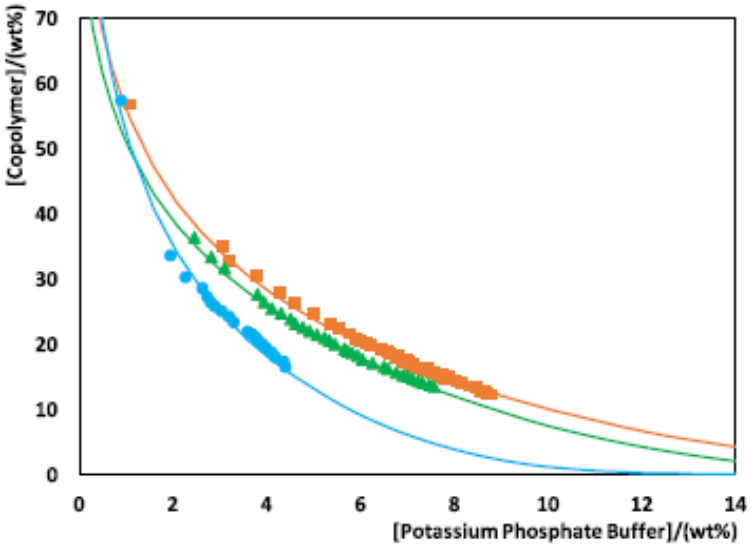

Fig. 2.18. Phase diagrams obtained for the copolymers: Pluronic 17R4 (●); Pluronic 10R5 (▲); and Pluronic L-35 (■) + potassium phosphate buffer (pH = 6.6), at 25ºC. The lines represent the Merchuk fit through **Eq.1**.

3.1.2. Measurement of the AMTPS coexisting curves

As thermo-responsive copolymers, these systems can be induced to form two-phases using temperature as the driving force. The cloud points were determined, and the phase diagrams are presented in **Fig. 2.19.** These results show that the copolymer nature and composition display a major effect on the AMTPS formation, namely upon the cloud points. Once again, the ability of the copolymers to form the biphasic region follows the tendency of Pluronic 14R4 > Pluronic 10R5 > Pluronic L-35. The main difference is that now, there is the formation of an AMTPS instead of a simpler ATPS, which means that the phase separation occurs due to the micelles coalescence in one phase and is not a result of the copolymer being *salted-out* by the salt. Herein, there is a complex balance of distinct interactions (electrostatic interactions, hydrophobic associations, hydrogen bonds and van der Waals forces), which in turn affects both solute-solute and solute-solvent interactions.[25] Moreover, it is well known that the addition of a co-surfactant can, not only reduce the system cloud points, but also improve the system extractive performance.[25,26] This is the best option in terms of the cloud point extraction of labile proteins, and thus, the quaternary system composed of Pluronic L-35 + potassium phosphate buffer (+ water) + Triton X-114 was also characterized and depicted in **Fig.**

2.19. (dashed line and square symbol).

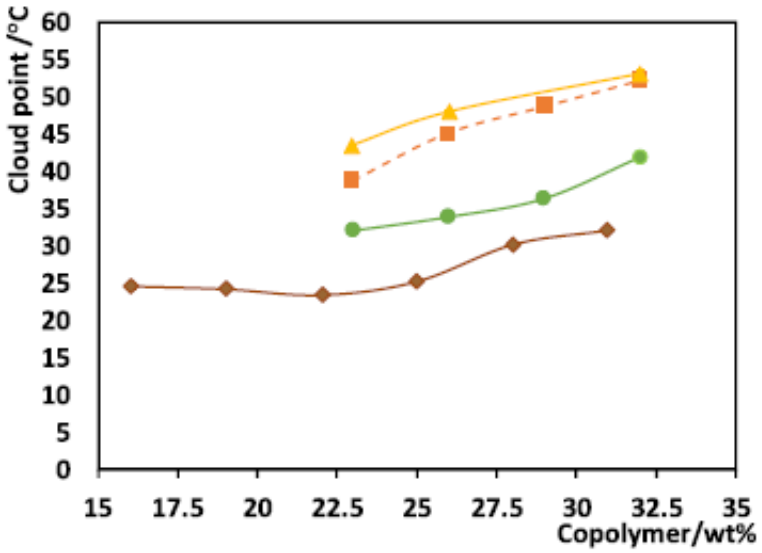

Fig. 2.19. Coexistence curves for the ternary systems with potassium phosphate buffer + water + Pluronic 17R4 (♦); Pluronic 10R5 (●); and Pluronic L-35 (▲); and for the quaternary system composed of potassium phosphate buffer + Pluronic L-35 + water + 1 wt% of Triton X-114 (--■--).

Through these results, it is visible a slight reduction of the cloud point temperatures of this system in comparison with the pseudo-ternary system composed of Pluronic L-35, but in absence of Triton X-114 as co-surfactant. Since both Pluronic L-35 and Triton X-114 are non-ionic surfactants above their CMC, non-ionic mixed micelles are formed. Nevertheless, it seems that there is a dominance of the copolymer in the aggregate's formation, since it is present in higher concentration.

3.2. Optimization of the proteins partition applying ATPS and AMTPS

Once the phase diagrams had been characterized, a mixture point was selected, considering two criteria, the water content, and an appropriate temperature, above the system cloud point, but not too high to maintain the proteins thermal stability. As previously mentioned, cytochrome c, azocasein and ovalbumin were the model proteins selected (*cf.* properties in **Table A.8 at Appendix A**). The ternary system composed of Pluronic 17R4 was not used due to experimental restrictions imposed by its very low cloud point (25ºC).

Thus, the systems studied in the partition of proteins were the ones constituted by Pluronic L-35 and Pluronic 10R5 and the quaternary system composed of Pluronic L-35 + potassium phosphate buffer + water + Triton X-114. The ATPS and AMTPS prepared to

perform the partition tests are exemplified by the case of Pluronic L-35 as presented in **Fig. A.1** of **Appendix A**.

The recovery and partition coefficient data obtained for each model protein in both (top and bottom) phases of the ATPS and AMTPS were determined, and the results presented in **Figs 2.20.**, **2.21.**, **A.2** and **A.3** (**Appendix A**). From the Recovery results displayed in **Figs 2.20.** and **2.21.** and corroborated by the partition coefficient data **(Figs A.2** and **A.3** of **Appendix A**), it is clear the cytochrome c (red bars) preferential partition to the bottom/salt-rich phase whereas azocasein (blue bars) was completely recovered in the top/copolymer-rich phase. Contrarily, the ovalbumin (green bars) partition was found to be dependent on the system, since for Pluronic L-35-based AMTPS, ovalbumin is mainly recovered in the top phase, while for Pluronic 10R5, this protein partitions preferably for the bottom-phase of the ATPS.

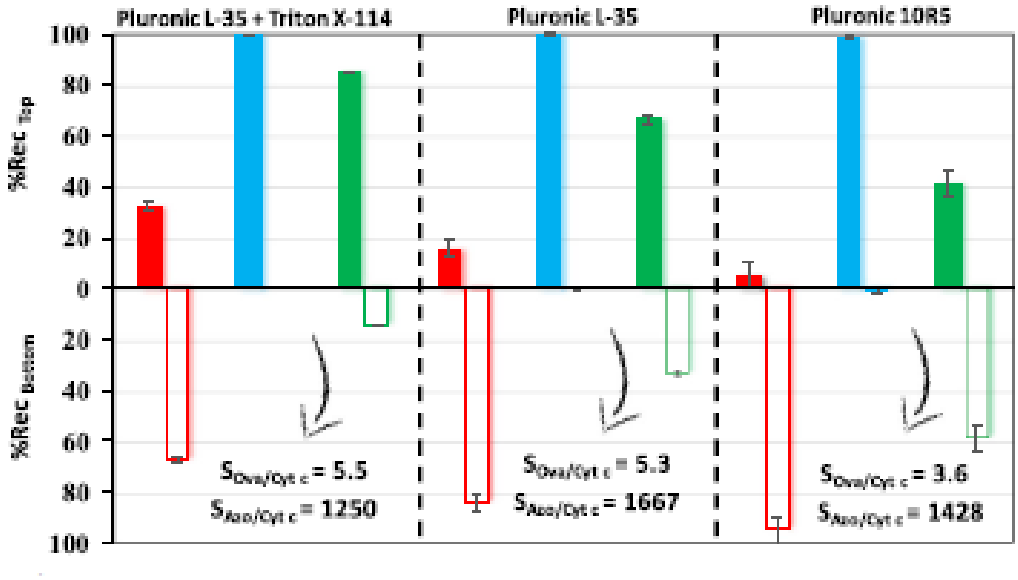

Fig. 2.20. Recovery data obtained for the three proteins regarding top/copolymer-rich phase (*%Rec Top*) and bottom/salt-rich phase (*%Rec Bottom*) and respective standard deviations (σ) by using the different ATPS: cytochrome c, Cyt c (■); azocasein, Azo (■); and ovalbumin, Ova (■). For each system studied the selectivity results are reported.

The cytochrome c preferential partition to the salt-rich phase can be improved by the proper choice of the copolymer, being this partition more pronounced for Pluronic 10R5 (*%Rec Bottom* = 95 ± 5 %). It is also clear that electrostatic interactions between proteins and the buffer are not the only parameter influencing the proteins' partition behaviour since both cytochrome c and ovalbumin partition varies with the copolymer applied. For

instance, when the normal is replaced by the reverse Pluronic, the ovalbumin partition tendency completely changed with around 60% of this protein being concentrated not in the polymeric phase but in the salt-rich phase. This leads to the conclusion that some more specific interactions between the copolymers and ovalbumin should be occurring and dictating its partition. Likewise, cytochrome c recovery is also improved with this copolymer replacement, suggesting that the more hydrophobic character of Pluronic 10R5 might be forcing more cytochrome c to migrate towards the more hydrophilic phase.

Regarding the presence of Triton X-114 as co-surfactant, it was found that the ovalbumin recovery is enhanced by 20% to the copolymer-rich phase. This reinforces the notion that some specific interactions between the system phase formers and the proteins contribute to their partition.

To further elucidate the ability of these systems to separate the proteins, the ATPS selectivity was also determined. As expected, higher selectivity values were obtained for the Pluronic L-35 in the partition of ovalbumin and cytochrome c. Even though the presence of Triton X-114 affects the partition of proteins, a negligible effect is observed when the proteins selectivity (especially $S_{\text{Ova/Cyt c}}$) is investigated. Nevertheless, outstanding selectivity values were obtained for the partition of azocasein and cytochrome c in all the studied systems (S > 1250).

Sequentially, the ATPS top phase was submitted to a temperature above the cloud point of each system and allowed it to separate into two macroscopic phases, aiming at separating ovalbumin and azocasein in the end. Once again, azocasein migrated completely towards the top/surfactant-rich phase while ovalbumin partitioned mostly to the bottom/surfactant-poor phase. The ability to fractionate both model proteins in the AMTPS is described by the trend: Pluronic 10R5 < Pluronic L-35 + 1 wt% Triton X-114 < Pluronic L-35. The differential partition between the two proteins can be explained by their molecular weights and hydrophobic/hydrophilic character.[26,27] The smallest and more hydrophobic protein, in this case azocasein, is recovered inside the micelles, while ovalbumin, due to its higher molecular weight and more hydrophilic character, is excluded to the most hydrophilic phase, the surfactant-poor phase. As far as the pseudo-ternary and quaternary systems with Pluronic L-35 are concerned, it can be assumed

that the micelle complexity of the quaternary AMTPS hinders the partition of ovalbumin towards the surfactant-rich phase. Therefore, the addition of a co-surfactant is not so selective as it was in the first separation step, probably by the nature of the mixed micelles created.[26] Taking these results into account, the system with Pluronic L-35 was identified as the most selective system for the two fractionation steps.

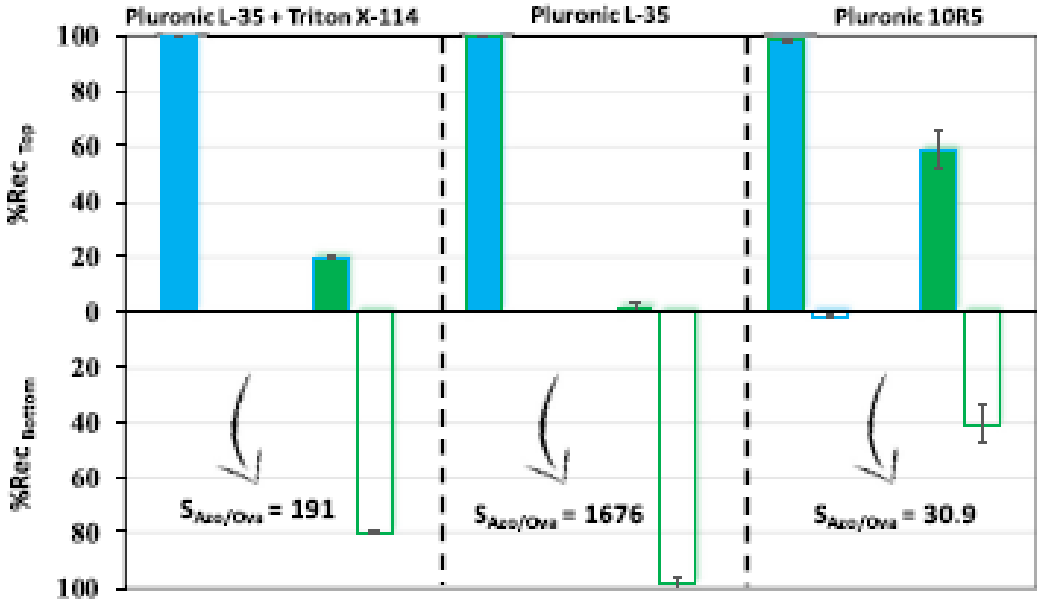

Fig. 2.21. Recovery values obtained for the surfactant-rich phase (*%Rec Top*) and surfactant-poor phase (*%Rec Bottom*), with the respective standard deviations (σ) by applying AMTPS to separate azocasein (■); and ovalbumin (■). For each system studied the selectivity results are presented.

3.3. Sequential fractionation of the protein mixture

The separation of the three proteins present in a single mixture was performed for the most selective system composed of Pluronic L-35 + potassium phosphate buffer + water. The isolation of each protein from the phase formers was a step also investigated in this work and corroborated by distinct techniques. Herein, two different parameters were considered to analyse the proteins purification owing to the use of a complex protein mixture, namely the proteins recovery (R_x) in each phase and their purity (P_x). This data is presented in **Figs 2.22.** and **A.4** (of **Appendix A**). As expected, the protein partition of ovalbumin, azocasein and cytochrome c maintained almost the same partition profile as previously observed for each protein when individually tested (section 2.2 of this work). Herein, cytochrome c was completely recovered in the salt-rich phase of the ATPS ($R_{Cyt\ c}$ = 100% and $P_{Cyt\ c}$ = 14%), which was an improvement compared to the results previously

obtained for each protein tested individually. However, ovalbumin partitioned almost completely to the salt-rich phase contrarily to the expected (R_{Ova}= 96% and P_{Ova} = 86%), being the remaining concentration separated from azocasein in the second fractionation step, applying the AMTPS. In this case, azocasein was completely recovered in the surfactant-rich phase (R_{Azo} = 100% and P_{Azo} = 100%), whereas the ovalbumin still present in the system was totally concentrated in the surfactant-poor phase (R_{Ova}= 4% and P_{Ova} = 100%). In the end, an ultrafiltration step was applied to isolate cytochrome c and ovalbumin, obtaining a cytochrome c recovery of 89% with a 74% purity and recovering 97% of an almost pure (99%) ovalbumin. Aiming at the industrial potential of the integrated process developed, an isolation step was considered in this integrated process enabling the reuse of copolymer for additional cycles of purification. For this step, an acid precipitation of Azo was carried using TCA (0.1 M at pH 3-4) to promote the azocasein isolation from Pluronic L-35, as represented in **Figure A.5** of **Appendix A**. After Azo precipitation, the pellet was microfuged at maximum speed and the supernatant was discharged, being applied a solution of NaOH (0.1 M) to further dissolve the precipitated protein. Both the azocasein isolation and copolymer recovery were confirmed through ^{1}H NMR and FTIR, as shown in **Figs A.6** and **A.7** of **Appendix A**, respectively. The NMR data seems identical before and after the polishing step, **Fig. A.6**, however, the FT-IR spectra were different. In **Fig. A.7**, the main differences between the aqueous copolymer solution (black line) and the supernatant (red line) presenting essentially Pluronic L-35 correspond to the amount of water present in the solutions (*cf*. 1625 cm^{-1}: water H-O-H bend and 3400-3200 cm^{-1}: water O-H stretch). The potassium phosphate buffer was not recovered since it is a common media used to stabilize proteins.

Overall, high purities (> 74 %) were obtained for the four distinct polished streams: *iv)*, *v)*, *vii)* and *ix)*, as presented in **Fig. 2.22**. It should be stressed that *circa* of 5 wt% of Pluronic L-35 is still present in stream ix); yet, this copolymer concentration is at an acceptable concentration approved by FDA.[28] Summing up, a high-performance separation process was here developed by the sequential application of ATPS and AMTPS to separate ovalbumin (maximum yield and purity of 97% and 99%, respectively),

azocasein (maximum yield and purity of 100%) and cytochrome c (maximum yield and purity of 89% and 74%, respectively).

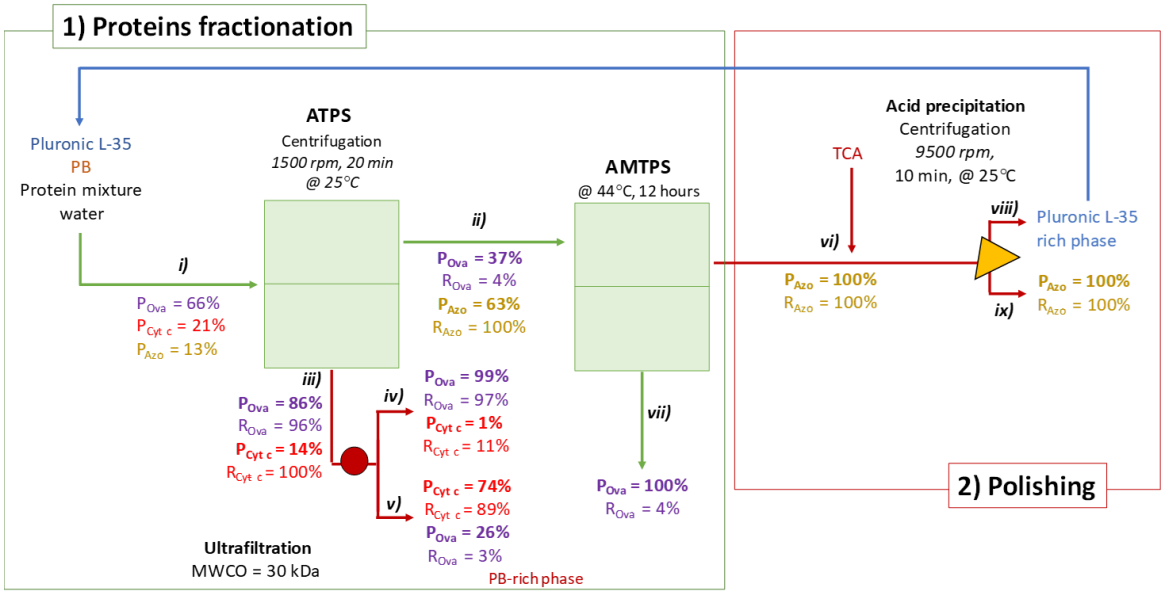

Fig. 2.22. Diagram of the integrated process to selectively separate cytochrome c (Cyt c), ovalbumin (Ova) and azoasein (Azo). The proposed strategy includes two steps of purification using, respectively, ATPS and AMTPS based on Pluronic L-35 and potassium phosphate buffer - PB (pH = 6.6). The purity (P_x) and recovery (R_x) of each step is provided in the present diagram. An ultrafiltration was applied to improve the separation of Cyt c and Ova and an acid precipitation was applied to isolate the Azo from Pluronic L35. The potassium phosphate buffer was maintained in the Azo-rich phase as a stabilizing solution.

3.4. Environmental assessment

Fig. 2.23. shows the results of the carbon footprint of the novel purification platform of proteins complex matrices *per* 1 kg of aqueous system. The total carbon footprint is equal to 117 kg $CO_{2\,eq}$. The contribution of the fractionation process (79 kg $CO_{2\,eq.}$), which includes the ATPS, AMTPS and ultrafiltration steps, represents ~67% of the total carbon footprint, is dominated by the ultrafiltration step (~49%). The proteins isolation process contributes with 39 kg $CO_{2\,eq}$. This process encompasses the acid precipitation step, representing ~33% of the total carbon footprint. The main contribution to the carbon footprint comes from the electricity consumption, more precisely, the electricity consumption in the centrifugation processes of the ultrafiltration and acid precipitation steps (representing a contribution of 99.6 % and 99.9 % of the carbon footprint for each step, respectively). The carbon footprint of the ATPS step is also dominated by electricity consumption, mainly by the centrifuge, contributing to 95 % of the carbon footprint.

However, it should be noted that the energy consumption of some equipment should be reviewed in view of the system industrial implementation.

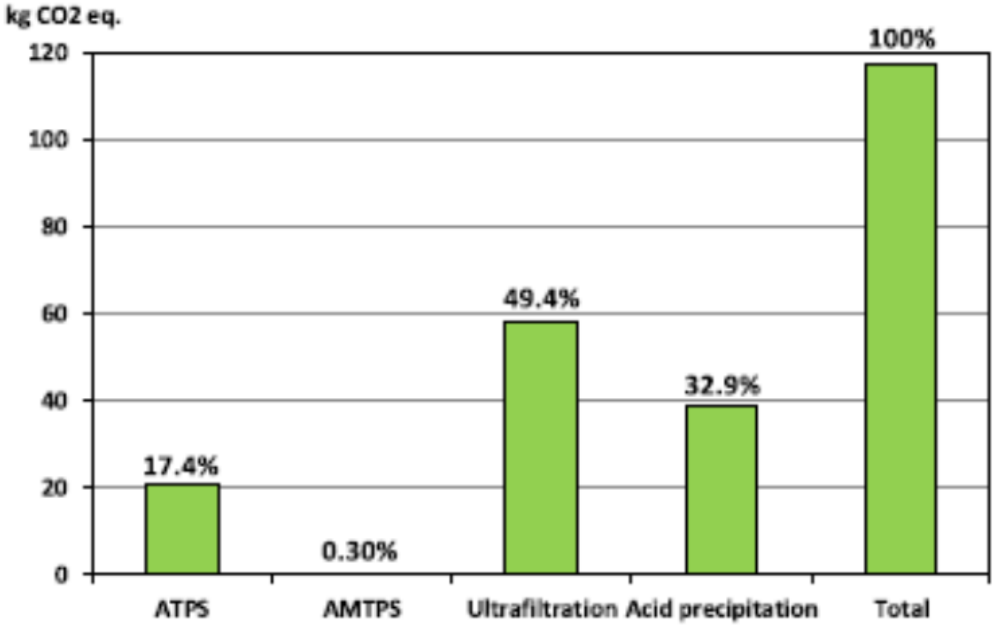

Fig. 2.23. Carbon footprint for the two scenarios proposed for 1 kg of aqueous system.

4. Conclusions

An integrated purification platform composed of ATPS and AMTPS was here proposed for the fractionation of different biomolecules present in complex matrices. Both the ATPS and AMTPS were first characterized, and then applied in the fractionation of a mixture of three model proteins, namely cytochrome c, azocasein and ovalbumin. The results herein obtained showed that the ternary system composed of Pluronic L-35 (23 wt%) + potassium phosphate buffer (6 wt%) was the most selective system as proved by the selectivity values achieved: $S_{Azo/Cyt}$=1667, $S_{Ova/Cyt}$=5.33 and $S_{Azo/Ova}$=1676. The combination of these two liquid-liquid extraction units emerged as an attractive platform to improve the extraction and purification of proteins, with a final fractionation of cytochrome c and ovalbumin being achieved through ultrafiltration and an acid precipitation carried out to isolate azocasein from the copolymer. Finally, the carbon footprint was evaluated to better understand the environmental impacts of this new protein purification process. The main contribution to the total carbon footprint of the system comes from the ultrafiltration (~49%) and acid precipitation (~33%) steps mainly due to their energy consumption.

References

1. Abhinav A. Shukla, Mark R. Etzel, S. G. *Process Scale Bioseparations for the Biopharmaceutical Industry*. (CRC Press, 2006).
2. Berg, J. M., Tymoczko, J. L. & Stryer, L. *Biochemistry.: Section 4.1 The Purification of Proteins Is an Essential First Step in Understanding Their Function*. (New York: WH Freeman, 2002).
3. Ventura, S. P. M., Nobre, B. P., Ertekin, F., Hayes, M., Garciá-Vaquero, M., Vieira, F., Koc, M., Gouveia, L., Aires-Barros, M. R. & Palavra, A. M. F. in *Microalgae-Based Biofuels Bioprod.* 461–483 (Elsevier, 2018).
4. Balina, K., Romagnoli, F. & Blumberga, D. Seaweed biorefinery concept for sustainable use of marine resources. *Energy Procedia* **128,** 504–511 (2017).
5. Asenjo, J. A. & Andrews, B. A. Protein purification using chromatography: selection of type, modelling and optimization of operating conditions. *J. Mol. Recognit. An Interdiscip. J.* **22,** 65–76 (2009).
6. Asenjo, J. A. & Andrews, B. A. Aqueous two-phase systems for protein separation: A perspective. *J. Chromatogr. A* **1218,** 8826–8835 (2011).
7. Wan, Y., Cui, Z. & Ghosh, R. Fractionation of Proteins Using Ultrafiltration: Developments and Challenges. *Dev. Chem. Eng. Miner. Process.* **13,** 121–136 (2008).
8. Cui, Z. Protein separation using ultrafiltration — an example of multi-scale complex systems. *China Particuology* **3,** 343–348 (2005).
9. Zittle, C. A. & DellaMonica, E. S. Separation of proteins by gradient solvent extraction of a protein precipitate. *Arch. Biochem. Biophys.* **58,** 31–36 (1955).
10. Yu, H. & Ito, Y. Preparative separation of proteins using centrifugal precipitation chromatography based on solubility in ammonium sulfate solution. *Prep. Biochem. Biotechnol.* **34,** 1–12 (2004).
11. Yau, Y. K., Ooi, C. W., Ng, E.-P., Lan, J. C.-W., Ling, T. C. & Show, P. L. Current applications of different type of aqueous two-phase systems. *Bioresour. Bioprocess.* **2,** 49 (2015).
12. Molino, J. V. D., Viana Marques, D. de A., Júnior, A. P., Mazzola, P. G. & Gatti, M. S. V. Different types of aqueous two-phase systems for biomolecule and

bioparticle extraction and purification. *Biotechnol. Prog.* **29,** 1343–1353 (2013).

13. Ventura, S. P. M., e Silva, F. A., Quental, M. V, Mondal, D., Freire, M. G. & Coutinho, J. A. P. Ionic-Liquid-Mediated Extraction and Separation Processes for Bioactive Compounds: Past, Present, and Future Trends. *Chem. Rev.* **117,** 6984–7052 (2017).
14. Iqbal, M., Tao, Y., Xie, S., Zhu, Y., Chen, D., Wang, X., Huang, L., Peng, D., Sattar, A., Shabbir, M. A. B., Hussain, H. I., Ahmed, S. & Yuan, Z. Aqueous two-phase system (ATPS): an overview and advances in its applications. *Biol. Proced. Online* **18,** 18 (2016).
15. Alexandridis, P. Poly(ethylene oxide)/poly(propylene oxide) block copolymer surfactants. *Curr. Opin. Colloid Interface Sci.* **2,** 478–489 (1997).
16. Persson, J., Nyström, L., Ageland, H. & Tjerneld, F. Purification of recombinant and human apolipoprotein A-1 using surfactant micelles in aqueous two-phase systems: Recycling of thermoseparating polymer and surfactant with temperature-induced phase separation. *Biotechnol. Bioeng.* **65,** 371–381 (2000).
17. Merchuk, J. C., Andrews, B. a & Asenjo, J. a. Aqueous two-phase systems for protein separation. *J. Chromatogr. B Biomed. Sci. Appl.* **711,** 285–293 (1998).
18. Chakraborty, A. & Sen, K. Impact of pH and temperature on phase diagrams of different aqueous biphasic systems. *J. Chromatogr. A* **1433,** 41–55 (2016).
19. Shahriari, S., Neves, C. M. S. S., Freire, M. G. & Coutinho, J. A. P. Role of the Hofmeister Series in the Formation of Ionic-Liquid-Based. *J Phys Chem B.* **116,** 7252–7258 (2012).
20. Vicente, F. A., Cardoso, I. S., Sintra, T. E., Lemus, J., Marques, E. F., Ventura, S. P. M. & Coutinho, J. A. P. Impact of Surface Active Ionic Liquids on the Cloud Points of Nonionic Surfactants and the Formation of Aqueous Micellar Two-Phase Systems. *J. Phys. Chem. B* **121,** 8742–8755 (2017).
21. Vicente, F. A., Malpiedi, L. P., Silva, F. A. e, Jr., A. P., Coutinho, J. A. P. & Ventura, S. P. M. Design of novel aqueous micellar two-phase systems using ionic liquids as co-surfactants for the selective extraction of (bio)molecules. *Sep. Purif. Technol.* **135,** 259–267 (2014).
22. Liu, C. L., Nikas, Y. J. & Blankschtein, D. Novel bioseparations using two-phase

aqueous micellar systems. *Biotechnol. Bioeng.* **52,** 185–92 (1996).

23. Safety Assessment of Poloxamers 101, 105, 108, 122, 123, 124, 181, 182, 183, 184, 185, 188, 212, 215, 217, 231, 234, 235, 237, 238, 282, 284, 288, 331, 333, 334, 335, 338, 401, 402, 403, and 407, Poloxamer 105 Benzoate, and Poloxamer 182 Dibenzoate as Use. *Int. J. Toxicol.* **27,** 93–128 (2008).
24. Ventura, S. P. M., Neves, C. M. S. S., Freire, M. G., Marrucho, I. M., Oliveira, J. & Coutinho, J. A. P. Evaluation of Anion Influence on the Formation and Extraction Capacity of Ionic-Liquid-Based Aqueous Biphasic Systems. *J. Phys. Chem. B* **113,** 9304–9310 (2009).
25. Louros, C. L. S., Cláudio, A. F. M., Neves, C. M. S. S., Freire, M. G., Marrucho, I. M., Pauly, J. & Coutinho, J. A. P. Extraction of Biomolecules Using Phosphonium-Based Ionic Liquids + K3PO4 Aqueous Biphasic Systems. *Int. J. Mol. Sci.* **11,** 1777–1791 (2010).
26. Blankschtein, D., Thurston, G. M. & Benedek, G. B. Phenomenological theory of equilibrium thermodynamic properties and phase separation of micellar solutions. *J. Chem. Phys.* **85,** (1986).
27. Ecoinvent, http://www.ecoinvent.org. (2018).
28. Lemos, D., Dias, A. C., Gabarrell, X. & Arroja, L. Environmental assessment of an urban water system. *J. Clean. Prod.* **54,** 157–165 (2013).

3. PEGylation Reaction

3.1. Novel biobetter of monoPEGylated ASNase for the treatment of acute lymphoblastic leukemia

Meneguetti, G. P., **Santos, J. H. P. M**., Obreque, K. M. T., Barbosa, C. M. V., Monteiro, G., Farsky, S. H. P., Oliveira, A. M., Angeli, C. B., Palmisano, G., Ventura, S. P. M., Junior, A. P. & Rangel-Yagui, C. O. *Plos One*, 2019, 14(2): e0211951. https://doi.org/10.1371/journal.pone.0211951.[5]

Abstract

L-asparaginase (ASNase) from *Escherichia coli* is currently used in some countries in its PEGylated form (ONCASPAR®, pegaspargase) to treat acute lymphoblastic leukemia (ALL). PEGylation refers to the covalent attachment of poly(ethylene) glycol to the protein drug and it not only reduces the immune system activation but also decreases degradation by plasmatic proteases. However, pegaspargase is randomly PEGylated and, consequently, with a high degree of polydispersity in its final formulation. In this work we developed a site-specific N-terminus PEGylation protocol for ASNase. The monoPEG-ASNase was purified by anionic followed by size exclusion chromatography to a final purity of 99%. The highest yield of monoPEG-ASNase of 42% was obtained by the protein reaction with methoxy polyethylene glycol-carboxymethyl *N*-hydroxysuccinimidyl ester (10 kDa) in 100 mM PBS at pH 7.5 and PEG:ASNase ratio of 25:1. The monoPEG-ASNase was found to maintain enzymatic stability for more days than ASNase, also was resistant to the plasma proteases like asparaginyl endopeptidase and cathepsin B. Additionally, monoPEG-ASNase was found to be potent against leukemic cell lines (MOLT-4 and REH) *in vitro* like polyPEG-ASNase. MonoPEG-ASNase demonstrates its potential as a novel option for ALL treatment, being an inventive novelty that maintains the benefits of the current enzyme and solves challenges.

Keywords: N-terminal PEGylation, biobetters, biopharmaceutics, therapeutic enzymes, acute lymphoblastic leukemia.

[5] Contributions: GM, JS, KO, CB, CA and GP acquired the experimental data. The conceptualization of this work was done by CY. The manuscript was mainly written by GM and JS, with contributions from all the authors.

1. Introduction

PEGylation is one of the most effective approaches to solve intrinsic problems of protein drugs, such as immunogenicity and short half-life. It refers to the covalent attachment of polyethylene glycol (PEG) on the protein surface.[1] PEG is a highly water-soluble polymer, with low immunogenicity and approved by the US Agency for Food and Drug Administration (FDA). PEG-protein conjugates have several advantages as increased solubility and stability, prolonged half-life in the body and decreased metabolic degradation by enzymes.[2] Thus, PEGylation has become a well-established technology, increasing the therapeutic potential of biopharmaceutics like the L-asparaginase (ASNase).[3]

L-asparaginase (L-asparagine amidohydrolase) is an enzyme used on chemotherapy schemes to treat acute lymphocytic leukemia (ALL). More than 95% complete remission is observed within 4 to 6 weeks of treatment of children with ALL.[4] More recently, researchers also showed that treatment with ASNase or dietary asparagine restriction reduces metastasis of breast cancer, what improves the potential uses of this drug.[5] However, hypersensitivity due to anti-ASNase antibodies is frequent with the use of the native enzyme from *Escherichia coli*. One available option to minimize hypersensitivity is pegaspargase (Oncaspar®), the PEGylated form of the enzyme. Pegaspargase also presents longer biological half-life than the native enzyme.[6] The FDA approval for pegaspargase to treat patients with hypersensitivity to the native form of the enzyme was granted in 1994 and in 2006, it was approved as treatment for children and adults with newly diagnosed ALL.[7] Nonetheless, only in 2015 the European Medicine Agency (EMA) granted a marketing authorization for the drug.[8] The method used for pegaspargase production is the conjugation of PEG to free amines, typically at lysine residues and at N-terminus. An important limitation of this approach is that proteins typically contain many lysine residues and, therefore, PEGylation is random, leading to a high degree of polydispersity on the resulting preparations.[9] Approximately 69-82 molecules of 5 kDa methoxylated PEG are conjugated to ASNase.[4] The main concern related to random PEGylation is that different PEGylated species often have different pharmacokinetic profiles and possibly different intrinsic biological activities.[10] One strategy to tackle the problem of random PEGylation is N-terminal site-specific

PEGylation (**Fig. B.1 at Appendix B**). It involves the conjugation of one PEG molecule to protein N-terminus, taking advantage of lower pKa of N-terminal α-amino group (7.5 to 8.5) compared with that of the ε-amino group in lysine (pK ≈ 10.5).[2] Therefore, at pH values between 7.0 and 8.5 the lysine amine residues are predominantly protonated and thus unreactive to PEG. A considerable fraction of N-terminus, in turn, is unprotonated and available for conjugation with PEG, resulting in monoPEGylated protein.[11]

In this work, an optimized protocol to synthesize an N-terminus PEGylated ASNase was developed. The monoPEG-ASNase produced is more stable over the time and *in vitro* resistant to plasma proteases than the non-PEGylated enzyme, while keeping the same activity against leukemic cell lines.

2. Materials and methods

2.1. Materials

E.C.3.5.1.1 L-asparaginase enzyme was commercially obtained from ProSpec Tany (Ness-Ziona, Central District, ISR). The reactive PEG polymers, methoxy polyethylene glycol-carboxymethyl *N*-hydroxysuccinimidyl ester 2, 5 and 10 kDa (mPEG-NHS) were purchased from NANOCS (New York, NY). All buffer solutions (phosphate buffered saline, PBS and tris(hydroxymethyl)aminomethane hydrochloride, Tris-HCl) were prepared with purified water from a Millipore Milli-Q system (Bedford, MA) and pH adjusted at room temperature (22 to 25 °C). All other reagents used were of analytical grade. Proteases asparagine endopeptidase (AEP) and a cathepsin B (CTSB) were purchased from Abcam (Cambrigde, Cambridgeshire, ENG). Leukemia cell lines, acute T-cell lymphoblastic leukemia (MOLT-4) and B-cell lines (REH), and healthy cell line, Human Umbilical Vein Endothelial Cells (HUVEC), were obtained from Rio de Janeiro (Brazil) cell bank.

2.2. ASNase PEGylation

The influence of the buffer ionic strength (10, 100 or 200 mM of PBS), PEG:ASNase molar ratio (25:1 or 50:1) and pH (6.0, 6.5, 7.0, 7.5 or 8.0) on site-specific PEGylation of ASNase was first investigated using a 2 kDa of mPEG-NHS. This molecular size presents a smaller hydrodynamic volume than the market attached 5 kDa mPEG-NHS, facilitating PEG

conjugation and initial understanding of how PEGylation happens. Nonetheless, PRG MW does not influence reaction conditions. The initial use of 2 kDa mPEG was a proof of concept, since this reactive PEG is relatively cheaper. Additionally, a significant excess of mPEG-NHS was used due to its susceptibility to suffer hydrolysis in aqueous solutions; these values of molar ratio are in accordance with previous works.[12-14] Each system, at selected conditions, was kept under mechanical stirring at room temperature (22 to 25 °C) for 30 minutes. After that, 20 mM hydroxylamine was added to cleave any unstable PEGylation site formed. All samples were analyzed by electrophoresis (SDS-PAGE). Reaction yields were obtained based on electrophoresis band intensity using the ImageJ software.[15]

After defining the best ionic strength, PEG:ASNase ratio and pH for N-terminal PEGylation, an experiment was carried out to define the reaction time for higher yields of monoPEG-ASNase. Considering that time is very important parameter for the PEGylation reaction, the same protocol described above was employed at the best conditions and just changing time reaction. The samples were withdrawn every 15 minutes until 90 minutes, and PEG-ASNase concentration quantified based on electrophoresis band intensity. Subsequently, ultrafiltration (Amicon Ultra-15, 30 kDa MWCO) was used for buffer exchange, concentration of samples and removal of hydroxylamine and unreacted PEG from reaction. The final protocol was also applied to ASNase PEGylation with 10 kDa mPEG-NHS.

A similar pegaspargase (polyPEGylated ASNase) was also synthesized as a reference, by a random PEGylation protocol. Briefly, 5 kDa of mPEG-NHS and ASNase at 50:1 ratio were reacted for 1 h in 100 mM of PBS at pH 10.0, under magnetic stirring. Then, the reaction was stopped with 20 mM of hydroxylamine as described above.

2.3. Electrophoresis in polyacrylamide gel

Samples from PEGylation reactions were analyzed by SDS-PAGE[16] and to observe the enzymatic integrity of ASNase, the samples after the purification process were analyzed by native-PAGE. Proteins were stained with Coomassie Brilliant Blue, CBB[17] or silver.[18] Electrophoretic gel for separation was prepared with 522 mM of Tris-HCl (pH 8.8), 6%, 10% or 12% of acrylamide/bis-acrylamide, 0.09% (w/v) of ammonium persulphate (PSA),

and 0.19% (v/v) of tetramethylethylenediamine (TEMED). The packing gel was prepared with 116 mM of Tris-HCl (pH 6.8), 5% of acrylamide/bis-acrylamide, 0.14% (w/v) of PSA, and 0.29% (v/v) of TEMED. For SDS-PAGE, 0.1% (w/v) of sodium dodecyl sulfate (SDS) was added to the gels. Samples were prepared with 4x of protein buffer and 25 mM of dithiothreitol (DTT) for SDS-PAGE. The running buffer was Tris-Glycine/SDS 1x (pH 8.3) for SDS-PAGE and the gel was kept under 80 mA at room temperature (22 to 25 ºC). For native-PAGE, the buffer was Tris-Glycine 1x (pH 8.8) and the gel was kept under 100 mA at 4 ºC.

2.4. Purification of PEGylated ASNase

Purification was performed on a Fast Protein Liquid Chromatography GE Healthcare AKTA Explorer 100. The monoPEG-ASNase was purified with an anionic column Resource Q 6 mL (GE Healthcare Life Science, Marlborough/USA), equilibrated with buffer A (Tris-HCl, 20 mM at pH 7.0) and eluted with buffer B (Tris-HCl, 20 mM at pH 7.0, with 1 M of NaCl). The running protocol corresponded to 12 column volumes up to 170 mM of NaCl of linear gradient at a flow rate of 3 $mL.min^{-1}$. The protein elution profile was monitored by UV absorbance at 280 nm. Size exclusion chromatography (SEC), Superdex 200 Increase 10/300 GL (GE Life Sciences), was performed as a polishing step and also to estimate the monoPEG-ASNase molecular mass. This purification protocol corresponded to an isocratic elution with 50 mM of Tris-HCl (pH 8.6) buffer at a flow rate of 0.5 $mL.min^{-1}$.

Reference sample (polyPEG-ASNase) was also purified by SEC in isocratic elution with a flow rate of 0.5 $mL.min^{-1}$, but with 100 mM of PBS (pH 7.0) + 0.9% of NaCl buffer. Four standards from GE Healthcare Life Sciences were used: ferritin (440 kDa), conalbumine (75 kDa), carbonic anhydrase (29 kDa) and ribonuclease A (13.7 kDa). Dead column volume was determined by blue dextran 2000.

2.5. Determination of protein concentration

ASNase concentration was determined by the bicinchoninic acid (BCA) kit method (Merck-Sigma, Darmstadt, Germany), which is based on the detection of a purple copper complex that absorbs at 562 nm.[19] Spectrophotometric measurements were performed

in a Biophotometer Plus (Eppendorf) spectrophotometer. Samples were incubated with the BCA reagent for 30 minutes at 37 °C. Total protein concentration was obtained by interpolating the values of absorbance on a calibration curve of bovine serum albumin (BSA).

2.6. Determination of enzymatic activity of ASNase

Enzymatic activity of ASNase was determined by the Nessler method.[20] The method is based on the release of ammonium by ASNase enzymatic cleavage, which interacts with the Nessler's reagent giving rise to a brown colored compound (maximum absorption at 436 nm). One enzyme unit (U) is defined as the amount of enzyme required to produce 1 µmol of ammonia *per* minute, at pH 7.3 and 37 °C. The reaction system was composed of 24 mM of Tris-HCl buffer (pH 8.6), 9 mM of L-asparagine and the sample. The system was kept in a water bath at 37 °C for 30 minutes; the reaction was stopped with 68 mM of trichloroacetic acid (TCA). All experiments were performed in triplicate. Specific activity ($U.mg^{-1}$ of protein) was calculated based on protein concentration and ASNase activity determinations at the same day.

2.7. Kinetic analysis

The kinetic parameters of ASNase samples were determined by means of the NADH-coupled method.[21] The β-NADH oxidation was measured spectrophotometrically at 340 nm ($\varepsilon_{\beta\text{-NADH}} = 6.1\ \mu mol^{-1} \cdot cm^{-1}$) and 37 °C. Assays were performed in 96-well microplates. Each well received, final concentration, 50 mM of Tris–HCl, pH 8.6; L-asparagine at different concentrations (0.07, 0.1, 0.3, 0.5, 0.7, 1.5, 2.0 and 2.5 mM); 0.13 mM of β-NADH, 1 mM of α-ketoglutarate, 0.5 U of glutamate dehydrogenase (diluted in 50 mM of PBS, pH 7.4; 50% of glycerol) and 1.8 ± 0.2 U of the enzyme sample (ASNase, monoPEG-ASNase or polyPEG-ASNase), 30 minutes reaction time. Data analysis and statistical analysis (F-test) were done using the GraphPad Prism 5.0 program (La Jolla, California/USA).

2.8. Determination of PEGylated ASNase activity over time

Samples of monoPEG-ASNase, polyPEG-ASNase and free ASNase were maintained at 4 °C for 21 days to verify activity over storage time by quantifying protein concentration and enzymatic activity. Measurements were done in triplicate and a non-linear regression was fit using GraphPad Prism 5.0.

2.9. Dynamic light scattering - DLS

Dynamic light scattering (DLS) was used to determine the hydrodynamic *radius* of the conjugate samples. All measurements were performed on a Zetasizer Nano ZS, a DLS instrument, using non-invasive backscatter (NIBS) detection. The protein samples were at 1.0 $mg.mL^{-1}$ in saline buffer (50 mM of Tris-HCl, pH 8.6) where, for each protein, no subunit dissociation is expected. All samples were filtered before measurement using 0.22 µm or smaller pore size to remove large aggregates and the quantification of number size distributions was performed for each sample at 25ºC.

2.10. MALDI-TOF mass spectrometry

Matrix-assisted laser desorption/ionization (MALDI) coupled to time of flight (TOF) was used to determine the position of PEGylation. The proteins samples with and without PEG of 2 kDa and 10 kDa were treated initially with 10mM DTT to reduce disulfide bonds and alkylated with 55mM iodoacetamide to block the reduced thiols. Subsequently, trypsin was added to each protein sample in a 1:50 enzyme:protein ratio. The enzymatic reaction was blocked with 1%TFA and the tryptic peptides were desalted using R3 micro-columns as previously reported.[22] The tryptic digests were co-crystallized with α-Cyano-4-hydroxycinnamic acid matrix dissolved in 30:70 (v/v) (acetonitrile : 0.1% TFA in water) at a concentration of 10 $mg.mL^{-1}$. The MS spectra were acquired in reflectron positive ion mode in a 700-4000 m/z range. External calibration was performed for all spectra. The mzXML files were processed using Mass-Up.[23] The MALDI-TOF MS spectra were processed using baseline subtraction and smoothing. Subsequently, MS spectra were overlaid in order to evaluate the signal intensity of the tryptic peptides obtained from ASNase without PEG and with PEG 2 kDa and 10 kDa.

2.11. Evaluation of ASNase resistance to plasmatic proteases

The evaluation of resistance to proteolytic cleavage by asparaginyl endopeptidase (AEP) and cathepsin B (CTSB) was based on an adaptation of Patel et al. method.[24] Briefly, 4 µg of sample was added to 2 µg of CTSB or 1.8 µg AEP in 20 µL of Tris-HCl buffer (50 mM, pH 8.8) and kept under bath stirring at 37 °C for 84 hours. After, a Native-PAGE electrophoresis was performed. Zymography was also performed to detect enzyme activity.[25] After the Native-PAGE running, the gel was submerged in an enzyme reaction medium (30 mM of Tris-HCl, 38 mM of L-asparagine and 0.2 M of hydroxylamine hydrochloride at pH 7.0) and incubated at 37 °C for 30 minutes. Subsequently, the gel was washed with ultra-pure water and revealed with chromogenic iron chloride solution ($FeCl_3$, 10%, and TCA, 3.3 % (w/v), in 0.7 M of HCl). After 24 h the gel was flushed with CBB.

2.12. *In vitro* cytotoxicity assays

Mitochondrial viability (hence cell viability) was quantified by the reduction of MTT (3-(4,5-dimethylthiazol-2yl)-2,5-diphenyl tetrazoline bromide) by the enzyme succinate dehydrogenase present in the mitochondrial membrane, resulting in crystals of formazan, whose production is proportional to the number of metabolically active cells.[26] The assay was performed as described by Costa et al.[27]with acute T-cell lymphoblastic leukemia (MOLT-4) and B-cell lines (REH), and healthy human umbilical vein endothelial cell line (HUVEC). The cell lines were maintained in the Roswell Park Memorial Institute medium (RPMI 1640) with 10% of fetal bovine serum (v/v), L-glutamine and sodium pyruvate, incubated at 37 °C in a 5% of CO_2. Cells were pealed after reaching a high cell density, confluence greater than 90%. HUVEC line had its cells trypsinized with 0.05 $mL.cm^2$ of Trypsin/EDTA solution, ressuspended in fresh medium. After reaching confluence, cell lineages were centrifuged at 600 xg at 4 °C for 10 min and suspended in fresh RPMI medium. The visualization of cell viability was done with Trypan blue (Sigma-Aldrich, Darmstadt, Hessen, GER). Cells were counted in Neubauer's chamber. MOLT-4 or REH, at 1.0 x 10^4 cells/well and HUVEC, at 2.0 x 10^4 cells/well, were incubated in 96-well microplates with 0.01, 0.05, 0.1, 0.3 and 0.6 $U.mL^{-1}$ of ASNase samples (free, monoPEGylated and polyPEGylated) in 20 mM sodium phosphate buffer

pH 7.4. Ultrafiltration method (Amicon Ultra-30 kDa MWCO) was used for buffer SEC elution exchange and samples were filtered with 0.22 µm steric filter. MOLT-4 and REH were tested at the same plate. Control cells were RPMI medium and protein buffer (50 mM of Tris–HCl, pH 8.8) without enzyme. Then, 48 or 72 h later (at 37 °C in a 5% CO_2 incubator) a 0.25 $mg.mL^{-1}$ MTT solution was added. After 4 h, 1% of SDS was added and cells were incubated under the same conditions for more 24 h. The optical density reading was performed in a spectrophotometer at the wavelength of 540 nm. The results were expressed as a percentage of MTT reduction, having as parameter the control group, for which 100% reduction was attributed. The assays were done in triplicate and data analysis was carried with the program GraphPad Prism 5.0.

3. Results

3.1. ASNase PEGylation

Site-specific PEGylation at N-terminal region is highly influenced by pH, temperature, reaction time and ionic strength.[11] The latest is mainly determined by the ions dissolved and, therefore, the total concentration of electrolytes in solution.[28] Buffer ionic strength effect on conjugation of PEG to ASNase was investigated by varying molarity of PBS (pH 7.5): 10, 100 and 200 mM were investigated. Results presented in **Fig 3.1.A** show that best PEGylation yields were obtained with 100 mM of PBS. Regarding PEG:ASNase ratio, similar yields (42-45%) were observed for both 25:1 and 50:1 molar ratios (**Fig 3.1.B**). Nonetheless, at a PEG:ASNase ratio of 25:1, less polyPEGylated species were formed in comparison to 50:1 (7% and 19%, respectively).

After defining the best PBS molarity (ionic strength) and PEG:ASNase ratio, we investigated the effect of pH on PEGylation yields. Since ASNase N-terminal has a pKa_{LEU} of 7.6 (**Table B.1 at Appendix B**), we investigated the PEGylation reaction at a pH range from 6.5 to 8.0 and found that PEGylation increases with pH (**Fig 3.1.C, Fig. B.2 at Appendix B**). However, at pH 8.0 the monoPEGylation yield decreased with the concomitant increase of polyPEGylation. According to the results, PEGylation at pH 7.5 provides better yields with less than 10% of polyPEGylated species.

The effect of different reaction times from 0 to 90 minutes (**Fig 3.1.D, Fig. B.3 at Appendix B**) was also evaluated, and a maximum yield of 41% was observed in

monoPEGylated ASNase after 30 minutes of reaction, compared to 28% at 15 minutes and 40% at 45 minutes. Although the reaction time of 45 minutes showed similar yields to 30 minutes, the concentration of polyPEGylated species, in other words the polydispersity, was higher (13 and 17%, respectively). Additionally, the polydispersity increased with time and reached a maximum of 30% at 75 minutes of reaction time. At 30 minutes, polyPEGylation rate (13%) was nearly a half of the value observed at 90 minutes.

The best conditions for ASNase monoPEGylation were defined as 100 mM of PBS, pH 7.5, PEG:ASNase ratio 25:1 and reaction time of 30 min. This protocol was applied for ASNase PEGylation with 10 kDa of mPEG-NHS resulting in about 40% of monoPEG-ASNase yields. Moreover, a polyPEGylated ASNase was also prepared as previously described, to be the reference of the commercially available drug pegaspargase.

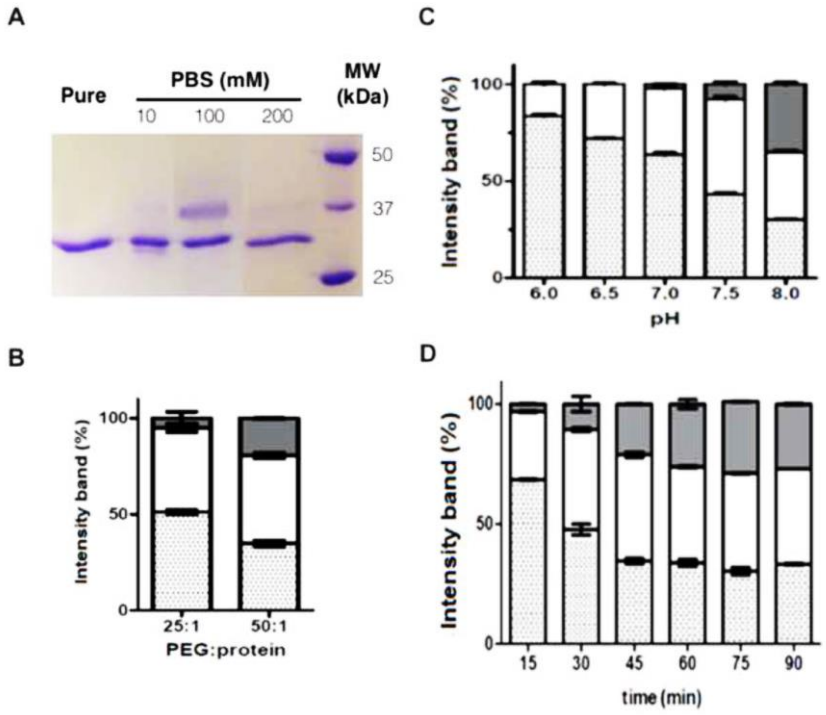

Fig 3.1. Reaction conditions to produce monoPEGylated L-asparaginase (monoPEG-ASNase). (**A**) Electrophoresis (SDS-PAGE) showing the influence of PBS buffer ionic strength on N-terminal PEGylation with pH 7.5 (PEG:ASNase ratio of 25:1, 2 kDa mPEG-NHS): Column 1- ASNase (control), column 2- reaction in 10 mM PBS, column 3- reaction in 100 mM of PBS, column 4- reaction in 200 mM PBS, and column 5- Molecular weight (BioRad). (**B**) Percentage of PEGylation at different PEG:ASNase ratios, 25:1 and 50:1, in 100 mM of PBS pH 7.5, 30 min of time reaction. (**C**) Percentage of PEGylation at different pH values (6.0, 6.5, 7.0, 7.5 or 8.0) in 100 mM of PBS, PEG:ASNase ratio of 25:1 and 30 min of reaction time. (**D**) Percentage of PEGylation on different reaction times (15 to 90 minutes) in 100 mM of PBS, pH 7.5, PEG:ASNase ratio of 25:1. Grey bars - polypegylated ASNase, white bars - monoPEGylated ASNase, dotted bars - free ASNase. Percentage of PEGylation was based on gel analysis by band intensity.

3.2. Purification of PEGylated ASNase

A strong anion exchange column (Resource Q, GE Healthcare) was used to purify the monoPEG-ASNase. At this stage of the purification, all different forms of protein present in the reaction medium were separated: free enzyme (unreacted ASNase) with 92 mM of NaCl, monoPEGylated enzyme (78 mM of NaCl) and polyPEGylated forms of the enzyme with 67 mM of NaCl (**Fig. B.4 at Appendix B**). Anion exchange chromatography resulted in monoPEG-ASNase with 70% of purity and 57% of yield. To confirm the molecular mass of the monoPEG-ASNase and to refine purification, the fractions eluted with 78 mM of NaCl were subjected to size exclusion chromatography (**Fig. B.5 at Appendix B**). MonoPEG-ASNase was eluted at 10.65 mL, while free ASNase (pure enzyme) was eluted at 11.39 mL, corresponding to 187 ± 10 kDa and 146 ± 6 kDa, respectively. Therefore, we obtained 99% of purity monoPEG-ASNase with 45% of yield. Only SEC was necessary for polyPEG-ASNase, once size difference between unreacted and polydisperse ASNase is high.[4] PolyPEGylated ASNase sample was eluted at 8.28 mL to 9.61 mL (**Fig. B.6 at Appendix B**), corresponding to a polydispersity range weight from 264 ± 3 to 410 ± 9 kDa and 28 to 57 units of PEG 5 kDa.

3.3. Determination of kinetic parameters

The kinetics of an enzyme allows to elucidate its catalytic mechanism, its role in metabolism and how its activity in the cell is controlled. The mathematical model of Michaelis-Menten[24] was used to determine the kinetic parameters. Different concentrations of the substrate L-asparagine (5 to 1,470 µM) and respective rates of saturation of ASNase fractions were studied (**Fig. 3.2.**).

The kinetic parameters obtained for ASNase, monoPEG-ASNase and polyPEG-ASNase are shown in **Table 3.1.**. All samples presented Michaelian behavior with similar K_m values of 20 µM, 35 µM and 65 µM respectively (**Table 3.1.**). In fact, the turnover values were similar to those described in literature for ASNase.[27]

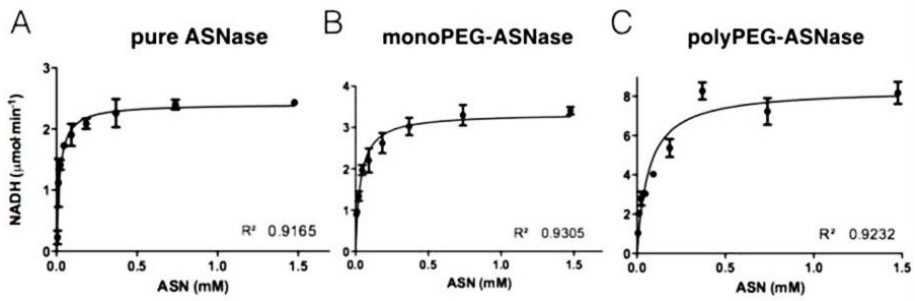

Fig 3.2. Enzymatic behavior of monoPEG-ASNase compared to ASNase (control) and polyPEGylated form. (**A**) Enzymatic kinetics of ASNase. (**B**) Enzymatic kinetics of monoPEG-ASNase. (**C**) Enzymatic kinetics of polyPEG-ASNase. Data analysis and statistical analysis (F-test) were done using GraphPad Prism 5.0 software. All trials were in triplicates and error bars represent the standard deviation.

Table 3.1. Kinetic parameters of L-asparaginase (ASNase), monoPEG-ASNase and own produced pegaspargase reference (polyPEG-ASNase).[a]

Enzyme	K_m (µM)	v_{max} (µmol.min^{-1})
ASNase	19.58 ± 0.003	2.36 ± 0.015
monoPEG-ASNase	34.67 ± 0.005	3.34 ± 0.007
polyPEG-ASNase	65.21 ± 0.005	8.36 ± 0.065

[a] All experiments were done in triplicate and error bars represent the standard deviation. The kinetic parameters were calculated by non-linear regression analysis using GraphPad Prism 5.0 software.

3.4. PEGylated ASNase activity over time

Enzymatic activity of polyPEG-ASNase, monoPEG-ASNase and free ASNase over time was studied for 21 days (**Fig. 3.3.A**). After purification, the monoPEG-ASNase maintained its initial specific activity (233 ± 8.1 U.mg^{-1}). However, the excess of PEG units randomly conjugated to ASNase, in polyPEG-ASNase similarly to pegaspargase, decreased the specific activity to 21% of the pure enzyme activity, getting 50 ± 0.6 U.mg^{-1}. After seven days, pure ASNase (control) lost 53% of specific activity. On the other hand, the monoPEG-ASNase and polyPEG-ASNase remained stable up to 21 days (*p*-value = 0.005).

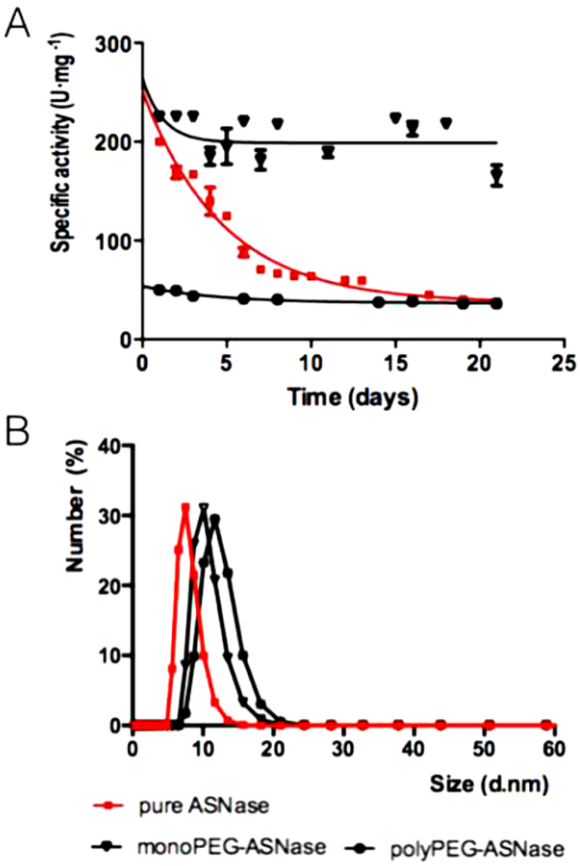

Fig 3.3. PEG attachment influence on native enzyme. (**A**) Enzymatic activity *versus* storage time at 4 °C for ASNase control, monoPEG-ASNase and polyPEG-ASNase. (**B**) Dynamic light scattering profiles of unreacted ASNase, mono and polyPEGylated ASNase. The hydrodynamic radius were 7.53 nm, 9.85 nm and 11.75 nm, respectively.

3.5. Dynamic light scattering

The PEGylation of ASNase caused an increase in the hydrodynamic diameter of the protein, through the binding of the PEG structure to the protein (**Fig 3.3.B**), an effect well-described in literature.[30-31] The hydrodynamic radius values are 7.53 nm, 9.85 nm, and 11.75 nm for ASNase, monoPEG-ASNase and polyPEG-ASNase, respectively. Comparing both PEGylated proteins, the polyPEG-ASNase has the highest hydrodynamic diameter, related to the higher amount of PEG attached to the protein.

3.6. MALDI-TOF mass spectrometry

To confirm site-specific PEGylation, the signal intensity of MS peak corresponding to the N-terminal and internal peptides were compared between the PEGylated and not PEGylated protein. **Fig. 3.4.A**, represents the first peak at 2028.1809 corresponding to

the N-terminal peptide LPNITILATGGTIAGGGDSATK.(S) and **Fig 3.4.B** represents MS peak corresponding to peptide SVFDTLATAAK.(T) at m/z 1123.6, an internal peptide that contains a lysine residue.

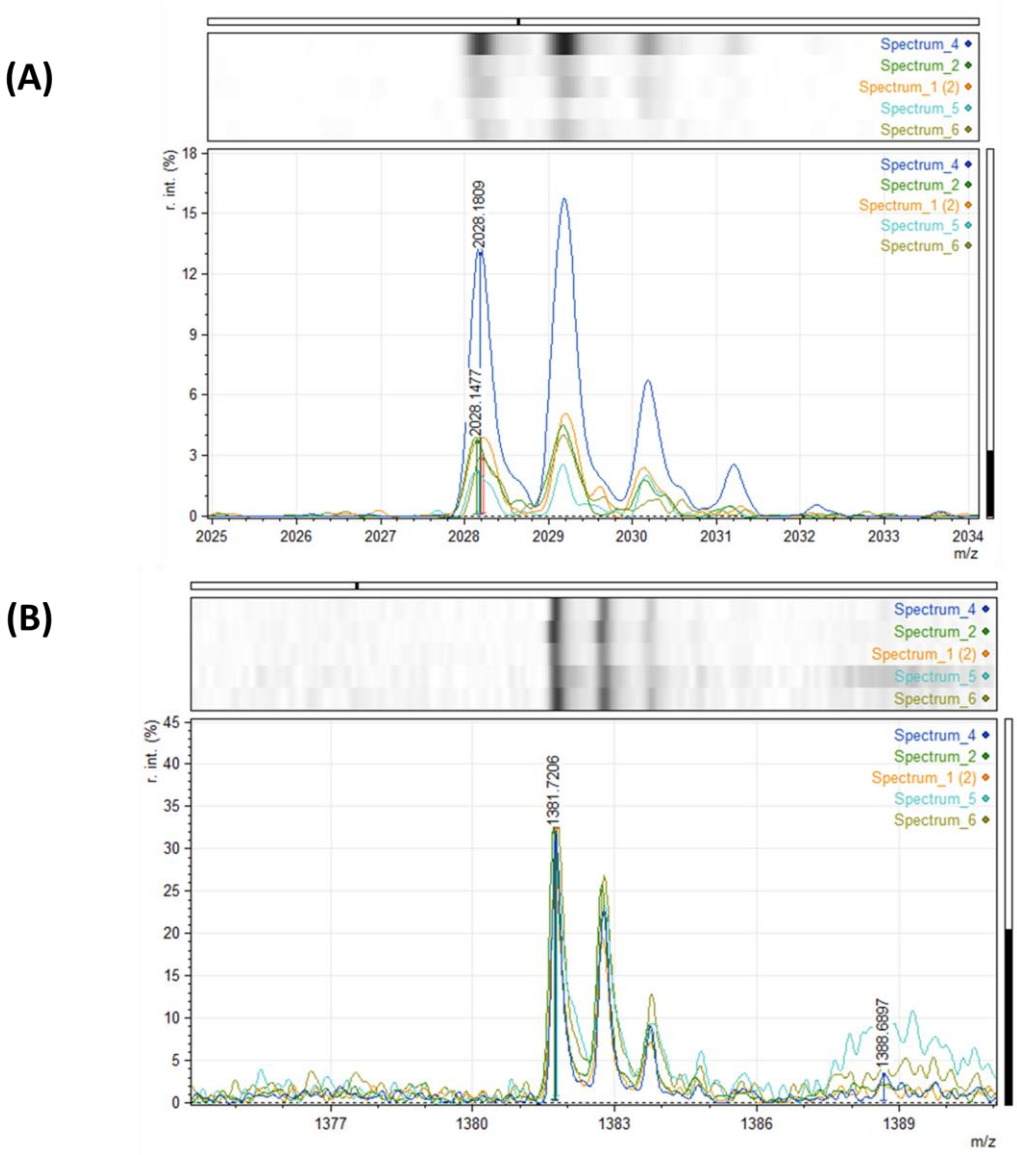

Fig 3.4. MALDI-TOF of free ASNAse and monoPEG-ASNase (with 2 kDa and 10 kDa PEG). **(A)** N-terminal peptide LPNITILATGGTIAGGGDSATK.(S) at m/z 2028.1809 and **(B)** lysine peptide SVNYGPLGYIHNGK.(I), at m/z 1518.7. Samples were acquired in duplicate. ASNase; blue line (spectrum 4), monoPEG-ASNase 2 kDa light and dark green line (spectrum 6 and 2), and monoPEG-ASNase 10 kDa; light blue line and orange (spectrum 5 and 1).

The MS signal of the N-terminal peptide derived from free ASNase is higher than the others samples (PEGylated forms), **Fig. 3.4.A**, indicating that this peptide sequence has been modified during PEGylation. It should be noted, that all the intensities were normalized to avoid sample loading bias. In order to prove that this reduction was not

due to other factors, we analyzed other MS peaks (**Fig. 3.4.B**) corresponding to internal peptides with lysine residues since the PEG reacts with lysine. The MS signal intensity of all peptides were equal between the different conditions showing that PEGylation was site-specific to ASNase N-terminal.

3.7. Proteolytic degradation

Fig. 3.5. presents the electrophoretic profile of ASNase samples after exposition to two human blood proteases related to the decrease in ASNase plasma half-life, AEP and CTSB.[32] AEP specifically cleaves asparagine and aspartate residues.[25] To date, the proteolytic sites for CTSB have not been defined, but it is known that this enzyme can recognize a wide range of residues combinations.[28]

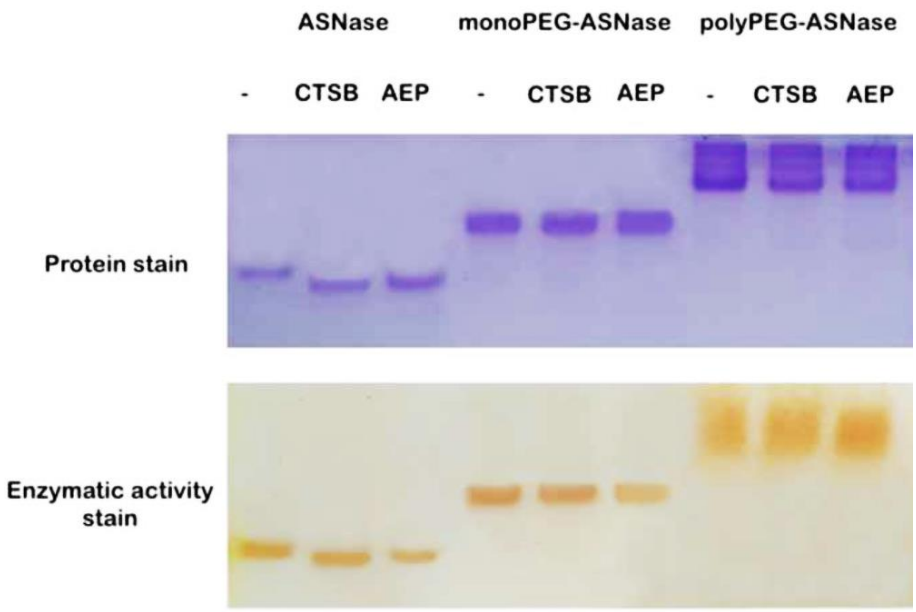

Fig 3.5. Electrophoresis gel (native-PAGE) showing the proteolytic degradation /resistance of native ASNase and PEGylated forms. ASNase, monoPEG-ASNase and polyPEG-ASNase in presence of asparagine endopeptidase (AEP) and cathepsin B (CTSB) after 84 h at 37 °C, stained with CBB (top gel) and stained with ferric chloride (bottom gel). Column 1- Protease-free ASNase, column 2- ASNase with CTSB, column 3- ASNase with AEP, column 4- protease-free monoPEG-ASNase, column 5- monoPEG-ASNase with CTSB, column 6- monoPEG-ASNase with AEP, 7- protease-free polyPEG-ASNase, column 8- polyPEG-ASNase with CTSB and column 9- polyPEG-ASNase with AEP.

The polyethylene glycol chain is known to protect protein sites susceptible to proteolytic degradation.[34] This protective effect was present for PEGylated forms, either as mono or polyPEGylated, when incubated with both tested proteases since no shifts were

observed in the electrophoretic bands. Conversely, the native ASNase presented degradation in the presence of the proteases and electrophoretic shifts were observed corresponding to smaller protein structures. Activity staining also showed that ASNase activity decreased more with AEP cleavage than CTSB, while no activity change was observed for monoPEG-ASNase and polyPEG-ASNase in presence of both proteases.

3.8. Cytotoxicity

In vitro assays using MOLT-4 (T lymphocytes) and REH (B lymphocytes) ALL cell lines were performed to test the cytotoxic potential of monoPEG-ASNase (**Fig. 3.6**.). REH line is considered to be resistant to ASNase, since it expresses considerable levels of asparagine synthetase[35] and MOLT-4 is described as an ASNase-sensitive strain.[36] As a control, HUVEC cells were used (**Fig. B.7 at Appendix B**).

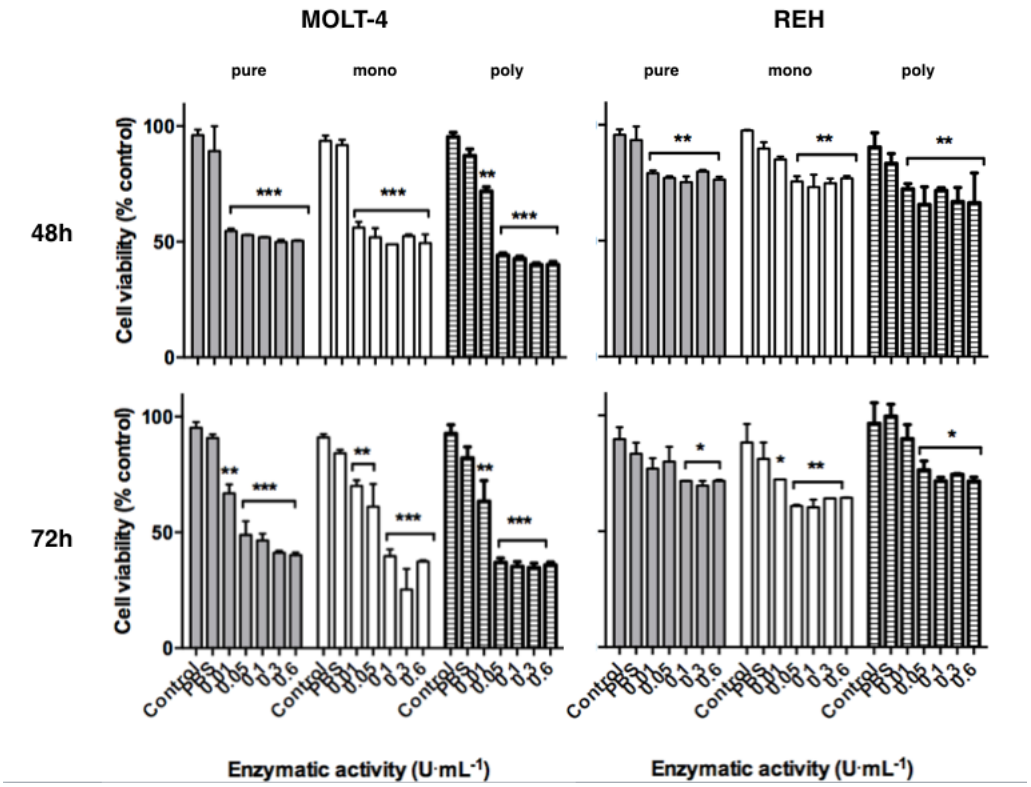

Fig 3.6. Cytotoxicity of monoPEG-ASNase in MOLT-4 and REH cells. Assays performed at 48 h and 72 h, with cells alone (control), without enzyme (PBS) and at different concentrations of enzymatic activity (0.01, 0.05, 0.1, 0.3 or 0.6 U.mL^{-1}). Grey bars - free ASNase and white bars - monoPEGylated ASNase. Error bars represent the standard deviation. Likelihood of significance less than 0.05 (*), less than 0.01 (**) and less than 0.001 (***) when compared with the control.

All ASNase samples (PEGylated or native) presented similar cytotoxicity to leukemic cells. For the sensitive strain MOLT-4 treated with monoPEG-ASNase, we detected

reductions of 48% and 62% in cell viability after 48 h and 72 h, respectively. PolyPEG-ASNase reduced 55% and 68% of cell viability after 48 h and 72 h. Additionally, no statistically significant differences were observed in cytotoxicity among PEGylated species and free enzyme. Reductions around 23% to 26% in REH cell viability were observed after 48 h for ASNase and monoPEG- ASNase, while polyPEG-ASNase reduced 35% of REH cell viability. For 72 h reaction, the reduction was approximately 33% - 39% for all the samples tested. Therefore, PEGylation preserved ASNase cytotoxic activity against leukemic lines. Moreover, both ASNase and monoPEG-ASNase were not toxic to healthy HUVEC cells (**Fig. B.7 at Appendix B**).

4. Discussion

In this work we developed a site-specific N-terminal PEGylation protocol for *E. coli* ASNase, currently employed in the treatment of ALL, to overcome the high degree of polydispersity of the commercial pegaspargase. According to our results, the increase of the ionic strength from 10 to 100 mM provided counter ions that contributed to protonation of protein residues stabilizing them and favoring PEGylation at unprotonated N-terminal amino acid.[28] At higher molarity (200 mM), PEGylation rate was lower probably due to mPEG-NHS instability. Usually, an excess molar ratio of reactive PEG over the protein amount is added to increase PEGylation and overcome reactive PEG hydrolysis.[37] However, the PEG:enzyme ratio of 25:1 resulted in less polyPEGylated forms when compared to ratio 50:1 (7% and 19%, respectively).

An adequate pH value is crucial for PEGylation as it determines the nucleophiles reactivity. Nucleophilic attack occurs at pH values closer or higher than the pKa value of the amino acid residue, because they will be predominantly deprotonated.[38] Since all lysine residues of ASNase present pKa ≥ 10.5, while N-terminal pK ≈ 7.6, the best pH value for ASNase PEGylation was 7.5. By increasing pH values around 7.5, the reaction gradually lost specificity, since other amine residues were PEGylated.

Hydrolysis of mPEG-NHS, *i.e.* the half-life of succinimidyl group hydrolysis by nucleophilic attack on the ester group depends directly on its molecular structure and the ester-binding site on the structural chain.[39] The hydrolysis half-life of the PEG with an aliphatic C4 ester linkage (such as the one used in the present work) is around 44 minutes,

whereas for PEG with a C2 ester linkage it is around 3 minutes, at pH 8.0.[40] Therefore, the best conditions to favor ASNase monoPEGylation were defined as 100 mM of PBS (pH 7.5), PEG:protein ratio of 25:1 and reaction time of 30 min.

Even with the N-terminal site-specific PEGylation protocol, multiple PEGylated enzyme structures can be produced and must be removed of the final preparation.[41] A common purification technique is size exclusion chromatography (SEC).[42-43] However, to obtain high chromatographic resolution, samples species must have at least 20% of difference in size.[44] PEGylation also alters the isoelectric point (pI) of the protein. The change in charge depends on the size of the protein, the number of conjugated PEG molecules and the residues to which PEG chains bind.[45]

Pabst et al.[46] purified PEGylated bovine serum albumin (monoPEG-BSA) by anion exchange chromatography with a yield of 50% and Subramanian[47] purified monoPEGylated α-lactalbumin from the reaction mixture by SEC with 56% of yield and 93% of purity. For polyPEG-ASNase, we obtained 58% of yield and purity of 98% by applying a one-step purification using SEC and considering desired polydispersity in the final sample. On the other hand, when the PEGylated and nonpegylated proteins are close in molecular mass (such as ASNase and monoPEG-ASNase) another purification step is required. In this sense, we used strong anion exchange chromatography (55% yield) followed by size exclusion chromatography (45% yield) to a final preparation with 99% of purity of monoPEG-ASNase. The confirmation of N-terminal PEGylation was also determined by the significant reduction in the MS signal intensity for the N-terminal peak, compared to other lysine containing peptides that do not change after PEGylation, indicating that the PEG was added to the N-terminal residue.

Data on SEC usually presents good size correlations for globular proteins, regarding the molecular mass. Based on SEC, we obtained 146 ± 6 kDa for ASNase molecular mass, corroborating the literature data that describes this enzyme with 136 to 150 kDa.[9,48] When flexible linear chains of PEG are attached to a protein, the SEC power of prediction decreases and usually size is underestimated. MonoPEG-ASNase was estimated to have 187 ± 10 kDa, what is consistent with the attachment of four 10 kDa PEG chains to the protein (one at each monomer N-terminal). PolyPEG-ASNase was estimated to present a range of 264 ± 3 kDa to 410 ± 9 kDa, what is below the expected considering that 69

to 82 units of 5 kDa PEG should be attached to the protein.[4] One possibility for such a difference is that, as explained, the high number of linear PEG chains attached, and the fact that the PEG chains are shorter (10 kDa for monoPEG-ASNase and 5 kDa for polyPEG-ASNase) resulted in a stronger influence in protein elution and the underestimation of polyPEG-ASNase size by SEC.

The kinetic properties of the purified monoPEG-ASNase were determined to investigate whether N-terminal PEGylation would result in significant differences in ASNase activity. Kinetic properties as the maximum saturation velocity (V_{max}) and the Michaelis constant (K_m), allows not only the formulation of hypotheses on the enzyme behavior in a cellular environment, but also to predict on how ASNase will respond to changes in environmental conditions.[49] ASNase is described as a Michaelian enzyme with high affinity for the substrate. In this work, a K_m of 20 µM for ASNase was obtained, which is in agreement with the values defined in literature, from 12.5 to 22 µM.[50-51] For monoPEG-ASNase, as expected, a higher K_m (35 µM) was obtained since the PEG moieties may hinder substrate access to the enzyme and also difficult enzyme-substrate molecular interactions. The same effect occured with polyPEG-ASNase presenting a higher K_m of 65 µM. Previous studies report a K_m of 12 to 40 µM for pegaspargase.[6,52] The N-terminal site-specific PEGylation significantly preserved ASNase affinity for the substrate, since the K_m of monoPEG-ASNase was still in the micromolar range and lower than the value observed for polyPEG-ASNase.

One of the main concerns about the site-specific N-terminal PEGylation was if the lower number of PEG moieties would be enough to provide protein stability. Our results showed that both monoPEG-ASNase and polyPEG-ASNase remained stable for 21 days, while free ASNase lost approximately 50-70% of its activity in just one week. However, the large number of PEG molecules conjugated to ASNase in random PEGylation significantly decreased the enzymatic activity of polyPEG-ASNase in 79%. Pegaspargase is marketed with at least 85 $U.mg^{-1}$, that is, 65% smaller than the nonpegylated form. Therefore, site specific N-terminal PEGylation indicates enzymatic stability to further studies with longer storage times, once that commercially available pegaspargase in buffer saline solution is valid for 8 months when stored at 2 to 8 °C.[53]

The commercially available pegaspargase has a longer plasma half-life than the free ASNase due to steric hindrance of PEG to proteases. Therefore, the determination of monoPEG-ASNase stability to proteases degradation is pivotal. Our results confirmed ASNase cleavage by the proteases, but cleavage by CTSB did not completely inactivate the enzyme. Nonetheless, CTSB cleavage is intracellular, after enzyme capturing by phagocytic cells.[33] Proteolytic degradation by AEP, on the other hand, resulted in a significant loss of ASNase activity by the protease mechanism of action that involves interaction with Asn248 and Asp90 residues of ASNase active site.[50] MonoPEG-ASNase was found to be stable in presence of both AEP and CTSB cells, demonstrating that the binding of four PEG moieties to the enzyme was enough to provide plasma stability. This study also suggests that monoPEG-ASNase may be less immunogenic, as degradation by proteases may lead to the exposition of epitopes that activate the immune response.[24]
Besides stability in solution and resistance to proteases cleavage, monoPEG-ASNase presented similar *in vitro* cytotoxicity against leukemic cell lines (MOLT-4 and REH) in comparison to polyPEG-ASNase and free enzyme. Costa et al.[27] demonstrated that 10 $U.mL^{-1}$ of ASNase reduced almost 100% of MOLT-4 cells and 20% of REH cells viability in 72 h of incubation. The ASNase activity of a therapeutic dose must be at least 0.1 to 0.2 $U.mL^{-1}$ and,[6,52] in this sense, the range of 0.01 to 0.6 $U.mL^{-1}$ was tested in the present work. MonoPEG-ASNase resulted in 62% and 33% viability reduction of MOLT-4 and REH cells, respectively, considering 72 h of incubation. Cytotoxicity against healthy cell lines (HUVEC) was also investigated and monoPEG-ASNase was found to be safe with no cytotoxic effect. HUVEC cells were used as control since they are highly metabolic cells covering the vessels wall and, consequently, in contact with circulating substances. Hence, we showed that any physical or metabolic alteration that could lead to cell death was caused by the enzymes.
In conclusion, it was developed an optimized protocol for site-specific N-terminal PEGylation of ASNase to produce a novel enzyme variant, monoPEG-ASNase, with similar yield of monoPEGylation as literature,[46-47] with reaction time of 30 minutes which represent a great industrial production time and also less cost with raw material since the reaction needs less PEG than unspecific PEGylation. Also this novel enzyme variant promote a kinetic profile and activity towards leukemic cell lines in comparison to the

free and polyPEGylated enzyme. The N-terminal site-specific PEGylation provides batch-to-batch control over pegaspargase (commercially available ASNase) and an enhanced long-term stability, being considered a better biobetter than the polyPEGylated form. In addition, monoPEG-ASNase is at least three-times more stable than native ASNase and resistant to cleavage by serum proteases. This monoPEG-ASNase can be considered as a potential novel biopharmaceutical to treat ALL, as well as possibly other types of cancer.

References

1. Pasut, G., Sergi, M. & Veronese, F. M. Anti-cancer PEG-enzymes: 30 years old, but still a current approach. *Advanced Drug Delivery Reviews*. **60**, 69–78 (2008).
2. Veronese, F. M. & Pasut, G. PEGylation: successful approach to drug delivery. *Drug Discovery Today*, **10**, 1451-1458 (2005).
3. Soares, A. L., Guimarães, G. M., Polakiewicz, B., Pitombo, R. N. M. & Abrahão-Neto, J. Effects of polyethylene glycol attachment on physicochemical and biological stability of *E. coli* L-asparaginase. *Int J Pharm*. **237**, 163-170 (2002).
4. Sigma-Tau. Pharmaceuticals. Oncaspar®. Highlights of prescribing information U.S. License No. 1850 I-301-21-US-B, 1994.
5. Knott, S. R. V., Wagenblast, E., Khan, S., Kim, S. Y., Soto, M., Wagner, M., *et al*. Asparagine bioavailability governs metastasis in a model of breast cancer. Nature. **554**, 378–381 (2018).
6. Avramis, V. I., Sencer, S., Periclou, A. P., Sather, H., Bostrom, B. C., Cohen, L. J., *et al*. A randomized comparison of native *Escherichia coli* asparaginase and polyethyleneglycol conjugated asparaginase for treatment of children with newly diagnosed standard-risk acute lymphoblastic leukemia: a Children's Cancer Group study. *Blood.* **99**, 1986-1994 (2002).
7. Dinndorf, P. A., Gootenberg, J., Cohen, M. H., Keegan, P. & Pazdur, R. FDA Drug Approval Summary: Pegaspargase (Oncaspar) for the First-Line Treatment of Children with Acute Lymphoblastic Leukemia (ALL), *The Oncologist*. **12**, 991-998 (2007).

8. European Medicine Agency, EMA. Oncaspar – pegaspargase. 2015. EMA/CHMP/734982/2015.
9. Loureiro, C. B., Borges, K. S., Andrade, A. F., Tone, L. G. & Said, S. Purification and biochemical characterization of native and PEGylated form of L-asparaginase produced by *Aspergillus terreus*: evaluation in vitro of antineoplasic activity. *Adv Microbiol.* **2**, 138–145 (2012).
10. Pisal, D. S., Kosloski, M. P. & Balu-Iyer, S. V. Delivery of therapeutic proteins. *J Pharm Sci.* **99**, 2557–2575 (2010).
11. Abe, M., Akbarzaderaleh, P., Hamachi, M., Yoshimoto, N. & Yamamoto, S. Interaction mechanism of mono-PEGylated proteins in electrostatic interaction chromatography. *Biotechnology Journal*. **5**, 477–483 (2010).
12. Lee, S., Wylie, D. C. & Cannon-Carlson, S. V. Pegylated interleukin-10. U.S. Grant No. US7052686B2, 2000.
13. Santos, J. H. P. M., Carretero, G., Coutinho, J. A. P., Rangel-Yagui, C. O. & Ventura, S. P. M. Multistep purification of cytochrome c PEGylated forms using polymer-based aqueous biphasic systems. *Green Chem*., **19**, 5800-5808 (2017).
14. Jin, M., Chen, W., Huang, W., Rong, L. & Gao, Z. Preparation of pegylated lumbrokinase and an evaluation of its thrombolytic activity both *in vitro* and *in vivo*. *Acta Pharmaceutica Sinica B.* **3**, 123–129 (2013).
15. Rashband, W. S. ImageJ, U.S. National Institute of Health, Bethesda, Maryland, USA. 1997-2016.
16. Laemmli, U. K. Cleavage of structural proteins during the assembly of the head of bacteriophage T4. *Nature*. **227**,680-685 (1970).
17. Blum, H., Beier, H. & Gross, H. J. Improved silver staining of plant proteins, RNA and DNA in polyacylamide gels. *Electrophoresis*. **8**, 93-99 (1987).
18. Mattos, A., Jager-Krikken, A., Haan, M., Beljaars, L. & Poelstra, K. PEGylation of interleukin-10 improves the pharmacokinetic profile and enhances the antifibrotic effectivity in CCl4-induced fibrogenesis in mice. *J Control Release*. **162**, 84-91 (2012).
19. Sigma-Aldrich. M6768 SIGMA/ Methoxypolyethylene glycol 350, 2013. CAS Number 9004-74-4.

20. Imada, A., Igarasi, S., Nakahama, K. & Isono, M. Asparaginase and Glutaminase Activities of Micro-organisms. *J Gen Microbiol*. **76**, 85-99 (1973).
21. Balcão, V. M., Mateo, C., Fernández–Lafuente, R., Malcata, F. X. & Guisán, J. M. Structural and functional stabilization of L-asparaginase via multisubunit immobilization onto highly activated supports. *Biotechnol Prog.* **17**,537–542 (2001).
22. Fernandes, L. R., Stern, A. C. B., Cavaglieri, R. C., Nogueira, F. C. S., Domont, G., Palmisano, G. & Bydlowski, S. P. 7-Ketocholesterol overcomes drug resistance in chronic myeloid leukemia cell lines beyond MDR1 mechanism. *Journal of Proteomics.* **151**,12-23 (2017).
23. Lopez-Fernandez, H., Santos, H. M., Capelo, J. L., Fdez-Riverola, F., Glez-Peña, D. & Reboiro-Jato, M. Mass-Up: an all-in-one open software application for MALDI-TOF mass spectrometry knowledge discovery. *BMC Bioinformatics*. **16**,318 (2015).
24. Patel, N., Krishnan, S., Offman, M. N., Krol, M., Moss, C. X., Leighton, C., *et al*. A dyad of lymphoblastic lysosomal cysteine proteases degrades the antileukemic drug l-asparaginase. *Journal of Clinical Investigation*. **119**, 1964-1973 (2009).
25. Mesas, J. M., Josk, A. G. & Martin, J. F. Characterization and partial purification of L-asparaginase from *Corynebaeterium glutamicurn*. *Journal of General Microbiology*. **136**, 515-519 (1990).
26. Mosmann, T. Rapid colorimetric assay for cellular growth and survival: application to proliferation and cytotoxicity assays. *Journal of Immunological Methods*. **65**, 55-63 (1983).
27. Costa, I. M., Schultz, L., Pedra, B. A. B., Leite, M. S. M., Farsky, M. A., Oliveira, A., Pessoa, A., *et al*. Recombinant L-asparaginase 1 from *Saccharomyces cerevisiae*: an allosteric enzyme with antineoplastic activity. *Scientific Reports*. **6**, 36239 (2016).
28. Glasstone, S. An introduction to electrochemistry. New York: D. Van Nostrand Company Inc, 2007.
29. Ebbing, D. D. General chemistry. Boston: Houghton Mifflin Harcourt, 1993.

30. Akbarzadehlaleh, P., Mirzaei, M., Mashahdi-Keshtiban, M., Shamsasenjan, K. & Heydari, H. PEGylated Human Serum Albumin: Review of PEGylation, Purification and Characterization Methods. *Adv Pharm Bull*. **6**, 309–317 (2016).
31. Gokarn, Y. R., McLean, M. & Laue, T. M. Effect of PEGylation on protein hydrodynamics. *Mol Pharm*. **9**, 762-773 (2012).
32. Offman, M. N., Krol, M., Patel, N., Krishnan, S., Liu, J., Saha, V., *et al*. Rational engineering of L-asparaginase reveals importance of dual activity for cancer cell toxicity. *Blood*. **117**, 1614-1621 (2011).
33. Der Meer, L. T., Waanders, E., Levers, M., Venselaar, H., Roeleveld, D., Boos, J., *et al*. A germ line mutation in cathepsin B points toward a role in asparaginase pharmacokinetics. *Blood.* **124**, 3027-3079 (2014).
34. Abuchowsi, A., Van Es, T., Palczuk, N. C. & Davis, F. F. Alteration of immunological properties of bovine serum albumin by covalent attachment of polyethylene glycol. *Journal of Biological Chemistry*. **252**, 3578-3581 (1997).
35. Hermanova, I., Zaliova, M., Trka, J. & Starkova, J. Low expression of asparagine synthetase in lymphoid blasts precludes its role in sensitivity to L-asparaginase. *Experimental Hematology*. **40**, 657-665 (2012).
36. Aslanian, A. M., Fletcher, B. S. & Kilberg, M. S. Asparagine synthetase expression alone is sufficient to induce L-asparaginase resistance in MOLT-4 human leukaemia cells. *Biochem J*. **357**, 321-328 (2001).
37. Veronese, F. M. Peptide and protein PEGylation: a review of problems and solutions. *Biomaterials*. **22**, 405-417 (2001).
38. Roberts, M. J., Bentley, M. D. & Harris, J. M. Chemistry for peptide and protein PEGylation*. Adv Drug Delivery Rev.* **54**, 459–476 (2002).
39. Zalipsky, S. Alkyl succinimidyl carbonates undergo Lossen rearrangement in basic buffers. *Chem Commun*. 1998; 69-70. DOI: 10.1039/A706713E.
40. Hermanson, G. T. Bioconjugation Protocols: Strategies and Methods, in: Audet J (ed.), *Bioconjugate Techniques*. San Diego: Elsevier Inc, 2013; pp.790.
41. Yu, D. & Ghosh, R. Purification of PEGylated protein using membrane chromatography. *J Pharm Sci*. **99**, 3326-3333 (2010).

42. Pfister, D. & Morbidelli, M. Integrated process of high conversation and high yield protein PEGylation. *Biotechnology & Bioengineering*. **113**, 1711-1718 (2016).
43. Jevsevar, S., Kundstelj, M. & Porekar, V. G. PEGylation of therapeutic proteins. *Biotechnology Journal*. **5**, 113-128 (2010).
44. Hagel, L. Gel Filtration: Size Exclusion Chromatography, in: Janson JC (ed.), *Protein Purification: Principles, High Resolution Methods, and Applications*. Hoboken:John Wiley & Sons, Inc. 2011; pp.51-91.
45. Pasut, G. & Veronese, F. M. State of the art in PEGylation: the great versatility achieved after forty years of research. *J Control Release*. **161**, 461-72 (2012).
46. Pabst, T. M., Buckley, J. J., Ranasubramanyan, N. & Hunter, A. K. Comparison of strong anion-exchangers for the purification of a PEGylated protein. *Journal of Chromatography A*. **1147**, 172–182 (2007).
47. Subramanian, G. Continuous processing in pharmaceutical manufacturing. Weinheim:Wiley-VCH, 2015.
48. Aghaiypour, K., Wlodawer, A. & Lubkowski, J. Structural basis for the activity and substrate specificity of *Erwinia chrysanthemi* L-Asparaginase. *Biochemistry.* **40**, 5655–5664 (2001).
49. Nelson, D. L. & Cox, M. M. Lehninger Principles of Biochemistry. New York:WH Freeman and Company, 2005.
50. Anishkin, A., Vanegas, J. M., Rogers, D. M., Lorenzi, P. L., Chan, W. K., Purwaha, P., *et al.* Catalytic Role of the Substrate Defines Specificity of Therapeutic L-Asparaginase. *J Mol Biol*. **427**, 2867-2885 (2015).
51. Derst, C., Henseling, J. & Röhm, K. Engineering the substrate specificity of *Escherichia coli* asparaginase II. Selective reduction of glutaminase activity by amino acid replacements at position 248. *Protein Science*. **9**, 2009–2017 (2000).
52. Douer, D., Yampolsky, H., Cohen, L. J., Watkins, K., Levine, A. M., Periclou, A. P., *et al.* Pharmacodynamics and safety of intravenous pegaspargase during remission induction in adults aged 55 years or younger with newly diagnosed acute lymphoblastic leukemia. *Blood*. **109**, 2744-2750 (2007).

53. European Medicine Agency, EMA. EPAR - Human product information. WC500200735, 2005.

3.2. Site-specific PEGylated cytochrome c as biosensor: PEGylation reaction to enhance its long-term stability

Santos, J. H. P. M., Meneguetti, G. P., Carreto, G., Coutinho, J. A. P., Ventura, S. P. M. & Rangel-Yagui, C. O. 2019 (manuscript in preparation).[6]

Abstract

Cytochrome c (Cyt-c) has been currently employed in bioelectrochemical applications for redox sensing due to its peroxidase-like activity. Nevertheless, its potential as a biosensor is significantly reduced due to low long-term and thermal stability, generally attributed to the fragile conformation of proteins. To overcome these drawbacks, in this work, a site-specific PEGylation protocol for Cyt-c was developed. The PEG derivative used was a 5kDa methoxy polyethylene glycol succinimidyl NHS ester (mPEG-NHS) and a site-directed PEGylation at the lysine amino-acids was performed. In this case, the aim was to establish an optimized protocol to control the number of PEGylated amino acid residues at specific sites. The effects of reactional medium pH, molar proportion (Cyt-c:mPEG-NHS) and reaction time were evaluated. The best conditions were defined as pH 7, 1:25 Cyt-c:mPEG-NHS and 15 min reaction time resulting in PEGylation yields of 45% for the attachment of 4 PEG molecules (Cyt-c-PEG-4) and 34% for the binding of 8 PEG molecules (Cyt-c-PEG-8). Circular dichroism spectra demonstrated that Cyt-c PEGylation did not cause significant changes to the secondary and tertiary structures of the PEGylated forms. The long-term stability of free and PEGylated Cyt-c was also investigated in terms of catalytic activity of ABTS oxidation by hydrogen peroxidase. The main results demonstrate that both Cyt-c-PEG-4 and Cyt-c-PEG-8 were found to be more stable than the free protein. In particular, Cyt-c-PEG-8 presented great potential as a biosensor, since its structure and activity was found to be three times higher than that defined for the free protein over 60-days of storage, at distinct temperatures of 4 ^{o}C and 25 ^{o}C.

Keywords: cytochrome c; PEGylation; lysine amino-acid residues; stability; biosensor.

[6] Contributions: JS performed the PEGylation and long-term stability assays, GC performed the circular dichroism assays and GM performed the *in silico* analysis. JS interpreted the experimental data. CY conceived this work. The manuscript was mainly written by JS with contributions for the remaining authors.

1. Introduction

Cytochrome c (Cyt-c) is a small protein with 104 amino acids and about 12 kDa molecular weight. It is is a heme protein involved in mitochondrial electron transfer, even though not considered as an enzyme in nature, it catalyzes several chemical reactions including the hydrogen peroxide reduction, aromatic oxidation, hydroxylation, epoxidation and N-demethylation.[2] Based on the broad heterogeneity obtained in biotransformation reactions catalyzed by Cyt-c, along side with the high reactivity towards different substrates and the electron transfer capability, this protein has been recently explored as a biosensor of hydrogen peroxide, nitric oxide and polycyclic aromatic hydrocarbon.[2–4] However, the potential biosensing applications of Cyt-c are compromised by irreversible denaturation, aggregation and/or precipitation. This short-term stability condition results from the fragile conformation shared by most proteins, where Cyt-c is also included.

The stability of biosensors during storage is crucial to guarantee reproducibility and feasibility of biochemical measurements. Generally, long-term stability of protein-based sensors is the major problem associated with their potential application.[5] In this sense, chemical modifications in proteins are a key solution to overcome these drawbacks. PEGylation is one of the most common chemical modifications applied in protein-based biosensing field, mostly due to the advantages it may bring to proteins.[3] Chemical bonding of poly(ethylene glycol) (PEG) to the protein enhances the protein solubility in water and some organic solvents, confers long-term stability while reduces denaturation, aggregation, and precipitation, as well as prevents immunogenicity and proteolytic degradation due to the PEG shielding effect.[6–8] Literature shows that many redox proteins with sensing applications have already been PEGylated to improve stability, *e.g.* horseradish peroxidase,[9] hemoglobin,[10] myoglobin.[11] Recent studies showed that PEGylation could kinetically stabilize the Cyt-c structure through the maintenance of the heme group, while decreasing the unfolding rate.[3,4,12] However, most of the PEGylation reactions presented in literature included in the field of biosensors are not site-specific, resulting in the random production of PEGylated conjugates with increased polydispersity.[4,13] This unspecific reaction leads to a decreased bioactivity and lack of batch to batch control, resulting in a mixture of protein-

based biosensors with differential biosensing activity.[6,14] To overcome this problem, we developed a site-specific PEGylation protocol for Cyt-c through the conjugation of methoxy PEG succinimidyl NHS ester (mPEG-NHS). This functionalized PEG is attached to the protein through a nucleophilic attack of primary protein amine groups forming an ester bond and releasing an NHS group. Reaction conditions such as pH, molar proportion of protein:mPEG-NHS and reaction time were studied to obtain an enhanced yield of site-specific PEGylated conjugates. Furthermore, the effect of PEGylation on Cyt-c chemical structure, function and stability over the time was also examined. The main results obtained identified the Cyt-c-PEG-8 (with eight PEG molecules attached) as the conjugate with the highest stability, proving that this chemical alteration is actually preserving the protein structure and function.

2. Materials and methods

2.1. Materials

Horse heart cytochrome c (Cyt-c, ≥ 95% purity), 2,2'-azino-di-(3-ethylbenzthiazoline sulfonic acid) (ABTS, ≥ 95% purity), hydrogen peroxide (99% purity), hydroxylammonium chloride (99% purity) were obtained from Sigma-Aldrich. The methoxy PEG N-hydroxysuccinimide ester (mPEG-NHS, 5 kDa) was acquired from Nanocs with high purity. The aqueous buffer used in PEGylation reaction was the potassium phosphate buffer (100 mM). All other reagents were of analytical grade. The water used was double distilled, passed by a reverse osmosis system and further treated with a Milli-Q plus 185 water purification apparatus.

2.2. Cyt-c PEGylation

The PEGylation reaction was carried following the method provided by the PEG derivative supplier.[16] Briefly, Cyt-c was dissolved in 0.1 M of sodium phosphate buffer and allow to react with mPEG-NHS at room temperature and constant magnetic stirring of 400 rpm. Several parameters were optimized, namely the pH (7 - 12), protein:mPEG-NHS molar proportion (1:5, 1:10, 1:25 and 1:35) and reaction time (15, 30 and 45 min). At the end, 2 M of hydroxylamine (1:10 v/v) was added to stop the reaction as well as to avoid the production of undesirable and unstable products (such as ester conjugation).

2.3. Purification of PEGylated conjugates

PEGylation reaction mixtures were purified by size exclusion chromatography (SEC), using a Superdex 200 Increase 10/300 GL column (crosslinked agarose-dextran resin) (GE Healthcare) in an AKTA™ purifier system (GE Healthcare). The column was equilibrated with 0.01 M phosphate buffer (0.14 M NaCl, pH 7.4) and eluted with the same buffer at the flow of 0.75 mL min^{-1}. The protein fractions (determined by U.V. at 280 nm), corresponding to the unreacted Cyt-c and modified proteins Cyt-c-PEG-4 (protein with 4 PEG molecules attached) and Cyt-c-PEG-8 (protein with 8 PEG molecules attached) were stored at -20^{o}C for further studies. The determination of Cyt-c concentration was carried out by the use of a calibration curve established in the SEC-FPLC at the conditions described before. The retention time of Cyt-c (confirmed with the commercial and pure sample) was found to be *ca.* 24 min within an analysis time of 40 min. The percentage yield of Cyt-c and Cyt-c modified conjugates was calculated dividing the FPLC peak area corresponding to the target protein by the total area of all peaks corresponding to all proteins and conjugates present in the sample.

2.4. Determination of PEGylation degree of Cyt-c conjugates by SEC

The PEGylation degree of the Cyt-c conjugates was determined by SEC.[17,18] The determination of the molecular weight (MW) of protein conjugates and, consequently, the degree of PEGylation can be accomplished by the column calibration with several proteins with a known molecular weight. The column (Superdex 200 Increase 10/300 GL) was calibrated using several proteins as MW markers: thyroglobulin 669 kDa, ferritin 450 kDa, catalase 232 kDa, lactate dehydrogenase 136. 7 kDa, bovine serum albumin 67 kDa, ovalbumin 45 kDa, carbonic anhydrase 31 kDa, soybean trypsin inhibitor 20.1 kDa, α-lactalbumin 14.4 kDa, cytochrome c 12.2 kDa, and the void volume (V_0) was determined using blue dextran 2000. All standards were used from GE Healthcare. The standard proteins were run at the same conditions assayed for the SEC purification of Cyt-c conjugates, 0.01 M phosphate buffer (0.14 M NaCl, pH 7.4), at 0.75 mL min^{-1} of flow rate. The MW of the protein conjugates was determined by the linear relationship obtained by plotting the K_{av} value of the proteins calculated by the equation 1, and the logarithms of their MW. The calibration curve is presented in **Fig. B.8 at Appendix B**.

$$K_{av} = \frac{(V_e - V_0)}{(V_T - V_0)} \quad \textbf{(1)}$$

The elution volume (V_e) is the amount of eluent collected from the start of loading the sample to the point of its maximal elution; the (V_T) corresponds to the total volume of the column.

Nevertheless, the MW derived by this technique with globular proteins seems to be accurate to about ± 10%, resulting in uncertainty in the average number of PEG's per Cyt-c inferior to ± 1. An example of each chromatogram corresponding to a specific PEGylation condition is depicted in **Fig. B.9 at Appendix B**.

2.5. Circular dichroism (CD) spectroscopy

CD spectra of Cyt-c and its modified forms were obtained in a Jasco J-720 Spectropolarimeter (Tokyo, Japan). The final spectra were the average of six scans with subtraction of the buffer spectrum (0.01 M phosphate buffer, 0.14 M NaCl, pH 7.4). CD spectra were obtained in the far (190-260 nm) and near (250-350 nm) UV ranges. Far-UV samples were placed in 1 mm optical length quartz cells with concentration ranging from 6 to 15 µM. Near-UV samples, with concentration ranging from 14 to 41 µM, were placed in 5 mm optical length quartz cells. Spectra intensities (θ, mdeg) were converted to residual molar ellipticity ([θ], deg.cm^2.dmol^{-1}) based on equation 2:

$$[\theta] = \frac{\theta}{10.\ C.\ l.n} \quad \textbf{(2)}$$

where (C) is the protein concentration in mol L^{-1}, (l) is the optical length in cm and (n) is the number of residues in the protein, in this case, 104 residues.

2.6. Determination of Cyt-c long-term stability

Long-term stability was performed for both storage conditions, namely room (~25 °C) and refrigerated (4 °C) temperature. The peroxidase activity was measured during 60 days and the residual activity (%) calculated taking into consideration the activity on day 1 as 100%. The enzymatic activity of Cyt-c was determined by the catalytic oxidation of 50 µM ABTS in the presence of 0.5 mM hydrogen peroxide.[15] The concentration of non-PEGylated and PEGylated Cyt-c was 10 µM in 0.01 M phosphate buffer (0.14 M NaCl, pH 7.4). The reaction was initiated by the addition of hydrogen peroxide and the increase

in absorbance at 418 nm was measured in a SpectraMax plus 384 (Molecular Devices) spectrophotometer.

2.7. SDS-PAGE

Protein samples with 20 µL of volume were applied to a 12% polyacrylamide gel (10 x 10.5 cm x 0.75 mm thick) under reducing conditions in accordance with Laemmli method.[19] The electrophoretic run was performed by applying a 120 V potential difference for approximately 1h 30 min using vertical Mini Protean™ system (Bio-Rad, Hercules, CA, USA). Protein marker Precision Plus Protein was used (Bio-Rad). Gels were stained with Coomassie Brilliant Blue R-250 for visualization of protein bands.

2.8. *In silico studies*: Molecular visualization of PEGylation

The pKa of N-terminal and lysine residues based on Cyt-c crystal structure (PDB code, 1HRC) and using the software H++ were determined to understand the location of PEG attachment in Cyt-c. Additionally, molecular models of Cyt-c were constructed using PyMOL (Molecular Graphics System, version 1.3, Schrödinger, LLC) based on the protein crystal structure. The *in silico* conjugation of four and eight molecules of mPEG (5 kDa) in lysine residues of Cyt-c to form Cyt-c-PEG-4 (LYS 22, 25, 27 and 39) and Cyt-c-PEG-8 (LYS 22, 25, 27, 39, 55, 79, 86 and 87), was respectively performed. All PEG chains were auto-sculpted to adjust the proper molecular conformation.

2.9. *Statistical analysis*

PEGylation yields were experimentally quantified in triplicate for the three parameters under study, namely the pH, molar ratio and reaction time (each set of three determinations was used to calculate the average and respective standard deviations). Statistical data analysis was performed using one-way Analysis of Variance (ANOVA) and Tukey's post-test, at a 5% level of significance.

3. Results and discussion

3.1. Cyt-c PEGylation

The selection of an appropriate PEGylation reaction in the design of site-specific polymer-protein conjugates to be applied in the biosensing field is the first step to obtain

a successful PEGylated product. Several of the final properties of the conjugate are directly related to the physical and chemical features of the selected PEG derivative.[8,20,21] Moreover, the number and local reactivity of available attachment sites in the amino acid sequence of the target protein are important criteria to choose the type of PEGylation reaction.[20] Therefore, the reaction design must be tailored to the protein of interest, depending on its physicochemical properties, amino acid sequence and final application.[7,22] Taking this into account, the amino (-NH_2) reactive PEGylation, using N-hydroxysuccinimide (NHS) functionalized poly(ethylene glycol) (mPEG-NHS) was selected, due to its inherent advantages. In this kind of PEGylation, the PEG polymer is generally attached to the ε amino group of lysine by a nucleophilic attack of the amine group to the ester carbonyl of the reactive PEG, releasing NHS as a byproduct (**Fig. 3.7.**).[16,23,24] Compared to other PEG-NHS ester derivatives, succinimidyl carbonate (SC) functionalized mPEG-NHS offers superior reactivity and higher stability in aqueous solution.[16]

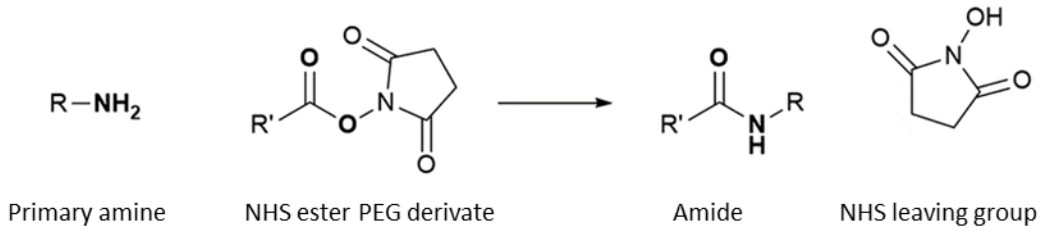

Fig. 3.7. Schematic overview of PEGylation reaction.

The PEGylation of Cyt-c by reacting it with mPEG-NHS, resulted in three different degrees of polymer conjugation, these representing the attachment of four PEG molecules (Cyt-c-PEG-4), eight PEG molecules (Cyt-c-PEG-8), and a poly-PEGylated form (Cyt-c-Poly-PEG). In order to understand the location of PEGylation in Cyt-c, bioinformatics studies were conducted to determine the pKa of the amino acids that can be PEGylated (**Table 3.2**.) and to construct the molecular scheme of the Cyt-c PEGylated forms (**Fig. 3.8.**).

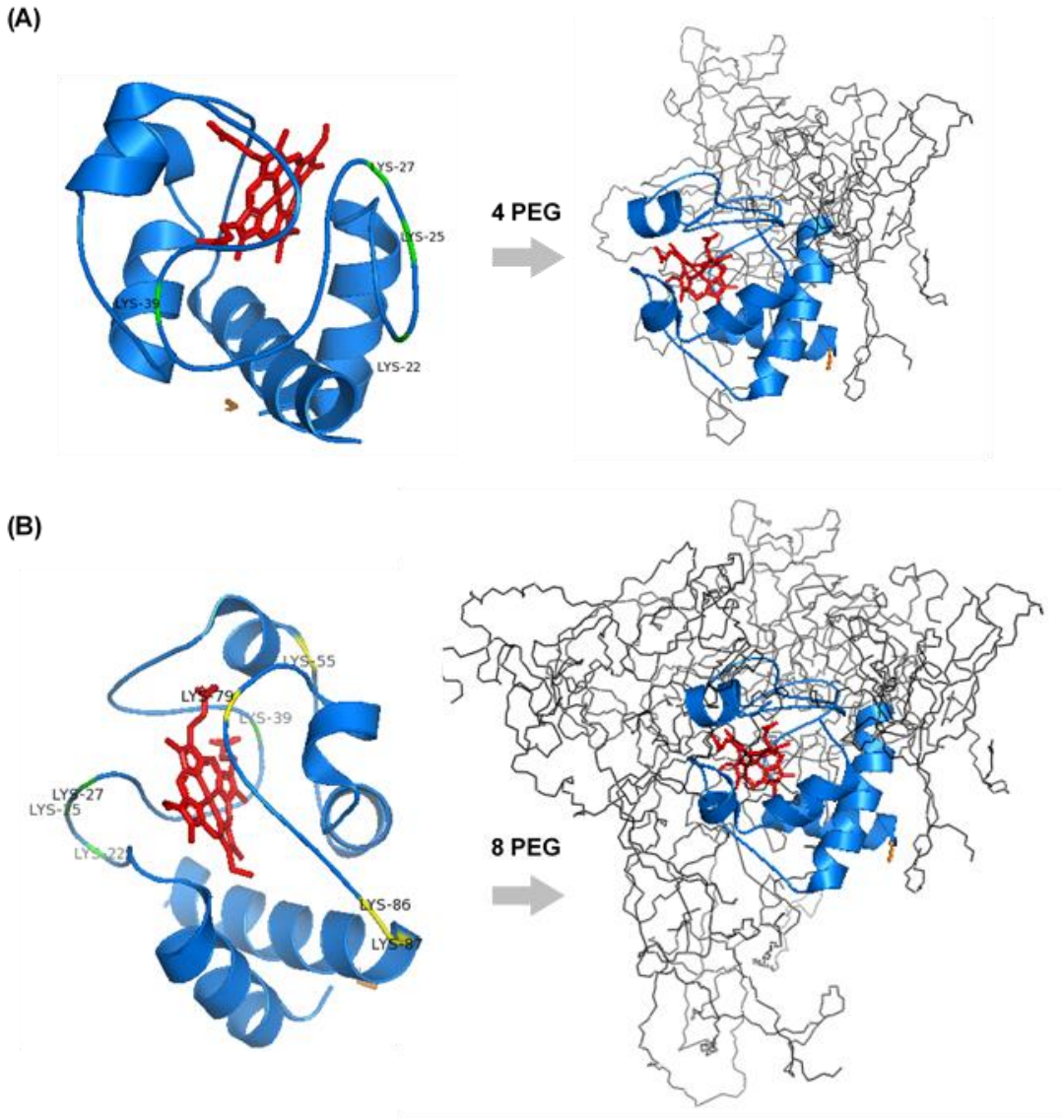

Fig. 3.8. Molecular visualization of theoretical lysine residues (LYS) of cytochrome c (Cyt-c, PDB code 1HRC) PEGylated, using the Software PyMOL. **(A)** Four residues of conjugation are highlighted: LYS - 22, 25, 27 and 39, resulting in Cyt-c-PEG-4. **(B)** Eight residues of conjugation are defined i.e. LYS - 22, 25, 27, 39, 55, 79, 86 and 87 resulting in Cyt-c-PEG-8.

Primary amines exist at the N-terminus of each polypeptide chain and in the side-chain of lysine (Lys, K) amino acid residues. PEGylation in amine groups preferentially takes place in deprotonated primary amines, in which the lone pair of electrons is freely available for the nucleophilic attack; therefore it deppends on the pKa of the residues. The location in the polypeptide chain is also important, since amino acids more exposed to the solvent and located in flexible regions of the protein are more likely to be PEGylated. Cyt-c contains 19 Lys residues and one N-terminal residue that can be potentially modified by PEG covalent binding. Of these, six are part of loop regions (four

in the largest loop more accessible to PEG and two in an intermediate loop), three are in the alpha-helix transition and the remaining are located in the alpha-helix composition (**Table 3.2.**). According to previous studies, the lysines more available for PEG attachment are Lys22, Lys25, Lys27, and Lys39, all located in the flexible region (Ω loop) of Cyt-c polypeptide chain. In this sense, the site-specific PEGylated form Cyt-c-PEG-4 refers to PEG attachment to those amino acid residues. Regarding the other four lysines covalently bound to PEG in Cyt-c-PEG-8, Lys55, Lys60, Lys79, and Lys86 are the most probable binding sites. These lysines are present in flexible regions of the protein (Ω loop and alpha-helix transition). The N-terminal group cannot be PEGylated at neutral pH due to the extremely high pKa (**Table 3.2.**) that makes it preferentially protonated at most pH values and, therefore, enabling the occurrence of the nucleophilic attack.

Table 3.2. pKa and location of the lysines (Lys) and N-terminal residue of Cyt-c (1HRC, PDB code).

Residue	pKa	Location
NT	11.8	N terminal
Lys5	>12	alpha-helix
Lys7	10.9	alpha-helix
Lys8	9.7	alpha-helix
Lys13	10.8	alpha-helix
Lys22	9.9	Ω loop
Lys25	11.2	Ω loop
Lys27	10.9	Ω loop
Lys39	10.3	Ω loop
Lys53	10.7	alpha-helix
Lys55	10.4	alpha-helix transition
Lys60	10.4	alpha-helix transition
Lys72	8.6	alpha-helix
Lys73	11.0	alpha-helix
Lys79	10.4	Ω loop
Lys86	10.3	Ω loop
Lys87	10.7	alpha-helix transition
Lys88	10.4	alpha-helix
Lys99	>12	alpha-helix
Lys100	10.7	alpha-helix

3.1.1. Effect of pH in the PEGylation of Cyt-c

PEGylation reactions are mostly conducted in single-step unidirectional batch systems to guarantee that all products have followed the same procedure, enhancing validation, reproducibility, and optimization of the reaction. One of the key parameters to design a

site-specific PEGylation reaction is the pH. By the control of pH, PEGylation can be directed to produce specific conjugates, an essential feature to promote batch-to-batch control. The effect of pH in Cyt-c PEGylation is presented in **Fig. 3.9.** and, as can be seen, the number of PEGylated forms increases with the pH due to the higher probability of lysines to react with PEG derivative since in pH > pKa they are deprotonated. The unreacted protein quantity is also decreased in more alkaline pH as a result of a higher degree of PEGylation. An opposite trend is observed for pH > 10; the degree of PEGylation decreases and the concentration of unreacted protein increases to 66% at pH 12. This behavior could be explained due to the higher hydrolysis rate of the PEG derivate used when in alkaline solution, leading to lower concentrations of reactive PEG and consequently decreasing the yields of PEGylation. The highest yields of Cyt-c-PEG-4 (38%) and Cyt-c-PEG-8 (26%) were both observed at pH 7, defined as the optimal pH in this specifc case.

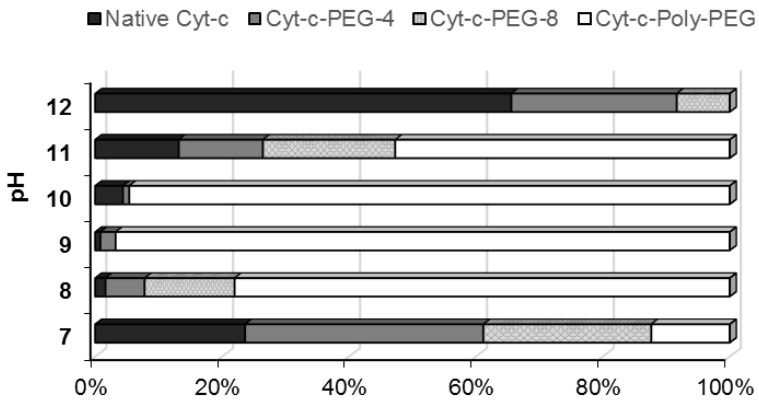

pH	Percentage of unreacted Cyt-c ± std (%)	Percentage of Cyt-c-PEG-4 ± std (%)	Percentage of Cyt-c-PEG-8 ± std (%)	Percentage of Cyt-c-Poly-PEG ± std (%)
7	23.63 ± 0.55 B	37.54 ± 0.47 A	26.48 ± 0.55 A	12.35 ± 0.63 D
8	1.63 ± 0.04 DE	6.16 ± 0.38 D	14.18 ± 0.01 C	78.03 ± 0.41 B
9	0.83 ± 0.26 E	2.40 ± 0.06 E	0 E	96.77 ±0.32 A
10	4.39 ± 0.79 D	0.99 ± 0.05 E	0 E	94.62 ± 0.84 A
11	13.18 ± 0.52 C	13.25 ± 0.32 C	20.86 ± 1.13 B	52.71 ± 1.33 C
12	65.60 ± 1.83 A	26.06 ± 1.51 B	8.34 ± 0.32 D	0 E

Note: All experiments were carried in triplicate.

Fig. 3.9. Effect of pH on Cyt-c PEGylation yields. The PEGylation reaction was performed in 0.1 M phosphate buffer (at different pHs), 1:25 molar proportion (protein:mPEG-NHS, 5 KDa), at room temperature, for 30 minutes, and with a constant stirring of 400 rpm. Different letters indicate significant differences ($P < 0.05$) between conditions (A-E).

Fig. 3.10. shows the electrophoretic profile (SDS-PAGE) of PEGylation reaction of Cyt-c at different pH values. The results depicted in this figure seem to corroborate the PEGylation yield data previously shown with each band representing one site-specific Cyt-c-PEGylated form. The bands presenting higher intensity correpond to pH 7 - 12, in opposition to those obtained for pH range between 8 and 10, in which the most intense bands are identifying the poly-PEGylated forms.

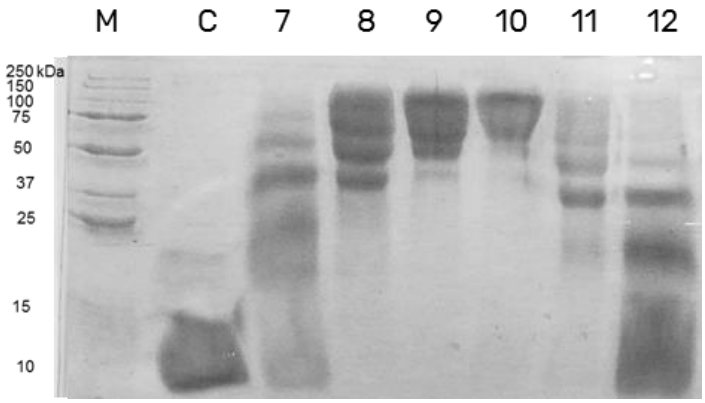

Fig. 3.10. SDS-PAGE for the mixture obtained after PEGylation of Cyt-c with mPEG-NHS, at different pH values. Lane 1: molecular weight marker, Lane 2: Cyt-c. The protein mixtures obtained after PEGylation of Cyt-c were: Lane 3: pH = 7, Lane 4: pH = 8, Lane 5: pH = 9; Lane 6: pH = 10, Lane 7: pH = 11, Lane 8: pH = 12.

3.1.2. Effect of PEG derivative concentration in the PEGylation of Cyt-c

The effect of PEG derivative concentration is a very important parameter to evaluate in order to attain a site-specific PEGylation. The effect of PEG derivate concentration on the PEGylation yield is depicted in **Fig. 3.11.** and **Fig. 3.12.** corresponds to the representative SDS-PAGE image of the reaction results. The lowest molar ratio values, specifically 1:5 and 1:10, resulted in less PEGylation extents and higher quantities of unreacted protein present. In addition, no band of poly-PEGylated forms was obtained at those experimental conditions. The optimal result was obtained at molar ratio 1:25 corresponding to higher yields of site-specific Cyt-c-PEGylated forms. The upper molar ratio (1:35) promoted polydispersity of the PEGylated products due to the excess of PEG-derivate.

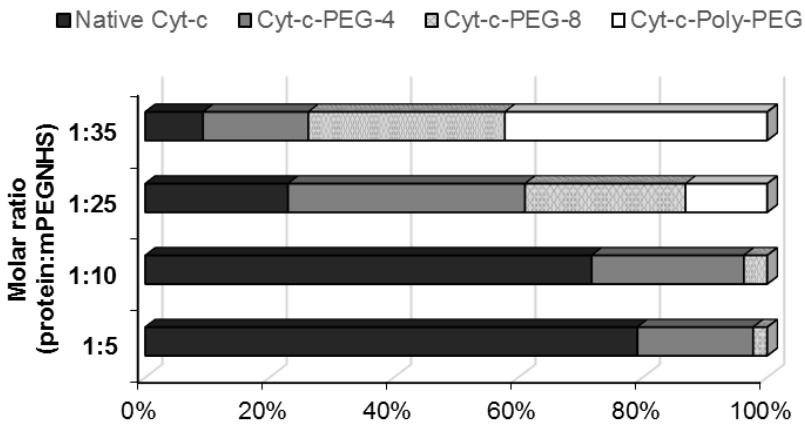

Molar ratio (protein:mPEG - NHS)	Percentage of unreacted Cyt-c ± std (%)	Percentage of Cyt-c-PEG-4 ± std (%)	Percentage of Cyt-c-PEG-8 ± std (%)	Percentage of Cyt-c-Poly-PEG ± std (%)
1:5	79.65 ± 0.41 A	17.80 ± 0.65 B	2.55 ± 0.25 C	0 C
1:10	77.21 ± 4.42 A	20.04 ± 3.62 B	2.75 ± 0.80 C	0 C
1:25	23.63 ± 0.55 B	37.54 ± 0.47 A	26.48 ± 0.55 B	12.35 ± 0.63 B
1:35	9.44 ± 0.11 C	17.00 ± 0.06 B	32.10 ± 0.41 A	41.46 ± 0.59 A

*All experiments were carried in triplicate.

Fig. 3.11. Effect of molar ratio (protein:mPEG-NHS) on Cyt-c PEGylation yields. The PEGylation reaction was performed in 0.1 M phosphate buffer (pH = 7), at room temperature, for 30 minutes, and with a constant stirring of 400 rpm. Different letters indicate significant differences ($P < 0.05$) between conditions (A-C).

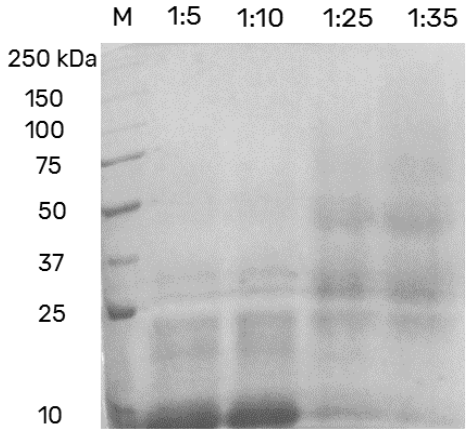

Fig. 3.12. SDS-PAGE for the mixture obtained after PEGylation of Cyt-c at different molar proportions (protein:mPEG-NHS). Lane 1: molecular weight marker, Lane 2: 1:5, Lane 3: 1:10, Lane 4: 1:25, Lane 5: 1:35.

3.1.3. Effect of time of reaction in the PEGylation of Cyt-c

The reaction time for Cyt-c PEGylation was also investigated during 15, 30 and 45 min (**Figs. 3.13. and 3.14.**). Results showed that the poly-PEGylation yield increases with the reaction time. Therefore, higher yields of Cyt-c-PEG-4 (45%) and Cyt-c-PEG-8 (32%) were obtained in the shortest time of 15 min, with no poly-PEGylated forms produced, what could facilitate the purification process. Furthermore, the shorter times required in this process will translate into economic advantage.

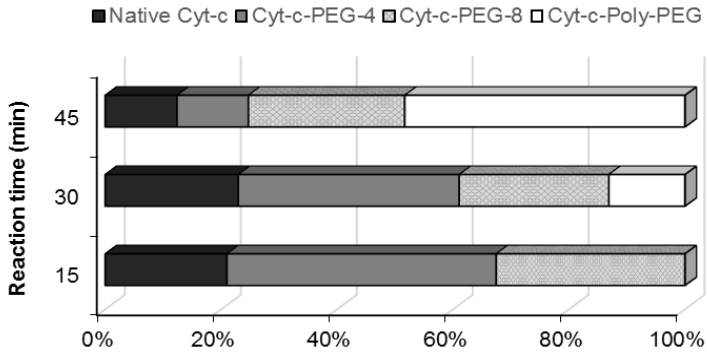

Reaction time (min)	Percentage of unreacted Cyt-c ± std (%)	Percentage of Cyt-c-PEG-4 ± std (%)	Percentage of Cyt-c-PEG-8 ± std (%)	Percentage of Cyt-c-Poly-PEG ± std (%)
15	23.37 ± 1.93 A	44.70 ± 1.43 A	31.93 ± 0.51 A	0 C
30	23.63 ± 0.55 A	37.54 ± 0.47 B	26.48 ± 0.55 B	12.35 ± 0.63 B
45	11.42 ± 0.79 B	12.47 ± 0.13 C	26.13 ± 0.68 B	49.98 ± 1.34 A

*All experiments were carried in triplicate.

Fig. 3.13. Effect of reaction time on Cyt-c PEGylation yields. Effect of molar ratio (protein:mPEG-NHS) on Cyt-c PEGylation yields. The PEGylation reaction was performed in 0.1 M phosphate buffer (pH = 7), 1:25 molar proportion (protein:mPEG-NHS, 5 KDa), at room temperature, and with a constant stirring of 400 rpm. Different letters indicate significant differences ($P < 0.05$) between conditions (A-C).

In summary, a designed and tailor-made PEGylation reaction was developed and the best experimental conditions were set as pH 7, 1:25 molar ratio (Cyt-c:mPEG-NHS) and 15 min reaction time. At these conditions we obtained two forms of site-specific PEGylated Cyt-c with no undesirable poly-PEGylated forms. Those PEGylated Cyt-c forms were then isolated through SEC-FPLC and then further applied in spectroscopic studies to understand the effect of PEGylation on the Cyt-c structure, as well as in the long-term stability of the conjugates.

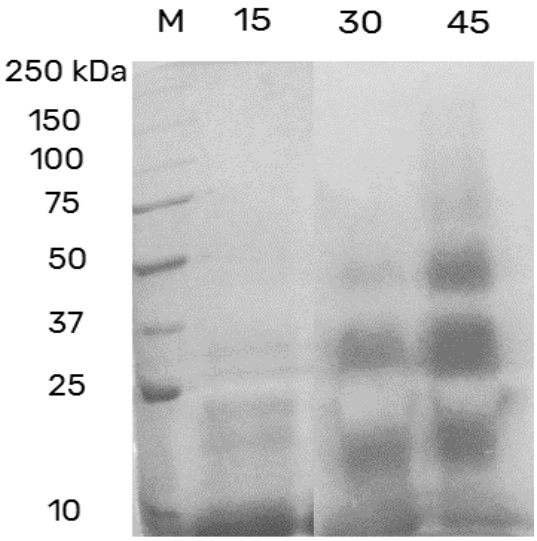

Fig. 3.14. SDS-PAGE for the mixture obtained after PEGylation of Cyt-c with mPEG-NHS at different reaction times. Lane 1: molecular weight marker, Lane 2: 15 min, Lane 3: 30 min, Lane 4: 45 min.

3.2. Effect of PEGylation on Cyt-c structure

To verify the effect of PEGylation on Cyt-c secondary and tertiary structures, CD measurements were performed. The UV CD spectra (**Fig. 3.15. and 3.16**.) showed the characteristic tertiary and secondary structural fingerprints of Cyt-c. The spectrum shows a peak at around 330 nm with a small peak at 290 nm, characteristic of Trp. Between 280 and 290 nm, the Tyr peaks can be observed and at around the 255–270 nm a weak peak of Phe is present. PEGylation of Cyt-c caused no significant spectral changes demonstrating that PEGylation did not disrupt Cyt-c tertiary structure (**Fig. 3.15**.). Similarly, no spectral changes were found by observation of the far-UV CD spectra upon PEGylation (**Fig. 3.16**.); the different proteinic forms exhibited negative intensity bands centered at 208 and 222 nm and a positive peak at the 195-200 nm region of the spectrum, characteristic of a predominant α-helical secondary structure. Our results corroborate with previous studies,[12] in which other types of Cyt-c PEGylation also did not compromise the protein stability.

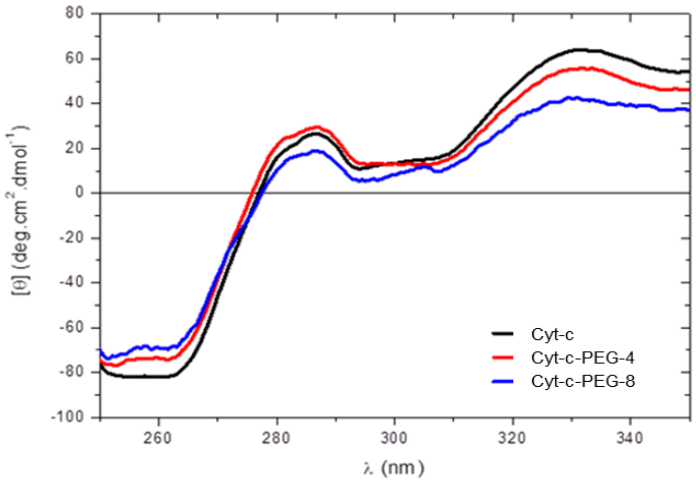

Fig. 3.15. Near-UV CD spectra of Cyt-c (—), Cyt-c-PEG-4 (—) and Cyt-c-PEG-8 (—) in 0.01 M sodium phosphate buffer (0.14 M NaCl, pH = 7.4) in the region reflecting the protein tertiary structure.

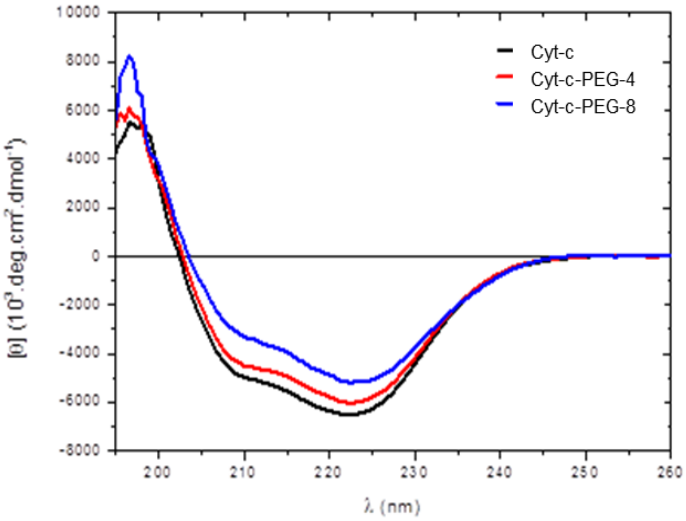

Fig. 3.16. Far-UV CD spectra of Cyt-c (—), Cyt-c-PEG-4 (—) and Cyt-c-PEG-8 (—) in 0.01 M sodium phosphate buffer (0.14 M NaCl, pH = 7.4) in the region reflecting the protein secondary structure.

3.3. Effect of PEGylation on the long-term stability of native and PEGylated forms

To study the Cyt-c long-term stability in its native and PEGylated forms (in solution), it was measured the residual Cyt-c activity using the ABTS oxidation procedure during 60 days at different temperatures (**Fig. 3.17.**). Both Cyt-c PEGylated conjugates showed higher residual activity than free Cyt-c from room and refrigirated temperatures. When stored for 60 days at 4 °C, Cyt-c-PEG-8 retained 80% of its activity and Cyt-c-PEG-4 retained 63%, while the free Cyt-c retained only 30% of its activity. As expected, Cyt-c (free and PEGylated forms) was more stable at lower temperature. At room

temperature storage (25 ºC) the free Cyt-c residual activity was only 22% contrasting with ≥53% for both Cyt-c PEGylated forms. The Cyt-c with higher mPEG content (Cyt-c-PEG-8) presented superior stability than Cyt-c-PEG-4, particularly at low temperature. These results demonstrate that the site-specific PEGylation is a valuable strategy to increase Cyt-c stability during storage.

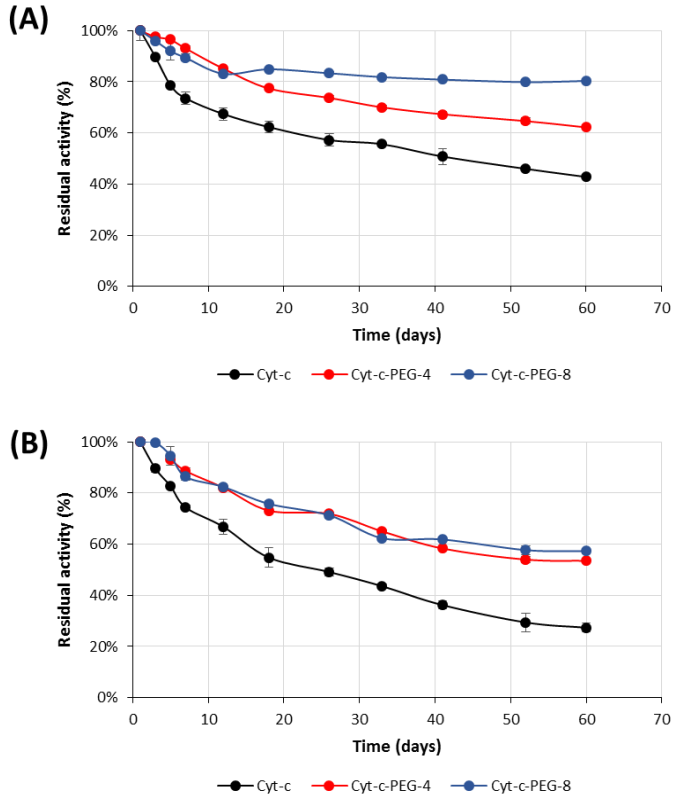

Fig. 3.17. Plot of the residual activity of Cyt-c and PEGylated protein forms (Cyt-c-PEG-4 and Cyt-c-PEG-8) determined during 60 days at 4ºC **(A)** and room temperature of 25ºC **(B)**.

4. Conclusions

In this work, Cyt-c PEGylated conjugates, namely Cyt-c-PEG-4 and Cyt-c-PEG-8 were produced, and their potential demonstrated as biosensors. The optimal PEGylation conditions for site-specific reaction were optimized; pH 7, 1:25 molar ratio (Cyt-c:mPEG-NHS) and 15 min of reaction, resulting in yields of 45% for Cyt-c-PEG-4 and 32% for Cyt-c-PEG-8. The Cyt-c PEGylation caused no significant structural changes, which was evaluated through CD analysis, demonstrating that PEGylation did not compromise the protein conformation. Additionally, Cyt-c-PEGylated forms were found to be significantly more stable over the time than the free protein, with the higher stability

observed for the Cyt-c-PEG-8. The improved stability of PEGylated Cyt-c conjugates clearly brings advantages for its use as a biosensor by the possibility of extending its product half-life time.

References

1. Bertini, I., Cavallaro, G. & Rosato, A. Cytochrome c: Occurrence and functions. *Chem. Rev.* **106,** 90–115 (2006).
2. Vazquez-Duhalt, R. Cytochrome c as a biocatalyst. in *J. Mol. Catal. - B Enzym.* **7,** 241–249 (1999).
3. Santiago-Rodríguez, L., Méndez, J., Flores-Fernandez, G. M., Pagán, M., Rodríguez-Martínez, J. A., Cabrera, C. R. & Griebenow, K. Enhanced stability of a nanostructured cytochrome c biosensor by PEGylation. *J. Electroanal. Chem.* **663,** 1–7 (2011).
4. García-Arellano, H., Buenrostro-Gonzalez, E. & Vazquez-Duhalt, R. Biocatalytic Transformation of Petroporphyrins by Chemical Modified Cytochrome C. *Biotechnol. Bioeng.* **85,** 790–798 (2004).
5. Tothill, I. E. Biosensors developments and potential applications in the agricultural diagnosis sector. *Comput. Electron. Agric.* **30,** 205–218 (2001).
6. Pasut, G. & Veronese, F. M. State of the art in PEGylation: The great versatility achieved after forty years of research. *J. Control. Release* **161,** 461–472 (2012).
7. Veronese, F. M. Peptide and protein PEGylation: a review of problems and solutions. *Biomaterials* **22,** 405–417 (2001).
8. Pfister, D. & Morbidelli, M. Process for protein PEGylation. *J. Control. Release* **180,** 134–149 (2014).
9. Kawahara, N.Y., Muneyasu, K., Ohno, H. Conformation and redox reaction of poly(ethylene oxide)-modified horseradish peroxidase in poly(ethylene oxide) oligomers. *Chem. Lett.* 381–382 (1997).
10. Ohno, H. & Yamaguchi, N. Redox reaction of poly(ethylene oxide)-modified hemoglobin in poly(ethylene oxide) oligomers at 120 degrees C. *Bioconjug. Chem.* **5,** 379–381 (1994).
11. Kawahara, N. Y., Ohkubo, W. & Ohno, H. Effect of cast solvent on the electron

transfer reaction for poly(ethylene oxide)-modified myoglobin on the electrode in poly(ethylene oxide) oligomers. *Bioconjug. Chem.* **8,** 244–248 (1997).

12. Mabrouk, P. A. Effect of pegylation on the structure and function of horse cytochrome c. *Bioconjug. Chem.* **5,** 236–241 (1994).
13. Zhou, J. Q., He, T. & Wang, J. W. PEGylation of cytochrome c at the level of lysine residues mediated by a microbial transglutaminase. *Biotechnol. Lett.* **38,** 1121–1129 (2016).
14. Da Silva Freitas, D., Mero, A. & Pasut, G. Chemical and enzymatic site specific pegylation of hGH. *Bioconjug. Chem.* **24,** 456–463 (2013).
15. Kim, N. H., Jeong, M. S., Choi, S. Y. & Kang, J. H. Peroxidase activity of cytochrome c. *Bull. Korean Chem. Soc.* **25,** 1889–1892 (2004).
16. Nanocs. Succinimidyl PEG NHS, mPEG-NHS(SC). (2017). at <http://www.nanocs.net/mPEG-SC-5k-1g.htm>
17. Tayyab, S., Qamar, S. & Islam, M. Size exclusion chromatography and size exclusion HPLC of proteins. *Biochem. Educ.* **19,** 149–152 (1991).
18. Hong, P., Koza, S., Bouvier, E. S. P. & Corporation, W. Size-Exclusion Chromatography for the Analysis of Protein Biotherapeutics and their Aggregates. *J. Liq. Chromatogr. Relat. Technol.* **35,** 2923–2950 (2012).
19. Laemmli, U. Cleavage of structural proteins during the assembly of the head of bacteriophage T4. *Nature* **227,** 670–685 (1970).
20. González-Valdez, J., Rito-Palomares, M. & Benavides, J. Advances and trends in the design, analysis, and characterization of polymer-protein conjugates for 'pEGylaided' bioprocesses. *Anal. Bioanal. Chem.* **403,** 2225–2235 (2012).
21. Ginn, C., Khalili, H., Lever, R. & Brocchini, S. PEGylation and its impact on the design of new protein-based medicines. *Future Med. Chem.* **6,** 1829–46 (2014).
22. Roberts, M. J., Bentley, M. D. & Harris, J. M. Chemistry for peptide and protein PEGylation. *Adv. Drug Deliv. Rev.* **64,** 116–127 (2012).
23. Harris, J. M. & Chess, R. B. Effect of pegylation on pharmaceuticals. *Nat. Rev. Drug Discov.* **2,** 214–221 (2003).
24. Palm, T., Esfandiary, R. & Gandhi, R. The effect of PEGylation on the stability of small therapeutic proteins. *Pharm. Dev. Technol.* **16,** 441–448 (2011).

3.3. PEGylation as an efficient tool to enhance protein thermostability: a kinetic and thermodynamic study on cytochrome c

Santos, J. H. P. M., Carretero, G., Coutinho, J. A. P., Ventura, S. P. M., Converti, A. & Rangel-Yagui, C. O. *International Journal of Biological Macromolecules*, 2019, submitted.[7]

Abstract

Cytochrome-c from equine heart was kinetically and thermodynamically investigated either in its native (Cyt-c) and PEGylated forms. In this work, two Cyt-c-PEG conjugates with different PEGylation degrees, namely 4 and 8, represented by Cyt-c-PEG-4 and Cyt-c-PEG-8, were tested. The main results exhibited maximum activities at 80°C, and their irreversible deactivation was well described by a first-order kinetic. The results of activity collected at different temperatures (T = 30-100°C) were then used to estimate the activation energy of the catalysed Cyt-c reaction (E^* = 10.22, 7.51 and 8.87 kJ.mol^{-1} for Cyt-c, Cyt-c-PEG-4 and Cyt-c-PEG-8) and the standard enthalpy variation of enzyme unfolding (ΔH^o_U = 33.82, 109.44 and 58.43 kJ.mol^{-1} for Cyt-c, Cyt-c-PEG-4 and Cyt-c-PEG-8, respectively). When temperature increased in the range of temperatures 70-95 °C, the deactivation rate constant (k_d) increased from 0.17 to 0.59 h^{-1}, while the half-life ($t_{1/2}$) decreased from 4.00 to 1.18 h for unreacted Cyt-c. However, for the PEGylated conjugates, the k_d was reduced in the whole range of temperatures, while the $t_{1/2}$ was doubled for Cyt-c-PEG-8 and increased 1.1-1.7-fold for Cyt-c-PEG-4. The results of residual activity tests carried in the temperature range 70–95 °C allowed to estimate the activation energy (E^*_d = 50.51, 72.63 and 63.36 kJ.mol^{-1} for Cyt-c, Cyt-c-PEG-4 and Cyt-c-PEG-8), enthalpy (ΔH^*_d), entropy (ΔS^*_d) and Gibbs free energy (ΔG^*_d) of the enzyme irreversible denaturation. The higher enthalpic contributions of PEGylated conjugates in addition to the increase in ΔG^*_d, compared to the native protein, indorsed the protective role of PEGylation. Negative values of ΔS^*_d suggest the occurrence of aggregation phenomenon by increasing the temperature, further confirmed by thermal studies with circular dichroism where the change on the conformational protein structure was shown. The thermodynamic parameters determined suggest that the PEGylated Cyt-c has an enhanced thermostability, being this important for industrial biosensing applications.

Keywords: Thermodynamics; thermostability; cytochrome c; protein PEGylation; bioconjugation; enzyme unfolding.

[7] Contributions: JS and GC acquired all the experimental data. CY and AC conceived and directed this work. JS, CY and AC interpreted the experimental data. The manuscript was mainly written by JS with contributions from the remaining authors.

1. Introduction

Horse heart cytochrome c (Cyt-c) is a heme protein involved in mitochondrial electron transfer with bio-electrochemical applications for hydrogen peroxide, polycyclic aromatic hydrocarbons (PAHs), and nitric oxide biosensing.[1] Cyt-c is recurrently applied on the catalysis of several chemical reactions including hydrogen peroxide reduction,[1] lipid peroxidation,[2] oxidation[3] and hydroxylation[4] of aromatic compounds. The peroxidase-like activity of Cyt-c has been demonstrated by the oxidation of various electron donors, among which are the 2,2'-azino-bis(3-ethylbenzothiazoline-6-sulphonic acid) (ABTS) and PAHs.[5] This enzyme is considered an important redox biocatalyst since it is resistant to catalysis in organic solvents due to the covalent binding of the heme prosthetic group to the protein, it is stable in a wide range of pH (from 2 to 11), and of low cost. However, there is a need to improve its thermostability to increase the spectrum of applicability of Cyt-c as a biocatalyst and biosensor. One of the approaches followed to improve the thermostability of proteins is related with their chemical modification by bioconjugation.[6–8] This process is carried by the covalent link of a protective polymer to the biomolecule being thermostabilized. The poly(N-(2-hydroxypropyl) methacrylamide) (PHPMA), poly(oligoethylene glycol methyl ether methacrylate) (POEGMA), poly(D,L-lacticco-glycolic acid) (PLGA), poly(glutamic acid) (PGA), poly(N-isopropyl acrylamide) (PNIPAM), poly(N,N'-diethyl acrylamide) (PDEAM), polystyrene, and poly(ethylene glycol) (PEG), are some examples of polymers of biological and synthetic origin used for this purpose. PEG is a biocompatible polymer, with low immunogenicity, antigenicity and toxicity, it is soluble in water and other organic solvents. It has a high mobility in solution, making it one of the polymers most used for bioconjugation.[9] In addition, PEG is, among the few synthetic polymers, considered safe by the Food and Drug Administration (FDA) and European Medicine Agency (EMA).[10] The concept of protein PEGylation has been applied to several enzymes, leading to a new era of polymeric conjugate biocatalysts with improved properties. In the particular case of Cyt-c, PEGylation appears to be the first line option to enhance its thermostability.[11] Behind the improvement of the thermostability, PEGylation improves several other properties, including its long-term stability, solubility in water, resistance to organic solvents and biocompatibility.[10,12] These conditions are

exceptionally important taking into account that Cyt-c is used as a model biocatalyst in the biosensing field. The Cyt-c PEGylation was shown to kinetically stabilize the protein tertiary structure[7], with the additional advantage of preserving the catalytic activity of enzymes at high temperatures.[8] Nevertheless, a thermostability study on the effect of PEGylation on this specific redox enzyme has never been reported.

The thermodynamic and kinetic studies can provide valuable information about the thermostability of enzymes at the operating temperature. Concerning the kinetic modelling of thermostability, a first-order deactivation reaction is usually adopted, describing its irreversible inactivation (denaturation), whose kinetics is usually expressed in terms of enzyme half-life ($t_{1/2}$).[13] On the other hand, the activation energy and the changes in the Gibbs free energy, enthalpy and entropy of irreversible inactivation are important parameters widely reported in literature to describe the thermodynamic behaviour of the enzyme denaturation phenomenon.[14]

In this work, the kinetic and thermodynamic parameters of the activity and thermostability of two PEGylated conjugates, Cyt-c-PEG-4 and Cyt-c-PEG-8, were investigated and compared with the behaviour of the native protein.

2. Materials and Methods

2.1. Materials

Horse heart cytochrome c (Cyt-c, ≥ 95% purity), 2,2'-azino-di-(3-ethylbenzthiazoline sulfonic acid) (ABTS, ≥ 95% purity), hydrogen peroxide (99% purity), and hydroxylammonium chloride (99% purity) were obtained from Sigma-Aldrich/Merck (Darmstadt, Germany). High-purity methoxy poly(ethyleneglycol) N-hydroxysuccinimide ester (mPEG-NHS, 5 kDa) was acquired from Nanocs (New York, USA). The aqueous medium used to perform the PEGylation reaction is composed of potassium phosphate buffer at 100 mM. All other reagents were of analytical grade. All solutions were prepared using double distilled water, passed through a reverse osmosis system and further treated with a Milli-Q plus 185 water purification apparatus (Millipore/Merck, Darmstadt, Germany).

2.2. PEGylation reaction and purification of PEGylated products

The PEGylation reaction was carried according to the PEG derivative supplier.[15] Briefly, Cyt-c was dissolved in 0.1 M of sodium phosphate buffer and allowed to react with mPEG-NHS at room temperature (25 ± 1°C) and constant magnetic stirring of 400 rpm. The experimental conditions of the reaction were pH = 7.0, 1:25 protein:mPEG-NHS molar proportion and reaction time of 15 min. At the end, 2.0 M of a hydroxylamine solution (1:10 v/v) was added to stop the reaction as well as to avoid the formation of undesirable and unstable byproducts like conjugated esters.

After PEGylation and considering that the reaction is not complete, a complex media was obtained, composed of native Cyt-c, and two PEGylated forms, the Cyt-c-PEG-4 and Cyt-c-PEG-8. The PEGylated forms and unreacted Cyt-c were then separated by fast protein size exclusion liquid chromatography (SEC-FPLC), For that, a Superdex 200 Increase 10/300 GL column filled with crosslinked agarose-dextran resin (GE Healthcare Life Sciences, Chicago, USA), in an AKTA™ purifier system (GE Healthcare) was used. The column was equilibrated with 0.01 M of potassium phosphate buffer (0.14 M of NaCl, pH 7.4) and eluted with the same buffer at a flow rate of 0.75 $mL.min^{-1}$. Protein fractions with UV absorption at 280 nm, corresponding to the unreacted Cyt-c and PEGylated proteins were stored at -20°C for further studies. Concentrations of Cyt-c and Cyt-c-PEG conjugates were determined using a calibration curve established in the SEC-FPLC under the conditions previously described. The PEGylation degree of Cyt-c conjugates was determined by SEC and eletrophoresis.[16] The determination of the molecular weights of the protein conjugates and, consequently, the degree of PEGylation was based on a calibration curve with several proteins with known molecular weights.

2.3. Cyt-c activity assay

The enzymatic activity of Cyt-c was determined by the catalytic oxidation of 50 µM of 2,2'-azino-bis(3-ethylbenzothiazoline-6-sulphonic acid) (ABTS) in presence of 0.5 mM of hydrogen peroxide.[5,6] The concentration of non-PEGylated and PEGylated forms was 10 µM in 0.01 M of potassium phosphate buffer (0.14 M of NaCl, pH 7.4). The reaction was started by the addition of hydrogen peroxide and followed by the absorbance' increase at 418 nm.

2.4. Circular dichroism spectroscopy

Circular dichroism (CD) spectra of Cyt-c and PEGylated conjugates were acquired either in far-UV (190-260 nm) or near-UV (250-350 nm) range using a spectropolarimeter, model Jasco J-720 (Jasco, Tokyo, Japan). The final spectra were the average of 6 scans, followed by subtraction of the spectrum of 0.01 M of potassium phosphate buffer (0.14 M of NaCl, pH = 7.4) obtained under the same conditions. Samples were placed in 1.00 mm optical length quartz cells with concentrations ranging from 13 to 15 μM. the spectra intensities (θ, mdeg) were converted to residual molar ellipticity ([θ], deg.cm^2.dmol^{-1}) by the following expression:

$$[\theta] = \frac{\theta}{10.C.l.n} \quad \textbf{(1)}$$

where *C* is the protein concentration expressed in M, *l* is the optical length expressed in cm and *n* is the number of amino acid residues in the protein (104 in this case).

The thermal stability of Cyt-c and its modified forms was also investigated by CD. Temperature was scanned from 30 to 90°C, at a rate of 1°C.min^{-1}, and back from 90 to 30°C to study, respectively, the unfolding and refolding processes suffered by the enzyme. Samples with concentrations ranging from 2 to 4 μM were placed in 5.00 mm optical length quartz cells, and the intensities of ellipticity at 222 nm (θ_{222}, mdeg) were recorded throughout the experiment. Intensities of ellipticity were then converted to residual molar ellipticity ($[\theta]_{222}$, deg.cm^2.dmol^{-1}).

2.5. Determination of kinetic parameters

The Michaelis constant (K_m) and the maximum rate (v_{max}) of the enzyme-catalyzed reaction were determined through a double reciprocal (Lineweaver–Burk) plot of Cyt-c activity *versus* ABTS concentrations (0.025-0.300 mM). The turnover number (k_{cat}), defined as the maximum number of chemical conversions of substrate molecules *per* second that a single catalytic site executes at a given enzyme concentration, was calculated for Cyt-c and both PEGylated conjugates. The kinetic parameters were measured in triplicate and expressed as means ± standard deviations. All experimental data were analysed using the Prism 6.0 software (Graphpad Software, San Diego, CA,

USA) for non-linear regression applied to Michaelis-Menten equation, and the determination coefficient (R^2) was used to compare the fitting performance. The Michaelis-Menten curves of Cyt-c, Cyt-c-PEG-4 and Cyt-c-PEG-8 are provided in **Fig. B.10 at Appendix B**.

2.6. Thermodynamic study

As described by Converti *et al.*,[17] the thermal inactivation of enzymes can be described by an enzyme unfolding equilibrium:

$$E \quad \leftrightarrows \quad E_u$$

where E and E_u are the folded and unfolded forms of the enzyme, respectively, with equilibrium constant K_U, coupled with a time-dependent irreversible denaturation, characterized by a first-order rate constant (k_d). At temperatures below the optimum temperature ($T < T_{opt}$), the equilibrium is shifted to the left side favouring the native, folded form of the enzyme, being the rate constant of the enzyme-catalysed reaction (k_0) described by the Arrhenius model. Conversely, when $T > T_{opt}$, the equilibrium is shifted to the right side favouring the unfolded form[18] and leading, after substitution of enzyme material balance in the K_U definition and Michaelis-Menten equation, to Eq. (2):

$$k_0 = \frac{A \exp(-E^*/RT)}{1 + B \exp(-\Delta H^o_U/RT)} \qquad \textbf{(2)}$$

where E^* is the activation energy of Cyt-c-catalyzed reaction, R the ideal gas constant (8.314 $J.K^{-1}.mol^{-1}$), A and B, the Arrhenius and an additional pre-exponential factors, and ΔH^o_U the standard enthalpy variation of the inactivation equilibrium previously described. If the unfolded form of the enzyme becomes predominant, what is observed while raising the temperature, Eq. (2) may be simplified originating Eq. (3):

$$k_0 = \frac{A}{B} \exp\left(\frac{\Delta H^o_U - E^*}{RT}\right) \qquad \textbf{(3)}$$

For the protein conjugates Cyt-c-PEG-4 and Cyt-c-PEG-8, the calculation of k_0 values is a challenge. Therefore, the proportionality existing between this parameter and the initial enzyme activity (v_0) was adopted. The E^* and ΔH^o_U were then estimated, either for

native or PEGylated forms of Cyt-c, from the slopes of the straight lines of lnv_0 vs. 1/T, according to the Arrhenius equation and Eq. (3), respectively.

A different approach was used for the enzyme irreversible thermo-inactivation (denaturation), which was described by a first-order reaction kinetics – Eq. (4):

$$v_d = k_d E \quad \textbf{(4)}$$

where v_d is the rate of enzyme denaturation and E represents the concentration of its active form. Introducing the activity coefficient (ψ), defined as the ratio between E and the enzyme concentration before exposition to different temperatures (E_0), k_d was estimated at each temperature from the slope of the straight line of lnψ vs. time. The activation energy of irreversible enzyme denaturation (E^*_d) was then estimated from the slope of the straight line of lnk_d vs. 1/T. The activation enthalpy (ΔH^*_d), Gibbs free energy (ΔG^*_d) and entropy (ΔS^*_d) of denaturation either for the native or PEGylated forms of Cyt-c were finally estimated, as described by Melikoglu *et al.*,[19] and through Eqs. (5) to (7):

$$\Delta H_d^* = E_d^* - RT \quad \textbf{(5)}$$

$$\Delta G_d^* = -RT \ln\left[\frac{k_d\, h}{k_B\, T}\right] \quad \textbf{(6)}$$

$$\Delta S_d^* = \frac{\Delta H_d^* - \Delta G_d^*}{T} \quad \textbf{(7)}$$

where k_B and h are the Boltzmann and Planck constants, respectively.

The enzyme half-life ($t_{1/2}$) was defined as the time of exposure at a given temperature to reduce E to one half of E_0 and calculated by Eq. (8):[19]

$$t_{1/2} = \frac{\ln 2}{k_d} \quad \textbf{(8)}$$

3. Results and discussion

3.1. Structural effects of Cyt-c PEGylation

Cyt-c was modified with mPEG-NHS (5 kDa) forming a heterogeneous mixture of unreacted protein, two PEGylated conjugates with different PEGylation degrees (number of grafted polymer chains) and PEGylation by-products (*e.g.* salts and PEG derivative). Fast protein size exclusion liquid chromatography was applied in the separation of the different PEGylated forms as well as on the determination of the PEGylation degree, *i.e.* the number of PEG chains attached to Cyt-c. In particular, the PEGylation reaction led to two purified fractions with four and eight mPEG chains *per* Cyt-c molecule (on average), similarly to other PEGylated conjugates previously reported in literature for this enzyme.[6,20]

To determine the effect of PEGylation on the Cyt-c secondary and tertiary structures, circular dichroism spectroscopy was employed. The far-UV and near-UV circular dichroism spectra of unreacted Cyt-c and both PEGylated conjugates were evaluated being the main results depicted in **Figs. 3.18.A** and **1B**. In these figures, the characteristic secondary and tertiary structural fingerprints of Cyt-c are identified. The peak around 330 nm and the small peak at 300 nm are characteristic of tryptophan (Trp), those between 280 and 290 nm representative of tyrosine (Tyr) and the ones around 255–270 nm typical of phenylalanine (Phe). However, as previously observed by other authors,[7,20] the PEGylation reaction did not cause any significant spectral change either in the far (**Fig. 3.18.A**) or the near (**Fig. 3.18.B**) UV region, thus proving that the protein tertiary structure was maintained (**Fig. 3.18.B**). Moreover, the different protein forms exhibited negative intensity bands centred at 208 and 222 nm and a positive peak in the 195-200 nm region of the spectrum, which are characteristic of a predominant α-helical secondary structure.

The Cyt-c thermal stability (folding/unfolding) was also investigated through circular dichroism (**Fig. 3.18.C**). The unfolding curves showed similar behaviour between the three Cyt-c forms. In this case, the proteins were found to be stable up to 75°C and unfolded above this temperature. Nevertheless, the results demonstrated that the unreacted Cyt-c has refolded more efficiently than Cyt-c-PEG-4, followed by Cyt-c-PEG-

8, suggesting that the PEG chain interferes with the refolding process, probably by steric hindrance of the unfolded protein chain during refolding.[21]

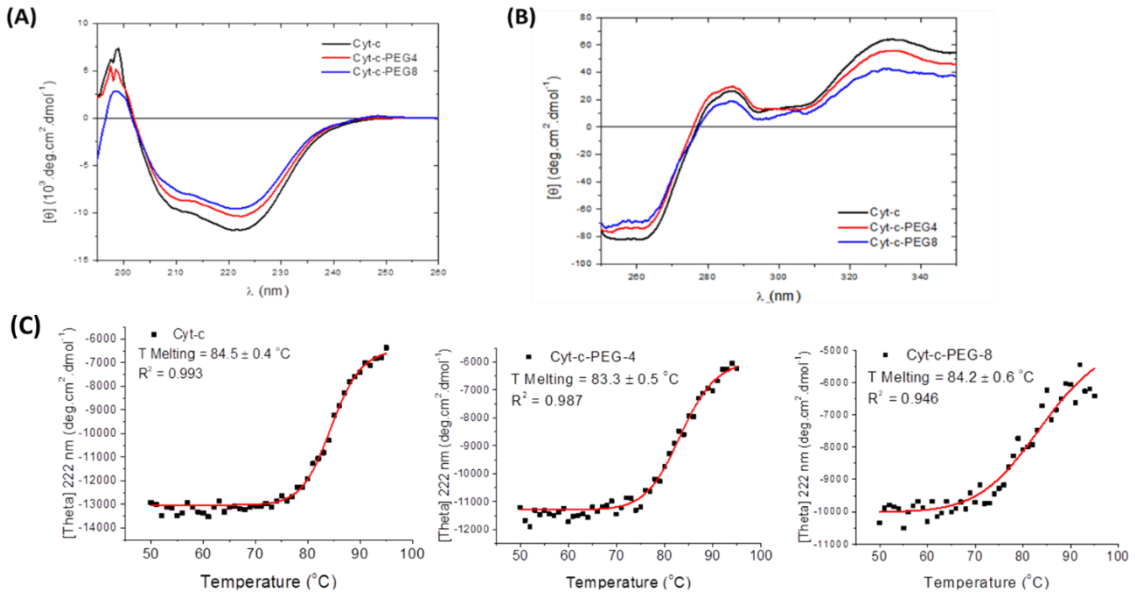

Fig. 3.18. (A) Far-UV and **(B)** Near-UV circular dichroism spectra of equine heart cytochrome c either in native form (Cyt-c, —) or PEGylated with 4 (Cyt-c-PEG-4, —) or 8 (Cyt-c-PEG-8, —) PEGs. Experiments were carried out with 13-15 µM of Cyt-c/Cyt-c-PEG-4/Cyt-c-PEG-8 in 0.01 M phosphate buffer (0.14 M NaCl, pH = 7.4) at room temperature (25±1°C). **(C)** Thermal stability curves of unfolding (■) and refolding (—) processes of the same enzyme preparations.

3.2. Kinetic parameters

To demonstrate the influence of PEGylation on the kinetics of enzyme-catalysed reaction, the activity of unreacted Cyt-c and the PEGylated conjugates was evaluated in terms of their capacity to oxidize ABTS in presence of 0.25 mM of hydrogen peroxide (**Table 3.3.**). The main kinetic parameters of this reaction, namely the Michaelis constant (K_m), the turnover number (k_{cat}) and the maximum reaction rate (v_{max}), were calculated from the experimental results of activity carried by varying the initial substrate concentration (S_0) from 0.025 to 0.300 mM. The nonlinear regression of the experimental data of reaction rate vs. the ABTS concentration revealed that all the three enzyme preparations presented, with good correlation ($R^2 > 0.95$), a Michaelis-Menten kinetics. The kinetic parameters estimated for the three preparations varied in the ranges of 36.00 ± 6.24 µM < K_m < 85.21 ± 11.23 µM, 0.34 ± 0.03 min^{-1} < k_{cat} < 0.91 ± 0.05 min^{-1} and 0.41 ± 0.02 $nmol.min^{-1}$ < v_{max} < 1.09 ± 0.05 $\mu mol.min^{-1}$. The slight decrease of k_{cat} and v_{max}, along with the increase in K_m observed for PEGylated conjugates in

comparison with the native protein, indicate the negative effect of the PEGylation on the Cyt-c catalytic performance. This effect was confirmed by the improvement of the catalytic activity by decreasing the PEGylation degree, in which Cyt-c-PEG-8 presented lower k_{cat} and higher K_m than Cyt-c-PEG-4. This behaviour was already observed in previous works, where the decrease of the activity of several enzymes after PEGylation was reported.[22,23] Moreover, the PEGylation ability to stabilize the enzymes structure, even at high temperatures, compensates the decay of the kinetic parameters (*i.e.* k_{cat}/K_m ratio).[22,24,25] Laccase is an example where the PEGylation was shown to reduce the k_{cat}/K_m ratio for the ABTS oxidation.[24] Since in the present study the circular dichroism data excluded significant structural alterations of Cyt-c induced by PEGylation, these variations in the kinetic parameters may be attributed to (i) minor structural alterations in the heme environment[7] and/or (ii) to the loss of enzyme structural flexibility caused by the polymer binding[26]. In terms of oxidation of polyaromatic hydrocarbons (PAHs), the effect of Cyt-c PEGylation was different from that observed for other electron donors. For instance, in the specific case of tetrahydrofuran, the Cyt-c PEGylation was reported to induce a positive effect on the kinetics parameters, with an increase in the k_{cat}/K_m ratio from 4.1 $min^{-1}.mM^{-1}$ to 132 $min^{-1}.mM^{-1}$.[8,27] Nevertheless, the oxidation of electron donors such as ABTS by Cyt-c-PEGylated proteins would still be advantageous taking into consideration the various beneficial effects of attaching PEG to the protein structure, for example its improved thermostability.

Table 3.3. Kinetic parameters of Cyt-c-catalysed reaction for the native cytochrome c (Cyt-c) or PEGylated conjugates, the Cyt-c-PEG-4 and Cyt-c-PEG-8. The catalytic oxidation of ABTS was performed in the presence of 0.5 mM of H_2O_2, at 25±1°C and pH 7.4.

Protein	K_m **(μM)**[a]	v_{max} **(nmol.min^{-1})**[b]	k_{cat} **(min^{-1})**[c]	k_{cat}/K_m **(min^{-1}.mM^{-1})**	R^2
Cyt-c	36.00 ± 6.24	1.09 ± 0.05	0.91 ± 0.05	25.30	0.956
Cyt-c-PEG-4	73.24 ± 6.40	0.73 ± 0.04	0.61 ± 0.03	8.33	0.958
Cyt-c-PEG-8	85.21 ± 11.23	0.41 ± 0.02	0.34 ± 0.03	4.04	0.975

[a]Michaelis constant.
[b]Maximum reaction rate.
[c]Turnover number.

3.3. Thermodynamic study

Thermodynamic studies are important to understand the role of temperature on the enzymes activity. Here, the effect of the Cyt-c PEGylation degree on the protein reversible unfolding and long-term thermostability was investigated.

3.3.1. Thermal inactivation – Enzyme unfolding

The optimum temperature in terms of Cyt-c activity was identified by performing activity tests varying the temperature (T) from 30 to 100 °C. To minimize the influence of the irreversible denaturation on the activity of Cyt-c, only the initial values of enzyme activity (v_0) were taken into account. Cyt-c and Cyt-c-PEG conjugates proved to be active on the range of temperatures from 30 to 80 °C, with an optimum temperature at 80 °C, in accordance with literature.[1]

The semi-log plot of $\ln v_0$ vs. $1/T$ showed two tendencies. At temperatures below 80°C, a linear decrease was found **(Fig. 3.19.B)**, following the typical Arrenhius-type behaviour. Contrariwise, beyond 80°C, the opposite trend was observed **(Fig. 3.19.A)**, suggesting temperature-driven enzyme unfolding. That being the case, from the slopes of the straight lines in the temperature ranges 30-80°C ($T < T_{opt}$) and 80-100°C ($T > T_{opt}$), the activation energies of the enzyme-catalysed reaction (E^*) and the standard enthalpy changes of enzyme unfolding (ΔH^o_U) were estimated for the native and PEGylated forms with satisfactory correlations ($R^2 > 0.84$ and > 0.97, respectively) (**Table 3.4.**). E^* was 15-36% higher for the native protein (10.22 $kJ.mol^{-1}$) than the value estimated for the PEGylated conjugates, suggesting the reduction of the energy of the transition state promoted by the PEGylation. The very low E^* values estimated for all preparations indicate that little energy was required to form the transition state of ABTS oxidation, thus highlighting an effective oxidation capacity. Apparently, they seem to be inconsistent with the lower catalytic performance at mild temperatures ($T < T_{opt}$) of PEGylated conjugates, denoted by lower v_{max} and higher K_m values, compared to the native enzyme. This apparent inconsistency may be the result of (i) enzyme unfolding and/or irreversible denaturation interference (see the following section) on the starting activity, (ii) insufficient predominance of enzyme unfolding at $T > T_{opt}$, thereby making simplification of Eq. (1) to Eq. (2) not fully applicable.

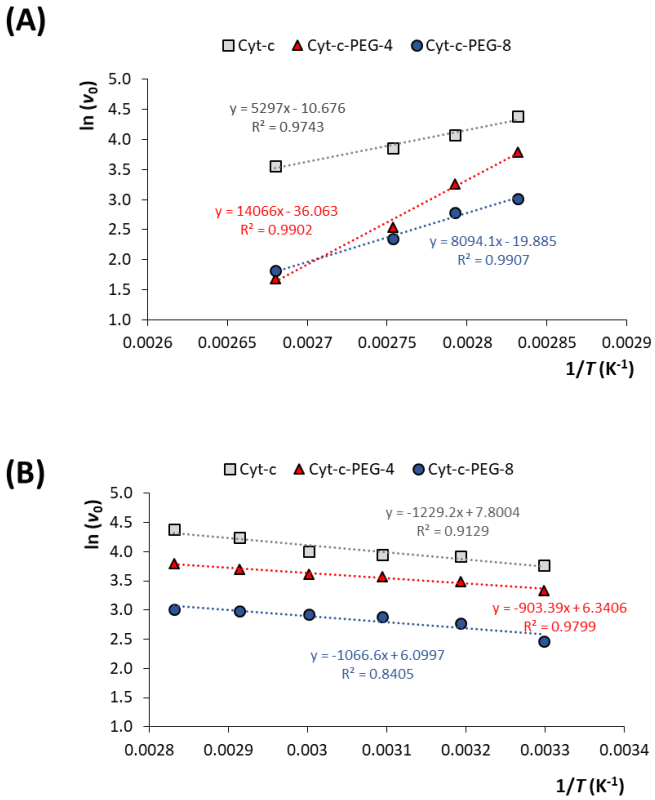

Fig. 3.19. Arrhenius-type plots of initial activity of Cyt-c and PEGylated conjugates with 4 (Cyt-c-PEG-4) or 8 (Cyt-c-PEG-8) PEGs attached, using 0.300 mM ABTS as a substrate.

Table 3.4. Thermodynamic parameters of Cyt-c-catalyzed reaction and reversible unfolding of native Cyt-c, Cyt-c-PEG-4 and Cyt-c-PEG-8 estimated according to the Arrhenius equation. The concentration of non-PEGylated and PEGylated Cyt-c was 10 µM in 0.01 M of potassium phosphate buffer (0.14 M of NaCl, pH 7.4). The catalytic oxidation of the substrate ABTS was performed in the range of T = 30 – 100 °C (ΔT = 10 °C).

Protein	***E**** **(kJ.mol^{-1})**	**ΔH^{o}_{U} (kJ.mol^{-1})**
Cyt-c	10.22	33.82
Cyt-c-PEG-4	7.51	109.44
Cyt-c-PEG-8	8.87	58.43

Note: Activation energy of Cyt-c constant.

PEGylation also increased the ΔH^{o}_{U} of thermal inactivation from 33.82 kJ.mol^{-1} for the native protein up to 109.44 kJ.mol^{-1} for Cyt-c-PEG-4. These results suggest the enzyme stabilization against unfolding at $T > T_{opt}$. Additionally, the higher ΔH^{o}_{U} value for Cyt-c-

PEG-4 compared with Cyt-c-PEG-8 makes reasonable the hypothesis that excess PEGylation partially reduced this benefit. As suggested by Gaertner and Puigserver,[28] the entropic penalty related to the restricted motion of some amino acid groups on the protein surface due to the shell-like structure formed by coiled PEG chains influences protein stability.

3.3.2. Thermostability – Irreversible enzyme denaturation

Long-term residual activity tests were carried in the temperature range 70–95 °C, being the results in terms of residual activity coefficient (ψ) illustrated in the semi-log plots of **Fig. B.11 at Appendix B**. The residual activities of Cyt-c and PEGylated conjugates followed the typical first-order decay due to denaturation already observed for other oxidoreductases.[29] For biosensors, the enzyme half-life ($t_{1/2}$) is a key parameter in terms of economic feasibility and resistance to thermal inactivation, that has become a required property for industrial applications of catalysts.[30,31]

The thermodynamic and kinetic parameters of the irreversible denaturation process are summarized in **Table 3.5.**. As can be seen, $t_{1/2}$ progressively decreased and the rate of the first-order Cyt-c thermo-inactivation (k_d) progressively increased with the increase in temperature, which means that its irreversible denaturation is more extensive. Regarding the effect of PEGylation, the protective role of PEG conjugation is confirmed, since both Cyt-c-PEG-4 and Cyt-c-PEG-8 exhibited higher $t_{1/2}$ compared to the native protein. Additionally, the number of PEGs grafted to the protein greatly enhanced the enzyme long-term thermostability. Indeed, the higher the PEGylation degree, the longer the $t_{1/2}$ (about twice and 1.1-1.7-fold that of Cyt-c than the values obtained for Cyt-c-PEG-8 and Cyt-c-PEG-4, respectively).

Semi-log plot of $\ln k_d$ vs. $1/T$ allowed estimating, with good correlation ($R^2 > 0.96$), the activation energies of denaturation (E^*_d) (**Fig. 3.20.**). In this case, 50.51 kJ.mol^{-1}, 72.63 kJ.mol^{-1} and 63.36 kJ.mol^{-1} were the data obtained for Cyt-c, Cyt-c-PEG-4 and Cyt-c-PEG-8, respectively. The higher values of E^*_d obtained for the PEGylated conjugates when compared to the one found for the native protein confirmed the thermostability promoted by PEGylation. Moreover, the higher E^*_d value for Cyt-c-PEG-4 compared to Cyt-c-PEG-8 indicated that excess PEGylation has a negative impact, not only for enzyme unfolding, as previously discussed, but also on the conjugates thermostability. The

comparison of E^*_d data with the values found in literature is challenging, mainly due to the large variability resulting from the source and purity of the enzymes, as well as, the substrates used in the thermostability assays.[30,32,33]

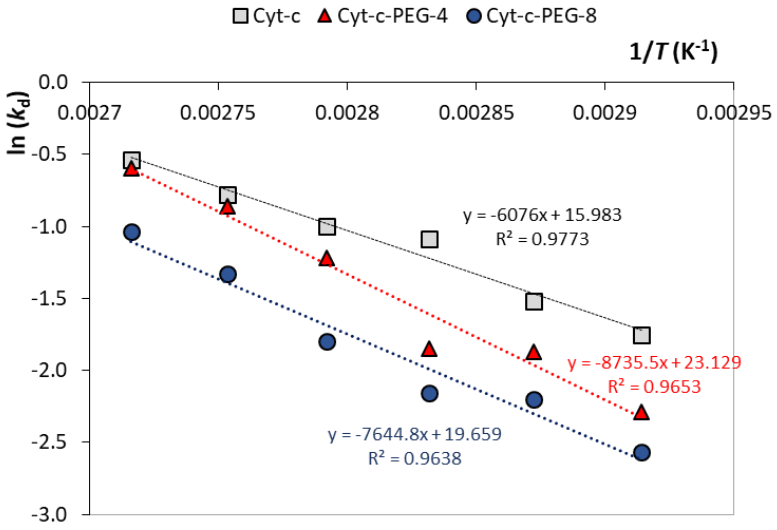

Fig. 3.20. Semi-log plots of the first-order denaturation constant (k_d) vs. the reciprocal temperature ($1/T$). The slopes of the resulting straight lines used were used to estimate the activation energies (E^*_d) of irreversible inactivation (denaturation) of native cytochrome c (Cyt-c) and PEGylated conjugated with 4 (Cyt-c-PEG-4) or 8 (Cyt-c-PEG-8) PEGs attached.

Applying Eqs. (5–7), it was possible to calculate the activation enthalpy (ΔH^*_d), Gibbs free energy (ΔG^*_d) and entropy (ΔS^*_d) of denaturation for Cyt-c and PEGylated conjugates (**Table 3.5.**). These results indicate that the enzyme denaturation process is (i) exothermic ($\Delta H^*_d > 0$), (ii) not spontaneous ($\Delta G^*_d > 0$), and (iii) implies, at all tested temperatures (T = 70-95 °C), a transition state with an unexpected more rigid structure than the reacting system ($\Delta S^*_d < 0$), either for native or PEGylated forms. In particular, the ΔH^*_d is an important thermodynamic parameter to consider, since it expresses the total amount of energy required to promote the enzyme denaturation,[13] which is accompanied by the disruption of non-covalent linkages, including hydrophobic interactions, hydrogen bonds, and van der Waals forces.[19] Lower ΔH^*_d values at higher operating temperatures indicate that enzyme thermo-inactivation is boosted at higher temperatures. So, the higher enthalpic contributions of PEGylated conjugates compared to the native protein mean that higher energy is needed to denature the PEGylated conjugates, thereby endorsing the protective role of PEG coupling. The extent of the

enzyme thermostability also depends on the ΔS^*_d, which expresses the amount of energy *per* temperature degree involved in the transition from a native to a denatured state.[13] Negative values of ΔS^*_d, like those estimated in this study, suggest the occurrence of an aggregation process in which a few inter- and/intra-molecular bonds are formed.[34] Thermal circular dichroism studies (**Fig. 3.18.C**) revealed a change in the protein conformation at temperatures at *circa* 75°C, suggesting that steric hindrance may have influenced the entropic variations. When an enzyme proceeds to the aggregated complex, the state of order of the system increases ($\Delta S^*_d < 0$), reducing the consequent randomness degree of such a transition. Negative values of ΔS^*_d were also found for other redox enzymes[29], hydrolases[35] and proteases[36,37] at high temperatures. Finally, the ΔG^*_d combines both enthalpic and entropic contributions.[13] When $\Delta S^*_d < 0$ and $\Delta H^*_d > 0$, the denaturation process is not spontaneous ($\Delta G^*_d > 0$), as it was found in this work. A negative value of ΔG^*_d is associated with a spontaneous process, meaning that the protein is less thermostable. An increase in ΔG^*_d, on the contrary, can be understood as an increase in the enzyme' resistance to denaturation, *i.e.* increased thermostability. Even though the ΔG^*_d values listed in **Table 3.5.** are similar for the three enzyme preparations, the highest ΔG^*_d data were obtained for the PEGylated conjugates in the entire range of temperatures, and especially for Cyt-c-PEG-8, which is consistent with the thermoprotective role of PEG previously discussed. However, contrary to what was observed for reversible unfolding, no negative impact of excess PEGylation was detected for irreversible thermo-inactivation of the enzyme.

Table 3.5. Thermodynamic and kinetic parameters of the irreversible thermal deactivation (denaturation) of native Cyt-c, Cyt-c-PEG-4 and Cyt-c-PEG-8

Cyt-c						Cyt-c-PEG-4					Cyt-c-PEG-8				
T (°C)	k_d (h^{-1})	$t_{1/2}$ (h)	ΔH^*_d (kJ/mol)	ΔG^*_d (kJ/mol)	ΔS^*_d (J/mol.K)	k_d (h^{-1})	$t_{1/2}$ (h)	ΔH^*_d (kJ/mol)	ΔG^*_d (kJ/mol)	ΔS^*_d (J/mol.K)	k_d (h^{-1})	$t_{1/2}$ (h)	ΔH^*_d (kJ/mol)	ΔG^*_d (kJ/mol)	ΔS^*_d (J/mol.K)
70	0.173	4.00	47.65	101.13	-155.83	0.101	6.84	69.78	102.66	-95.82	0.077	9.05	60.50	103.46	-125.18
75	0.219	3.17	47.61	101.97	-156.13	0.154	4.49	69.74	102.98	-95.48	0.111	6.26	60.46	103.94	-124.89
80	0.339	2.05	47.57	102.19	-154.67	0.157	4.41	69.69	104.45	-98.41	0.116	5.97	60.42	105.33	-127.18
85	0.369	1.88	47.53	103.43	-156.08	0.295	2.35	69.65	104.09	-96.16	0.165	4.19	60.38	105.82	-126.87
90	0.459	1.51	47.49	104.25	-156.31	0.422	1.64	69.61	104.50	-96.09	0.264	2.63	60.34	105.92	-125.53
95	0.587	1.18	47.45	104.98	-156.28	0.551	1.26	69.57	105.17	-96.70	0.352	1.97	60.30	106.55	-125.63

4. Conclusions

In this work, the kinetic and thermodynamic properties of PEGylated Cyt-c, a model redox protein, were determined. A maximum activity was observed at 80 °C for Cyt-c and both PEGylated forms, Cyt-c-PEG-4 and Cyt-c-PEG-8. The half-life for PEGylated conjugates, as well as the thermodynamic parameters of the enzyme denaturation were estimated based on tests of the residual activity. The Gibbs free energy and activation enthalpy was higher for PEGylated conjugates showing the protective role of this polymer, more pronounced at higher temperatures. Our results highlight the improved thermostability of the PEGylated forms of Cyt-c that could be profitably exploited for future industrial applications, especially in the biosensing and pharmaceutical sectors.

References

1. Vazquez-Duhalt, R. Cytochrome c as a biocatalyst. in *Journal of Molecular Catalysis - B Enzymatic* **7,** 241–249 (1999).
2. Radi, R., Turrens, J. F. & Freeman, B. A. Cytochrome c-catalyzed membrane lipid peroxidation by hydrogen peroxide. *Arch. Biochem. Biophys.* **288,** 118–125 (1991).
3. García-Arellano, H., Buenrostro-Gonzalez, E. & Vazquez-Duhalt, R. Biocatalytic Transformation of Petroporphyrins by Chemical Modified Cytochrome C. *Biotechnol. Bioeng.* **85,** 790–798 (2004).
4. Florence, T. M. The degradation of cytochrome c by hydrogen peroxide. *J. Inorg. Biochem.* **23,** 131–141 (1985).
5. Kim, N. H., Jeong, M. S., Choi, S. Y. & Kang, J. H. Peroxidase activity of cytochrome c. *Bull. Korean Chem. Soc.* **25,** 1889–1892 (2004).
6. Santiago-Rodríguez, L. *et al.* Enhanced stability of a nanostructured cytochrome c biosensor by PEGylation. *J. Electroanal. Chem.* **663,** 1–7 (2011).
7. Mabrouk, P. A. Effect of pegylation on the structure and function of horse cytochrome c. *Bioconjug. Chem.* **5,** 236–241 (1994).
8. Tinoco, R. & Vazquez-Duhalt, R. Chemical modification of cytochrome C improves their catalytic properties in oxidation of polycyclic aromatic hydrocarbons. *Enzyme Microb. Technol.* **22,** 8–12 (1998).
9. Presolski, S. I., Hong, V. P. & Finn, M. G. Chemistry for Bioconjugation. *Chem. Biol.*

3, 153–162 (2011).

10. Pfister, D. & Morbidelli, M. Process for protein PEGylation. *Journal of Controlled Release* **180,** 134–149 (2014).
11. Kwon, O. H. & Ito, Y. Bioconjugation for enzyme technology. *Biotechnol. Genet. Eng. Rev.* **18,** 237–263 (2001).
12. Jevševar, S., Kunstelj, M. & Porekar, V. G. PEGylation of therapeutic proteins. *Biotechnol. J.* **5,** 113–128 (2010).
13. Marangoni, A. G. *Enzyme Kinetics: A Modern Approach*. (John Wiley & Sons, 2003).
14. Saqib, A. A. N., Hassan, M., Khan, N. F. & Baig, S. Thermostability of crude endoglucanase from Aspergillus fumigatus grown under solid state fermentation (SSF) and submerged fermentation (SmF). *Process Biochem.* **45,** 641–646 (2010).
15. Nanocs. Succinimidyl PEG NHS, mPEG-NHS(SC). (2017). Available at: http://www.nanocs.net/mPEG-SC-5k-1g.htm.
16. Santos, J. H. P. M., Carretero, G., Coutinho, J. A. P., Rangel-Yagui, C. O. & Ventura, S. P. M. Multistep purification of cytochrome c PEGylated forms using polymer-based aqueous biphasic systems. *Green Chem.* **19,** 5800–5808 (2017).
17. Converti, A. *et al.* Reactivity and stability of mycelium-bound carboxylesterase from Aspergillus oryzae. *Biotechnol. Bioeng.* **77,** 232–237 (2002).
18. Roels, J. *Energetics and kinetics in biotechnology*. (1983).
19. Melikoglu, M., Lin, C. S. K. & Webb, C. Kinetic studies on the multi-enzyme solution produced via solid state fermentation of waste bread by Aspergillus awamori. *Biochem. Eng. J.* **80,** 76–82 (2013).
20. Zhou, J. Q., He, T. & Wang, J. W. PEGylation of cytochrome c at the level of lysine residues mediated by a microbial transglutaminase. *Biotechnol. Lett.* **38,** 1121–1129 (2016).
21. Parrott, M. C. & DeSimone, J. M. Relieving PEGylation. *Nat. Chem.* **4,** 13–14 (2012).
22. Hsieh, Y. P. & Lin, S. C. Effect of PEGylation on the activity and stability of horseradish peroxidase and L-N-carbamoylase in aqueous phases. *Process Biochem.* **50,** 1372–1378 (2015).

23. Santos, J. H. P. M., Torres-Obreque, K. M., Pastore, G. M., Amaro, B. P. & Rangel-Yagui, C. O. Protein PEGylation for the design of biobetters: from reaction to purification processes. *Brazilian J. Pharm. Sci.* **54,** (2018).
24. López-Cruz, J. I., Viniegra-González, G. & Hernández-Arana, A. Thermostability of native and pegylated Myceliophthora thermophila laccase in aqueous and mixed solvents. *Bioconjug. Chem.* **17,** 1093–1098 (2006).
25. Rodríguez-Martínez, J. A., Rivera-Rivera, I., Solá, R. J. & Griebenow, K. Enzymatic activity and thermal stability of PEG-α-chymotrypsin conjugates. *Biotechnol. Lett.* **31,** 883–887 (2009).
26. Morgenstern, J., Baumann, P., Brunner, C. & Hubbuch, J. Effect of PEG molecular weight and PEGylation degree on the physical stability of PEGylated lysozyme. *Int. J. Pharm.* **519,** 408–417 (2017).
27. Vazquez-Duhalt, R., Semple, K. M., Westlake, D. W. S. & Fedorak, P. M. Effect of water-miscible organic solvents on the catalytic activity of cytochrome c. *Enzyme Microb. Technol.* **15,** 936–943 (1993).
28. Gaertner, H. F. & Puigserver, A. J. Increased activity and stability of poly(ethylene glycol)-modified trypsin. *Enzyme Microb. Technol.* **14,** 150–155 (1992).
29. Eze, S. Kinetic analysis of the thermostability of peroxidase from African oil bean (Pentaclethra macrophylla Benth) seeds. *J Biochem Tech* **4,** 459–463 (2012).
30. Rigoldi, F., Donini, S., Redaelli, A., Parisini, E. & Gautieri, A. Review: Engineering of thermostable enzymes for industrial applications. *APL Bioeng.* **2,** 011501 (2018).
31. Haki, G. D. & Rakshit, S. K. Developments in industrially important thermostable enzymes: A review. *Bioresource Technology* **89,** 17–34 (2003).
32. Saqib, A. A. N. & Siddiqui, K. S. How to calculate thermostability of enzymes using a simple approach. *Biochem. Mol. Biol. Educ.* **46,** 398–402 (2018).
33. Korkegian, A., Black, M. E., Baker, D. & Stoddard, B. L. Computational thermostabilization of an enzyme. *Science (80-.).* **308,** 857–860 (2005).
34. Anema, S. G. & McKenna, A. B. Reaction kinetics of thermal denaturation of whey proteins in heated reconstituted whole milk. *J. Agric. Food Chem.* **44,** 422–428 (1996).

35. Maisuria, V. B., Patel, V. A. & Nerurkar, A. S. Biochemical and thermal stabilization parameters of polygalacturonase from Erwinia carotovora subsp. carotovora BR1. *J. Microbiol. Biotechnol.* **20,** 1077–1085 (2010).

36. Gohel, S. D. & Singh, S. P. Purification strategies, characteristics and thermodynamic analysis of a highly thermostable alkaline protease from a salt-tolerant alkaliphilic actinomycete, Nocardiopsis alba OK-5. *J. Chromatogr. B Anal. Technol. Biomed. Life Sci.* **889-890,** 61–68 (2012).

37. Hernández-Martínez, R. *et al.* Purification and characterization of a thermodynamic stable serine protease from Aspergillus fumigatus. *Process Biochem.* **46,** 2001–2006 (2011).

4. Development of Novel Purification Platforms using ABS

4.1. Multistep purification of cytochrome c PEGylated forms using polymer-based aqueous biphasic systems

Santos, J. H. P. M., Carretero, G., Coutinho, J. A. P., Rangel-Yagui, C. O. & Ventura, S. P. M. *Green Chemistry*, 2017, **19**, 5800-5808.[8]

Abstract

Chemical PEGylation of proteins has been used to improve their physicochemical properties and kinetics. However, the PEGylation reactions lead to a heterogeneous mixture of PEGylated conjugates and unreacted protein, which is a challenge for the design of an efficient downstream process. The purification of PEGylated proteins should address the two main issues: the separation of PEGylated conjugates from the unreacted protein and the fractionation of the PEGylated conjugates on the basis of their degree of PEGylation. The present study aims at the development of liquid-liquid extraction processes for the purification of PEGylated conjugates. An initial study of the partition behavior of cytochrome c and their PEGylated conjugates (Cyt-c-PEG-4 and Cyt-c-PEG-8) on polyethylene-glycol (PEG) + potassium phosphate buffer (pH = 7) aqueous biphasic systems (ABS) shows that PEGs with intermediate molecular weights (PEG MW = 1000-2000) allow the separation of the PEGylated conjugates from the unreacted protein in a single step. It is further shown that the PEGylated conjugates can be efficiently separated using ABS based in PEGs with high molecular weight (PEG MW = 6000-8000) and a study of the proteins stability after purification was carried using circular dichroism. A downstream process to separate Cyt-c, Cyt-c-PEG-4 and Cyt-c-PEG-8 with high purities (96.5% Cyt-c, 85.8% Cyt-c-PEG-4, and 99.0% Cyt-c-PEG-8) was developed. The process proposed addresses not only the efficient separation of each of the protein forms but also the recycle of the unreacted protein purified and the ABS phases, which was successfully used in a new step of PEGylation.

Keywords: Multi-stage aqueous biphasic systems; cytochrome c; PEGylation; PEGylated proteins; fractionation.

[8] Contributions: JS and GC acquired the experimental data. All the authors interpreted the experimental data. JC, CY and SV conceived and directed this work. The manuscript was mainly written by JS with contributions from the remaining authors.

1. Introduction

The use of PEGylation as a drug delivery technology was firstly proposed by Abuchowski *et al.*[1] It consists in the covalent attachment of polyethylene glycol (PEG) chains to proteins. This approach can be used for drug delivery of biopharmaceuticals, its success depending on the characteristics of the PEGylated conjugates obtained, namely its enhanced pharmacokinetics properties, increased blood residence time and reduced immunological response and proteolytic degradation.[2–4] This protein modification technique can enhance the "green" character of the final product, by preserving the efficacy of the function, while decreasing its toxicity,[5] and thus their impact to the user and the environment. Through PEGylation, novel biobetters[6,7] have been developed and commercialized. Pegadamase (Adagen), a PEGylated form of the enzyme adenosine deaminase[8] used in the treatment of severe combined immunodeficiency disease (SCID),[9] and Pegaspargase (Oncaspar), a PEGylated form of the enzyme asparaginase[10] used for the treatment of childhood acute lymphoblastic leukemia (ALL)[11] are just two examples. In the field of biosensors, the PEGylation also showed to be a promising approach to enhance the thermal and long-term stability of the protein-based bionsensors.[12–14]

Given the interest of the applications of protein PEGylation, the downstream processing of the PEGylated conjugates remains a bottleneck to its widespread use.[15] The PEGylation reaction normally results in a heterogeneous mixture of unreacted protein with a variety of PEGylated conjugates with different degrees of PEGylation.[16] The purification of the PEGylated conjugates implies thus three main challenges: (i) the isolation and recycling of the unreacted protein from the PEGylated conjugates, (ii) the fractionation of PEGylated conjugates according to their degrees of PEGylation , and (iii) the isolation of each protein form from the reaction products (*e.g.* PEG derivate, hydroxylamine and buffer).[17] Nowadays, the downstream processes most used to fractionate the PEGylated conjugates are based on size exclusion chromatography (SEC)[18,19] and ion exchange chromatography (IEX).[20–22] Recently, non-chromatographic techniques such as capillary electrophoresis,[23,24] ultrafiltration[25–28] and aqueous biphasic systems (ABS)[29,30] have been proposed to selectively purify the PEGylated conjugates.

Aqueous biphasic systems (ABS) were originally proposed by Albertsson[31] as a cleaner and more biocompatible alternative to conventional liquid-liquid extraction processes that often use hazardous volatile organic solvents while ABS present a high water content, providing milder and more biocompatible conditions for bioseparations.[32] ABS are designer processes, with a wide range of compounds that can be combined as phase formers, *e.g.* polymer + polymer,[33–35] polymer + salt,[36,37] salt + salt,[38] among others.[39–41] This tailoring ability allows the design of specific downstream processes for a wide range of biomolecules.[42–45] Furthermore, the scale-up of these systems is rather straightforward.

The use of PEG + salt, PEG + polymer and PEG + polymer + salt (adjuvant) ABS for the separation of the PEGylated conjugates has been described for several proteins, *e.g.* bovine serum albumin,[46] immunoglobulin G,[46] α-lactalbumin,[29] RNase A,[29,47] lysozyme[48] and glycoproteins granulocyte-macrophage colony-stimulating factor (GM-CSF).[30,46] Delgado *et al.*[30,46] reported a correlation between log K and the PEGylation degree of the conjugates that allowed the purification of protein conjugates from the unreacted protein. González-Valdez *et al.*[29] proved that PEG + phosphate buffer ABS were able to efficiently fractionate the PEGylated conjugates from their unreacted precursors for two proteins: RNase A and α-lactalbumin. Nevertheless, the most remarkable application of ABS considering the downstream PEGylation process was attributed to Sookumnerd and Hsu,[48] which used PEG + phosphate buffer countercurrent distribution in aqueous biphasic systems (CCD-ABS) to selectively fractionate the unmodified lysozyme, and its mono- and di-PEGylated forms. Galindo-López & Rito-Palomares[47] also attempted the separation of mono-PEGylated and di-PEGylated RNase A, using CCD-ABS followed by an ultrafiltration. However, low selectivities (*i.e.* co-elution of mono-PEGylated RNase A and di-PEGylated RNase A in the purified fractions) were obtained and significant product loss (%*Rec* mono-PEGylated RNase A = 34% and %*Rec* di-PEGylated RNase A = 45% of 50 kDa of PEG) occurred for both PEGylated conjugates. Despite the promising results of ABS in the fractionation of different protein PEGylated forms, their use is still compromised by the poor results obtained. While Cyt-c has been purified with ABS[49,50] and stabilized with ionic liquids,[51,52] results for the purification of PEGylated cytochrome c (Cyt-c) with ABS are, to the best of our knowledge, previously inexistent. Cyt-c is a

biocatalyst[53–56] used as a biosensor,[12,57] and enzyme-based biosensors suffer from the fact that proteins have a fragile conformation, being affected by several exogenous conditions, namely pH, salt concentration, presence of proteases, and temperature, among others.[12,58] In order to overcome those drawbacks, the chemical modification of proteins and enzymes is frequently employed.[13,59] Actually, the chemical modification of protein-based biosensors through PEGylation improves their properties, like their biocompatibility, long-term stability, enhanced thermal stability, and solubility in organic solvents.[2] In this context, some authors have already shown the potential of PEGylation in nanostructured Cyt-c biosensor, by improving its long-term stability even under accelerated conditions.[12] However, there is a need to purify the PEGylated conjugates of Cyt-c in order to have a control batch-to-batch and guarantee that all purified conjugates have a similar biosensing activity.

In this work, polymer-based ABS were used to develop an integrated process to fractionate different cytochrome c PEGylated forms and separate them from the unreacted protein. In the optimization of this integrated process, a multistep strategy was developed to separate firstly the unreacted protein from the conjugates and, secondly, the conjugates form each other. Aiming at the industrial application of the process, the recycling of the unreacted protein to a novel PEGylation cycle was also investigated, as well as the recycling and reuse of each phase former used in the ABS preparation.

2. Materials and Methods

2.1. Materials

Horse heart cytochrome c (Cyt-c) was acquired in Sigma-Aldrich with a purity of ≥ 95%. The PEG derivative used in the PEGylation reaction was the methoxyl polyethylene glycol succinimidyl NHS ester (mPEG-NHS or just mPEG), obtained from Nanocs (purity > 95%). Hydroxylammonium chloride acquired from Sigma-Aldrich was used to stop the PEGylation reaction and to avoid the formation of undesirable and instable products. The aqueous buffer used in the PEGylation reaction was 100 mM potassium phosphate buffer, being the pH adjusted using a solution of NaOH 2 M. The inorganic salts, K_2HPO_4 and K_2HPO_4, were purchased from Sigma-Aldrich (purity of 95%). The phase formers used to prepare the different ABS were the polyethylene glycol (PEG) with different MW

(300, 600, 1000, 1500, 2000, 4000, 6000, and 8000), obtained from Sigma-Aldrich with high purity and the potassium phosphate buffer was prepared using K_2HPO_4 and K_2HPO_4.

2.2. PEGylation reaction of Cyt-c

The PEGylation reactions were conducted according to the literature.[60] Briefly, 1 mL of a Cyt-c solution (0.5 $mg.mL^{-1}$) in potassium phosphate buffer (100 mM, pH = 7) was added to a flask containing 5.2 mg mPEG with 5 kDa. The mixtures were stirred at 400 rpm, for 15 min at room temperature with a magnetic stirrer, and then stored at -20^{o}C for further use.

2.3. Purification studies of unreacted Cyt-c and PEGylated forms using ABS

Ternary mixtures of PEG + potassium phosphate buffer were used to study the fractionation of the unreacted Cyt-c and PEGylated forms. In these systems, the top phase corresponds to the PEG-rich phase while the bottom phase is mainly composed by potassium phosphate buffered salt. The mixture points used in the purification studies were chosen based on phase diagrams described in literature.[61,62]

For the first screening, the effect of the PEG molecular weight was evaluated (PEG 300, 600, 1000, 1500, 2000, 4000, 6000 and 8000 $g.mol^{-1}$) considering a fixed mixture with 15 wt% of PEG + 20 wt% of phosphate buffer (pH 7). Regarding the second set of experiments carried, in which the water content of the top phase was studied, the PEG 1500 + potassium phosphate buffer (pH = 7) system was studied considering the mixture points: (15; 15 wt%), (17.5; 15 wt%), (20; 15 wt%), (22.5; 15 wt%), (25; 15 wt%), (potassium phosphate buffer; PEG 1500). The tie-lines (TLs) were calculated for all the mixture points aforementioned as previously reported.[63,64]

For the study of the multistep ABS strategy three consecutive ABS were implemented: first step - **ABS I** using PEG 8000 + potassium phosphate buffer (pH = 7); second step - **ABS II** using PEG 8000 + potassium phosphate buffer (pH = 7); and third step - **ABS III** using PEG 1500 + potassium phosphate buffer (pH = 7). In the case of **ABS II** and **ABS III** the top-phase was recovered and used in the next step of purification.

For the partition studies the preparation of ABS were carried in eppendorfs, with a total volume of 2 mL, being the aqueous mixture vigorously homogenised in vortex. After the

homogenisation, the systems were centrifuged for 15 min at 3500 rpm to induce the phase separation and both phases were carefully separated and weighted. After separation, both top and bottom phases were injected into an AKTA™ purifier system (GE Healthcare) size exclusion chromatographer equipped with a Superdex 200 Increase 10/300 GL chromatographic column prepacked with crosslinked agarose-dextran high resolution resin (GE Healthcare) in order to separate and quantify each PEGylated conjugate and the unreacted protein. The column was equilibrated with 0.01 M of a sodium phosphate buffer solution (0.14 M NaCl, pH = 7.4) and eluted with the same buffer with a flow of 0.75 mL min^{-1}. The quantification of the unreacted Cyt-c and each conjugate was carried at 280 nm by FPLC/UV size-exclusion method.

All experiments were performed in triplicate, where the final absorbance was reported as the average of three independent assays with the respective standard deviations calculated.

To assess the performance of the purification parameters for the different ABS, the partition coefficients in log scale (log K) of the unreacted Cyt-c and the PEGylated conjugates (Cyt-c-PEG-4 and Cyt-c-PEG-8), their recovery in the top (*Rec* Top - %) and bottom (*Rec* Bot - %) phases were determined (eqns. 1 to 3, respectively):

$$\log K = \log\left(\frac{[Prot]top}{[Prot]bot}\right) \quad \textbf{(1)}$$

$$Rec\ Top\ (\%) = \frac{100}{1 + \left(\frac{1}{K \times Rv}\right)} \quad \textbf{(2)}$$

$$Rec\ Bot\ (\%) = \frac{100}{1 + Rv \times K} \quad \textbf{(3)}$$

where $[Prot]_{top}$ and $[Prot]_{bot}$ represent the protein concentration in the top and bottom phases, respectively. Rv represents the volume ratio between the top and bottom phase volumes. The purity of the three Cyt-c proteins was calculated considering the ratio between the (SEC-FPLC) peak area representing the target protein and the peak area defined for the sum of all proteins present in the phase.[65] The purification parameters were calculated for the unreacted Cyt-c and the PEGylated conjugates, respectively Cyt-

c-PEG-4 and Cyt-c-PEG-8. The mass balance (*MB*) was calculated for the three Cyt-c based products, considering each separation unit, and the overall process (*OMB*).

2.4. Recycling of unreacted Cyt-c and its application in a new cycle of PEGylation

In order to prove the reuse of the unreacted protein in a subsequent cycle of PEGylation, after its recovery from the reactional mixture using the ABS two approaches were tested. The first strategy consists in adding directly to the reaction media the salt-rich phase with the unreacted Cyt-c. The second approach tested was the use of the unreacted Cyt-c free of the salt-rich phase, which was removed by precipitation using cold acetone. In this last approach, the unreacted protein was re-suspended in the same buffer used for the PEGylation reaction. For both cases, the quantification of the PEGylation conjugates and unreacted protein was performed by FPLC/UV SEC methodology. A SDS-PAGE of the samples was carried to evaluate the PEGylation yield.

2.5. Circular Dichroism (CD) experiments

CD spectra of Cyt-c before and after ABS purification were obtained in a Jasco J-720 Spectropolarimeter (Jasco, Tokyo, Japan). The final spectra were the average of 6 scans, following subtraction of the spectrum representing 0.01 M of sodium phosphate buffer (0.14 M NaCl, pH = 7.4) obtained under the same conditions. CD spectra were obtained in the far-UV range (190-260 nm). Samples were placed in quartz cells (1.00 mm of optical length) with the concentration ranging from 13 to 15 µM. Spectra intensities (θ, mdeg) were converted to residual molar ellipticity ([θ], deg.cm^2.dmol^{-1}) by the following expression:

$$[\theta] = \frac{\theta}{10.C.l.n} \quad \textbf{(5)}$$

where *C* is the protein concentration in mol.L^{-1}, *l* is the optical length in cm and *n* is the number of residues in the protein, that for this specific case is 104 residues.

3. Results and discussion

3.1. Partition studies

PEGylation is one of the most attractive strategies used to increase the half-life time of therapeutic proteins. Despite its high applicability, the efficiency of the PEGylation reaction is low, thus compromising the production of site-specific PEGylated proteins. In order to establish an efficient process to separate the PEGylated forms from the unreacted protein, polymer-based ABS composed of PEG and potassium phosphate buffer were investigated. The influence of the various process and system variables on the partition of these biomolecules was evaluated by using the heterogeneous mixture obtained after PEGylation. From the PEGylation reaction three forms were obtained, the unreacted Cyt-c, the Cyt-c PEGylated 4 times (Cyt-c-PEG-4) and the Cyt-c PEGylated 8 times (Cyt-c-PEG-8). The recovery results at the ABS top and bottom phases are reported in **Table C.1-2 at Appendix C**.

The effect of the PEG MW was the first variable studied. A fixed mixture point with 15 wt% of PEG + 20 wt% of potassium phosphate buffer (pH = 7) was adopted and the partition of Cyt-c, Cyt-c-PEG-4 and Cyt-c-PEG-8 is shown in **Fig. 4.1**.. From the data it is possible to observe that the native/unreacted Cyt-c has a clear tendency to partition towards the salt rich (bottom) phase. This tendency is even more pronounced with the increase of the MW of PEG (*i.e.* PEG MW ≥ 1000), thus with the increased hydrophobicity of the PEG-rich phase. Since Cyt-c is a small (12 kDa) and highly hydrophilic heme protein,[53] its higher affinity towards the most hydrophilic phase is thus expected. The PEGylated conjugates, by their turn, exhibited a different behaviour, their partition being dependent on the PEG MW. For PEGs with lower MW (*i.e.* PEG MW ≤ 2000) both conjugates partition towards the PEG-rich (top) phase, however for PEGs with higher MW the partition of the PEGylated forms towards the bottom phase becomes more significant. This is especially true for the form with lower degree of PEGylation (Cyt-c-PEG-4) that exhibits a pronounced preference for the bottom phase in ABS with the heavier PEGs. The partition coefficients obtained for the different protein forms show that these ABS can be applied as purification platforms for (i) the separation of unreacted protein from the PEGylated conjugates using the ABS composed of PEG 1000/1500 + potassium phosphate buffer (Rec $Bot_{Cyt\text{-}c}$ > 99% and Rec $Top_{Cyt\text{-}c\text{-}PEG\text{-}4}$ > 99%

and Rec $Top_{Cyt\text{-}c\text{-}PEG\text{-}8}$ > 99%) and (ii) the partial fractionation of the PEGylated conjugates according to their degree of PEGylation considering the use of ABS based in PEG 6000/8000 + potassium phosphate buffer (*Rec* $Bot_{Cyt\text{-}c}$ > 99% and *Rec* $Bot_{Cyt\text{-}c\text{-}PEG\text{-}4}$ > 99% and *Rec* $Top_{Cyt\text{-}c\text{-}PEG\text{-}8}$ ≈ 45%).

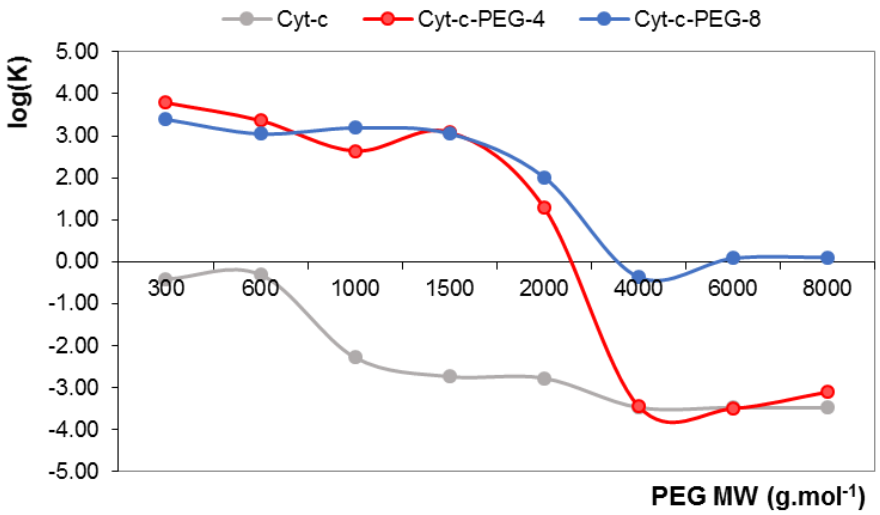

Fig. 4.1. Effect of polymer MW on log(*K*) of Cyt-c and PEGylated forms (Cyt-c-PEG-4 and Cyt-c-PEG-8) in PEG-phosphate buffer ABS (pH = 7). The PEG MW 300, 600, 1000, 1500, 2000, 4000, 6000 and 8000 $g.mol^{-1}$ were studied in a fixed mixture point 15 wt% PEG + 20 wt% phosphate buffer.

In order to fully explore the potential for the separation of the PEGylated forms, and aiming at increasing the selectivity of the systems previously studied towards the fractionation of these conjugates, different tie-lines were studied using mixture points with variable concentration of water. The ABS was chosen aiming at promoting the total partition of the PEGylated conjugates towards the top phase and the unreacted protein towards the opposite phase. The phase diagram and the respective tie-lines (*TLs*) of the selected ABS (PEG 1500 + potassium phosphate buffer, pH = 7) are depicted in **Fig. 4.2.**. The *TLs* were studied for the following mixture points: (15; 15 wt%), (17.5; 15 wt%), (20; 15 wt%), (22.5; 15 wt%), (25; 15 wt%) potassium phosphate buffer; PEG 1500 wt%. The composition of the top phase was determined as described in **Table C.3 at Appendix C**. **Table C.3** presents for the mixture points studied, their compositions, respective *TLs* and tie-line lengths (*TLLs*) obtained. As can be noticed from the results of **Table 4.1.**, by increasing the tie-line length (*TLL*), the water content in the top phase decreases (from 56.89 to 38.98 wt%). The partition behaviour of both unreacted Cyt-c and Cyt-c-PEG-8 showed no significant dependency with the *TLL* as shown in **Fig. 4.3**.. On the other hand,

the partition of Cyt-c-PEG-4 is shown to decrease with the increase of the *TLL*. This could be explained by the fact that, when the concentration of water in the top phase decreases, these less PEGylated proteins, with intermediate hydrophobicity, start to be excluded from the most hydrophobic phase towards the bottom phase (decrease of 3 fold on the log (*K*) from 3.42 to 1.40). The amount of water in top phase, has been described in literature as one of the driving-forces controlling the partition of PEGylated proteins.[29] Analysing the results, it can observed that the effect of volume exclusion only affects the PEGylated conjugate with less degree of PEGylation, thus "PEG-PEG" interactions between the PEG phase forming agent and the PEG covalently bounded to the protein are most certainly occurring. Those specific "PEG-PEG" interactions were already observed by other authors.[29] Previous PEGylated protein partition studies in PEG-dextran ABS showed partition coefficients to increase exponentially with the amount of PEG bound to the protein and a linear relationship between log K values and the number of grafted PEG chains.[30] Other studies also assume that as the number of chains linked to the protein increase "PEG-PEG" interactions become an important driving-force for the partition on this ABS, since conjugates with a higher degree of PEGylation will have stronger interactions with the PEG-rich phase. Overall, in the polymer-salt studied ABS, the partition of the protein conjugates seems to be driven by "PEG-PEG" interactions, while the partition of the unreacted protein is dominated by its hydrophilic character, promoting hydrophilic interactions with the most polar phase.

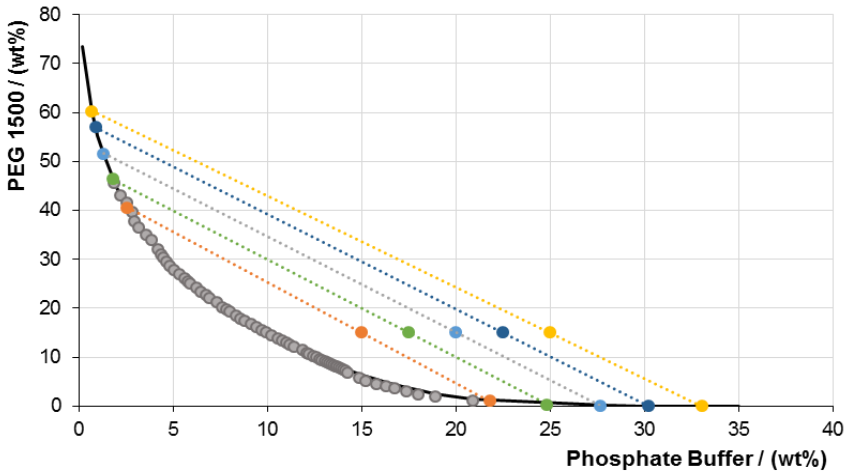

Fig. 4.2. Phase diagram (●) and respective tie-lines; *TLs* defined for the ABS composed of PEG 1500 + potassium phosphate buffer (pH = 7). The TLs were calculated considering the following mixture points (potassium phosphate buffer; PEG 1500 wt%): ■ (15; 15 wt%), ▪ (17.5; 15 wt%), ◆ (20; 15 wt%), ● (22.5; 15 wt%), ▲ (25; 15 wt%).

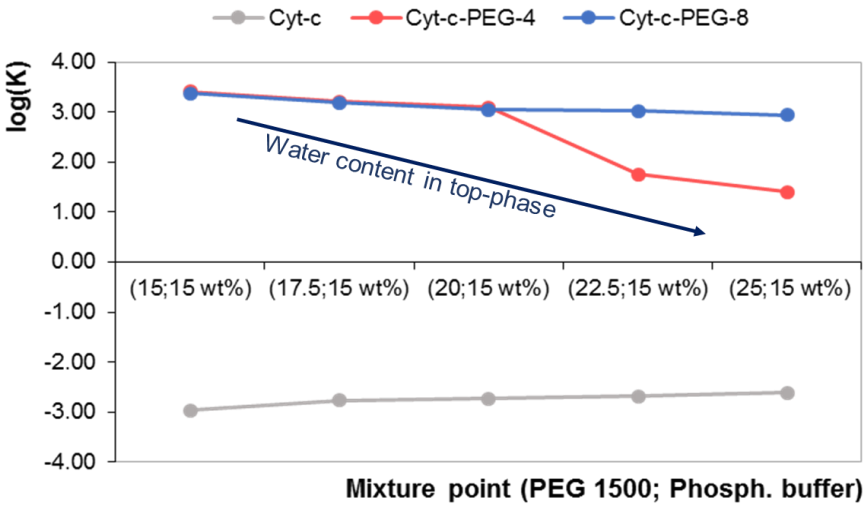

Fig. 4.3. Effect of water content in the top-phase on log(*K*) of Cyt-c and PEGylated forms (Cyt-c-PEG-4 and Cyt-c-PEG-8) in PEG 1500 + phosphate buffer ABS (pH = 7). The studied mixture points were: (15; 15 wt%), (17.5; 15 wt%), (20; 15 wt%), (22.5; 15 wt%) (25; 15 wt%) phosphate buffer; PEG 1500 wt%.

3.2. Process design

Considering the application of the various PEGylated forms, their use as both pure compounds or mixtures can be envisaged since PEGylated protein mixtures may result in a synergetic performance in terms of bioactivity, and for that reason in specific cases, *e.g* biosensing applications,[17] the fractionation of PEGylated forms could not be necessary.

If only the extraction of the PEGylated forms from the reaction mixture is required, a simplified process can be designed, as sketched in **Fig. C.1 at Appendix C** to achieve the separation of the unreacted protein from the PEGylated forms. Using this approach, the isolation and recycling of the unreacted protein from the PEGylated conjugates can be accomplished with recoveries higher than 99% for both the PEGylated forms, at the top, PEG 1500-rich phase, while more than 99% of the unreacted protein is recovered at the bottom, salt-rich phase. This means that, when the PEGylation reaction is not complete the reuse of the non-reacted proteins is possible, thus increasing the efficiency and sustainability of the overall process. To date, to the best of our knowledge, no studies were reported on the possibility of to purify and reuse the unreacted protein.

The most important challenge in terms of purification is, however, the complete separation of each PEGylated conjugate obtained. The selective fractionation of each conjugate was achieved through a multistep strategy of purification sketched in **Fig. 4.4.**

In this process, two liquid-liquid separation units were applied, namely those based in PEG 8000 + potassium phosphate buffer (pH = 7) (ABS I and ABS II), representing two stages of the same unit, and the second unit corresponding to ABS III, PEG 1500 + potassium phosphate buffer (pH = 7). The first unit was used in the separation of each PEGylated form, in which the conjugates were partially concentrated in opposite phases. The Cyt-c-PEG-4 was concentrated in the bottom phase, rich in salt, and Cyt-c-PEG-8 preferentially partitions towards the most hydrophobic phase, rich in polymer. With the application of the first process unit, the complete separation of both PEGylated forms was achieved, as demonstrated by the recoveries reported in **Fig. 4.4.**.

In the final of ABS II, the continuous removal of Cyt-c-PEG-8 was assessed and then, ABS III was applied to carry the final step of purification, in which the Cyt-c-PEG-4 was removed from the unreacted protein. From the results of log (K) for Cyt-c, Cyt-c-PEG-4 and Cyt-c-PEG-8 showed in **Table 4.1.** it is possible to reinforce that the application of the multistep process is effectively contributing to efficiently fractionate and purify each PEGylated form and the unreacted protein with high selectivity. High purities for each compound were obtained by applying this multistep approach as shown in **Table 4.1**., those being really appealing for the application of these biomolecules in the field of biosensors (purity of Cyt-c = 96.5%, purity of Cyt-c-PEG-4 = 85.8% and purity of Cyt-c-PEG-8 = 99.0%). Additionally, the analysis of the overall mass balance (OMB) of the protein conjugate, shows that the protein losses during the multistep ABS are small. The detailed composition of the streams of the process are presented in **Table C.4 at Appendix C**. It should be taken in consideration that the water content contemplates the Cyt-c based products, since their quantity in terms of weight is comparatively smaller than the phase forming agents (initial Cyt-c solution = 0.5 $mg.mL^{-1}$). This is the first report of a multistep approach using ABS in cascade being efficiently applied in the development of an effective downstream process to purify PEGylated conjugates according to their degree of PEGylation.

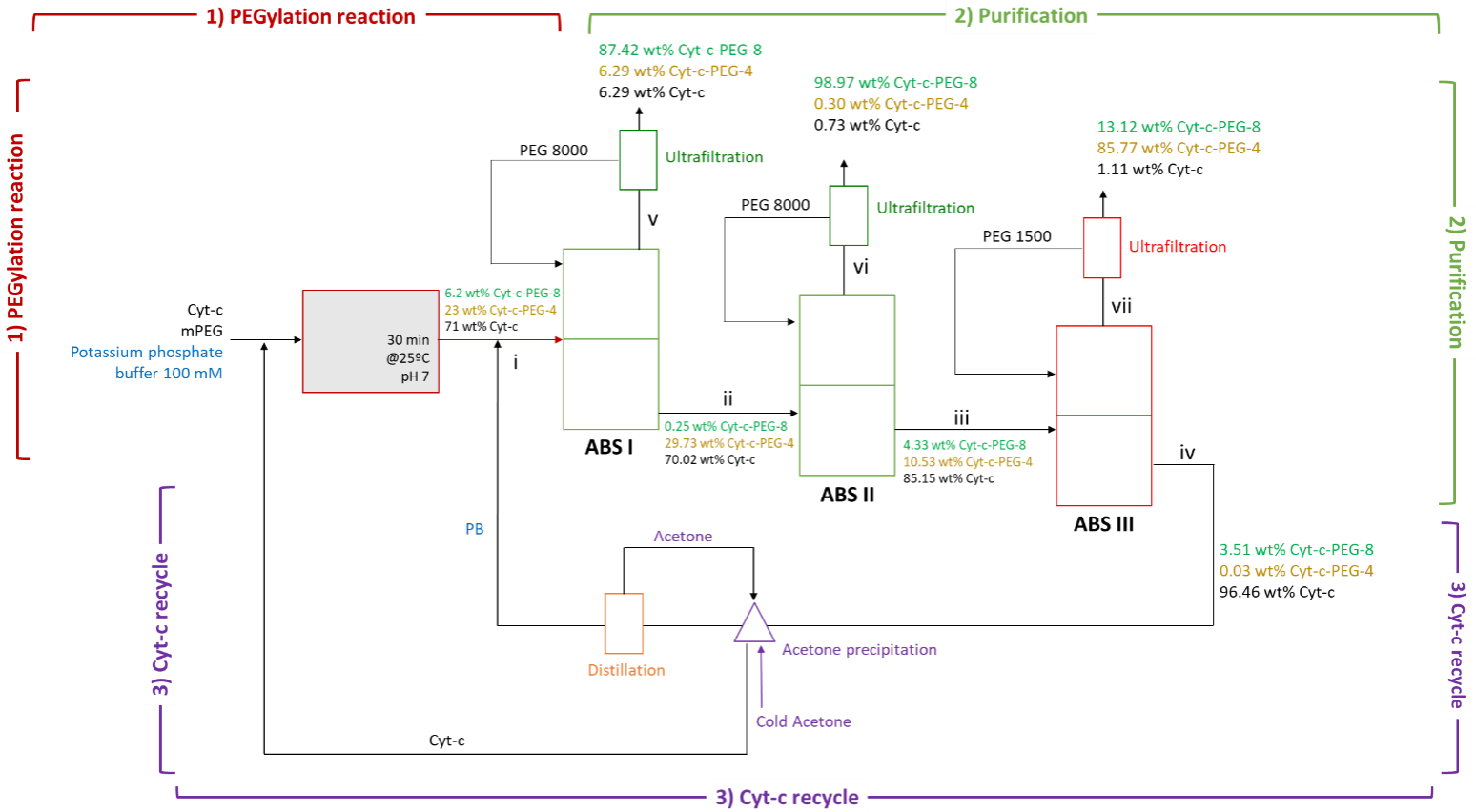

Fig. 4.4. Diagram of multistep process to fractionate selectively the unreacted cytochrome c and each one of the PEGylated conjugates (Cyt-c-PEG-4 and Cyt-c-PEG-8). The proposed strategy includes three steps of purification using ABS, namely considering the ABS I and ABS II composed of PEG 8000 + potassium phosphate buffer (pH = 7) to separate Cyt-c-PEG-8 and ABS III using PEG 1500 + potassium phosphate buffer (pH = 7) to fractionate the unreacted Cyt-c from the Cyt-c-PEG-4 conjugate. The recovery yield of each step is also provided in the present diagram. The recycle and reuse of the unreacted Cyt-c in a new PEGylation cycle after recovery in the last step is also demonstrated.

Table 4.1. Recoveries towards top and bottom phases, log (K), purities and mass balances (MB) obtained for the unreacted Cyt-c and for the PEGylated conjugates, respectively Cyt-c-PEG-4 and Cyt-c-PEG-8, in the integrated multistep process using polymer-based ABS as purification platforms, for the system using PEG (8000 and 1500) + potassium phosphate buffer (pH = 7). The overall mass balance (OMB) is also depicted in this table for unreacted and Cyt-c PEGylated forms.

	Cyt-c					**Cyt-c-PEG-4**					**Cyt-c-PEG-8**				
	Rec Top (%)	Rec Bot (%)	log(K)	Purity (%)	MB (%)	Rec Top (%)	Rec Bot (%)	log(K)	Purity (%)	MB (%)	Rec Top (%)	Rec Bot (%)	log(K)	Purity (%)	MB (%)
ABS I	0.02	99.98	-3.48	70.0	90.65	0.05	99.95	-3.10	29.7	93.74	45.78	54.22	0.11	87.4	88.23
ABS II	0.04	99.96	-3.13	85.2	92.59	0.13	99.87	-2.63	10.5	94.32	50.74	49.26	0.28	99.0	85.23
ABS III	0.09	99.91	-2.80	96.5	84.78	99.56	0.44	2.63	85.8	85.62	21.79	78.21	-0.28	99.0	96.52
OMB (%)		71.16					75.70					72.66			

The development of recycling strategies aiming at the reuse of the recovered unreacted Cyt-c to be used in new cycles of PEGylation is required. For that reason, two different approaches were tested: (i) the direct PEGylation of the salt-rich aqueous phase in which the purified Cyt-c is concentrated and (ii) the use of an acetone precipitation step to isolate the purified Cyt-c from the salt-rich layer as represented in **Fig. 4.5**.. After the precipitation step the unreacted protein is ressuspended in the same buffer used in the PEGylation. The results obtained, presented in **Fig. 4.5**., show the first approach to be inefficient due to the absence of any PEGylation of the recycled Cyt-c as can be gauged from the chromatogram presented in **Fig. 4.5.A**, which could be due to the higher amounts of salt present. However, the approach based in the acetone precipitation proved to be efficient for the recovery of the Cyt-c for further PEGylation, as shown in the chromatogram presented in **Fig. 4.5.B** and Lane 2 of the SDS-PAGE in **Fig. 4.5.C**, thus increasing the viability of the overall process.

Finally, the stability and integrity of the unreacted Cyt-c purified was accessed using far-CD. Both the control and purified Cyt-c present a CD spectrum (**Fig. 4.6.**) characteristic of α-helical secondary structures, displaying negative intensity bands centred at 208 and 222 nm and a positive peak at the 195-200 nm region of the spectrum, proving thus the structural integrity of the protein structure. Moreover, the PEGylated forms were also stable after the multistep downstream processing and confirmed by far-UV CD (**Fig. C.2 at Appendix C**).

The results reported highlight the potential of the downstream process here proposed for an efficient fractionation of the Cyt-c PEGylated conjugates and recovery of unreacted Cyt-c.

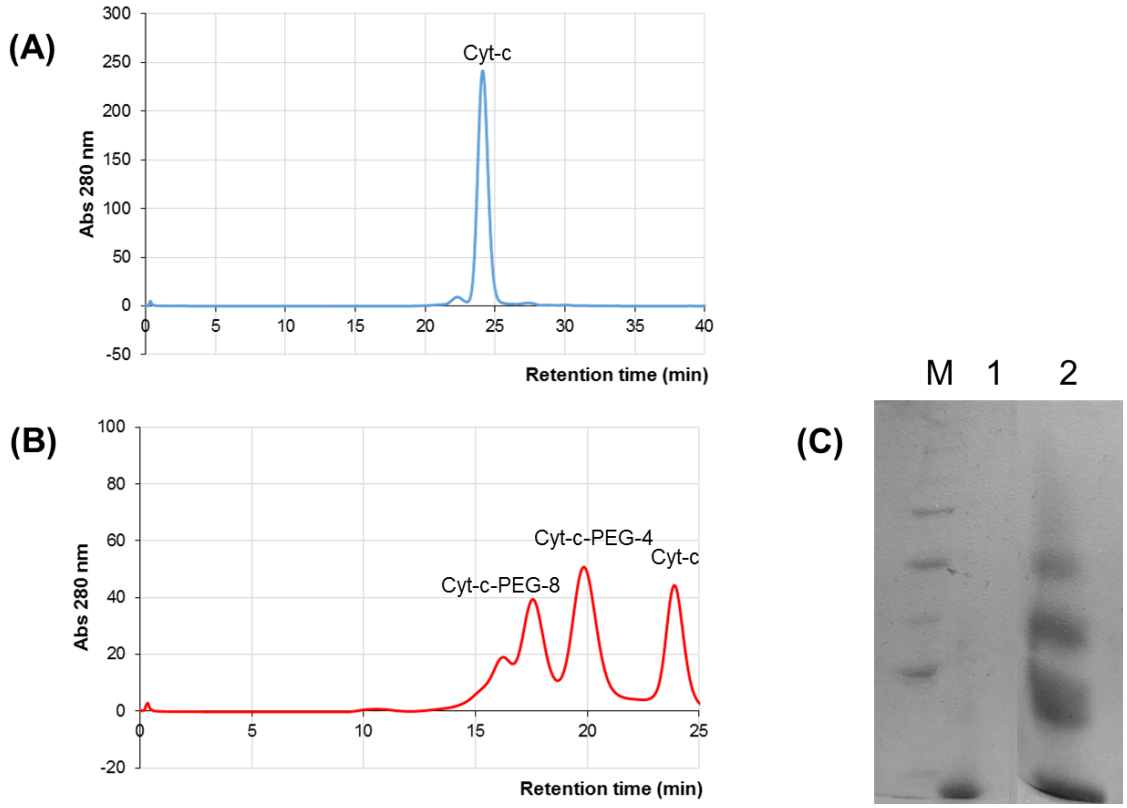

Fig. 4.5. SEC-FPLC chromatogram of **(A)** unreacted Cyt-c concentrated in the bottom-phase used directly in a new cycle of PEGylation; **(B)** unreacted Cyt-c used in a new cycle of PEGylation but after its isolation from the bottom phase through precipitation with cold acetone. **(C)** SDS-PAGE showing the successful use of the recycled Cyt-c in a new cycle of PEGylation: Lane M – Molecular Marker, Lane 1 – commercial equine heart Cyt-c, Lane 2 – PEGylation mixture obtained after a new cycle of PEGylation using the purified Cyt-c.

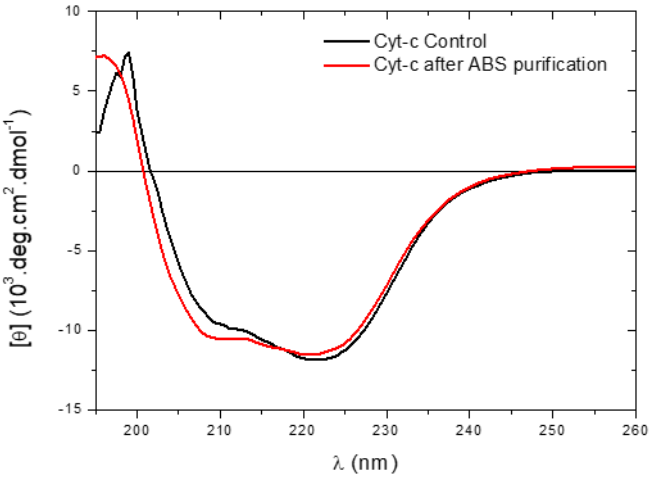

Fig. 4.6. Far-UV CD spectra of Cyt-c control (—) and Cyt-c purified through aqueous biphasic system (—). Cyt-c concentrations used are 15 and 13 µM for the control and purified forms, respectively.

4. Conclusions

In order to overcome the difficulty to obtain pure site-specific PEGylated conjugates of Cyt-c-based biosensors, an alternative process of downstream was here proposed. For that, the use of consecutive steps of purification using polymeric-based ABS were applied on the separation of (i) the unreacted protein from the PEGylated forms and (ii) each PEGylated conjugate. From the main results obtained in the partition studies, it was assessed the impact of the molecular weight of PEG and water content composing the top phase enriched in PEG. These two conditions have a significant impact on the partition profile of the unreacted Cyt-c and the different PEGylated forms obtained in non-site-specific PEGylation reactions (in this case, specifically Cyt-c-PEG-4 and Cyt-c-PEG-8) towards opposite phases. The different partition trend obtained for each class of proteins is actually explained by the presence of two major driving-forces occurring, namely the exclusion volume of the polymer-rich phase and "PEG-PEG" interactions. Considering thus the main applications of each PEGylated form and the unreacted protein, different processes of purification were defined to achieve different purposes. Thus, a single step process using the ABS composed of PEG 1500 was successfully developed for the isolation of the unreacted protein from the PEGylated conjugates. Rec Bot of 99.88 ± 0.05% of Cyt-c towards the bottom phase were achieved while in the top phase, Rec Top of 99.31 ± 0.62% and 99.87 ± 0.01% were obtained for Cyt-c-PEG-4 and Cyt-c-PEG-8. For the case when each PEGylated form is required in its purer form, a multistep process was developed by the conjugation of three different steps, all using the polymer-based ABS studied. This multi-step approach strategy was efficiently developed for the fractionation of the three protein species, namely Cyt-c, Cyt-c-PEG-4 and Cyt-c-PEG-8, allowing recoveries higher than 99% of the unreacted Cyt-c and Cyt-c-PEG-4 and more than 76.90% of recovery for Cyt-c-PEG-8 in the final of Step II. Envisaging the industrialization of these integrated processes, the recycling of the unreacted Cyt-c for a novel PEGylation reaction was successfully achieved by applying a precipitation step carried with cold acetone, in which it was proved the successfully reuse of the unreacted Cyt-c after purification, while maintaining the structural integrity of the protein. In this work, an efficient process of PEGylation and purification of different site-specific PEGylated forms was developed with high efficiency.

References

1. Abuchowski, A., van Es, T., Palczuk, N. C. & Davis, F. F. Alteration of immunological properties of bovine serum albumin by covalent attachment of polyethylene glycol. *J. Biol. Chem.* **252,** 3578–81 (1977).
2. Palm, T., Esfandiary, R. & Gandhi, R. The effect of PEGylation on the stability of small therapeutic proteins. *Pharm. Dev. Technol.* **16,** 441–448 (2011).
3. Harris, J. M. & Chess, R. B. Effect of pegylation on pharmaceuticals. *Nat. Rev. Drug Discov.* **2,** 214–221 (2003).
4. Ryu, J. K., Kim, H. S. & Nam, D. H. Current status and perspectives of biopharmaceutical drugs. *Biotechnol. Bioprocess Eng.* **17,** 900–911 (2012).
5. W. Roy Jackson, E. M. C. and M. T. W. H. Closing Pandora's box: chemical products should be designed to preserve efficacy of function while reducing toxicity. *Green Chem.* **18,** 4140–4144 (2016).
6. Sassi, A. B., Nagarkar, R. & Hamblin, P. in *Nov. Approaches Strateg. Biol. Vaccines Cancer Ther.* 199–217 (2015). doi:10.1016/B978-0-12-416603-5.00009-2
7. Beck, A., Sanglier-Cianférani, S. & Van Dorsselaer, A. Biosimilar, biobetter, and next generation antibody characterization by mass spectrometry. *Anal. Chem.* **84,** 4637–4646 (2012).
8. Davis, S., Abuchowski, A., Park, Y. K. & Davis, F. F. Alteration of the circulating life and antigenic properties of bovine adenosine deaminase in mice by attachment of polyethylene glycol. *Clin. Exp. Immunol.* **46,** 649–52 (1981).
9. Kameoka, J., Tanaka, T., Nojima, Y., Schlossman, S. F. & Morimoto, C. Direct association of adenosine deaminase with a T cell activation antigen, CD26. *Science (80-.).* **261,** 466–9 (1993).
10. Fu, C. H. & Sakamoto, K. M. PEG-asparaginase. *Expert Opin. Pharmacother.* **8,** 1977–1984 (2007).
11. Keating, M. J., Holmes, R., Lerner, S. & Ho, D. H. L-asparaginase and PEG asparaginase--past, present, and future. *Leuk. Lymphoma* **10 Suppl,** 153–157 (1993).
12. Santiago-Rodríguez, L., Méndez, J., Flores-Fernandez, G. M., Pagán, M., Rodríguez-Martínez, J. A., Cabrera, C. R. & Griebenow, K. Enhanced stability of a

nanostructured cytochrome c biosensor by PEGylation. *J. Electroanal. Chem.* **663,** 1–7 (2011).

13. García-Arellano, H., Buenrostro-Gonzalez, E. & Vazquez-Duhalt, R. Biocatalytic Transformation of Petroporphyrins by Chemical Modified Cytochrome C. *Biotechnol. Bioeng.* **85,** 790–798 (2004).
14. Ohno, H. & Yamaguchi, N. Redox reaction of poly(ethylene oxide)-modified hemoglobin in poly(ethylene oxide) oligomers at 120 degrees C. *Bioconjug. Chem.* **5,** 379–381 (1994).
15. Mayolo-Deloisa, K., González-Valdez, J., Guajardo-Flores, D., Aguilar, O., Benavides, J. & Rito-Palomares, M. Current advances in the non-chromatographic fractionation and characterization of PEGylated proteins. *J. Chem. Technol. Biotechnol.* **86,** 18–25 (2011).
16. Pasut, G. & Veronese, F. M. State of the art in PEGylation: The great versatility achieved after forty years of research. *J. Control. Release* **161,** 461–472 (2012).
17. González-Valdez, J., Rito-Palomares, M. & Benavides, J. Advances and trends in the design, analysis, and characterization of polymer-protein conjugates for 'PEGylaided' bioprocesses. *Anal. Bioanal. Chem.* **403,** 2225–2235 (2012).
18. Hong, P., Koza, S. & Bouvier, E. S. P. Size-Exclusion Chromatography for the Analysis of Protein Biotherapeutics and their Aggregates. *J. Liq. Chromatogr. Relat. Technol.* **35,** 2923–2950 (2012).
19. Fee, C. J. Size-exclusion reaction chromatography (SERC): A new technique for protein PEGylation. *Biotechnol. Bioeng.* **82,** 200–206 (2003).
20. Maiser, B., Kröner, F., Dismer, F., Brenner-Weiss, G. & Hubbuch, J. Isoform separation and binding site determination of mono-PEGylated lysozyme with pH gradient chromatography. *J. Chromatogr. A* **1268,** 102–108 (2012).
21. Moosmann, A., Müller, E. & Böttinger, H. Purification of PEGylated Proteins, with the example of PEGylated lysozyme and PEGylated scFv. *Methods Mol. Biol.* **1129,** 527–538 (2014).
22. Pabst, T. M., Buckley, J. J., Ramasubramanyan, N. & Hunter, A. K. Comparison of strong anion-exchangers for the purification of a PEGylated protein. *J. Chromatogr. A* **1147,** 172–182 (2007).

23. Li, W., Zhong, Y., Lin, B. & Su, Z. Characterization of polyethylene glycol-modified proteins by semi-aqueous capillary electrophoresis. *J. Chromatogr. A* **905,** 299–307 (2001).

24. Lee, K. S. & Na, D. H. Capillary electrophoretic separation of poly(ethylene glycol)-modified granulocyte-colony stimulating factor. *Arch. Pharm. Res.* **33,** 491–495 (2010).

25. Kwon, B., Molek, J. & Zydney, A. L. Ultrafiltration of PEGylated proteins: Fouling and concentration polarization effects. *J. Memb. Sci.* **319,** 206–213 (2008).

26. Molek, J. R. & Zydney, A. L. Ultrafiltration characteristics of pegylated proteins. *Biotechnol. Bioeng.* **95,** 474–482 (2006).

27. Molek, J., Ruanjaikaen, K. & Zydney, A. L. Effect of electrostatic interactions on transmission of PEGylated proteins through charged ultrafiltration membranes. *J. Memb. Sci.* **353,** 60–69 (2010).

28. Ruanjaikaen, K. & Zydney, A. L. Purification of singly PEGylated α-lactalbumin using charged ultrafiltration membranes. *Biotechnol. Bioeng.* **108,** 822–829 (2011).

29. González-Valdez, J., Cueto, L. F., Benavides, J. & Rito-Palomares, M. Potential application of aqueous two-phase systems for the fractionation of RNase A and α-Lactalbumin from their PEGylated conjugates. *J. Chem. Technol. Biotechnol.* **86,** 26–33 (2011).

30. Delgado, C., Malik, F., Selisko, B., Fisher, D. & Francis, G. E. Quantitative analysis of polyethylene glycol (PEG) in PEG-modified proteins/cytokines by aqueous two-phase systems. *J. Biochem. Biophys. Methods* **29,** 237–50 (1994).

31. Albertsson, P. A. Partition of cell particles and macromolecules in polymer two-phase systems. *Adv. Protein Chem.* **24,** 309–341 (1970).

32. Asenjo, J. A. & Andrews, B. A. Aqueous two-phase systems for protein separation: A perspective. *J. Chromatogr. A* **1218,** 8826–8835 (2011).

33. Johansson, H.-O., Feitosa, E. & Junior, A. P. Phase Diagrams of the Aqueous Two-Phase Systems of Poly(ethylene glycol)/Sodium Polyacrylate/Salts. *Polymers (Basel).* **3,** 587–601 (2011).

34. Karakatsanis, A. & Liakopoulou-Kyriakides, M. Comparison of PEG/fractionated

dextran and PEG/industrial grade dextran aqueous two-phase systems for the enzymic hydrolysis of starch. *J. Food Eng.* **80,** 1213–1217 (2007).

35. Diamond, A. D. & Hsu, J. T. Protein partitioning in PEG/dextran aqueous two-phase systems. *AIChE J.* **36,** 1017–1024 (1990).
36. Hirata, D. B., Badino, A. C. J. & Hokka, C. O. Utilization of PEG-phosphate aqueous two-phase system for clavulanic acid extraction from fermentation broth. in *2nd Mercosur Congr. Chem. Eng. 4th Mercosur Congr. Process Syst. Eng.* 1–6 (2005). at <http://www.enpromer2005.eq.ufrj.br/nukleo/pdfs/0124_trab.pdf>
37. Zafarani-Moattar, M. T. & Sadeghi, R. Phase diagram data for several PPG + salt aqueous biphasic systems at 25 °C. *J. Chem. Eng. Data* **50,** 947–950 (2005).
38. Bridges, N. J., Gutowski, K. E. & Rogers, R. D. Investigation of aqueous biphasic systems formed from solutions of chaotropic salts with kosmotropic salts (salt/salt ABS). *Green Chem.* **9,** 177 (2007).
39. Ooi, C. W., Tey, B. T., Hii, S. L., Kamal, S. M. M., Lan, J. C. W., Ariff, A. & Ling, T. C. Purification of lipase derived from Burkholderia pseudomallei with alcohol/salt-based aqueous two-phase systems. *Process Biochem.* **44,** 1083–1087 (2009).
40. Da Silva, L. H. M. & Meirelles, A. J. A. Phase equilibrium and protein partitioning in aqueous mixtures of maltodextrin with polypropylene glycol. *Carbohydr. Polym.* **46,** 267–274 (2001).
41. Freire, M. G., Cláudio, A. F. M., Araújo, J. M. M., Coutinho, J. A. P., Marrucho, I. M., Lopes, J. N. C. & Rebelo, L. P. N. Aqueous biphasic systems: a boost brought about by using ionic liquids. *Chem. Soc. Rev.* **41,** 4966 (2012).
42. Viana Marques, D. A., Pessoa-Júnior, A., Lima-Filho, J. L., Converti, A., Perego, P. & Porto, A. L. F. Extractive fermentation of clavulanic acid by Streptomyces DAUFPE 3060 using aqueous two-phase system. *Biotechnol. Prog.* **27,** 95–103 (2011).
43. Ventura, S. P. M., Santos-Ebinuma, V. C., Pereira, J. F. B., Teixeira, M. F. S., Pessoa, A. & Coutinho, J. A. P. Isolation of natural red colorants from fermented broth using ionic liquid-based aqueous two-phase systems. *J. Ind. Microbiol. Biotechnol.* **40,** 507–516 (2013).
44. Santos, J. H. P. M., Martins, M., Silvestre, A. J. D., Coutinho, J. A. P. & Ventura, S.

P. M. Fractionation of phenolic compounds from lignin depolymerisation using polymeric aqueous biphasic systems with ionic surfactants as electrolytes. *Green Chem.* **18,** 5569–5579 (2016).

45. Johansson, H.-O., Magaldi, F. M., Feitosa, E., Pessoa Jr, A. & Pessoa, A. Protein partitioning in poly(ethylene glycol)/sodium polyacrylate aqueous two-phase systems. *J. Chromatogr. A* **1178,** 145–53 (2008).
46. Delgado, C., Malmsten, M. & Van Alstine, J. M. Analytical partitioning of poly(ethylene glycol)-modified proteins. *J. Chromatogr. B Biomed. Appl.* **692,** 263–272 (1997).
47. Galindo-López, M. & Rito-Palomares, M. Practical non-chromatography strategies for the potential separation of PEGylated RNase A conjugates. *J. Chem. Technol. Biotechnol.* **88,** 49–54 (2013).
48. Sookkumnerd, T. & Hsu, J. T. Purification of PEG-protein conjugates by countercurrent disturbution in aqueous two-phase systems. *J. Liq. Chromatogr. Relat. Technol.* **23,** 497–503 (2000).
49. Pei, Y., Wang, J., Wu, K., Xuan, X. & Lu, X. Ionic liquid-based aqueous two-phase extraction of selected proteins. *Sep. Purif. Technol.* **64,** 288–295 (2009).
50. Santos, J. H. P. M., e Silva, F. A., Coutinho, J. A. P., Ventura, S. P. M. & Pessoa, A. Ionic liquids as a novel class of electrolytes in polymeric aqueous biphasic systems. *Process Biochem.* **50,** 661–668 (2015).
51. Tamura, K., Nakamura, N. & Ohno, H. Cytochrome c dissolved in 1-allyl-3-methylimidazolium chloride type ionic liquid undergoes a quasi-reversible redox reaction up to 140??C. *Biotechnol. Bioeng.* **109,** 729–735 (2012).
52. Kuroda, K., Kohno, Y. & Ohno, H. Renaturation of Cytochrome c Dissolved in Polar Phosphonate-type Ionic Liquids Using Highly Polar Zwitterions. *Chem. Lett.* **46,** 870–872 (2017).
53. Vazquez-Duhalt, R. Cytochrome c as a biocatalyst. in *J. Mol. Catal. - B Enzym.* **7,** 241–249 (1999).
54. Kawakami, N., Shoji, O. & Watanabe, Y. Use of perfluorocarboxylic acids to trick cytochrome P450BM3 into initiating the hydroxylation of gaseous alkanes. *Angew. Chemie - Int. Ed.* **50,** 5315–5318 (2011).

55. Cong, Z., Shoji, O., Kasai, C., Kawakami, N., Sugimoto, H., Shiro, Y. & Watanabe, Y. Activation of Wild-Type Cytochrome P450BM3 by the Next Generation of Decoy Molecules: Enhanced Hydroxylation of Gaseous Alkanes and Crystallographic Evidence. *ACS Catal.* **5,** 150–156 (2015).

56. Bisht, M., Mondal, D., Pereira, M. M., Freire, M. G., Venkatesu, P. & Coutinho, J. A. P. Long-term protein packaging in cholinium-based ionic liquids: improved catalytic activity and enhanced stability of cytochrome c against multiple stresses. *Green Chem.* (2017). doi:10.1039/C7GC02011B

57. Manickam, P., Kaushik, A., Karunakaran, C. & Bhansali, S. Recent advances in cytochrome c biosensing technologies. *Biosens. Bioelectron.* **87,** 654–668 (2017).

58. Gouda, M. D., Kumar, M. A., Thakur, M. S. & Karanth, N. G. Enhancement of operational stability of an enzyme biosensor for glucose and sucrose using protein based stabilizing agents. *Biosens. Bioelectron.* **17,** 503–507 (2002).

59. Boutureira, O. & Bernardes, G. J. L. Advances in chemical protein modification. *Chem. Rev.* **115,** 2174–2195 (2015).

60. Nanocs. Succinimidyl PEG NHS, mPEG-NHS(SC). (2017). at <http://www.nanocs.net/mPEG-SC-5k-1g.htm>

61. de Souza, R. L., Campos, V. C., Ventura, S. P. M., Soares, C. M. F., Coutinho, J. A. P. & Lima, Á. S. Effect of ionic liquids as adjuvants on PEG-based ABS formation and the extraction of two probe dyes. *Fluid Phase Equilib.* **375,** 30–36 (2014).

62. Giuliano, K. A. Aqueous two-phase partitioning. Physical chemistry and bioanalytical applications. *FEBS Lett.* **367,** 98 (1995).

63. Passos, H., Ferreira, A. R., Cláudio, A. F. M., Coutinho, J. A. P. & Freire, M. G. Characterization of aqueous biphasic systems composed of ionic liquids and a citrate-based biodegradable salt. *Biochem. Eng. J.* **67,** 68–76 (2012).

64. Almeida, M. R., Passos, H., Pereira, M. M., Lima, Á. S., Coutinho, J. A. P. & Freire, M. G. Ionic liquids as additives to enhance the extraction of antioxidants in aqueous two-phase systems. *Sep. Purif. Technol.* **128,** 1–10 (2014).

65. Ferreira, A. M., Faustino, V. F. M., Mondal, D., Coutinho, J. A. P. & Freire, M. G. Improving the extraction and purification of IgG by the use of ionic liquids as adjuvants in aqueous biphasic systems. *J. Biotechnol.* **236,** 166–175 (2016).

4.2. An integrated process combining the reaction and purification of PEGylated proteins

Santos, J. H. P. M., Mendonça, C. M. N., Silva, A. R. P., Oliveira, R. P. S., Junior, A. P., Coutinho, J. A. P., Ventura, S. P. M. & Rangel-Yagui, C. O., 2019 (manuscript in preparation)[9]

Abstract

A downstream process combining PEGylation reaction and the use of enzyme conjugates acting as phase-forming components of aqueous biphasic systems (ABS) is here proposed. On this approach, the citrate buffer (pH = 7.0) was used simultaneously to stop the reaction (avoiding the use of hydroxylamine) and as phase forming agent inducing the phase separation of the PEGylated proteins. The partition of the bioconjugates was assessed using two model enzyme of small size [cytochrome c (Cyt-c) and lysozyme (LYS)], and two of large size [L-asparaginase (ASNase) and catalase (CAT)] as well as, reactive PEG of 5, 10, 20 and 40 kDa. The effect of the reaction time in the PEGylation and recovery steps was also evaluated. All reactive PEGs allowed high selectivity in the separation of PEGylated from native forms (S > 100). A positive effect of increasing the time of reaction was denoted. It allows the formation of greater amounts of PEGylated proteins, with an increase of the PEG-protein conjugated phase volume (top phase), with those of the higher reaction times allowing 100 % of recovery. More selective systems were obtained for Cyt-c and LYS (S > 100) than for ASNase and CAT (40 < S < 60), nevertheless for all, the native and PEGylated proteins had its biological activity preserved. Envisioning the industrial potential evaluation of the processes developed in this work, an integrated process diagram was defined combining the PEGylation reaction with the purification of the protein conjugates. Two different scenarios were investigated considering the PEGylation reaction performance. For both approaches (complete and incomplete PEGylation reaction), high recovery yields and purities were obtained for the PEGylated conjugates (92.1 ± 0.4% < $\%RecT_{Cyt\text{-}c\text{-}PEG}$ < 98.1 ± 0.1%; 84.6% < purity < 100%) and for the unreacted enzyme ($\%RecB_{Cyt\text{-}c}$ = 81 ± 1%; purity = 97.7%), while maintaining their structural integrity.

Keywords: PEGylation; bioconjugation; separation; aqueous biphasic systems; protein recovery.

[9] Contributions: JS, CM and AS acquired the experimental data. JS, RO, SV, AP, JC and CY interpreted the experimental data. SV, JC and CY conceived and directed this work. The manuscript was mainly written by JS with contributions from the remaining authors.

1. Introduction

Therapeutic biological products based on proteins and peptides are of increasing interest in the pharmaceutical field.[1,2] This class of drugs is characterized by its high specificity, offering the possibility to treat complex diseases once considered untreatable. Nonetheless, protein drugs are usually associated to low solubility profiles, short shelf-lives, short circulating half-lives and susceptibility to cleavage by proteolytic enzymes.[2,3] To date, several techniques have been implemented to increase solubility, improve molecular stabilization and enhance proteins pharmacokinetics.[4–6] Most of those techniques focus in the bioconjugation of proteins with polymers, generating improved drugs, *i.e.* biobetters, which are superior when compared to the original biological.[7,8] Among the large array of bioconjugation techniques, PEGylation is the most auspicious alternative. This strategy is FDA and EMA approved and it has been used in the development of several protein drugs currently in the market.[7–9] Through careful selection of the reaction chemistry, one or more polyethylene glycol (PEG) molecules can be attached to the proteins, producing PEG-protein conjugated species with one or more grafted polymeric chains.[10–13]

The biological stability and activity of PEGylated proteins are influenced by the chemical reaction used. Usually, PEGylation results in a complex mixture of proteins with varying number of PEG chains attached to amino acid residues, which can also vary on the location at the protein surface. A narrow number of site-specific modifications is available, such as the *N*-terminal PEGylation and cysteine PEGylation. Nonetheless, even site specific reactions still present some degree of polydispersity.[9,12] The separation, sub fractionation and recovery of the target PEGamer among the different PEG-protein conjugated species is a crucial step in the PEGylation process.[14] Moreover, aqueous biphasic systems (ABS) stands out as interesting alternatives not only for the separation of the PEGylated proteins from the other reaction products,[15] but also for its sub-fractionation according to the number of grafted chains among the produced conjugates.[16–18] Aqueous biphasic systems (ABS) are clean alternatives for conventional organic-water solvent extraction systems. ABS are formed when either two polymers, one polymer and one kosmotropic salt, or two salts (one chaotropic salt and the other a kosmotropic salt) are mixed at appropriate concentrations.[19] The two phases are

mostly composed of water and non-volatile components, thus eliminating volatile organic compounds. They have been used for a plethora of purifications in biotechnological field, due to their intrinsic benign and non-denaturing character.[20,21] The technical and economic advantages offered by ABS regarding issues like increase of protein recovery yields, decrease of processing time, scale-up feasibility, as well as absence of specialized equipment or highly-trained personnel, have been further supporting the hypothesis of an industrial substitution of chromatographic-based downstream processes by ABS platforms.[22–24]

Despite the promising potential of ABS to separate PEGylated proteins, challenges like the recycling of phase-forming components and recovery of the target biological derivatives, have been pointed out as main limitations. Thus, novel insights into the development of innovative strategies to increase the industrial potential of ABS in PEGylation reactions still need to be explored. In this work, a novel integrated downstream process involving the simultaneous PEGylation reaction and ABS extraction of four model proteins (*i.e.* cytochrome-c, lysozyme, L-asparaginase and catalase) is proposed. In these systems, the PEG-protein conjugates are used as phase-forming components in ABS, together with citrate salt, allowing the formation of a biphasic system concurrently separating the PEGylated conjugates while simultaneously stopping the PEGylation reaction. Our results stand out as an attractive and simple in situ separation strategy for PEGylated proteins integrated with the bioconjugation reaction, without the need of toxic reagents to stop the reaction like hydroxylamine.[10] This research represents a pioneer study in the integration of PEGylation reaction and purification in a single step. By integrating the reaction and purification step by employing the PEGylated proteins as one of the ABS phase components, it was our intention to obtain a selective purification performance in the separation of the PEGylated conjugates from the unreacted proteins by a non-chromatographic and simple method. Following this approach, a successful integrated process was envisioned for a complete PEGylation reaction, but also for the most common scenario of an incomplete reaction (yield of reaction of 64 %). High recovery yields and purities were obtained for the PEGylated conjugates (92% < $\%RecT_{\text{Cyt-c-PEG}}$ < 98%; 85% < purity < 100%)

and for the unreacted enzyme (%$RecB_{Cyt\text{-}c}$ = 81%; purity = 98%), thus increasing the overall sustainability of the process and meeting the principles of Green Chemistry.

2. Materials and Methods

2.1. Materials

The four model proteins used were the horse heart cytochrome c (Cyt-c, ≈ 12 kDa, pI = 10.0–10.5) with purity of ≥ 95% from Sigma-Aldrich (St. Louis, MO), lysozyme from chicken egg white (LYS, ≈ 14 kDa, pI = 11.35) with purity of ≥ 90% from Sigma-Aldrich, L-asparaginase from *Escherichia coli* (ASNase, ≈ 130 kDa, pI = 4.9) 2500 IU with purity of ≥ 95% from Prospec-Tany (Ness Ziona, Israel), and catalase from bovine liver (CAT, ≈ 240 kDa, pI = 5.4) with a purity of ≥ 95% from Sigma-Aldrich.

The PEG derivatives used in the PEGylation reaction were methoxy polyethylene glycol succinimidyl NHS ester of 5, 10, 20 and 40 kDa (mPEG-NHS, purity > 95%), obtained from Nanocs (New York, NY). The aqueous buffer used in the PEGylation reaction was the potassium phosphate buffer (100 mM), pH adjusted to 7 through drop-wise addition of NaOH 2 M. Potassium citrate buffer was used to stop the PEGylation reaction and to promote the formation of the biphasic system. The salts potassium phosphate dibasic (K_2HPO_4, 95% of purity), potassium phosphate monobasic (KH_2PO_4, 95% of purity), citric acid, ($C_6H_8O_7$, purity ≥ 99%) and potassium citrate tribasic monohydrate ($C_6H_5K_3O_7{\cdot}H_2O$, purity ≥ 99%) were purchased from Sigma-Aldrich. Polyethylene glycols (PEG) and methoxy polyethylene glycol (mPEG) for phase diagrams determination were from Sigma-Aldrich with purity ≥ 95 %.

For the chromatography mobile phase, sodium chloride, NaCl, (purity ≥ 99 %; Sigma-Aldrich), sodium phosphate dibasic, Na_2HPO_4, (purity ≥ 99 %; Sigma-Aldrich), sodium phosphate monobasic, NaH_2PO_4, (purity ≥ 99 %; Sigma-Aldrich), and ultrapure water treated in a Mili-Q 185 water apparatus (Millipore, Bedford, MA) were used. Syringe filters (0.45 µm of pore size; Specanalitica, Portugal) and membrane filters (0.22 µm; Sartorius Stedim Biotech, Germany) were applied in the filtration steps.

2.2. Phase diagrams of polyethylene glycol + citrate buffer ABS

The experimental phase diagrams were determined gravimetrically, within an uncertainty of ± 10^{-4} g, using the cloud point titration method[22,23] at (298 ± 1) K and

atmospheric pressure. The phase diagrams were constructed for PEG 2, 6, 10, and 20 kDa + citrate buffer (pH = 7.0) and for mPEG 2 kDa + citrate buffer (pH = 7.0). Briefly, two stock solutions were prepared: 50 wt% of PEG and 50 wt% of citrate buffer, $C_6H_5K_3O_7$/ $C_6H_8O_7$, pH = 7.0. Drop-wise addition of buffer was carried to the polymer solution until the visual detection of a turbid system (biphasic region). Subsequently, drop-wise addition of the milli-Q water was conducted until the system became clear (monophasic region). This procedure was repeated several times in order to obtain the binodal curve, being performed under constant stirring and controlled temperature. The experimental phase diagrams data were correlated using the Merchuk equation[24] (Eq. 1):

$$[\mathrm{PEG}] = A \exp[(B \times [\mathrm{Citrate}]^{0.5}) - (C \times [\mathrm{Citrate}]^{3}) \quad \textbf{(1)}$$

where [PEG] and [Citrate] represent the weight percentages of PEG polymers and citrate buffer, respectively. *A*, *B* and *C* are constants obtained by the regression of the experimental data. The Merchuk equation was chosen since it has a low number of adjustable parameters to correlate these data and it is the most commonly applied.[24]

2.3. Combined PEGylation reaction and recovery step

The PEGylation reactions were conducted according to literature.[28] Briefly, 300 µL of a protein solution (2 mg.mL^{-1}, condition 1 and 4 mg.mL^{-1}, condition 2) in potassium phosphate buffer (100 mM, pH = 7.0) was added to a flask containing 50 mg of mPEG-NHS. The mixtures were magnetically stirred at 400 rpm for 7.5 min, at room temperature, and then the reaction was stopped through the drop-wise addition of 100 µL of potassium citrate buffer (pH=7.0, 50 wt% $C_6H_5K_3O_7$/$C_6H_8O_7$), consequently promoting the formation of two-phase systems composed by Prot-PEG-rich (top) phase and salt-rich (bottom) phase. The ABS applied were composed of 0.5 wt% of Prot + 12.5 wt% of Prot-PEG/PEG + 12.5 wt% of $C_6H_5K_3O_7$/$C_6H_8O_7$ (condition 1) and 1.0 wt% of Prot + 12.5 wt% of Prot-PEG/PEG + 12.5 wt% of $C_6H_5K_3O_7$/$C_6H_8O_7$ (condition 2). The two aqueous phases were carefully separated, and their volumes were measured.

Three variables were studied to develop and optimize the integrated conjugation-recovery process, namely the (i) mPEG-NHS molecular weight, (ii) reaction time and (iii) protein type. For the first study, four mPEG-NHS polymers of 5, 10, 20 and 40 kDa were conjugated with Cyt-c at 2 mg.mL^{-1} (condition 1) and 4 mg.mL^{-1} (condition 2). Following,

three reaction times were studied for Cyt-c PEGylation with mPEG-NHS of 20 kDa at condition 2, namely: 7.5, 15, and 30 min. Finally, to proof this one-step approach for more than one protein, different classes of proteins were tested: small proteins (Cyt-c and LYS, < 50 kDa) and large proteins (ASNase and CAT, > 100 kDa). In this step, the PEGylation reaction was performed with mPEG-NHS of 20 kDa, for 7.5 min at condition 2 and the ABS formed by potassium citrate buffer addition.

2.4. Quantification of PEGylated conjugates and unreacted protein: fractionation parameters

The quantification of unreacted protein (Cyt-c, LYS, ASNase, and CAT) and each conjugate (Cyt-c-PEG, LYS-PEG, ASNase-PEG, and CAT-PEG) at both top and bottom phases was carried out by size-exclusion chromatography and detection at 280 nm,[16] with a respective calibration curve for each protein and PEGylated conjugate. Samples of top and bottom phases were injected into an AKTA™ purifier system (GE Healthcare, United States) Fast Protein Liquid Chromatographer equipped with a Superdex 200 Increase 10/300 GL chromatographic column prepacked with crosslinked agarose-dextran high resolution resin (GE Healthcare). The column was equilibrated with 0.01 M of a sodium phosphate buffer solution (0.14 M NaCl, pH = 7.4) and eluted with the same buffer with a flow of 0.75 mL min^{-1}. All experiments were performed in triplicate and the final concentration was reported as the average of three independent assays with the respective standard deviations calculated.

The performance of the different ABS investigated was based on the following parameters: partition coefficients in log scale (log *K*) and recoveries in the top (*Rec Top* - %) and bottom (*Rec Bot* - %) phases of unreacted proteins and PEGylated conjugates, Eqs. 2 to 4, respectively:

$$\log K = \log\left(\frac{[\text{Prot}]\text{top}}{[\text{Prot}]\text{bot}}\right) \quad \textbf{(2)}$$

$$Rec\ Top\ (\%) = \frac{100}{1 + \left(\frac{1}{K \times Rv}\right)} \quad \textbf{(3)}$$

$$Rec\ Bot\ (\%) = \frac{100}{1 + Rv \times K} \quad \textbf{(4)}$$

where $[Prot]_{top}$ and $[Prot]_{bot}$ represent the protein concentration in the top and bottom phases, respectively. R_v represents the volume ratio between the top and bottom phase volumes.

The selectivity (*S*) is a key parameter to be measured, since the fractionation of PEGylated conjugates from the unreacted protein is under study. Therefore, the selective partition of the proteins (*i.e.* PEGylated protein from unreacted protein), can be assessed through Eq. 5:

$$S = \frac{K_{\mathrm{Prot-PEG}}}{K_{\mathrm{Prot}}} \quad \textbf{(5)}$$

2.5. Total protein concentration determination

The protein concentration was determined with the Pierce BCA Protein Assay and Micro BCA Protein Assay (Thermo Scientific, Schwerte, Germany) according to the product recommendations. Bovine serum albumin (albumin standard ampules, Thermo Scientific, Schwerte, Germany) was used as standard protein.

2.6. Protein activity assays

The activity of the proteins was determined for the top and bottom phase, in order to guarantee that the ABS platforms are gentle and maintain biological activity. The specific activity, SA, ($U.mg^{-1}$) represents the ratio between the volumetric activity of the respective protein ($U.mL^{-1}$) and the total protein concentration ($mg.mL^{-1}$) at a certain aqueous phase (top or bottom). Every sample was measured in triplicate and for calculation of reaction rate the average was used.

2.6.1. Cyt-c activity

The enzymatic activity of Cyt-c was determined by the catalytic oxidation of 50 µM of 2,2'-azino-bis(3-ethylbenzothiazoline-6-sulphonic acid), ABTS (Sigma–Aldrich, > 98%) in

the presence of 0.5 mM of hydrogen peroxide (Sigma–Aldrich, solution 30 wt% in H_2O).[29,30] The samples of both top and bottom phases were diluted to obtain a protein concentration of 10 µM in 0.01 M of potassium phosphate buffer (0.14 M of NaCl, pH 7.4). The reaction was started by adding hydrogen peroxide and followed by the absorbance increase at 418 nm.

2.6.2. LYS activity

The LYS activity was determined using *Micrococcus lysodeikticus*, *M. lysodeikticus* (Sigma–Aldrich) as substrate.[31] The kinetic assay is based on the lysis of the bacterial cells by lysozyme resulting in a decrease of turbidity over time. The *M. lysodeikticus* cells (0.015% w/v) were suspended in 50 mM of sodium phosphate buffer at pH 6.24. For the diluted samples of top and bottom phases, a volume of 0.1 mL was mixed with 2.5 mL of substrate solution. Absorption measurements at 450 nm were performed for 10 min in 30 s intervals with orbital shaking in between the measurements. The diluted samples of protein from both phases contained 200 400 $U.mL^{-1}$ of LYS. A blank consisting of 0.1 mL of sodium phosphate buffer (50 mM, pH 6.24) mixed with 2.5 mL of substrate solution was measured likewise. The absorbance values of the protein samples were subtracted from the absorbance values of the *M. lysodeikticus* blank, resulting in a positive slope of the measured values over time. One unit is equal to a decrease in turbidity of 0.001 per minute at 450 nm, pH 6.24 and 25°C under the specified conditions.

2.6.3. ASNase activity

The ASNase activity was based on the protocol of Drainas and co-workers.[32] Briefly, 0.1 mL of diluted sample (top and bottom phase), 0.7 mL of Tris-HCl buffer (50 mM, pH 8.6), 0.1 mL of ASNase (0.1 M) and 0.1 mL of hydroxylamine (1.0 M, pH 7.0) were incubated at 37°C and 30 min. The reaction was interrupted by adding 0.5 mL of 0.31 M of iron chloride reagent (dissolved in HCl 0.33 M and trichloroacetic acid 0.3 M solution, Sigma–Aldrich, > 97%). The reaction solution was centrifuged at 3220xg for 15 min and the iron chloride–hydroxamic acid complex produced was quantified at 500 nm. The calibration curve was prepared

from a β-aspartohydroxamic solution (Sigma-Aldrich, MO, USA, ≥ 98%). One unit of ASNase activity is defined as the amount of enzyme that produces 1 μmol of β-aspartohydroxamic acid per minute under the experiment conditions defined.

2.6.4. CAT activity

The CAT activity was quantified by the Iwase *et al.* method that measures the trapped oxygen gas generated by the catalase–hydrogen peroxide reaction, which is visualized as foam.[33] Each CAT sample from top and bottom phases (100 μL) was added in a Pyrex tube (13 mm diameter × 100 mm height, borosilicate glass; Corning, USA). Subsequently, 100 μL of 1% Triton X-100 (Sigma–Aldrich, 98%) and 100 μL of undiluted hydrogen peroxide (Sigma–Aldrich, solution 30 wt% in H_2O) were added to the CAT samples, mixed thoroughly and then incubated at room temperature. The CAT samples from top and bottom phases were diluted to stay in the linearity range of 20–300 units (U) of catalase activity. Following completion of the reaction, the height of O_2-forming foam that remained constant for 15 min in the test tube was finally measured using a ruler and correlated to CAT concentration based on a calibration curve.

2.7. FTIR-ATR spectra acquisition

The Fourier Transform Infrared Spectroscopy (FTIR) profile of standards (Cyt-c, model protein and PEG) and top and bottom phases were recorded using the FT RAMAN BRUKER 100/S spectrometer (Bruker, Billerica, MA) in mid-IR mode, equipped with an Universal ATR (attenuated total reflectance) sampling device containing diamond/ZnSe crystal. For powdered samples, an extra accessory plate with a conic awl was used, requiring only a few milligrams, without any previous sample preparation. The pressure applied to squeeze the powdered sample towards the diamond was approximately 148 ± 1 N. The spectra were scanned at room temperature in absorbance mode over the wave number range of 4000 to 50 cm^{-1}, with a scan speed of 0.20 $cm.s^{-1}$, and 30 accumulations at a resolution of 4 cm^{-1}. Triplicates of each sample were averaged to obtain an average spectrum. A background spectrum of air was scanned under the same instrumental

conditions before each series of measurements. The spectra acquired were processed with the Spectrum software version 6.3.2.

3. Results and Discussion

3.1. Phase diagrams and selection of mixture point for ABS preparation

Novel ternary phase diagrams were determined for the systems used in the integrated step (polyethylene glycol + $C_6H_5K_3O_7$/$C_6H_8O_7$ pH = 7 + water, 298 ± 1 K) to define a biphasic region and consequently, to choose a mixture point corresponding to phase separation on a top phase rich in PEG and a bottom one rich in salt. Citrate-based salts were chosen since they are biodegradable and nontoxic, with a strong salting-out ability.[34] The detailed experimental weight fraction data, Merchuk correlation parameters (*A*, *B* and *C*) and graphical representations of phase diagrams in mass fraction are reported at **Tables C.5-6** and **Fig. C.3 at Appendix C**. In the downstream process proposed to integrate the PEGylation reaction with the fractionation by ABS, the PEGylated protein is expected to work as one of the phase forming components. Since the grafted PEG groups are methoxylated and no previous reports on mPEG phase diagrams are available, novel experimental phase diagrams were mapped out. The phase diagrams for polyethylene glycol (PEG) and mPEG with the same molecular weight (2 kDa) + $C_6H_5K_3O_7$/$C_6H_8O_7$ (pH = 7) were studied and similar binodal curves were obtained (**Fig. C.3A at Appendix C**). Therefore, the methoxy group of the polymer chain has a negligible effect regarding the two-phase formation capability, and for larger polymer sizes the equivalent trend should be observed. Based on this result, phase diagrams of PEG/citrate systems were mapped out for regular PEGs of 2, 6, 10, and 20 kDa (**Fig. C.3B at Appendix C**). As extensively described in literature, for PEG/salt-based ABS, the increase of molecular weight contributes to a higher capacity to induce phase separation due to the hydrophobicity of the phase formed by longer polymeric PEG chains.[35,36] Based on the phase diagrams, a biphasic mixture point was chosen to be applied in the PEGylation reaction media (12.5 wt% of PEG + 12.5 wt% $C_6H_5K_3O_7$/$C_6H_8O_7$ pH = 7). This mixture point corresponds to the biphasic region in all phase diagrams evaluated (PEGs 6-20 kDa).

3.2. Process optimization

PEG/salt-based ABS are highlighted as promising for the recovery of PEGylated proteins, *i.e.* bovine serum albumin,[37,38] Cyt-c,[16] RNase A,[17,18,39] lactoalbumin,[17] LYS,[40] Immunoglobulin G,[37] and granulocyte-macrophage colony stimulation factor.[37,38] Nevertheless, the direct application of this operation on reaction media has not been extensively studied. The only previous report refers to an *in situ* ABS strategy formed by adding 4 mol.L^{-1} of ammonium sulphate in 20 mmol.L^{-1} Tris–HCl (pH 7.0) to lysozyme PEGylation reactions.[15] In this study, several polymers and salt solutions were tested as potential phase-forming agents with the further analysis of LYS-PEG and LYS partitioning behaviour. This manuscript showed some insights on the possibility to conceive a unidirectional and integrative process in the production of PEGylated proteins at large reaction volumes, which cannot be processed using packed bed or on-column PEGylation processes due to the limiting saturation capacities of the large columns. Yet, the need to deeply explore the *in-situ* potential of ABS in PEGylation reaction still demands to be addressed. Moreover, the idea of an integrative approach combining the bioconjugation reaction and ABS recovery, without the use of toxic reagents such as hydroxylamine to stop the reaction, neither the addition of more quantities of PEG to promote the phase separation is still a challenge. Given the well-established versatility of ABS regarding their integration capacity for chemical reactions in one-step and one-pot processes,[41,42] we investigated the full one-step potential of ABS combining PEGylation reaction and protein conjugates purification. The effect of the size of the reactive PEG on the integrated purification stage, the influence of the reaction time in the *in-situ* ABS for recovery of PEGylated proteins, and the proof of concept by investigating several proteins (with small and large sizes) were investigated.

Initially, mPEG-NHS of different molecular weights (5, 10, 20, and 40 kDa) were used for the PEGylation of Cyt-c. After PEGylation, the addition of salt promoted the phase separation with the top phase rich in PEGylated proteins (phase-forming compound) and excess of mPEG, while the bottom phase is rich in potassium citrate salt, for which the unreacted proteins preferentially partitioned. **Table 4.2.** presents the values of volume ratio (V_R) and recovery parameters for Cyt-c and Cyt-c-PEG, *i.e. K*, *%RecT, %RecB*, and *S* for both experimental conditions. **Fig. 4.7.** shows the data of *S* and the logarithm

function of *K* obtained after the study of two distinct protein concentrations (0.5 wt% and 1.0 wt% of protein, conditions 1 and 2, respectively) and different conditions of PEG MW, reaction time and type of protein. The positive values of log *K* depicted in **Fig. 4.7.** indicate the partition preference of the protein towards the top phase, while negative values indicate its preference for the bottom phase. *S* values above 1000 were represented as >1000, indicating the complete separation of PEGylated proteins from the unreacted protein. Our results show that V_R tends to increase with the PEG MW (*i.e.* $0.46 \leq V_R \leq 0.81$, condition 1) resulting on the increase of the upper volume of top phase rich in PEGylated protein. In the range of PEG MW studied (**Table 4.2.** and **Fig. 4.7.A**), higher selectivity values were obtained ($S \geq 61$ and $S \geq 87$, for conditions 1 and 2, respectively). In this sense, the unreacted protein partitioned preferentially to the bottom phase, predominantly in the systems with PEGs of smaller MW (%$RecB_{Cyt\text{-}c}$ > 85% for mPEG 40 kDa, %$RecB_{Cyt\text{-}c}$ = 100% for mPEG 5 kDa, condition 1). Moreover, the PEGylated protein migrates to the top phase, preferentially for systems with larger PEG MWs (%$RecT_{Cyt\text{-}c\text{-}PEG}$ > 90% for mPEG 5 kDa, %$RecT_{Cyt\text{-}c\text{-}PEG}$ > 97% for mPEG 40 kDa, condition 1). Indeed, the PEGylated Cyt-c is one of the main phase forming agents. Partition results were similar for both initial Cyt-c concentrations studied (conditions 1 and 2, respectively). Nonetheless, PEGylation yields were higher for condition 1 as a consequence of the higher mPEG-NHS:protein molar ratio.

The effect of PEGylation reaction tie was investigated for 1.0 wt% of Cyt-c (condition 2). As it can be seen in **Fig. 4.7.B** and **Table 4.3.**, high selectivity values were observed for all reaction times. The increase of reaction time resulted in higher PEGylation yields, with 100% of Cyt-c-PEG for the longer time of reaction (t = 30 min). Herein, for the complete reaction, it is also demonstrated the ability of this system to concentrate the PEGylated conjugates in the aqueous phase. As a result, the top-phase volume increases with the reaction time ($0.90 \leq V_R \leq 2.80$), as it can be seen by the photos depicted in **Fig. 4.7**.. Likewise, the recovery yields are enhanced with the extension of the reaction (%$RecT_{Cyt\text{-}c\text{-}PEG}$ = 98.5 ± 0.1% for 30 min, %$RecT_{Cyt\text{-}c\text{-}PEG}$ = 93.6 ± 0.3% for 7.5 min). Additionally, the efficiency of adding potassium citrate to end the PEGylation reaction was proved, since different degrees of PEGylation were obtained after adding it at

distinct reaction times. Therefore, it represents a non-toxic and eco-friendly alternative to replace hydroxylamine as a reagent to stop PEGylation.

Aiming at proving the transversal potential of integrating the PEGylation reaction and primary recovery as an alternative approach, three other enzymes were tested. In this sense, the mixture point (1.0 wt% of Protein + 12.5 wt% Prot-PEG + 12.5 wt% potassium citrate buffer, pH = 7.0) previously selected was tested for LYS, ASNase and CAT, using the PEG of 20 kDa (**Table 4.4.** and **Fig. 4.7.C**). Again, the preferential behaviour of native proteins towards the salt-rich phase and the PEGylated species to the top phase was observed with no exceptions. Nonetheless, a more selective performance was found for Cyt-c and LYS (smaller proteins), with *S* values of 123 and >1000, respectively. In the case of LYS, a complete separation was obtained (%$RecB_{LYS}$ = 100% and %$RecT_{LYS\text{-}PEG}$ = 100%) by our one-step *in-situ* approach. Regarding the larger enzymes, higher recovery yields were obtained for PEGylated conjugates towards the top phase, but recovery yields of the unreacted protein towards the opposite phase were lower (94 % > %$RecT_{PROT\text{-}PEG}$ > 98%, 58% > %$RecB_{PROT}$ > 66%). This decrease of recovery yield of unreacted protein in salt-rich phase may be a result of its higher molecular weight and consequent protein partition to the top phase by a salting-out phenomena caused by the potassium citrate salt presence.[43]

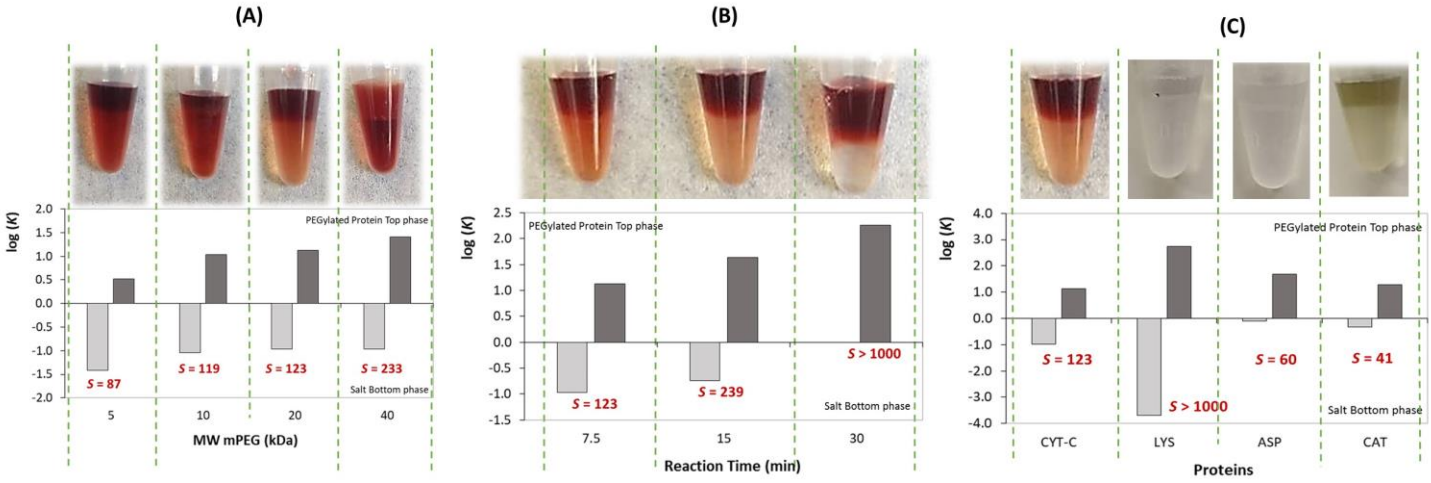

Fig. 4.7. Logarithm of *K* of both native (light grey bars) and PEGylated proteins (dark grey bars) in the one-step approach under development PEG-Prot + citrate (pH = 7) ABS [*1.0 wt% Protein (condition 2) + 12.5 wt% Prot-PEG/PEG + 12.5 wt% citrate buffer*]. The selectivity of each system (*S*) is presented in red. Pictures of each ABS prepared are depicted for each system.

Table 4.2. Effect of molecular weight (MW) of mPEG-NHS upon the volume ratio (V_R) and partitioning behaviour, represented as the partition coefficient (*K*), top and bottom-phase recoveries (%*RecT* and %*RecB*), and selectivity (*S*) of native and PEGylated Cyt-c in Cyt-c-PEG + potassium citrate buffer-based ABS.

MW mPEG-NHS	V_R	$K_{Cyt\text{-}c}$	$K_{Cyt\text{-}c\text{-}PEG}$	*S*	$\%RecT_{Cyt\text{-}c}$	$\%RecB_{Cyt\text{-}c}$	$\%RecT_{Cyt\text{-}c\text{-}PEG}$	$\%RecB_{Cyt\text{-}c\text{-}PEG}$
Condition 1: *0.5 wt% Cyt-c + 12.5 wt% Cyt-c-PEG + 12.5 wt% potassium citrate buffer*								
mPEG 5 kDa	0.46	0.00072 ± 0.00004	4.5 ± 0.2	>1000	0%	100%	90.7 ± 0.5%	9.3 ± 0.5%
mPEG 10 kDa	0.52	0.0051 ± 0.0003	2.2 ± 0.1	426	0.3 ± 0.1%	99.7 ± 0.1%	80.7 ± 1.0%	19.3 ± 1.0%
mPEG 20 kDa	0.73	0.115 ± 0.06	7 ± 0.4	61	7.8 ± 0.7%	92.3 ± 0.7%	90.6 ± 0.5%	9.4 ± 0.5%
mPEG 40 kDa	0.81	0.204 ± 0.01	31 ± 2	154	14.2 ± 0.7%	85.8 ± 0.7%	97.5 ± 0.1%	2.5 ± 0.1%
Condition 2*: 1.0 wt% Cyt-c + 12.5 wt% Cyt-c-PEG + 12.5 wt% potassium citrate buffer*								
mPEG 5 kDa	0.52	0.038 ± 0.002	3.3 ± 0.2	87	1.9 ± 0.1%	98.1 ± 0.1%	86.4 ± 0.7%	13.6 ± 0.7%
mPEG 10 kDa	0.58	0.090 ± 0.005	10.8 ± 0.5	119	5.0 ± 0.3%	95.0 ± .0.3%	94.9 ± 0.3%	5.1 ± 0.3%
mPEG 20 kDa	0.90	0.108 ± 0.005	13.3 ± 0.7	123	8.9 ± 0.4%	91.1 ± 0.4%	93.6 ± 0.3%	6.4 ± 0.3%
mPEG 40 kDa	2.17	0.109 ± 0.005	25 ± 1	233	19.1 ± 1.0%	80.9 ± 1.0%	92.1 ± 0.4%	7.9 ± 0.4%

Table 4.3. Effect of PEGylation reaction time on the volume ratio (V_R) and partition behaviour, represented as the partition coefficient (K), top and bottom-phase recoveries (%*RecT* and %*RecB*), and selectivity (S) of native and PEGylated Cyt-c in ABS composed of 1.0 wt% Cyt-c + 12.5 wt% Cyt-c-PEG/PEG + 12.5 wt% potassium citrate buffer, at pH 7.0.

Time (min)	V_R	$K_{Cyt\text{-}c}$	$K_{Cyt\text{-}c\text{-}PEG}$	S	$\%RecT_{Cyt\text{-}c}$	$\%RecB_{Cyt\text{-}c}$	$\%RecT_{Cyt\text{-}c\text{-}PEG}$	$\%RecB_{Cyt\text{-}c\text{-}PEG}$
7.5	0.90	0.108 ± 0.005	13.3 ± 0.7	123	8.9 ± 0.4%	91.1 ± 0.4%	93.6 ± 0.3%	6.4 ± 0.3%
15	1.24	0.181 ± 0.009	43.3 ± 2.2	239	18.3 ± 0.9%	81.7 ± 0.9%	97.2 ± 0.1%	2.8 ± 0.1%
30	2.80	*	180.8 ± 9.0	>1000	*	*	98.5 ± 0.1%	1.5 ± 0.1%

*Absence of unreacted Cyt-c since at 30 min the complete PEGylation reaction occurs.

Table 4.4. Partition parameters for Cyt-c, LYS, ASNase, and CAT for the *in-situ* approach under development: Volume ratio (V_R), partition coefficient (K), top and bottom-phase recoveries (%*RecT* and %*RecB*), and selectivity (S) of native and PEGylated enzyme conjugates in ABS composed of 1.0 wt% Protein + 12.5 wt% Prot-PEG/PEG + 12.5 wt% potassium citrate buffer.

Proteins	V_R	K_{PROT}	$K_{PROT\text{-}PEG}$	S	$\%RecT_{PROT}$	$\%RecB_{PROT}$	$\%RecT_{PROT\text{-}PEG}$	$\%RecB_{PROT\text{-}PEG}$
Cyt-c	0.90	0.108 ± 0.005	13.3 ± 0.7	123	8.9 ± 0.4%	91.1 ± 0.4%	93.6 ± 0.3%	6.4 ± 0.3%
LYS	0.73	0.0002 ± 0.0001	543 ± 27	>1000	0%	100%	100%	0%
ASNase	0.90	0.79 ± 0.04	47.5 ± 2.4	60	41.6 ± 2.1%	58.4 ± 2.1%	98.1 ± 0.1%	1.9 ± 0.1%
CAT	1.11	0.46 ± 0.02	18.8 ± 1.0	41	33.9 ± 1.7%	66.1 ± 1.7%	94.4 ± 0.3%	5.6 ± 0.3%

While developing a strategy able to efficiently produce PEGylated enzymes and purify them from the respective unreacted protein, the ABS used in this work proved to be simultaneously able to maintain the activity and structural integrity of each model enzyme. The enzyme activity was evaluated in both top and bottom phases, to guarantee the biological activity of both PEGylated and unreacted enzyme, since we expected to increase the sustainability of the process by reintroducing the unreacted enzyme in new cycles of PEGylation reaction.[16] **Table 4.5.** presents the specific activity (*SA*, $U.mg^{-1}$) and the volumetric activity (*A*, $U.mL^{-1}$) for each enzyme species concentrated in both top and bottom phases. In all cases, the enzyme activity was preserved, emphasizing the biocompatible and mild nature of the downstream process envisioned in this work. Moreover, and due to the enzymes' sensibility to small changes in their secondary structure, Fourier transform infrared spectroscopy (FTIR) was also applied to investigate PEG-proteins bioconjugation and partition. **Fig. 4.8.** shows the FTIR spectra of pure PEG and Cyt-c together with ABS top and bottom phases after PEGylation and phase separation. As observed, the IR spectra present three main spectral regions resultant from a complex combination of vibration modes from different infrared-activate functional groups typical of PEG and Cyt-c IR fingerprints: 3500-2700 cm^{-1}, 1700-1500 cm^{-1} and 1500-1000 cm^{-1}.[44,45] The appearance of two bands at 2921 and 2883 cm^{-1} assigned to aliphatic C-H asymmetric and symmetric stretching of PEG methylene groups at the top Cyt-c confirms the success of the PEGylation reaction while also demonstrates the presence of Cyt-c-PEG as main component of top-phase of ABS.[46] This is further supported by the occurrence of a broad envelope with maximum intensity centered on 1085 cm^{-1}, resultant of a band merging effect assigned to the combination of C–O, C–O–C stretches and C–O–H bending vibrations of the attached PEG.[44] The amide I band presented at 1638 cm^{-1} representing the C-O stretching vibration of peptide group, the amide II band at 1578 cm^{-1} corresponding primarily to N-H bending and contributions of C-N stretching vibrations, as well as, amide III at 1388 cm^{-1} representing the N-H bending and C-N stretching vibrations, prove that Cyt-c keeps its secondary structure after PEGylation.[47] Despite the fact that no changes are observed at the vibrational frequency of the studied proteins, an increase of intensity of amide I when compared with the amide II is observed for the ABS top

phase, and when compared with the data for both the pure Cyt-c and bottom phase of ABS.

Table 4.5. Proof of concept for four model enzymes: Cyt-c, LYS, ASNase, and CAT of one-pot conjugation + *in situ* ABS. The specific activity, SA, (units: $U.mg^{-1}$), the volumetric activity of the respective protein (units: $U.mL^{-1}$) and the total protein concentration (units: $mg.mL^{-1}$) of top and bottom phases of Prot-PEG + citrate ABS are depicted in this table.

Proteins	$[P]_T$ ($mg.mL^{-1}$)	$[P]_B$ ($mg.mL^{-1}$)	A_T ($U.mL^{-1}$)	A_B ($U.mL^{-1}$)	SA_T ($U.mg^{-1}$)	SA_B ($U.mg^{-1}$)
Cyt-c	0.352	0.070	1.11	0.17	3.15	2.40
LYS	0.437	0.039	2.55E+03	5.52E+03	5.84E+03	1.43E+05
ASNase	0.174	0.044	1.56E+01	2.78E+01	8.97E+01	6.28E+02
CAT	0.182	0.064	6.84E+04	1.22E+04	3.76E+05	1.91E+05

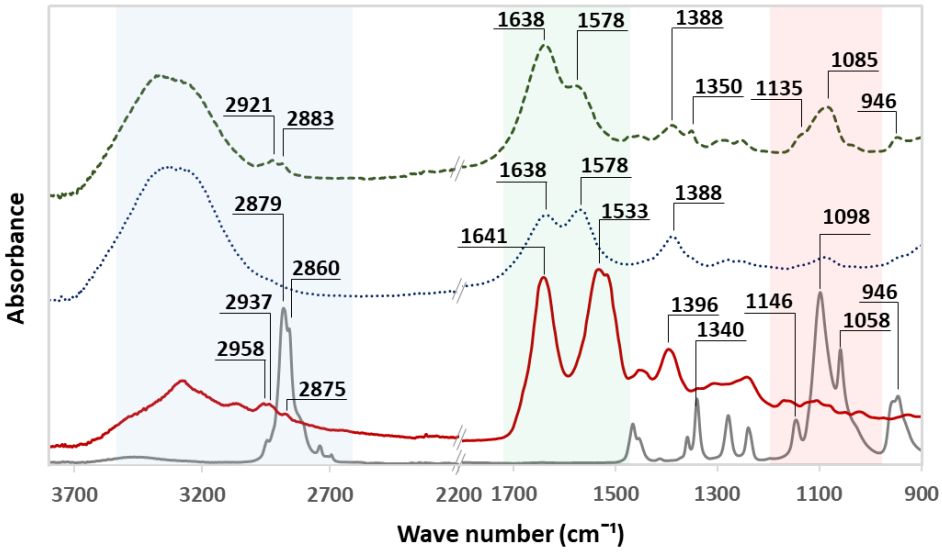

Fig. 4.8. FTIR-ATR spectrum of ABS (1.0 wt% Protein + 12.5 wt% Prot-PEG/PEG + 12.5 wt% citrate buffer) top-phase (---) bottom-phase (•••), pure Cyt-c (—) and PEG (—).

3.3. Process optimization

Three of the main criteria for the development of a sustainable process combining reaction and separation allied with the Green Chemistry principles, are the (i) need for a high yield of reaction, (ii) the possible recycle of main unreacted reagents and (iii) the possible recycle of the main solvents. In this work, a schematic diagram (**Figs. 4.9.** and **4.10.**) was defined combining the PEGylation reaction with the purification of the

protein conjugates. Here, two scenarios were considered. A first one were the PEGylation reaction is complete (1.0 wt% of Cyt-c + mPEG-NHS-20 kDa, 30 min), thus eliminating the need to recycle the unreacted enzyme (**Fig. 4.9.**). The second scenario (the worst but most common one) describes an incomplete PEGylation reaction (1.0 wt% of Cyt-c + mPEG-NHS-40 kDa, 7.5 min) and for which, the recycling of the unreacted enzyme was contemplated in the approach (**Fig. 4.10.**). In both cases, the dual role of the citrate salt was verified, namely as a phase-forming solvent but firstly, as an agent acting to stop the PEGylation reaction, which is also contributing for the higher sustainability of the process. Moreover, for both scenarios, the yield of reaction, as well as the recovery yields of both enzyme conjugates and unreacted enzyme (for the incomplete reaction), are represented in the respective diagram for both top and bottom phases. When the complete reaction is evaluated (**Fig. 4.9.**), the process is simpler, since after the reaction (PEGylation yield of 100%) the only demand is for the separation of the enzyme bioconjugates by ABS, followed by the recycle of the phase-forming solvents, which can be easily achieved by applying an ultrafiltration. Using this approach, the isolation of the citrate salt-rich phase from the PEGylated Cyt-c is accomplished with success. Since the presence of the Cyt-c conjugate is only residual (around 1.5%), the salt can be directly reintroduced in the process for new cycles of PEGylation + separation. Despite the good performance of this approach, the second scenario contemplating an incomplete reaction is the most common (**Fig. 4.10.**). Here, in addition to the recycle of the phase-forming solvents, the recycle and reuse of the unreacted enzyme in a new cycle of PEGylation was also contemplated. In this case, higher selectivity values were found for higher purity of both the PEGylated conjugates (purity = 84.6%) on the top phase and unreacted protein (purity = 97.7 %) on the bottom phase. Nevertheless, in both scenarios, the waste production was prevented by the addition of a recycling process using ultrafiltration, simultaneously allowing the reuse of (i) phase-forming components (citrate salt) in a consequent *in-situ* ABS purification, and (ii) unreacted protein for a novel PEGylation reaction, thus contributing for the higher sustainability and lower economic impact of the overall process. Allied with the good performance of the processes envisioned in this work, an enhanced capacity to improve the production of higher amounts of purified PEGylated proteins was obtained. The

strategy developed in this work combined the higher efficiency in the recovery of PEGylated proteins, with the possibility to re-use the unreacted protein and the phase former compounds (*i.e.* potassium citrate salt) to perform a second reaction.[16] In the end, an advantageous integrated process, in comparison with chromatographic techniques was here demonstrated, since the saturation limitations, especially in large scale[48] described for chromatography, were eliminated.

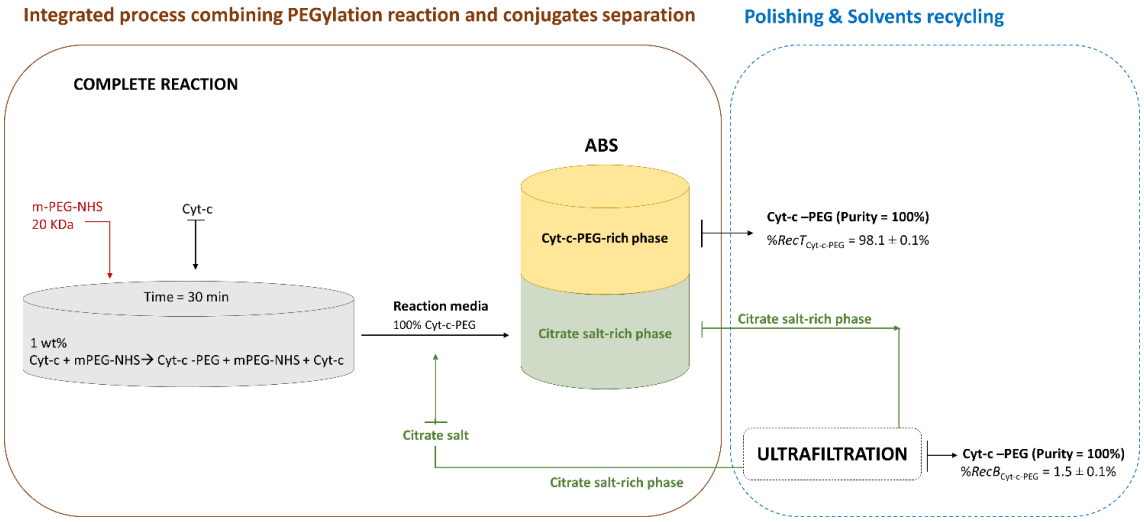

Fig. 4.9. Schematic diagram of the integrated process combining bioconjugation reaction and separation with the polishing step and solvent recycling process for a complete PEGylation reaction. The dashed line represents steps that were not experimentally developed.

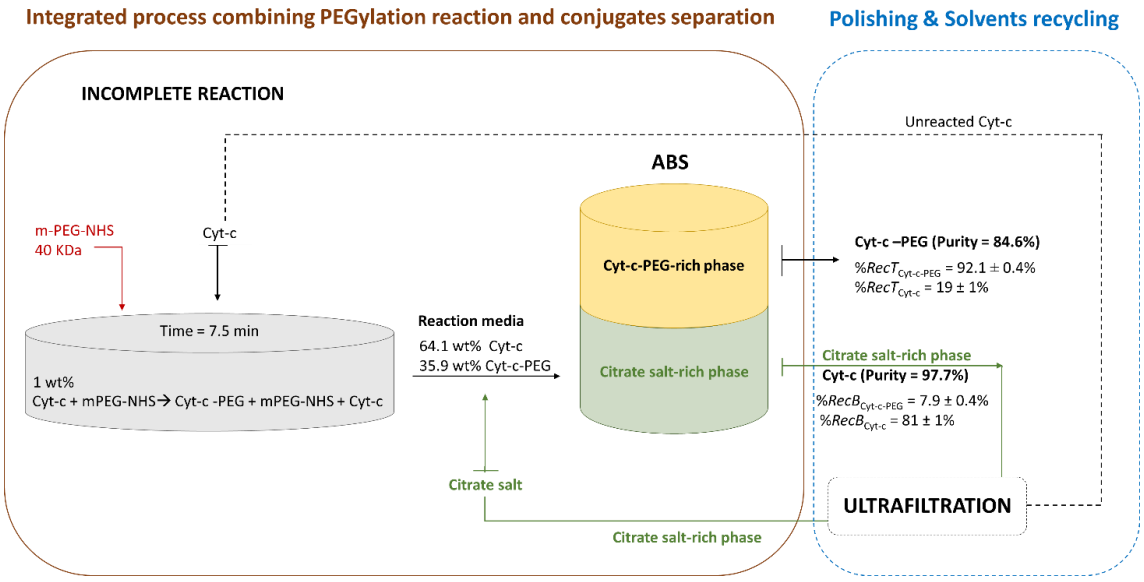

Fig. 4.10. Schematic diagram of the integrated process combining bioconjugation reaction and separation with the polishing step and solvent recycling process for an incomplete PEGylation reaction. The dashed line represents steps that were not experimentally developed.

4. Conclusions

In an era where the demand for more sustainable, cheap and "green" downstream processes is increasing, the need for improved downstream approaches is crucial. In this work, an alternative process was envisioned, by integrating the enzyme PEGylation with the separation of conjugates and unreacted enzyme. Aiming at simplifying the process, the PEGylated enzyme produced was used as one of the phase-forming agents, allowing the two-phase split after the direct addition of potassium citrate buffer. Despite the dual role of the enzyme conjugates as product of the reaction and phase forming agent, the citrate salt also acts as phase-forming agent, but firstly it is used to stop the PEGylation reaction, thus simplifying the process and avoiding the need for extra compounds on the reaction media. After optimization of the main conditions of reaction (time of reaction and PEG MW), an integrated process was successfully achieved for four model proteins, namely Cyt-c, LYS, ASNase and CAT.

Envisioning the industrial potential of the processes developed in this work, the schematic representation of the process diagram was defined combining PEGylation reaction with purification. Two different scenarios were here contemplated, the first one representing a complete PEGylation reaction (1.0 wt% of Cyt-c + mPEG-NHS-20 kDa, 30 min), and a second and most common, where an incomplete PEGylation reaction is represented (1.0 wt% of Cyt-c + mPEG-NHS-40 kDa, 7.5 min). For both approaches, high recovery yields and purities were obtained for the PEGylated conjugates (92.1 ± 0.4% < $\%RecT_{\text{Cyt-c-PEG}}$ < 98.1 ± 0.1%; 84.6% < purity < 100%) and for the unreacted enzyme ($\%RecB_{\text{Cyt-c}}$ = 81 ± 1%; purity = 97.7%), while maintaining their structural integrity.

The findings reported here open a new path for application of integrated bioconjugation + purification using ABS for the recovery of high-value biological products, like therapeutic biobetters and biosensors from larger reaction volumes, without compromising the success of the downstream process.

References

1. Zhu, M. M., Mollet, M., Hubert, R. S., Kyung, Y. S. & Zhang, G. G. in *Handb. Ind. Chem. Biotechnol.* 1639–1669 (2017). doi:10.1007/978-3-319-52287-6_29
2. Ryu, J. K., Kim, H. S. & Nam, D. H. Current status and perspectives of biopharmaceutical drugs. *Biotechnol. Bioprocess Eng.* **17,** 900–911 (2012).
3. Carter, P. H., Berndt, E. R., Dimasi, J. A. & Trusheim, M. Investigating investment in biopharmaceutical R&D. *Nat. Rev. Drug Discov.* **15,** 673–674 (2016).
4. Gong, Y., Leroux, J. C. & Gauthier, M. A. Releasable Conjugation of Polymers to Proteins. *Bioconjug. Chem.* **26,** 1179–1181 (2015).
5. Hermanson, G. T. Bioconjugation Techniques. *Bioconjugate Tech. (Third Ed.* 229–258 (2013). doi:10.1007/s00216-009-2731-y
6. Presolski, S. I., Hong, V. P. & Finn, M. G. Chemistry for Bioconjugation. *Chem. Biol.* **3,** 153–162 (2011).
7. Sassi, A. B., Nagarkar, R. & Hamblin, P. in *Nov. Approaches Strateg. Biol. Vaccines Cancer Ther.* 199–217 (2015). doi:10.1016/B978-0-12-416603-5.00009-2
8. Beck, A., Sanglier-Cianférani, S. & Van Dorsselaer, A. Biosimilar, biobetter, and next generation antibody characterization by mass spectrometry. *Anal. Chem.* **84,** 4637–4646 (2012).
9. Santos, J. H. P. M., Torres-Obreque, K. M., Pastore, G. M., Amaro, B. P. & Rangel-Yagui, C. O. Protein PEGylation for the design of biobetters: from reaction to purification processes. *Brazilian J. Pharm. Sci.* **54,** (2018).
10. Roberts, M. J., Bentley, M. D. & Harris, J. M. Chemistry for peptide and protein PEGylation. *Adv. Drug Deliv. Rev.* **64,** 116–127 (2012).
11. Jevševar, S., Kunstelj, M. & Porekar, V. G. PEGylation of therapeutic proteins. *Biotechnol. J.* **5,** 113–128 (2010).
12. Pasut, G. & Veronese, F. M. State of the art in PEGylation: The great versatility achieved after forty years of research. *J. Control. Release* **161,** 461–472 (2012).
13. González-Valdez, J., Rito-Palomares, M. & Benavides, J. Advances and trends in the design, analysis, and characterization of polymer-protein conjugates for 'PEGylaided' bioprocesses. *Anal. Bioanal. Chem.* **403,** 2225–2235 (2012).
14. Morgenstern, J., Baumann, P., Brunner, C. & Hubbuch, J. Effect of PEG molecular

weight and PEGylation degree on the physical stability of PEGylated lysozyme. *Int. J. Pharm.* **519,** 408–417 (2017).

15. Mejía-Manzano, L. A., Mayolo-Deloisa, K., Sánchez-Trasviña, C., González-Valdez, J., González-González, M. & Rito-Palomares, M. Recovery of PEGylated and native lysozyme using an in situ aqueous two-phase system directly from the PEGylation reaction. *J. Chem. Technol. Biotechnol.* **92,** 2519–2526 (2017).
16. Santos, J. H. P. M., Carretero, G., Coutinho, J. A. P., Rangel-Yagui, C. O. & Ventura, S. P. M. Multistep purification of cytochrome c PEGylated forms using polymer-based aqueous biphasic systems. *Green Chem.* **19,** 5800–5808 (2017).
17. González-Valdez, J., Cueto, L. F., Benavides, J. & Rito-Palomares, M. Potential application of aqueous two-phase systems for the fractionation of RNase A and α-Lactalbumin from their PEGylated conjugates. *J. Chem. Technol. Biotechnol.* **86,** 26–33 (2011).
18. González-Valdez, J., Rito-Palomares, M. & Benavides, J. Effects of chemical modifications in the partition behavior of proteins in aqueous two-phase systems: A case study with RNase A. *Biotechnol. Prog.* **29,** 378–385 (2013).
19. Hatti-Kaul, R. Aqueous two-phase systems. *Mol. Biotechnol.* **19,** 269–277 (2001).
20. Santos, J. H. P. M., Trigo, J. P., Maricato, É., Nunes, C., Coimbra, M. A. & Ventura, S. P. M. Fractionation of Isochrysis galbana Proteins, Arabinans, and Glucans Using Ionic-Liquid-Based Aqueous Biphasic Systems. *ACS Sustain. Chem. Eng.* **6,** 14042–14053 (2018).
21. Johansson, H.-O., Ishii, M., Minaguti, M., Feitosa, E., Penna, T. C. V. & Pessoa, A. Separation and partitioning of Green Fluorescent Protein from Escherichia coli homogenate in poly(ethylene glycol)/sodium-poly(acrylate) aqueous two-phase systems. *Sep. Purif. Technol.* **62,** 166–174 (2008).
22. Hatti-Kaul, R. Aqueous Two-Phase Systems: A General Overview. *Mol. Biotechnol.* **19,** 269–278 (2001).
23. Yau, Y. K., Ooi, C. W., Ng, E.-P., Lan, J. C.-W., Ling, T. C. & Show, P. L. Current applications of different type of aqueous two-phase systems. *Bioresour. Bioprocess.* **2,** 49 (2015).
24. Mekaoui, N., Faure, K. & Berthod, A. Advances in countercurrent chromatography

for protein separations. *Bioanalysis* **4,** 833–844 (2012).

25. Zafarani-Moattar, M. T. & Sadeghi, R. Phase diagram data for several PPG + salt aqueous biphasic systems at 25 °C. *J. Chem. Eng. Data* **50,** 947–950 (2005).
26. Santos, J. H. P. M., e Silva, F. A., Coutinho, J. A. P., Ventura, S. P. M. & Pessoa, A. Ionic liquids as a novel class of electrolytes in polymeric aqueous biphasic systems. *Process Biochem.* **50,** 661–668 (2015).
27. Merchuk, J. C., Andrews, B. a & Asenjo, J. a. Aqueous two-phase systems for protein separation. *J. Chromatogr. B Biomed. Sci. Appl.* **711,** 285–293 (1998).
28. Meneguetti, G. P., Santos, J. H. P. M., Obreque, K. M. T., Vaz Barbosa, C. M., Monteiro, G., Farsky, S. H. P., De Oliveira, A. M., Angeli, C. B., Palmisano, G., Ventura, S. P. M., Pessoa-Junior, A. & De Oliveira Rangel-Yagui, C. Novel site-specific PEGylated L-asparaginase. *PLoS One* **14,** (2019).
29. Santiago-Rodríguez, L., Méndez, J., Flores-Fernandez, G. M., Pagán, M., Rodríguez-Martínez, J. A., Cabrera, C. R. & Griebenow, K. Enhanced stability of a nanostructured cytochrome c biosensor by PEGylation. *J. Electroanal. Chem.* **663,** 1–7 (2011).
30. Kim, N. H., Jeong, M. S., Choi, S. Y. & Kang, J. H. Peroxidase activity of cytochrome c. *Bull. Korean Chem. Soc.* **25,** 1889–1892 (2004).
31. Aldrich, S. Enzymatic Assay of Lysozyme (EC 3.2.1.17). (2019). at <https://www.sigmaaldrich.com/technical-documents/protocols/biology/enzymatic-assay-of-lysozyme.html>
32. Drainas, C. & Pateman, J. A. L-Asparaginase activity in the fungus Aspergillus nidulans. *Biochem. Soc. Trans.* **5,** 259–261 (1977).
33. Iwase, T., Tajima, A., Sugimoto, S., Okuda, K. I., Hironaka, I., Kamata, Y., Takada, K. & Mizunoe, Y. A simple assay for measuring catalase activity: A visual approach. *Sci. Rep.* **3,** (2013).
34. Azevedo, A. M., Gomes, A. G., Rosa, P. A. J., Ferreira, I. F., Pisco, A. M. M. O. & Aires-Barros, M. R. Partitioning of human antibodies in polyethylene glycol–sodium citrate aqueous two-phase systems. *Sep. Purif. Technol.* **65,** 14–21 (2009).
35. Wu, Y.-T., Lin, D.-Q. & Zhu, Z.-Q. Thermodynamics of aqueous two-phase systems—the effect of polymer molecular weight on liquid–liquid equilibrium

phase diagrams by the modified NRTL model. *Fluid Phase Equilib.* **147,** 25–43 (1998).

36. Silvério, S. C., Wegrzyn, A., Lladosa, E., Rodríguez, O. & MacEdo, E. A. Effect of aqueous two-phase system constituents in different poly(ethylene glycol)-salt phase diagrams. *J. Chem. Eng. Data* **57,** 1203–1208 (2012).
37. Delgado, C., Malmsten, M. & Van Alstine, J. M. Analytical partitioning of poly(ethylene glycol)-modified proteins. *J. Chromatogr. B Biomed. Appl.* **692,** 263–272 (1997).
38. Delgado, C., Malik, F., Selisko, B., Fisher, D. & Francis, G. E. Quantitative analysis of polyethylene glycol (PEG) in PEG-modified proteins/cytokines by aqueous two-phase systems. *J. Biochem. Biophys. Methods* **29,** 237–50 (1994).
39. Galindo-López, M. & Rito-Palomares, M. Practical non-chromatography strategies for the potential separation of PEGylated RNase A conjugates. *J. Chem. Technol. Biotechnol.* **88,** 49–54 (2013).
40. Sookkumnerd, T. & Hsu, J. T. Purification of PEG-protein conjugates by countercurrent disturbution in aqueous two-phase systems. *J. Liq. Chromatogr. Relat. Technol.* **23,** 497–503 (2000).
41. Schaeffer, N., Gras, M., Passos, H., Mogilireddy, V., Mendonça, C. M. N., Pereira, E., Chainet, E., Billard, I., Coutinho, J. A. P. & Papaiconomou, N. Synergistic Aqueous Biphasic Systems: A New Paradigm for the 'One-Pot' Hydrometallurgical Recovery of Critical Metals. *ACS Sustain. Chem. Eng.* **7,** 1769–1777 (2019).
42. Ferreira, A. M., Passos, H., Okafuji, A., Tavares, A. P. M., Ohno, H., Freire, M. G. & Coutinho, J. A. P. An integrated process for enzymatic catalysis allowing product recovery and enzyme reuse by applying thermoreversible aqueous biphasic systems. *Green Chem.* **20,** 1218–1223 (2018).
43. Ventura, S. P. M., Santos-Ebinuma, V. C., Pereira, J. F. B., Teixeira, M. F. S., Pessoa, A. & Coutinho, J. A. P. Isolation of natural red colorants from fermented broth using ionic liquid-based aqueous two-phase systems. *J. Ind. Microbiol. Biotechnol.* **40,** 507–516 (2013).
44. Shameli, K., Ahmad, M. Bin, Jazayeri, S. D., Sedaghat, S., Shabanzadeh, P., Jahangirian, H., Mahdavi, M. & Abdollahi, Y. Synthesis and characterization of

polyethylene glycol mediated silver nanoparticles by the green method. *Int. J. Mol. Sci.* **13,** 6639–6650 (2012).

45. Kong, J. & Yu, S. Fourier transform infrared spectroscopic analysis of protein secondary structures. *Acta Biochim. Biophys. Sin. (Shanghai).* **39,** 549–559 (2007).
46. Natalello, A., Ami, D., Collini, M., D'Alfonso, L., Chirico, G., Tonon, G., Scaramuzza, S., Schrepfer, R. & Doglia, S. M. Biophysical characterization of Met-G-CSF: Effects of different site-specific mono-pegylations on protein stability and aggregation. *PLoS One* **7,** (2012).
47. Speare, J. O. & Rush, T. S. IR spectra of cytochrome c denatured with deuterated guanidine hydrochloride show increase in β sheet. *Biopolym. - Biospectroscopy Sect.* **72,** 193–204 (2003).
48. Fee, C. J. & Van Alstine, J. M. PEG-proteins: Reaction engineering and separation issues. *Chem. Eng. Sci.* **61,** 934–939 (2006).

5. CONTINUOUS PURIFICATION REGIME (CPC)

5.1. Continuous purification of PEG-Protein conjugates by fast centrifugal partition chromatography

Santos, J. H. P. M., Ferreira. A. M., Almeida, M. R., Coutinho, J. A. P., Freire, M. G., Rangel-Yagui, C. O. & Ventura, S. P. M. *Green Chemistry*, 2019, submitted.[10]

Abstract

This work proposes the application of aqueous biphasic systems (ABS) in FCPC for the purification of PEGylated cytochrome c conjugates. After the proper optimization of the processual conditions, the ABS composed of PEG 2000 + potassium phosphate buffer (at pH 7) was selected as the most performant to be applied on FCPC to separate unreacted Cytochromec (Cyt-c) from the PEGylated conjugate in continuous flow. Yields of purification (*Y*% > 88%) and purity levels around 100% were obtained, even after the reuse of both the unreacted Cyt-c in a new cycle of PEGylation + FCPC purification and the phase former components (PEG 2000 and potassium phosphate buffer), contributing towards the development of a sustainable fractionation approach in continuous regime for bioconjugates.

Keywords: cytochrome c; protein PEGylation; continuous purification regime; aqueous biphasic systems; fast centrifugal partition chromatography; countercurrent chromatography.

[10] Contributions: JS, AF and MA acquired the experimental data. The data was analysed by all the authors. JC, MF, CY and SV conceived and directed this work. The manuscript was mainly written by JS with contributions from the remaining authors.

1. Introduction

Protein PEGylation is widely used in the pharmaceutical industry,[1–4] yet, it can also be used to obtain novel protein-based biosensors.[5–8] PEGylated drugs are commonly classified as biobetters,[2,4,9] since the PEG attachment on the protein normally results in pharmacokinetic and pharmacodynamic improvements.[10,11] Generally, PEGylation enhances drug solubility and decreases immunogenicity.[1] PEGylation also increases plasma half-life by reducing drug proteolysis and clearance, thereby follow-on in a reduced dosing frequency to the patient.[2,12] Taking into consideration all these benefits, a wide variety of therapeutic proteins,[13–15] peptides,[16] and antibody fragments,[11] as well as small molecule drugs,[17] have been PEGylated. In terms of protein-based bionsensors, the PEGylation overcomes the crucial issue regarding the lack of long term stability of the protein since the PEGylated conjugate is more stable over extended periods of time while maintaining the biosensing aptitude.[5]

The conjugation reaction between PEG and protein is carried out by addition of activated PEG (also known as PEG derivative) and protein under the proper conditions (*i.e.* pH, molar ration PEG:protein, time, temperature and agitation speed).[18,19] The chemistry behind protein PEGylation is well-know, being extensively discussed in the literature.[9,19,20] While the conjugation reaction is rather straightforward, the fractionation and separation of PEGylated conjugates is troublesome, especially for continuous regime and scale-up processing.[21] Protein PEGylation results in a complex heterogeneous colloidal solution, consisting in residual polymer, native protein, reaction byproducts and in some cases different forms of the modified protein (*i.e.* different number of PEG molecules attached at different residues).[19] Therefore, there is the need to separate the PEGylated conjugates from the rest of the chemicals presented in the reaction.

Currently, purification processes of PEGylated proteins are based on chromatographic techniques, *i.e.* size exclusion chromatography (SEC)[22,23] and ion exchange chromatography (IEX).[24,25] Nonetheless, the separation of PEGylated proteins through conventional chromatographic based techniques showed to be, in a considerable number of cases, an unfeasible option, due to coelution of PEGylated products and native protein (*i.e.* poorer resolution at peak separation and peak overlapping).[26,27] This

occurs because separations by size (SEC) and charge (IEX) are ineffective to discriminate the PEG-protein conjugates from unreacted protein when the differences of molecular weight and charge between PEGylated conjugates and native protein are small. Recently, an effort has been noticed to seek for alternative non-chromatographic processes to fractionate PEGylated conjugates, through several techniques: membrane separations, electrophoresis, capillary electrophoresis, and aqueous biphasic systems (ABS).[28] In this way, the possibility to use aqueous biphasic systems principles in combination with chromatographic techniques, more specifically countercurrent chromatography (CCC), could be an interesting novel alternative for the separation of PEGylated proteins. Countercurrent chromatography consists in liquid–liquid chromatography which uses a support-free liquid stationary phase held in place by a simple centrifugal or complex centrifugal force field.[29] Countercurrent chromatography in aqueous two phase systems has been proven to be highly selective for closely related proteins, which have only slight differences in partitioning behavior.[29,30] In this case, it is studied the application of hydrostatic CCC columns, known as fast centrifugal partition chromatographs (FCPCs).[30–32] Their two main characteristics are: single axial rotation through a constant centrifugal field and enclosed geometrical volumes, tubes, channels, or locules that repeat themselves through connecting tubes forming a pattern.[29]

In this paper we evaluated the potential application of FCPC, for the separation of PEGylated species, using cytochrome c as a model protein. A previous report by our research group proved the potential application of PEG-phosphate ABS to separate the PEGylated cytochrome c (Cyt-c) from the unmodified form.[33] PEGylated Cyt-c forms are produced through an acylation reaction using NHS-PEG ester, which links to the protein in the amino groups. The continuous regime of purification through FCPC was evaluated, through the proper selection of mobile and stationary phases (*i.e*. mixture point and phase components) and possibility of recycling the unreacted protein to a novel PEGylation reaction and consequent FCPC purification.

2. Materials and Methods

2.1. Materials

Cytochrome c (Cyt-c) from equine heart (purity ≥ 95%) was acquired from Merck. The PEG derivative used in the PEGylation reaction was the methoxyl polyethylene glycol succinimidyl NHS ester (mPEG-NHS), obtained from Nanocs (purity > 95%) with a molecular weight of 20 kDa. The salts used on the protein PEGylation step were the potassium phosphate monobasic (KH_2PO_4), potassium phosphate dibasic (K_2HPO_4), and hydroxylammonium chloride all acquired from Merck, with purity of 95%.

For the FCPC separation process, the polyethylene glycol series (PEGs) used included PEG 600, 1000, 1500, 2000, and 4000. All these polymers were bought from Merck with high purity. The potassium phosphate buffer (PB) was prepared using the salts KH_2PO_4 and K_2HPO_4.

The mobile phase applied in the HPLC analysis was composed of acetonitrile (purity ≥ 99.9 wt%), trichloroacetic acid (purity ≥ 99.5 wt%) from Acros organics, both HPLC grade, and ultra-pure water, double distilled and passed through a Milli-Q plus 185 water purification apparatus. Syringe filters (0.45 μm) acquired from GE Healthcare, Whatman, were used.

2.2. PEGylation reaction of Cyt-c

The PEGylation reactions were conducted following standard protocols described in literature.[33,34] Briefly, 2 mL of a Cyt-c solution (0.5 $mg.mL^{-1}$) in 100 mM of PB (pH = 7) was added to a flask containing 20.8 mg of mPEG-NHS with 20 kDa (protein:PEG molar ratio = 1:25). The mixtures were stirred at 400 rpm, for 30 min at room temperature with a magnetic stirrer. To stop the PEGylation reaction 10% (v/v) of hydroxylammonium chloride (1 M) was added. After, the samples were stored at -20°C for further use in FCPC.

2.3. Fast Centrifugal Partition Chromatography Purification

2.3.1. FCPC equipment

A Fast Centrifugal Partition Chromatography (FCPC)® system, model FCPC-C, from Kromaton Rousselet-Robatel (Annonay, France), was used to investigate the continuous

separation of PEGylated and non-PEGylated proteins. The equipment used in this work is the same presented in our previous study, where phenolic compounds were purified in a continuous regime.[35] In order to verify the PEG + potassium phosphate buffer ABS behaviour in the equipment, increase the stationary phase retention ratio and decrease the purification time, operating conditions, such as flow-rate and rotation speed were investigated (**Table 5.1**.). The best flow rate and rotation speed found were of 2.5 mL.min^{-1} and 200 rpm with a S_f of 41.18%. The stationary phase retention, S_f, was calculated by the ratio of the stationary phase volume (V_S) and the column volume (V_C): $S_f = V_S/V_C$.

Table 5.1. FCPC assays with PEG 1000 + phosphate buffer ABS, mixture points adopted, stationary phase retention (S_f) achieved and operating conditions.

PEG (g.mol^{-1})	Potassium phosphate buffer	Mixture point (PEG; buffer wt%)	CPC	S_f	Flow rate (mL.min^{-1})	Rotation speed (rpm)
1000	pH 7	15; 20	✓	11.76	3.0	2000
		15; 20	✓	9.31	3.0	2500
		15; 20	✓	16.67	2.5	2500
		15; 20	✓	41.18	2.5	2000

2.3.2. FCPC purification of PEGylated and non-PEGylated Cyt-c

Ternary phase diagrams of PEG + potassium phosphate buffer were constructed through cloud point titration method[36] to further study the fractionation of the unreacted Cyt-c and PEGylated forms. In these systems, the top phase corresponds to the PEG-rich phase while the bottom phase is mainly composed by potassium phosphate buffer. The mixture point composed of 15 wt% of PEG + 20 wt% of potassium phosphate buffer (pH = 7) using different PEG molecular weights (Table 2) was selected. This system was set to work in the descending mode. The rotor was entirely filled with the PEG-(top)-rich phase at 5 mL.min^{-1} and 600 rpm to achieve the homogeneous solvent re-equilibration

on the rotor. Then, the rotation was set up at the highest speed (2000 rpm), needed for the appropriate stationary phase retention. After the set-up of the working rotational speed, the potassium phosphate buffer-rich-(bottom) phase was pumped (2.5 mL.min^{-1}) through the stationary phase to reach the equilibrium, *i.e.* when only the mobile phase came out of the column and the signal baseline is stabilized. The stationary phase retention parameter for all the ABS applied was calculated, ranging from 38% to 46%, depending on the PEG molecular weight used (**Table 5.2**.). The sample loop was filled with 2 mL of the PEGylation Cyt-c samples (obtained by the method 2.2.). An elution-extrusion countercurrent chromatography method was applied,[37,38] composed by two main steps: first an elution with potassium phosphate buffer-rich phase and then an extrusion with water. The first 20 min of elution were performed using the bottom(salt)-rich phase as mobile phase to extract the unreacted Cyt-c, then the PEGylated conjugates of Cyt-c were eluted with water by extrusion. By applying an elution-extrusion process, full sample recovery can be achieved with high resolution of the peaks.

2.3.4. Integrated process applying continuous purification by FCPC

An integrated process was created to reuse the unreacted Cyt-c in a novel PEGylation reaction. This integrated process combines the PEGylation reaction, followed by FCPC purification and then the isolation of the purified fractions of Cyt-c by applying an ultrafiltration step. The purified Cyt-c fractions were filtrated through Amicon Ultra centrifugal filters (Merck) with a MWCO of 4 kDa to remove the mobile phase (composed of potassium phosphate buffer with small quantities of PEG). The ultrafiltration step consisted in three washes of 100 mM of potassium phosphate buffer (pH = 7) to change the solvent of the unreacted Cyt-c to the appropriate PEGylation medium. The polished Cyt-c fraction was then PEGylated with a molar ratio of 1:25 (protein:PEG) and applying the same conditions of reaction time, temperature, and agitation speed, described in section 2.2. The yield of Cyt-c-PEG (*Y*%, corresponding to the weight of PEGylated protein in the purified fraction divided by the initial weight of PEGylated protein after bioconjugation reaction) was calculated for both the integrated and simple processes, meaning the process with and without recycling of Cyt-c.

2.4. Polishing of purified Cyt-c products (Cyt-c and Cyt-c-PEG) and recycling of phase components

Both purified fractions containing the PEGylated sample and the unreacted protein were ultrafiltrated through Amicon Ultra centrifugal filters (Merck) with a MWCO of 4 kDa for the removal of phase components of the mobile phase. The recycling of the phase components from the fractions without protein was achieved in the integrated process. This additional step aims to decrease the environmental impact and to seek for the higher sustainability of the purification process proposed.

2.5. Analytical procedures: HPLC quantification of Cyt-c and Cyt-c-PEG

The quantification of purified fractions of PEGylated Cyt-c and unreacted protein from the FCPC was carried by HPLC-DAD (Shimadzu, model PROMINENCE). HPLC analyses were performed with an analytical C18 reversed-phase column (250 × 4.60 mm), kinetex 5 µm C18 100 A, from Phenomenex. The mobile phase used was a gradient system of 0.1% of trifluoracetic acid (TFA)-ultra-pure water (phase A) and 0.1% TFA-acetonitrile (phase B), previously degassed by ultrasonication. The separation was conducted using the following gradient mode, 0 min 25% of B, 42 min 42% of B, 45 min of B, and then returning to initial conditions during 20 min to ensure the column stabilization. The flow rate used was 0.8 $mL.min^{-1}$ with an injection volume of 60 µL. DAD was set at 409 nm. Each sample was analysed at least in duplicate. The column oven and the autosampler operated at a controlled temperature of 25°C. Cyt-c and Cyt-c-PEG presented retention times of 16.5 and 19.3 minutes, respectively.

The purification performance of FCPC process was evaluated based on the purification yield (*Y*%) and purity (%) determined for both Cyt-c and Cyt-c-PEG. The purification yield was calculated by dividing the protein weight in the purified fraction (either Cyt-c or Cyt-c-PEG) by the initial protein weight (before purification). The purity (%) was calculated by the weight percentage of the desirable protein (either Cyt-c or Cyt-c-PEG) in the purified fraction.

3. Results and Discussion

3.1. FCPC purification step

The phase diagrams of the ABS formed by PEG and the potassium phosphate buffer solution were experimentally prepared under the scope of this work,[36] being the results depicted in **Fig. D.1 at Appendix D**. A well-established behaviour was observed for PEG/salt-based ABS, which correlates the increase of PEG molecular weight with the ability to form two aqueous phases.[39,40] The mixture point adopted to test the continuous purification using FCPC was 15 wt% of PEG + 20 wt% of potassium phosphate buffer (pH = 7), which represents a biphasic system (**Fig. 5.1**.). Furthermore, to better understand the separation of both proteins (unreacted and PEGylated conjugate) the partition of both protein structures, at lab scale, was determined, being the respective partition coefficients calculated for all the studied systems (**Table D.1 at Appendix D**). The results suggest the preferential partition of Cyt-c-PEG towards the PEG-rich phase and the unreacted protein towards the opposite phase (*i.e.* salt-rich phase), which results in high selectivity values, as previously shown in literature.[33,41–44] Due to the different characteristics of the proteins in terms of their relative hydrophilicity/hydrophobicity nature, the application of this type of systems in a continuous regime using the FCPC was investigated. The same five ABS composed of PEGs with different molecular weights + potassium phosphate buffer were investigated. The manipulation of PEG molecular weight was evaluated (ranging from 600 to 4000 $g.mol^{-1}$), maintaining fixed the mixture point and the FCPC operational conditions (*i.e.* flow rate and rotation speed), being the stationary phase retention and the capability to perform the purification runs calculated (**Table 5.2**.).

Table 5.2. PEG + potassium phosphate buffer ABS tested in FCPC, mixture points adopted, stationary phase retention and operating conditions.

PEG ($g.mol^{-1}$)	Potassium phosphate buffer	Mixture point (PEG; buffer wt%)	CPC	S_f	Operating conditions
600	pH 7	15; 20	✓	38.73	Flow: 2.5 $mL.min^{-1;}$ Rotation speed: 2000 rpm
1000		15; 20	✓	41.18	
1500		15; 20	✓	46.07	
2000		15; 20	✓	46.08	
4000		15; 20	×	--	Over-pressure Highly viscous top-phase

The polymer-based ABS designed with PEG of higher molecular weight (*i.e*. PEG 4000) resulted in a highly viscous top-phase, preventing the application of FCPC due to the over-pressure troubleshooting. Moreover, the polymer-based ABS using the PEG with the lower molecular weight (*i.e*. PEG 600) exhibited a lower value of S_f, indicating the weak capacity to retain the stationary phase. Taking into account all the processual restrictions previously identified, the work developed employing the FCPC was done using PEGs with intermediate molecular weights, namely PEG 1000, PEG 1500, and PEG 2000.

After selecting the most appropriate ABS to apply on FCPC, the next step was to perform the PEGylation of Cyt-c. For that, a PEG derivative (mPEG-NHS) of 20 kDa was used to perform the PEGylation, then forming a complex reaction medium, containing a heterogeneous mixture of proteins (Cyt-c and Cyt-c-PEG) and salts (hydroxylamine and potassium phosphate buffer). The yield of PEGylation observed was at *circa* 43.5%, with only one PEGylated conjugate formed (Cyt-c-PEG). This yield is quite reasonable when compared to other PEGylation yields obtained for Cyt-c.[5,6,45] **Fig. 5.1.** presents the chromatogram resulting from the batch injection of 2 mL of reaction medium, performed in the descending mode and with a mobile phase flow rate of 2.5 $mL.min^{-1}$.

The ascending mode was also tested resulting in lower fractionation performance, being for this reason discarded. The bottom potassium phosphate buffer-rich phase was used as mobile phase during the initial stage of elution (from 0 to 20 min).

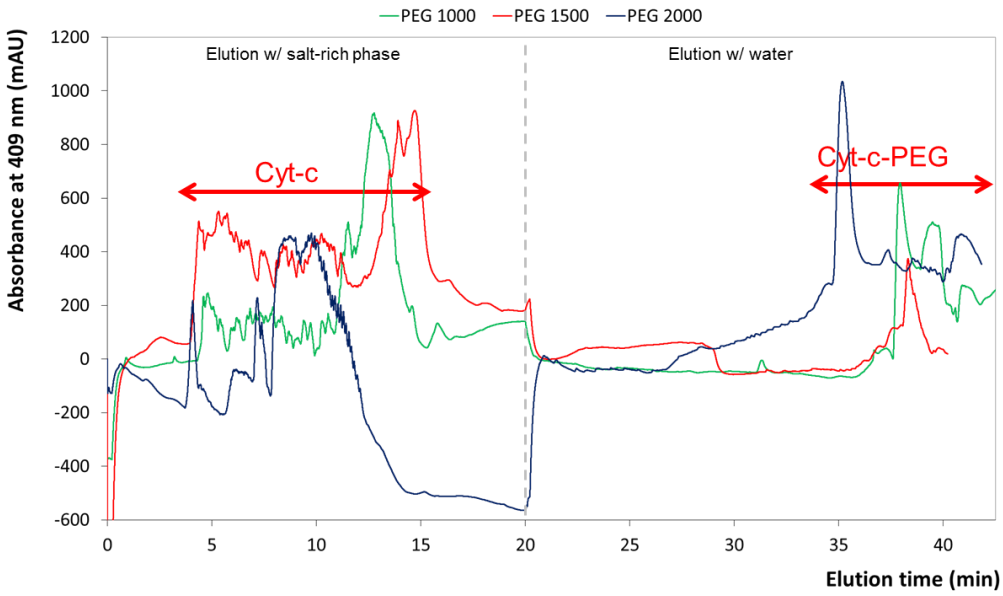

Fig. 5.1. Chromatogram of FCPC purification of Cyt-c and Cyt-c-PEG performed employing ABS comprising 15 wt% of PEG (1000, 1500 and 2000) + 20 wt% of potassium phosphate buffer, at pH 7.0.

Afterwards and, for the elution of unreacted Cyt-c, the mobile phase was changed to water and the extrusion method was applied[37,38] to efficiently separate the bioconjugates (from 20 to 40 min). This change on the mobile phase was required to decrease the elution time of Cyt-c-PEG, since the PEGylated form has a higher affinity to the stationary phase used during the initial stage of elution, the PEG-rich phase. Previous studies[33] and the partition tests here performed in lab scale for both proteins (**Table D.1 at Appendix D**) demonstrated that Cyt-c exhibits a $K < 1$, resulting in its favourable interaction with the most hydrophilic phase. On the contrary, the PEGylated form was concentrated mostly in the top-rich phase ($K > 1$). This behaviour is probably justified by the preferential PEG-PEG interactions and by some hydrophobic effects occurring. In this sense, the FCPC results agreed with the previous lab-scale partition assays, meaning that the unreacted protein migrating preferentially to the mobile phase, was firstly separated, followed the PEGylated conjugate further eluted by extrusion. No losses of stationary phase were observed during the separation run and the complete separation

of the two proteins was achieved with the Cyt-c elution observed in fractions 7-15, and the Cyt-c-PEG in fractions 35-39, depending on the PEG molecular weight used as phase component. After the removal of the phase components (PEG and potassium phosphate buffer) by ultrafiltration, using MWCO = 4 kDa Amicon centrifugal filter, both proteins were identified by HPLC (**Fig. 5.2.**), aiming at to prove the successful separation between the proteins and the solvents.

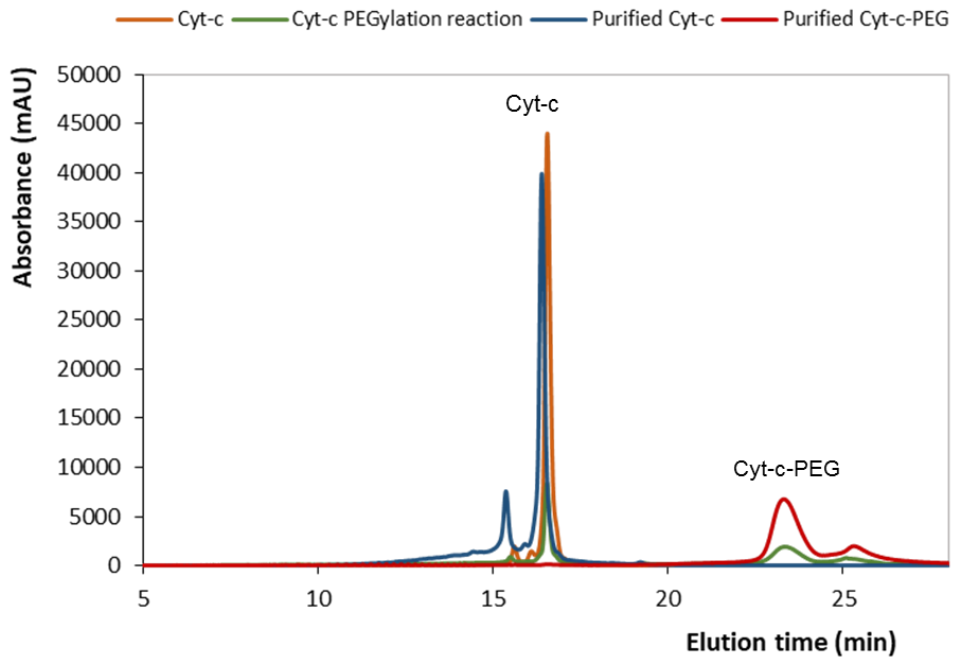

Fig. 5.2. HPLC chromatogram of the Cyt-c, Cyt-c PEGylation reaction media, purified Cyt-c and purified Cyt-c-PEG.

The results showed high yields and purities for both proteins (*i.e. Y*% > 96% and purity = 100% for Cyt-c; *Y*% > 88% and purity = 100% for Cyt-c-PEG) in all systems applied in FCPC (*cf.* **Table 5.3**.). Nonetheless, PEG 2000 can be highlighted as the most promising system due to the highest values of *Y*% for both unreacted and PEGylated protein. Therefore, the experiments and results discussed before demonstrated the potential of these specific ABS allowing the development of versatile approaches for the separation of PEGylated conjugates using FCPC in a continuous regime.

Table 5.3. Purified fractions, yield (%) and purity of Cyt-c and Cyt-c-PEG obtained after FCPC purification.

	Cyt-c			**Cyt-c-PEG**		
	Fractions	Y (%)	Purity	Fractions	Y (%)	Purity
PEG 1000	14-15	96.10%	100	39	88.23%	100
PEG 1500	12-14	98.91%	100	38-39	90.62%	100
PEG 2000	7-12	100.11%	100	35	99.18%	100

3.2. Integrated purification process: recycling of Cyt-c and ABS phase-forming compounds

Currently, the biopharmaceutical industries seek for the development of processes based on the principles of Green Chemistry and Sustainability, and in this sense, the profitability of the process has to be taken into account.[46] Based on the recent trends in the design of novel protein PEGylated products, it is herein proposed a novel recycling strategy composed of two steps: (i) the reuse of purified unreacted Cyt-c for a new cycle of PEGylation reaction and purification, and (ii) the reutilization of the phase-former solvents (PEG 2000 and potassium phosphate buffer) for a consequent FCPC purification step. **Fig. 5.3**. shows the simplified process without any recycling step (**Fig. 5.3.A**) and the integrated process contemplating the recycling of both Cyt-c and phase-forming components (**Fig. 5.3.B**). It must be highlighted that the polishing step was achieved using an ultrafiltration step (section 3.1.), since this allows the recovery and appropriate application of the PEGylated conjugate recycled.

(A)

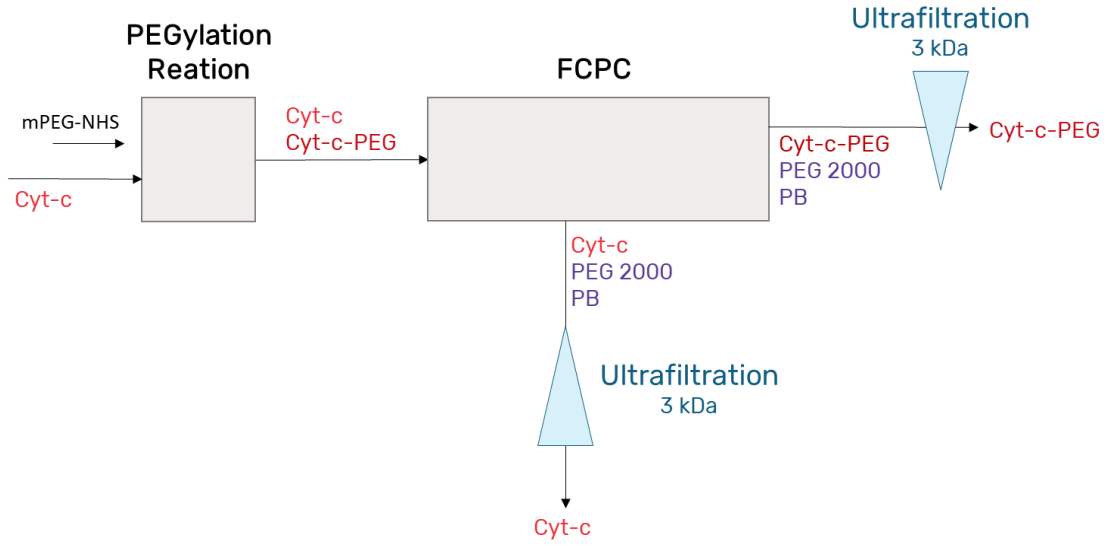

(B)

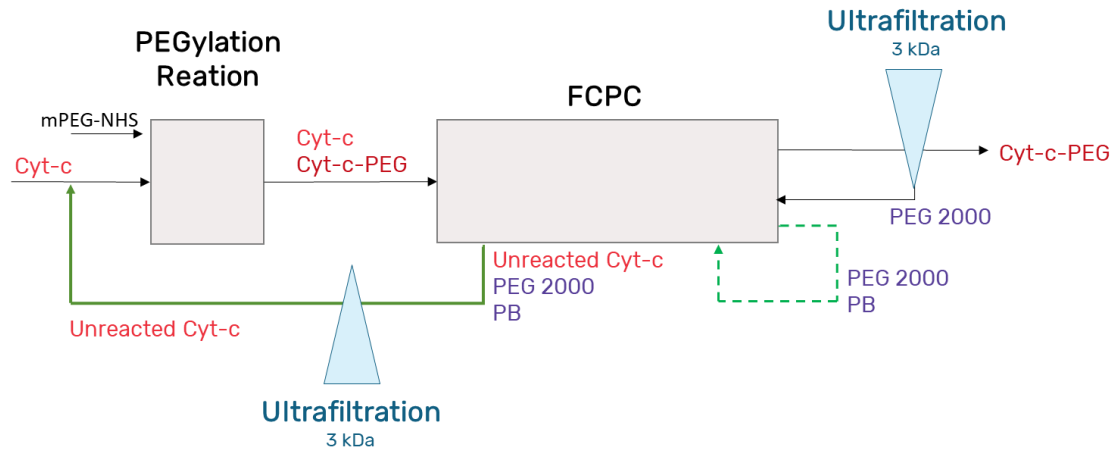

Fig. 5.3. Process diagram of the integrated process of purification in continuous regime applying FCPC without **(A)** and with the recycle of unreacted Cyt-c **(B).**

After the "re-PEGylation" process of the purified Cyt-c, a subsequent FCPC purification step was performed using the PEG 2000 + potassium phosphate buffer system, which was providing the highest purification yield, applying the same methodology of elution-extrusion CCC.[37,38] **Fig. 5.4.** depicts the chromatogram of each protein after FCPC application, where it can be seen the complete separation of the two protein products, using PEG 2000 after recycling, without losses of the stationary phase. The Cyt-c eluted is represented by fractions 10-12, and the Cyt-c-PEG corresponds to fractions 36-37.

Furthermore, remarkable purities and yields of purification (*Y*%) were obtained in this subsequent FCPC purification step. Indeed, the purity of both proteins was kept around 100% with minor losses of *Y*% (at *circa* 5% and 10% respectively for Cyt-c and Cyt-c-PEG, *cf.* **Table 5.4**.).

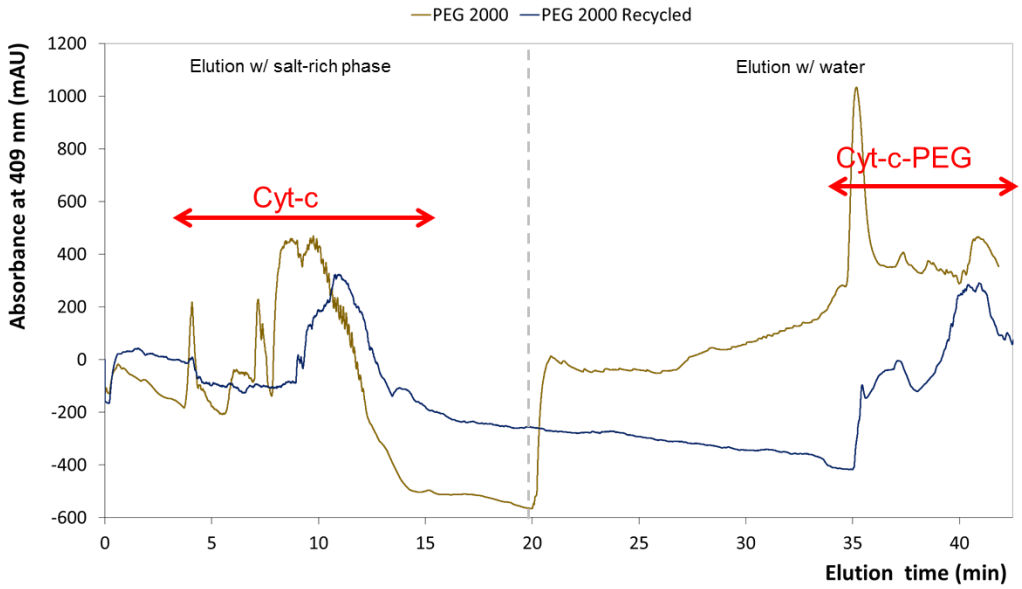

Fig. 5.4. Chromatogram of FCPC representing the separation of unreacted Cyt-c and Cyt-c-PEG, obtained after two-steps of PEGylation + fractionation using FCPC and the ABS comprising 15 wt% of PEG 2000 + 20 wt% of potassium phosphate buffer, at pH 7.0.

Table 5.4. Purified fractions, yield (*Y*%) and purity (%) of Cyt-c and Cyt-c-PEG obtained after FCPC purification in both processes designed.

	Cyt-c			**Cyt-c-PEG**		
	Fractions	*Y* (%)	Purity (%)	Fractions	*Y* (%)	Purity (%)
PEG 2000	7-12	100.11	100	35	99.18	100
PEG 2000 Recycled	10-12	95.95	100	36-37	90.85	100

Literature shows the use of CCC in the purification of PEGylated RNAse A[47] and lysozyme,[48] using the technique of countercurrent distribution (CCD). In comparision with FCPC, CCD is a preparative CCC scale technique firstly developed, it uses gravity to maintain the liquid stationary phase, resulting in very long elution times, lower resolution, and highly laborious work (no-automation), currently being an outdated

option.[49] Even so, Galindo-López *et. al.* attempted to purify mono and di-PEGylated products, applying PEG 8000 + PB ABS with CCD technology with ultrafiltration as polishing step. Accordingly, co-elution of both PEGylated forms was observed and lower yields were obtained when compared with FCPC results (*Y*% ranging from 38 to 60%).[47] Sookkumnerd *et. al.* also attempted to purify mono and di-PEGylated proteins, *i.e.* lysozyme, applying a PEG 3400 + PB ABS with CCD technology and showed difficulties in purifying PEGylated conjugates, resulting in lower purities in preparative scale and confirming FCPC a as better option.[48] In comparison with the results found in the literature, the newly designed centrifuges hydrostatic CCC columns (*i.e.* FCPC) allow greater yields and purity in the large scale purification of proteins, taking advantage of the several spotlights and commodities (**Table 5.5**.).[29,50] Further studies should be applied using other types of CCC columns (*i.e.* hydrodynamic) such as high-speed countercurrent chromatography (HSCCC) which can support more viscous polymers (high molecular weight PEGs as phase components) and can reveal a great opportunity to efficiently purify PEGylated conjugates with different degrees of functionalization.[51] In this work, with the integrated process (PEGylation reaction + separation of PEGylated products two times) contemplating the recycling of the phase forming compounds and unreacted Cyt-c, the overall cost of the PEGylation process was decreased, as a consequence of the high yields and purities obtained in the two consecutive purification steps studied. Overall, this findings opens up a novel path for engineering process in the developing of continuous purification steps that can easily be scaled-up through the combination of ABS and chromatography with CCC technology, in particular with hydrostatic columns (FCPC).

4. Conclusions

The present study reports two different strategies based upon aqueous two-phase systems and ultrafiltration for the potential separation of PEGylated conjugates of Cyt-c. The systems proposed exploiting the principle of CCC-ABS and applying FCPC resulted in the complete fractionation of PEGylated from unreacted protein. The manipulation of phase components was studied to establish the best purification condition in continuous purification regime. The protein polishing step was achieved by

ultrafiltration, removing the polymer and salts from the purified fractions. Additionally, an integrated process contempling the Cyt-c and phase forming compounds recycling was proposed, resulting in higher purification yields and purities, while increasing the overall sustainability of the process. In conclusion, the findings reported here point to the fractionation efficiency of novel continuous non-chromatography downstream processes in PEGylated proteins purification.

Table 5.5. Comparison of several types of columns used in countercurrent chromatography (CCC) regime of purification. Highlights and challenges of CCC technique.

Technology	Type	Advantages	Disadvantages
Countercurrent distribution (CCD)	Gravitational	• Easy operation and intrinsic simplicity.	• Highly laborious; • Preparative scale; • Long elution times (days); • Rudimentary technique; • Inefficient fractionation performance.
Fast centrifugal partition chromatography (FCPC)	Hydrostatic (constant centrifugal field, one axis of rotation)	• Versatile to work at ascending and descending modes; • Scale-up technique.	• Operational problems using solvents with medium and higher viscosity; • Maintenance, e.g. lubrication of rotating seals every 100 h; • Time-consuming purification method.
High-speed countercurrent chromatography (HSCCC)	Hydrodynamic (variable centrifugal field, two axes of rotation)	• Higher efficiency and peak resolution; • Greater versatility of solvents that can be used as mobile and stationary phases. • Shorter operational times; works more rapidly; • Scale-up technique.	• Possible noisy gear assembly; • Maintenance, e.g. connecting tube to change every 100 h.
Countercurrent chromatography (CCC)	**Highlights** • Quick (high throughput in preparative separation) • Inexpensive (contemplate only the cost of solvents, which are still significantly lower than the ones applied in HPLC) • Gentle and versatile, for separation of several compounds, with less chance of decomposition • Able to range from milligrams to tens of grams on the same instrument • Ability to switch between normal and reversed-phase • Free of irreversible adsorption to a solid support (recovery of sample at 100%)		**Challenges** • Aqueous solvents are not commonly used, more studies should be attained. • Higher cost of equipment investment, when compared with other fractionation technologies.

References

1. Turecek, P. L., Bossard, M. J., Schoetens, F. & Ivens, I. A. PEGylation of Biopharmaceuticals: A Review of Chemistry and Nonclinical Safety Information of Approved Drugs. *J. Pharm. Sci.* **105,** 460–475 (2016).
2. Ryu, J. K., Kim, H. S. & Nam, D. H. Current status and perspectives of biopharmaceutical drugs. *Biotechnol. Bioprocess Eng.* **17,** 900–911 (2012).
3. Harris, J. M. & Chess, R. B. Effect of pegylation on pharmaceuticals. *Nat. Rev. Drug Discov.* **2,** 214–221 (2003).
4. Sassi, A. B., Nagarkar, R. & Hamblin, P. in *Nov. Approaches Strateg. Biol. Vaccines Cancer Ther.* 199–217 (2015). doi:10.1016/B978-0-12-416603-5.00009-2
5. Santiago-Rodríguez, L., Méndez, J., Flores-Fernandez, G. M., Pagán, M., Rodríguez-Martínez, J. A., Cabrera, C. R. & Griebenow, K. Enhanced stability of a nanostructured cytochrome c biosensor by PEGylation. *J. Electroanal. Chem.* **663,** 1–7 (2011).
6. Mabrouk, P. A. Effect of pegylation on the structure and function of horse cytochrome c. *Bioconjug. Chem.* **5,** 236–241 (1994).
7. Hsieh, Y. P. & Lin, S. C. Effect of PEGylation on the activity and stability of horseradish peroxidase and L-N-carbamoylase in aqueous phases. *Process Biochem.* **50,** 1372–1378 (2015).
8. Liu, G., Lin, Y., Ostatná, V. & Wang, J. Enzyme nanoparticles-based electronic biosensor. *Chem. Commun.* 3481 (2005). doi:10.1039/b504943a
9. Santos, J. H. P. M., Torres-Obreque, K. M., Pastore, G. M., Amaro, B. P. & Rangel-Yagui, C. O. Protein PEGylation for the design of biobetters: from reaction to purification processes. *Brazilian J. Pharm. Sci.* **54,** (2018).
10. Da Silva Freitas, D., Mero, A. & Pasut, G. Chemical and enzymatic site specific pegylation of hGH. *Bioconjug. Chem.* **24,** 456–463 (2013).
11. Constantinou, A., Chen, C. & Deonarain, M. P. Modulating the pharmacokinetics of therapeutic antibodies. *Biotechnol. Lett.* **32,** 609–622 (2010).
12. Pasut, G. & Veronese, F. M. State of the art in PEGylation: The great versatility achieved after forty years of research. *J. Control. Release* **161,** 461–472 (2012).
13. Narta, U. K., Kanwar, S. S. & Azmi, W. Pharmacological and clinical evaluation of

l-asparaginase in the treatment of leukemia. *Crit. Rev. Oncol. Hematol.* **61,** 208–221 (2007).

14. Kurinomaru, T. & Shiraki, K. Noncovalent PEGylation of L-asparaginase using PEGylated polyelectrolyte. *J. Pharm. Sci.* **104,** 587–592 (2015).
15. Jevševar, S., Kunstelj, M. & Porekar, V. G. PEGylation of therapeutic proteins. *Biotechnol. J.* **5,** 113–128 (2010).
16. Liu, B. Peptide PEGylation: the next generation. *Pharm. Technol.* s26–s28 (2011).
17. Li, W., Zhan, P., De Clercq, E., Lou, H. & Liu, X. Current drug research on PEGylation with small molecular agents. *Prog. Polym. Sci.* **38,** 421–444 (2013).
18. Zalipsky, S. Chemistry of polyethylene glycol conjugates with biologically active molecules. *Adv. Drug Deliv. Rev.* **16,** 157–182 (1995).
19. Pfister, D. & Morbidelli, M. Process for protein PEGylation. *J. Control. Release* **180,** 134–149 (2014).
20. Roberts, M. J., Bentley, M. D. & Harris, J. M. Chemistry for peptide and protein PEGylation. *Adv. Drug Deliv. Rev.* **64,** 116–127 (2012).
21. González-Valdez, J., Rito-Palomares, M. & Benavides, J. Advances and trends in the design, analysis, and characterization of polymer-protein conjugates for 'PEGylaided' bioprocesses. *Anal. Bioanal. Chem.* **403,** 2225–2235 (2012).
22. Fee, C. J. & Alstine, J. M. Van. Separation of PEGylated Proteins by Size Exclusion Chromatography: Influence of PEGylation on Molecular Size. *APCChE Conf.* 1–10 (2004).
23. Fahrländer, E., Schelhaas, S., Jacobs, A. H. & Langer, K. PEGylated human serum albumin (HSA) nanoparticles: preparation, characterization and quantification of the PEGylation extent. *Nanotechnology* **26,** 145103 (2015).
24. Maiser, B., Kröner, F., Dismer, F., Brenner-Weiss, G. & Hubbuch, J. Isoform separation and binding site determination of mono-PEGylated lysozyme with pH gradient chromatography. *J. Chromatogr. A* **1268,** 102–108 (2012).
25. Abe, M., Akbarzaderaleh, P., Hamachi, M., Yoshimoto, N. & Yamamoto, S. Interaction mechanism of mono-PEGylated proteins in electrostatic interaction chromatography. *Biotechnol. J.* **5,** 477–483 (2010).
26. Fee, C. J. & Van Alstine, J. M. in *Protein Purif. Princ. High Resolut. Methods, Appl.*

Third Ed. 339–362 (2011). doi:10.1002/9780470939932.ch14

27. Yoshimoto, N. & Yamamoto, S. PEGylated protein separations: Challenges and opportunities. *Biotechnol. J.* **7,** 592–593 (2012).
28. Mayolo-Deloisa, K., González-Valdez, J., Guajardo-Flores, D., Aguilar, O., Benavides, J. & Rito-Palomares, M. Current advances in the non-chromatographic fractionation and characterization of PEGylated proteins. *J. Chem. Technol. Biotechnol.* **86,** 18–25 (2011).
29. Berthod, A., Maryutina, T., Spivakov, B., Shpigun, O. & Sutherland, I. a. Countercurrent chromatography in analytical chemistry (IUPAC Technical Report). *Pure Appl. Chem.* **81,** 355–387 (2009).
30. Michel, T., Destandau, E. & Elfakir, C. New advances in countercurrent chromatography and centrifugal partition chromatography: Focus on coupling strategy. *Anal. Bioanal. Chem.* **406,** 957–969 (2014).
31. Rolet, M. C., Thiebaut, D. & Rosset, R. *Centrifugal Partition Chromatography (Cpc)*. *Analusis* **20,** (1992).
32. Melorose, J., Perroy, R. & Careas, S. Introduction to Centrifugal Partition Chromatography CPC/CCC. *Statew. Agric. L. Use Baseline 2015* **1,** (2015).
33. Santos, J. H. P. M., Carretero, G., Coutinho, J. A. P., Rangel-Yagui, C. O. & Ventura, S. P. M. Multistep purification of cytochrome c PEGylated forms using polymer-based aqueous biphasic systems. *Green Chem.* **19,** 5800–5808 (2017).
34. Nanocs. Succinimidyl PEG NHS, mPEG-NHS(SC). (2017). at <http://www.nanocs.net/mPEG-SC-5k-1g.htm>
35. Santos, J. H. P. M., Almeida, M. R., Martins, C. I. R., Dias, A. C. R. V., Freire, M. G., Coutinho, J. A. P. & Ventura, S. P. M. Separation of phenolic compounds by centrifugal partition chromatography. *Green Chem.* **20,** 1906–1916 (2018).
36. Merchuk, J. C., Andrews, B. A. & Asenjo, J. A. Aqueous two-phase systems for protein separation. Studies on phase inversion. *J. Chromatogr. B. Biomed. Sci. Appl.* **711,** 285–293 (1998).
37. Berthod, A., Ruiz-Angel, M. J. & Carda-Broch, S. Elution-extrusion countercurrent chromatography. Use of the liquid nature of the stationary phase to extend the hydrophobicity window. *Anal. Chem.* **75,** 5886–5894 (2003).

38. Berthod, A., Friesen, J. B., Inui, T. & Pauli, G. F. Elution-extrusion countercurrent chromatography: Theory and concepts in metabolic analysis. *Anal. Chem.* **79,** 3371–3382 (2007).

39. Silvério, S. C., Wegrzyn, A., Lladosa, E., Rodríguez, O. & MacEdo, E. A. Effect of aqueous two-phase system constituents in different poly(ethylene glycol)-salt phase diagrams. *J. Chem. Eng. Data* **57,** 1203–1208 (2012).

40. Pereira, J. F. B., Kurnia, K. a, Cojocaru, O. A., Gurau, G., Rebelo, L. P. N., Rogers, R. D., Freire, M. G. & Coutinho, J. a P. Molecular interactions in aqueous biphasic systems composed of polyethylene glycol and crystalline vs. liquid cholinium-based salts. *Phys. Chem. Chem. Phys.* **16,** 5723–31 (2014).

41. Delgado, C., Malmsten, M. & Van Alstine, J. M. Analytical partitioning of poly(ethylene glycol)-modified proteins. *J. Chromatogr. B Biomed. Appl.* **692,** 263–272 (1997).

42. Delgado, C., Malik, F., Selisko, B., Fisher, D. & Francis, G. E. Quantitative analysis of polyethylene glycol (PEG) in PEG-modified proteins/cytokines by aqueous two-phase systems. *J. Biochem. Biophys. Methods* **29,** 237–50 (1994).

43. González-Valdez, J., Rito-Palomares, M. & Benavides, J. Effects of chemical modifications in the partition behavior of proteins in aqueous two-phase systems: A case study with RNase A. *Biotechnol. Prog.* **29,** 378–385 (2013).

44. González-Valdez, J., Cueto, L. F., Benavides, J. & Rito-Palomares, M. Potential application of aqueous two-phase systems for the fractionation of RNase A and α-Lactalbumin from their PEGylated conjugates. *J. Chem. Technol. Biotechnol.* **86,** 26–33 (2011).

45. Zhou, J. Q., He, T. & Wang, J. W. PEGylation of cytochrome c at the level of lysine residues mediated by a microbial transglutaminase. *Biotechnol. Lett.* **38,** 1121–1129 (2016).

46. Zhu, M. M., Mollet, M., Hubert, R. S., Kyung, Y. S. & Zhang, G. G. in *Handb. Ind. Chem. Biotechnol.* 1639–1669 (2017). doi:10.1007/978-3-319-52287-6_29

47. Galindo-López, M. & Rito-Palomares, M. Practical non-chromatography strategies for the potential separation of PEGylated RNase A conjugates. *J. Chem. Technol. Biotechnol.* **88,** 49–54 (2013).

48. Sookkumnerd, T. & Hsu, J. T. Purification of PEG-protein conjugates by countercurrent disturbution in aqueous two-phase systems. *J. Liq. Chromatogr. Relat. Technol.* **23,** 497–503 (2000).
49. Hawker, C. D. Countercurrent Chromatography and Countercurrent Distribution. *JALA - J. Assoc. Lab. Autom.* **14,** 242 (2009).
50. Mekaoui, N., Faure, K. & Berthod, A. Advances in countercurrent chromatography for protein separations. *Bioanalysis* **4,** 833–844 (2012).
51. Ito, Y. High-speed countercurrent chromatography. *Nature* **326,** 419–20 (2000).

6. Conclusions and Future Work

Conclusions and future work

This thesis is based on the development of site-specific protein PEGylation reactions and alternative purification platforms of PEGylated conjugates through the exploration of aqueous biphasic systems. For that reason two enzymes were studied under this scope: ASNase and Cyt-c, to produce, respectively, therapeutic and analytical proteins with enhanced properties.

In **Chapter 2**. the upstream and downstream processing for the production of a pharmaceutical grade ASNase through chromatographic (**Section 2.1.**) and non-chromatographic purification platforms was presented (**Section 2.2**). The optimized two-step FPLC purification method allowed successful purification of ASNase from *S. cerevisiae* expressed in *E. coli* BL21 (DE3). Alternatively, the design of an integrated process comprising the steps of production, cell disruption, and purification with an ammonium sulfate precipitation followed by the application of ABS with IL as adjuvant, and culminating in the ASNase isolation and phases reuse was achieved. This integrated non-chromatographic process lead to purification factor 20 times higher than chromatographic method. In **Section 2.3**, an efficient integrated ABS platform was developed to fractionate and recover Cyt-c from a complex protein mixture. An integrated purification platform composed of ABS and micellar-based ABS (AMTPS) was first characterized, through the construction of phase diagrams and then applied in the fractionation of Cyt-c from a protein mixture. The obtained results showed that the ternary system composed of Pluronic L-35 (23 wt%) + potassium phosphate buffer (6 wt%) was the most selective system, demonstrating the potential of combine these two liquid-liquid extraction units can lead to great selectivity performance. The carbon footprint was evaluated to better understand the environmental impacts of this novel protein purification process.

After carrying out the development of processes of production and purification of the proteins under study, the PEGylation reaction of both ASNase and Cyt-c was evaluated (**Chapter 3**). An optimized protocol for site-specific N-terminal PEGylation of ASNase was successfully developed in **Section 3.1.**, and adequate yields were obtained (monoPEGylation yield% = 41%). This novel biobetter, was produced in lower times (reaction time of 30 min), with less quantity of PEG reactive, which represent a great

industrial production time and also less cost with raw material since the reaction needs less PEG than unspecific PEGylation. Also this novel enzyme variant exhibited not only enhanced long-term stability, in comparison with to polyPEGylated form similar to the currently one on the market (ONCASPAR®), as well as higher protection to proteolytic activity in comparison with native ASNase. The kinetic profile and activity against leukemic cell lines were investigated and attested, this mono-PEG ASNase as a potential biobetter to treat acute lymphoblastic leukemia. In **Section 3.2.** a site-specific PEGylation reaction for Cyt-c was successfully developed. The best PEGylation conditions were pH 7, 1:25 Cyt-c:mPEG-NHS (molar ratio) and 15 min reaction time resulting in PEGylation yields of 45% for the attachment of 4 PEG molecules (Cyt-c-PEG-4) and 34% for the binding of 8 PEG molecules (Cyt-c-PEG-8). The PEGylated forms of Cyt-c exhibited enhanced long-term stability in terms of catalytic activity of ABTS oxidation by hydrogen peroxidase. Based on bioconjugation reaction engineering, the protective role of PEG considering the design of novel protein-based biosensors was demonstrated. The thermostability of PEG covalent conjugation of the protein-based biosensors were further evaluated in **Section 3.3**. From the thermodynamic parameters obtained, it was possible to conclude that PEGylation of Cyt-c enhanced its thermostability, proving to be an important tool for industrial biosensing applications. Such protection was even enhanced at higher temperatures.

Taking into account that the protein PEGylation reactions are not complete, with the formation of heterogeneous mixtures, there is a need to investigate sustainable processes for the purification of PEGylated conjugates. In this sense, batch ABS based platforms for the fractionation of site-specific PEGylated conjugates were studied in **Chapter 4**. The separation of PEGylated conjugates from the unreacted protein and the sub-fractionation of the PEGylated conjugates among themselves on the basis of their degree of PEGylation was successfully achieved with the use of multistage ABS based on PEG + phosphate buffer (pH = 7), the results are presented in **Section 4.1.**. This pioneer work, was the first to prove the possibility to fractionate site-specific PEGylated conjugates with the use of non-chromatographic ABS technology. Systems based on intermediate molecular weight (MW) PEGs showed to be promising platforms to selectively fractionate the PEGylated conjugates from the unreacted protein in a single

step, while ABS formed by higher MW PEGs exhibited higher selectivity in the purification of specific PEGylated conjugates. The two main driving-forces affecting the protein partitioning were the volume exclusion (of the polymer-rich phase) and the "PEG-PEG" interactions. In this sense, a multi-stage ABS strategy was developed to purify the three protein species, namely Cyt-c, Cyt-c-PEG-4 and Cyt-c-PEG-8 with high purities (96.5% Cyt-c, 85.8% Cyt-c-PEG-4, and 99.0% Cyt-c-PEG-8). Furthermore, an innovative recycling procedure of the purified Cyt-c for a novel PEGylation reaction was also achieved, increasing the feasibility and sustainability of the overall process (moving towards a circular economy). Within the ABS-based separation field, a novel one pot process designed with the integration of protein PEGylation reaction with the direct application of polymer + salt-based ABS on the reaction media was successfully developed for several model proteins: Cyt-c, LYS, ASNase, and CAT (**Section 4.2**.). The PEGylated protein was used as phase forming components, being concentrated and recovered in the top aqueous phase. The citrate buffer was applied not only to promote the formation of ABS through salting-out process, but also to stop the PEGylation reaction (a greener alternative to conventional reagents such as hydroxylamine, which exhibits high toxicity). The obtained results show high selectivies in the recovery of PEGylated Cyt-c from unreacted Cyt-c for several molecular weights reactive PEGs (5-40 kDa) and reaction times (7.5-30 min). The findings reported here open a new pathway for the application of one-pot bioconjugation + ABS step for the recovery of high-value biological products, such as therapeutic *biobetters* modified with different PEG sizes from large reaction volumes.

Looking for the need to transpose the efficient batch ABS-based separation units to a continuous purification regime, fast centrifugal partition chromatography (FCPC) applying ABS was investigated for the *in situ* fractionation of PEGylated protein conjugates (**Chapter 5**). In this sense, the application of PEG + phosphate buffer ABS in FCPC for the purification of PEGylated Cyt-c conjugates was effectively attained. The proportion of phase components in PEG + phosphate buffer ABS was evaluated in order to obtain the best purification yield and purity. An outstanding purification performance was obtained in the fractionation of Cyt-c from Cyt-c-PEG (Y% > 88% and purity = 100%). Furthermore, the recycling of unreacted Cyt-c for a novel PEGylation step and FCPC

purification was achieved, along with the reuse of phase components (PEG and phosphate buffer), towards the creation of a more sustainable process.

From the current work developed in this thesis, it is clear the great potential of ABS in the fractionation of PEGylated proteins, under batch and continuous regime. Moreover *in situ* recovery of the PEGylated products through one-pot integration of bioconjugation and ABS purification was successfully proved for both enzymes studied.

As future work and taking advantage of the results achieved and discussed above, it would be interesting to:

- Optimize site-specific protein PEGylation reactions with improved yields, through the application of alternative solvents in bioconjugation reactions, such as ionic liquids (ILs).
- Explore the potential of ionic liquids (ILs), deep eutectic solvents (DES), and copolymers as phase forming compounds of ABS to the purification of protein PEGylated conjugates.
- Test other continuous purification regimes based on ABS technology to fractionate site-specific PEGylated conjugates (*i.e*. high-speed countercurrent chromatography, HSCCC and continuous tubular separator).
- Use MALDI-TOF MS to do a better characterization of PEGylated Cyt-c conjugates (Cyt-c-PEG-4 and Cyt-c-PEG-8).
- Apply the site-specific PEGylated Cyt-c conjugates in bioelectrochemical redox sensing in order to develop an enhanced biosensor with long-term stability.
- Study the effect of PEGylation in thermal and kinetic stability of both ASNase and mono-PEGylated ASNase and other enzymes.
- Evaluate the *in vivo* drug clearance of ASNAse *vs* mono-PEGylated ASNase, through *in vivo* localization of labelled native and PEGylated asparaginase performed in mice with further *ex vivo* biodistribution studies.

List of Publications from PhD

Papers in international scientific periodicals with referees

1. Vicente, F. A., Santos, J. H. P. M., Pereira, I. M. M., Gonçalves, C. V. M., Dias, A. C. R. V, Coutinho, J. A. P. & Ventura, S. P. M. Integration of aqueous (micellar) two-phase systems on the proteins separation. *BMC Chem. Eng.* **1,** 4 (2019).

2. Santos, J. H. P. M., Torres-Obreque, K. M., Pastore, G. M., Amaro, B. P. & Rangel-Yagui, C. O. Protein PEGylation for the design of biobetters: from reaction to purification processes. *Brazilian J. Pharm. Sci.* **54,** (2018).

3. Santos, J. H. P. M., Almeida, M. R., Martins, C. I. R., Dias, A. C. R. V., Freire, M. G., Coutinho, J. A. P. & Ventura, S. P. M. Separation of phenolic compounds by centrifugal partition chromatography. *Green Chem.* **20,** 1906–1916 (2018).

4. Brumano, L. P., da Silva, F. V. S., Costa-Silva, T. A., Apolinario, A. C., Santos, J. H. P. M., Kleingesinds, E. K., Monteiro, G., Rangel-Yagui, C. de O., Benyahia, B. & Junior, A. P. Development of L-Asparaginase Biobetters: Current Research Status and Review of the Desirable Quality Profiles. *Front. Bioeng. Biotechnol.* **6,** 212 (2018).

5. Santos, J. H. P. M., Trigo, J. P., Maricato, É., Nunes, C., Coimbra, M. A. & Ventura, S. P. M. Fractionation of Isochrysis galbana Proteins, Arabinans, and Glucans Using Ionic-Liquid-Based Aqueous Biphasic Systems. *ACS Sustain. Chem. Eng.* **6,** 14042–14053 (2018).

6. Santos, J. H. P. M., Capela, E. V., Boal-Palheiros, I., Coutinho, J. A. P., Freire, M. G. & Ventura, S. P. M. Aqueous biphasic systems in the separation of food colorants. *Biochem. Mol. Biol. Educ.* **46,** 390–397 (2018).

7. Santos, J. H. P. M., Flores-Santos, J. C., Meneguetti, G. P., Rangel-Yagui, C. O., Coutinho, J. A. P., Vitolo, M., Ventura, S. P. M. & Pessoa, A. In situ purification of periplasmatic L-asparaginase by aqueous two phase systems with ionic liquids (ILs) as adjuvants. *J. Chem. Technol. Biotechnol.* **93,** 1871–1880 (2018).

8. Santos, J. H. P. M., Carretero, G., Coutinho, J. A. P., Rangel-Yagui, C. O. & Ventura,

S. P. M. Multistep purification of cytochrome c PEGylated forms using polymer-based aqueous biphasic systems. *Green Chem.* **19,** 5800–5808 (2017).

9. Santos, J. H. P. M., Costa, I. M., Molino, J. V.D., Leite, M. S. M., Pimenta, M. V., Coutinho, J. A. P., Pessoa, A., Ventura, S. P. M., Lopes, A. M. & Monteiro, G. Heterologous expression and purification of active L-asparaginase I of Saccharomyces cerevisiae in Escherichia coli host. *Biotechnol. Prog.* **33,** 416–424 (2017).

10. Santos, J. H. P. M., Martins, M., Silvestre, A. J. D., Coutinho, J. A. P. & Ventura, S. P. M. Fractionation of phenolic compounds from lignin depolymerisation using polymeric aqueous biphasic systems with ionic surfactants as electrolytes. *Green Chem.* **18,** 5569–5579 (2016).

Submitted papers

1. Capela, E. V., Santos, J. H. P. M., Palheiros, I. B., Coutinho, J. A. P., Ventura, S. P. M. & Freire, M. G. Determination of Ternary Phase Diagrams of Aqueous Biphasic Systems Composed of Water, Poly(ethylene glycol) and Sodium Carbonate. *Chemical Engineering Education*, 2019, submitted.

2. Santos, J. H. P. M., Carretero, G., Coutinho, J. A. P., Ventura, S. P. M., Converti, A., Rangel-Yagui, C. O. PEGylation as an efficient tool to enhance protein thermostability: a kinetic and thermodynamic study on cytochrome c. *Int. J. Biol. Macromol.*, 2019, submitted.

3. Santos, J. H. P. M., Ferreira. A. M., Almeida, M. R., Coutinho, J. A. P., Freire, M. G., Rangel-Yagui, C. O., Ventura, S. P. M. Continuous purification of PEG-Protein conjugates by fast centrifugal partition chromatography. *Green Chem.*, 2019, submitted.

Manuscripts under preparation

1. Santos, J. H. P. M., Meneguetti, G. P., Feitosa, V. A., Carreto, G., Coutinho, J. A. P., Ventura, S. P. M. & Rangel-Yagui, C. O. Site-specific PEGylated cytochrome c as biosensor: PEGylation reaction to enhance its long-term stability.

2. Santos, J. H. P. M., Mendonça, C. M. N., Silva, A. R. P., Oliveira, R. P. S., Junior, A. P., Coutinho, J. A. P., Ventura, S. P. M., Rangel-Yagui, C. O., An integrated one-pot process for the reaction and purification of PEGylated proteins.

Awards

1. Best work award presented as a poster: "Ionic Liquids as purification intensifiers for L-asparaginase produced by recombinant *Escherichia coli* through the use of aqueous biphasic systems", 1st Ibero-American Symposium on aqueous two-phase systems (SISAB), Aracaju, Brazil, 2018.

2. Best work award presented as oral presentation: "Purification in successive stages of PEGylated forms of cytochrome c using aqueous biphasic systems", 1st Ibero-American Symposium on aqueous two-phase systems (SISAB), Aracaju, Brazil, 2018.

3. Article selected at 2017 Green Chemistry Hot Articles: Multistep purification of cytochrome c PEGylated forms using polymer-based aqueous biphasic systems, Green Chemistry (Royal Society of Chemistry).

4. Front cover at *Green Chemistry*, v. 24., Multistep purification of cytochrome c PEGylated forms using polymer-based aqueous biphasic systems, Green Chemistry (Royal Society of Chemistry).

5. Best work award presented as a poster:"Purification of phenolic compounds in continuous flow by centrifugal partition chromatography", Biopartitioning and Purification 2017 Conference (BPP2017) Copenhagen, Denmark.

Work in the Press

YouTube (interview):

https://www.youtube.com/watch?v=ELgOL4dPFGM&feature=youtu.be&fbclid=IwAR0Xkm5g_uLndT_88l5hUAaR8SSL_SiG_1xgGnByi8Ox4Q3y3hXtuU2-5f4 (SISAB 2018)

Websites:

- http://agencia.fapesp.br/processo-alternativo-purifica-proteinas-usadas-como-biossensores/28079/ (Agência FAPESP – Brazil)
- http://rbp.fmrp.usp.br/processo-alternativo-purifica-proteinas-usadas-como-biossensores/
- https://www.diariodasaude.com.br/news.php?article=processo-limpo-purifica-proteinas-farmacos-biossensores&id=12873
- https://www.indice.eu/pt/noticias/saude/2018/07/05/criado-metodo-que-purifica-proteinas-para-farmacos-e-biossensores

APPENDIX A

SUPPORTING INFORMATION OF CHAPTER 2

Table A.1. *E. coli* strains used in this work.

E. coli strain	*Genotype*	*Selection marker*	*Manufacturer*
DH5α[1]	[deoR endA1 gyrA96 hsdR17 Δ(lac)U169 recA1 relA1 supE44 thi-1 (Φ 80 lacZΔM15)]	-	Novagen™
AD494[2]	[Δ(araABC-leu)7697 ΔlacX74 ΔmalF3 ΔphoAPvuII phoR trxB ::Kanr F'[lacIqlacZΔM15proAB+]	Kan	Novagen™
BL21(DE3)[3]	[F– ompT hsdSB(rB–, mB–) gal dcm (DE3)]	-	Life Technologies™
BL21 CodonPlus(DE3)[4]	[RIPL: endA gal ompT hsdSB Dcm+ Hte Tetr (pACYC-RIL argU ileY leuW Cam]r (DE3)	Cam and Strep	Agilent Technologies
Tuner™ (DE3)	gal hsdSB lacY1 ompT (DE3)		Novagen™
BL21pLyss(DE3)[5]	F–, ompT, hsdSB (rB–, mB–), dcm, gal, λ(DE3), pLysS, Cmr	Cam	Promega™
C43 (DE3)[6]	[F – ompT hsdSB (rB- mB-) gal dcm (DE3)]	-	Lucigen ™
Rosetta™(DE3)[7]	F– ompT hsdSB(rB – mB –) gal dcm (DE3) pRARE2 (CamR)	Cam	Novagen™
Origami(DE3)[8]	1Δ(ara–leu)7697 ΔlacX74 ΔphoA PvuII phoR araD139 ahpC galE galK rpsL F'[lac+ lacI q pro] (DE3) gor522::Tn10 trxB	Cam, Strep and Tetra	Novagen™

- = no selective marker, Kan = kanamycin, Cam = chloramphenicol, Tetra = tetracycline, Strep = streptomycin. Main reason to use this strain: [1] Cloning vectors; [2] (*trxB*) mutants that enable disulfide bond formation in the *E.coli* cytoplasm expressed proteins; [3] Expression of cytoplasmic proteins and deficient in both *lon* and *ompT* proteases; [4] extra copies of genes that encode the tRNAs that most frequently limit translation of heterologous proteins in *E. coli;* [5] high-stringency expression host due to expression of T7 lysozyme; [6] Effective in expressing toxic and membrane proteins; [7] Expresses six rare tRNAs that most frequently limit translation of heterologous proteins in *E. coli;* [8] *trxB/gor* mutant, greatly facilitates cytoplasmic disulfide bond formation.

Table A.2. Screening of expression conditions. I = Insoluble, S = Soluble, 0 = Do not express, .= Not tested.

Bacteria strain	pET15B									pET22B			pET28a+SUMO			T°C
	ASP3_1-362			ASP3_32-362			ASP3opt_26-362			ASP3_26-362			ASP3_26-362			
AD494	I	I	I	I	I	I	I	I	I	.	.	.	.	.	.	20°C
	I	I	I	I	I	I	.	.	.	.	.	.	.	.	.	37°C
BL21	I	I	I	I	I	I	I	I	I	.	.	.	I	I	I	20°C
	I	I	I	I	I	I	.	.	.	I	I	I	.	.	.	37°C
C43	I	I	I	I	I	I	0	0	0	.	.	.	.	.	.	20°C
	I	I	I	I	I	I	.	.	.	0	0	0	.	.	.	37°C
BL21 codon+	.	.	.	.	.	.	.	.	.	.	.	.	.	.	.	20°C
	I	I	I	I	I	I	.	.	.	.	.	.	.	.	.	37°C
BL21 tuner	I	I	I	I	I	I	I	I	I	.	.	.	.	.	.	20°C
	I	I	I	I	I	I	.	.	.	I	I	I	.	.	.	37°C
BL21pLyss	.	.	.	.	.	.	.	.	.	.	.	.	0	0	0	20°C
	.	.	.	.	.	.	.	.	.	0	0	0	.	.	.	37°C
Rosetta	.	.	.	.	.	.	.	.	.	.	.	.	0	0	0	20°C
	.	.	.	.	.	.	.	.	.	.	.	.	.	.	.	37°C
Origami	.	.	.	.	.	.	I	I	I	.	.	.	.	.	.	20°C
	.	.	.	.	.	.	.	.	.	0	0	0	.	.	.	37°C
IPTG (mM)	0.1	0.5	1.0	0.1	0.5	1.0	0. 01	0.1	1.0	0.1	0.5	1.0	0.01	0.1	1.0	

Table A.3. Merchuk parameters (*A*, *B* and *C*) used on the description of the experimental binodal data by Merchuk Equation.

Effect of the salt nature	**Pluronic L-35 (1.0% Triton X-100)**	$A \pm \sigma$	$B \pm \sigma$	$10^5(C \pm \sigma)$
	K_2HPO_4	82.56 ± 5.73	-0.45 ± 0.05	101.51 ± 22.32
	KH_2PO_4	154.70 ± 14.24	-0.64 ± 0.04	21.42 ± 5.29
	K_3PO_4	102.49 ± 7.83	-0.59 ± 0.05	92.40 ± 21.19
	K_2HPO_4/KH_2PO_4	108.03 ± 10.03	-0.62 ± 0.05	73.41 ± 16.07
Effect of the surfactant	**Pluronic L-35 + K_2HPO_4/KH_2PO_4**	$A \pm \sigma$	$B \pm \sigma$	$10^5(C \pm \sigma)$
	Triton X-114	96.16 ± 1.97	-0.59 ± 0.01	40.19 ± 3.66
	Triton X-100	108.03 ± 10.03	-0.62 ± 0.05	73.41 ± 16.07
Effect of the copolymer	**K_2HPO_4/KH_2PO_4**	$A \pm \sigma$	$B \pm \sigma$	$10^5(C \pm \sigma)$
	Pluronic L-35	109.62 ± 5.44	-0.67 ± 0.03	28.11 ± 9.74
	Pluronic 10R5	97.99 ± 7.87	-0.64 ± 0.05	51.81 ± 2.14
	Pluronic 17R4	137.31 ± 18.28	-0.95 ± 0.11	169.71 ± 1.42

Table A.4. Weight fraction data (*w*) for the systems composed of Pluronic L-35 (1) + Phosphate salts - K_2HPO_4; KH_2PO_4; K_3PO_4 and K_2HPO_4/KH_2PO_4 (2) + H_2O (3) determined in the present work at 25ºC.

Pluronic L-35 + K_2HPO_4		**Pluronic L-35 + KH_2PO_4**		**Pluronic L-35 + K_3PO_4**		**Pluronic L-35 + K_2HPO_4/KH_2PO_4**	
100 w_1	**100 w_2**	**100 w_1**	**100 w_2**	**100 w_1**	**100 w_2**	**100 w_1**	**100 w_2**
56.972	0.911	44.926	3.857	56.803	0.878	12.232	8.791
51.969	0.831	44.048	3.782	33.111	2.520	12.170	8.747
50.726	1.286	43.064	4.031	33.111	2.520	12.532	8.701
48.245	1.223	42.257	3.955	29.936	2.954	12.755	8.665
46.616	1.853	41.012	4.279	27.866	2.749	12.413	8.618
44.727	1.778	40.453	4.221	25.855	3.830	13.142	8.493
42.544	2.661	39.409	4.498	25.728	3.425	13.023	8.417
39.373	2.463	39.037	4.455	25.193	3.954	13.486	8.374
38.602	2.804	37.002	5.002	25.011	3.925	13.359	8.295
38.049	2.764	36.753	4.968	24.427	4.098	14.353	8.068
37.606	2.963	35.927	5.192	23.643	4.189	14.191	7.977
36.622	2.886	35.426	5.120	23.449	4.298	14.816	7.896
35.867	3.236	33.872	5.551	23.428	3.839	15.032	7.825
35.344	3.188	33.689	5.521	23.335	4.277	14.653	7.809
34.986	3.358	32.886	5.746	22.824	4.128	15.377	7.752
34.079	3.270	32.562	5.689	22.299	4.518	15.215	7.671
33.562	3.522	30.410	6.301	22.163	4.490	15.715	7.597
32.893	3.452	30.235	6.265	21.596	4.300	16.018	7.465
0.036	19.956	29.126	6.583	21.112	4.781	16.333	7.329
0.021	11.847	28.959	6.545	20.479	4.590	16.238	7.287
7.277	10.407	27.411	6.994	20.315	4.553	16.826	7.147
6.767	9.678	27.298	6.966	20.085	4.671	16.651	7.073
14.387	8.285	25.342	7.537	19.639	5.088	17.383	7.003
13.823	7.960	25.229	7.504	19.553	4.722	17.041	6.977
17.931	7.248	16.379	10.114	19.313	5.004	17.291	6.967
17.592	7.111	16.279	10.052	19.248	4.779	17.684	6.962
19.685	6.757	11.492	12.197	18.983	4.921	18.057	6.812
19.362	6.646	11.395	12.094	18.972	5.173	17.938	6.767
22.828	6.075	12.619	11.791	18.731	4.855	18.474	6.661
22.135	5.891	12.417	11.602	17.681	5.144	18.766	6.585
25.527	5.359	13.895	11.243	17.390	5.307	18.636	6.540
25.001	5.248	13.634	11.032	17.261	5.268	19.197	6.477
27.611	4.854	16.275	10.408	17.100	5.359	19.002	6.411
26.979	4.742	15.884	10.158	16.648	5.495	19.600	6.183
30.595	4.218	18.625	9.531	16.505	5.807	20.109	6.123
29.640	4.086	18.332	9.380	16.341	5.551	19.957	6.077
		20.460	8.904	16.001	5.630	20.461	6.014
		19.914	8.667	15.545	5.641	20.834	5.916
		22.299	8.155	15.266	5.974	20.666	5.869
		22.138	8.096	15.125	5.737	21.535	5.761
		23.696	7.765	14.972	6.246	22.287	5.564
		23.369	7.658	14.861	5.900	21.947	5.479
		25.283	7.261	14.756	5.858	23.148	5.363
		24.978	7.173	14.328	5.959	22.733	5.266
		27.839	6.592	14.114	6.095	24.627	5.023
		27.288	6.461	13.966	6.031	23.896	4.874
		34.449	5.059	13.680	6.426	27.827	4.298
		33.544	4.926	13.266	6.300	26.964	4.165
				12.755	6.432	30.458	3.807
				12.754	6.934	28.988	3.623
				12.446	6.767	32.624	3.215
				11.974	6.633	31.705	3.124
				11.833	6.555	33.141	2.941

Table A.5. Weight fraction data (*w*) for the systems composed of Pluronic L-35 (1) + Phosphate Buffer - K_2HPO_4/KH_2PO_4 (pH=6.6) (2) + H_2O (3) with 1 wt% of adjuvant, determined in the present work at 25ºC.

Pluronic L-35 + K_2HPO_4/KH_2PO_4 + Triton X-100		**Pluronic L-35 + K_2HPO_4/KH_2PO_4 + Triton X-114**	
100 w_1	**100 w_2**	**100 w_1**	**100 w_2**
56.901	1.206	57.611	0.809
48.911	1.036	55.462	0.779
45.641	2.336	52.969	1.655
39.386	2.016	46.695	1.459
37.048	3.112	42.470	2.114
34.055	2.861	40.365	2.009
32.273	3.783	39.375	2.457
30.509	3.577	37.977	2.370
29.778	3.982	36.559	2.614
28.976	3.875	35.052	2.765
27.042	4.266	34.672	2.955
26.399	4.652	33.372	2.999
26.070	4.594	32.640	3.148
25.603	4.878	32.146	3.407
24.967	4.757	31.499	3.338
24.063	5.327	29.746	3.897
23.433	5.187	28.718	4.122
23.085	5.414	28.261	4.056
22.459	5.267	26.966	4.454
21.695	5.784	26.252	4.602
21.107	5.628	25.982	4.555
20.476	6.072	25.605	4.782
20.117	5.966	24.411	4.927
19.618	6.326	23.778	5.094
19.215	6.196	23.452	5.302
18.822	6.489	23.157	5.235
18.506	6.380	21.956	5.735
18.022	6.749	21.389	5.906
17.701	6.629	21.233	5.863
		20.581	6.161
		20.016	6.360
		19.503	6.498
		19.288	6.426
		18.581	6.656
		18.227	6.798
		18.056	6.925
		17.930	6.876
		17.289	7.118
		17.126	7.242
		16.736	7.374
		16.169	7.475
		15.952	7.646
		15.857	7.601
		15.522	7.666
		14.876	7.998
		14.140	8.242

Table A.6. Weight fraction data (*w*) for the systems composed of copolymers (1) - Pluronic 17R4 or 10R5 + Phosphate Buffer- K_2HPO_4/KH_2PO_4 (pH=6.6) (2) + H_2O (3) determined in the present work at 25ºC.

Pluronic 17R4 + K_2HPO_4/KH_2PO_4		**Pluronic 10R5+ K_2HPO_4/KH_2PO_4**	
100 w_1	**100 w_2**	**100 w_1**	**100 w_2**
57.328	0.922	65.656	1.326
50.975	0.820	46.570	1.940
49.678	1.320	37.390	2.018
44.177	1.174	36.480	2.467
43.518	1.462	33.338	2.820
41.235	1.385	32.376	2.739
40.363	1.789	31.698	3.111
37.097	1.645	30.477	2.991
36.165	2.118	29.565	3.515
33.560	1.966	28.379	3.374
32.647	2.470	27.662	3.806
30.216	2.286	26.889	3.699
29.724	2.582	26.484	3.952
28.697	2.493	25.855	3.858
28.465	2.638	25.065	4.065
27.533	2.552	24.683	4.315
27.230	2.749	24.263	4.242
26.596	2.685	23.862	4.510
26.382	2.828	23.416	4.426
25.947	2.782	22.873	4.565
25.753	2.914	22.559	4.784
25.293	2.862	22.256	4.719
25.011	3.059	21.964	4.926
24.416	2.986	21.759	4.880
24.110	3.206	21.484	5.077
23.527	3.128	21.277	5.028
23.290	3.303	20.986	5.239
22.480	3.188	20.748	5.180
21.922	3.618	20.523	5.346
21.621	3.568	20.230	5.270
21.437	3.712	19.978	5.459
21.060	3.646	19.663	5.373
20.882	3.788	19.272	5.674
20.555	3.729	19.107	5.625
20.426	3.834	18.981	5.723
20.109	3.775	18.823	5.676

Table A.7. Experimental data of *TL*s and *TLL*s of the studied ATPS.

	Weight fraction composition ($wt\%$)						*TLL*
	$[\mathbf{Copol}]_{\mathbf{Top}}$	$[\mathbf{Salt}]_{\mathbf{Top}}$	$[\mathbf{Copol}]_{\mathbf{M}}$	$[\mathbf{Salt}]_{\mathbf{M}}$	$[\mathbf{Copol}]_{\mathbf{Bot}}$	$[\mathbf{Salt}]_{\mathbf{Bot}}$	
Pluronic L-35 + Potassium phosphate buffer	30.28	3.66	22.96	6.00	9.43	10.35	21.90
	34.83	2.93	26.04	6.02	4.79	13.47	31.84
	39.35	2.35	29.28	5.85	3.32	14.89	38.15
	43.33	1.94	32.02	6.00	1.87	16.84	44.06
	48.79	1.48	35.60	5.95	1.49	17.52	49.94
	50.37	1.36	37.98	6.00	0.59	20.00	53.15
Pluronic 10R5 + Potassium phosphate buffer	33.91	2.82	23.01	6.00	2.01	12.13	33.24
	39.97	2.32	25.98	5.99	1.87	12.32	39.40
	41.98	2.18	28.98	6.02	0.77	14.36	42.97
	42.94	2.12	31.99	6.00	0.16	17.27	45.38
	43.67	2.07	35.04	6.01	0.01	22.00	48.00
	51.20	1.66	37.91	6.00	0.08	18.37	53.79
Pluronic 17R4 + Potassium phosphate buffer	34.78	2.03	16.04	6.00	2.42	8.89	33.08
	38.18	1.77	19.02	5.99	1.32	9.89	37.75
	42.05	1.52	22.03	6.00	0.72	10.76	42.35
	46.02	1.30	25.01	6.01	0.40	11.52	46.75
	50.23	1.10	28.03	6.00	0.24	12.12	51.19
	58.46	0.79	30.96	6.00	0.32	11.80	59.17

Table A.8. Properties of the model proteins (Cyt c, Azo and Ova).

Model protein / **Properties**	**Cyt c**	**Azo**	**Ova**
Molecular weight (kDa)	~11.70	23.60	42.70
pI	9.60	4.60	4.50
ΔTemp	> 51ºC	> 42ºC	> 56ºC
λmax (nm)	409	342	280

Table A.9. Mixture points for each system constituted by copolymer + salt + water, to the determination of the *TL*s.

Copolymer	Salt	Mixture Points	
		$100\ w_{Copol}$	$100\ w_{Salt}$
Pluronic L-35	Phosphate buffer (pH = 6.6)	23 26 29 32 35 38	6
Pluronic 10R5	Phosphate buffer (pH = 6.6)	23 26 29 32 35 38	6
Pluronic 17R4	Phosphate buffer (pH = 6.6)	16 19 22 25 28 31	6

Table A.10. Inputs for 5 g of aqueous system considered.

Process	Step	Input	Value
Fractionation process	ATPS	Pluronic L-35 (g)	1.15
		Potassium phosphate buffer (g)	0.365
		Distilled water (g)	3.47
		Electricity (kWh)	0.233
	AMTPS	Electricity (kWh)	0.00425
	Ultrafiltration	NaOH (g)	3.98E-04
		Distilled water (g)	9.96E-02
		Electricity (kWh)	0.703
Isolation process	Acid precipitation	TCA (g)	1.61E-05
		Distilled water (g)	9.90E-04
		Electricity (kWh)	0.467

Table A.11. GHG emission factors and activity name taken from Ecoinvent version 3.4 used in the calculation of the carbon footprint.

Input	Reference unit	Activity name	GHG emissions (kg $CO_{2eq.}$/reference unit)[a]
Distilled water	kg	---	0.311
Electricity	kWh	Market for electricity, low voltage, Portugal	0.413
Pluronic L-35	kg	Ethylene glycol production, Europe[b]	1.841
		Propylene glycol production, Europe[b]	4.526
Potassium phosphate buffer	kg	Chemical production, inorganic, Global[c]	2.109
Trichloroacetic acid	kg	Trichloroacetic acid production, Europe	2.866
Sodium hydroxide	kg	sodium hydroxide to generic market for neutralizing agent, Global[d]	1.955

[a] Global warming potentials for converting the mass of each GHG into mass of CO_2 eq. are those recommended by the Intergovernmental Panel on Climate Change (IPCC)[3] for a time horizon of 100 years.

[b] In the absence of data for the production of Pluronic L-35, an average value of the two processes was calculated.

[c] In the absence of data for the production of Potassium phosphate buffer, this process was selected as more similar

Table A.12. Characteristics and chemical structure of the copolymers and non-ionic surfactants used in this work.

Copolymer/ Surfactant	Molecular weight ($g.mol^{-1}$)	Hydrophilic-lipophilic balance (HLB)	wt% PEG	Structure
Pluronic L-35	1900	18 - 23	50	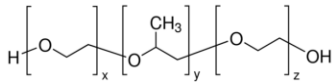
Pluronic 10R5	2000	12 - 18	50	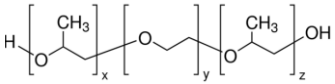
Pluronic 17R4	2700	7 - 12	40	
Triton X-100	647	13.5	---	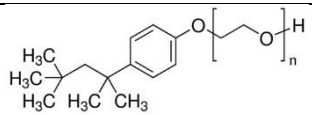 n = 7-8, Triton X-114 n = 9-10, Triton X-110
Triton X-114	537	12.4	---	

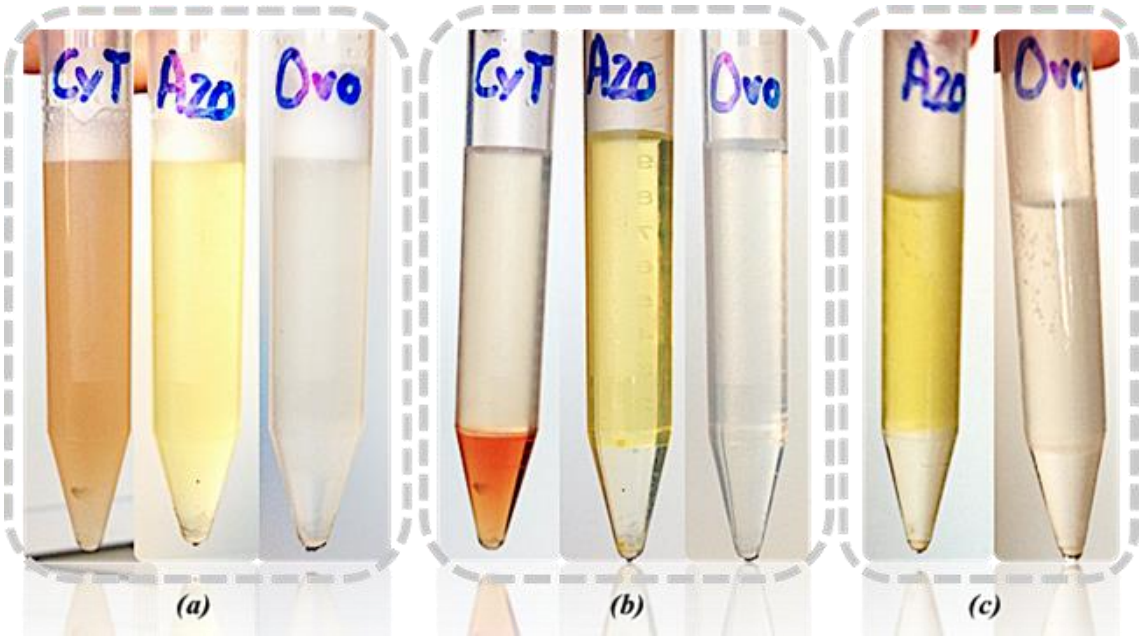

Fig. A.1. Macroscopic view of the pseudo-ternary system composed of Pluronic L-35. ***(a)*** Initial mixture for all extraction ATPS; ***(b)*** ATPS formation for the purification of the three model proteins, at 25ºC; ***(c)*** AMTPS formation for azocasein and ovalbumin purification, at a temperature above the cloud point (ºC) of the copolymer used.

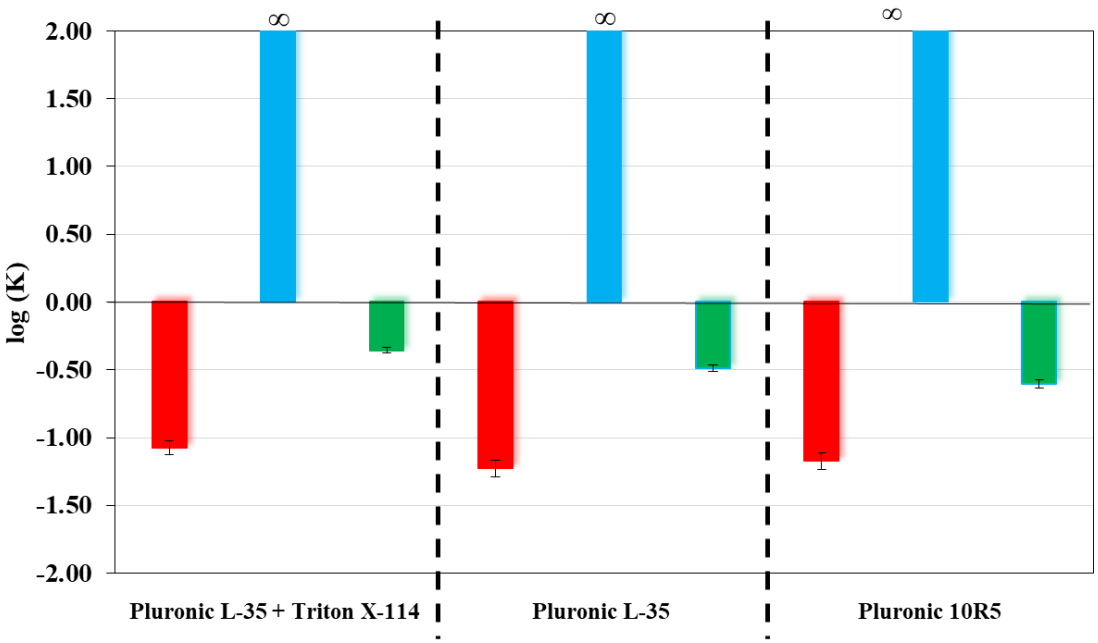

Fig. A.2. Partition coefficient - log(*K*) obtained for each studied system for: cytochrome c (■); azocasein (■); and ovalbumin (■), on the first purification step (ATPS).

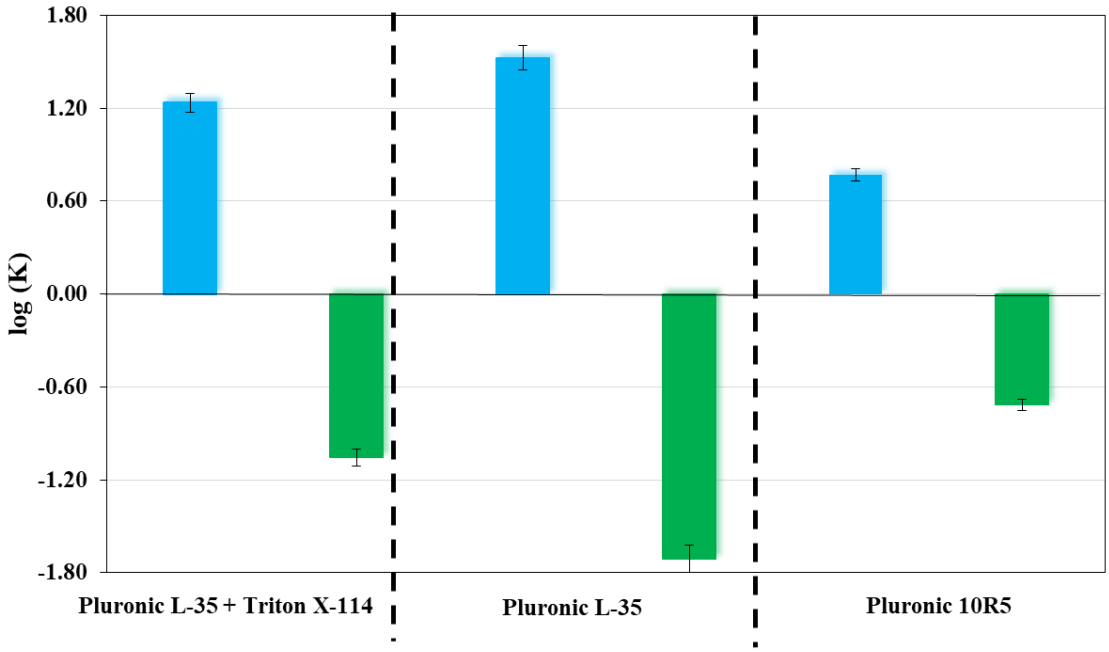

Figure A.3. Partition coefficient - log(*K*) obtained for each studied system for the azocasein (■); and ovalbumin (■), on the second purification step (AMTPS).

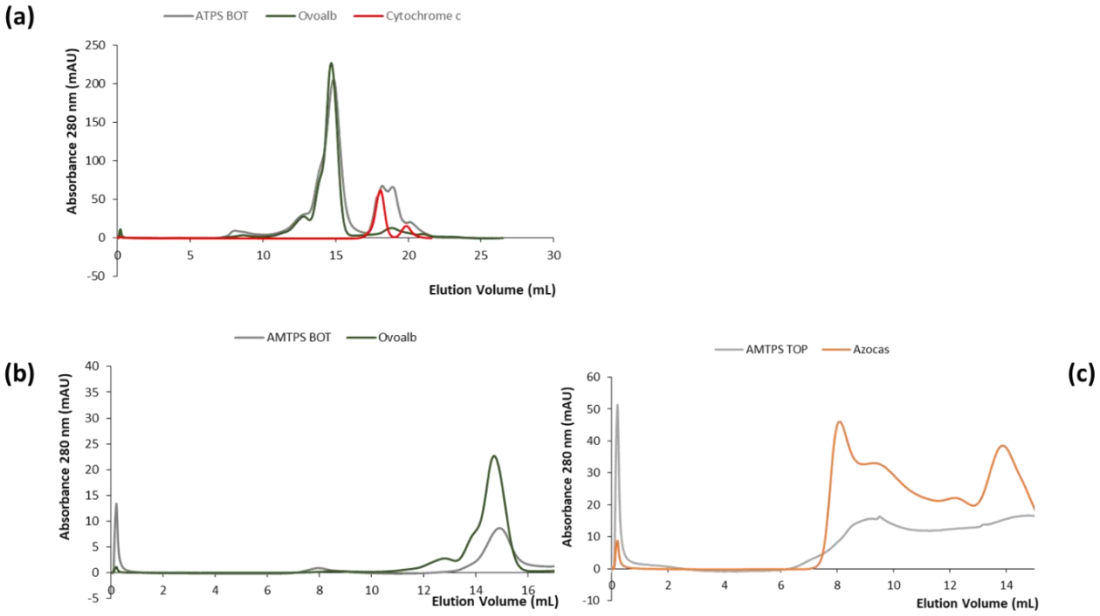

Figure A.4. FPLC-SEC chromatograms of the purified fractions of **(a)** ATPS bottom phase, **(b)** AMTPS bottom and **(c)** AMTPS top phase respectively.

Confirmation of Azocasein precipitation and refolding

1. Adjust the pH to 3-4 with TCA. This will precipitate the protein.
2. Pellet the precipitate in a microfuge at maximum speed (9500 rpm).
3. Discard the supernatant that contains excess dye.
4. Dissolve the pelleted protein in 0.1 M NaOH (10 mg/ml).

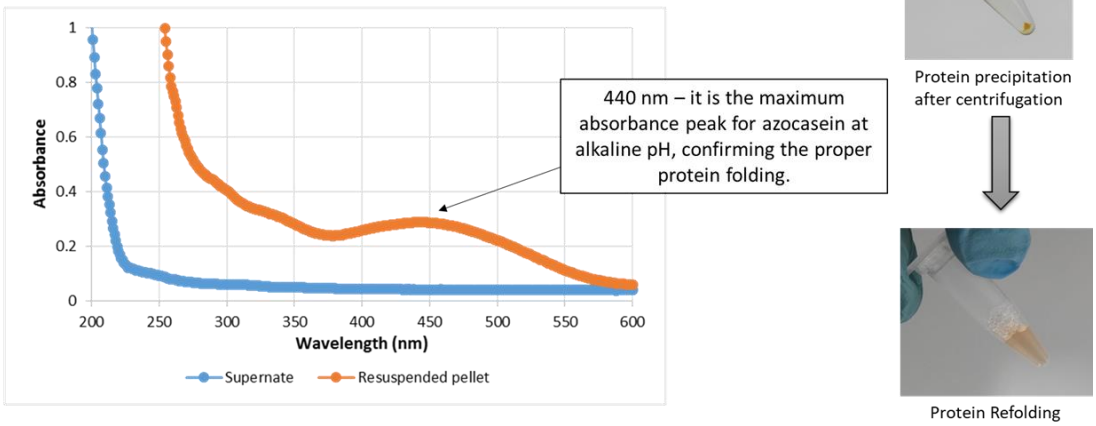

Fig. A.5. Polishing of azocasein through acid precipitation, confirming the protein proper refolding.

^{1}H NMR – Confirmation of Pluronic recovery (after Azo precipitation)

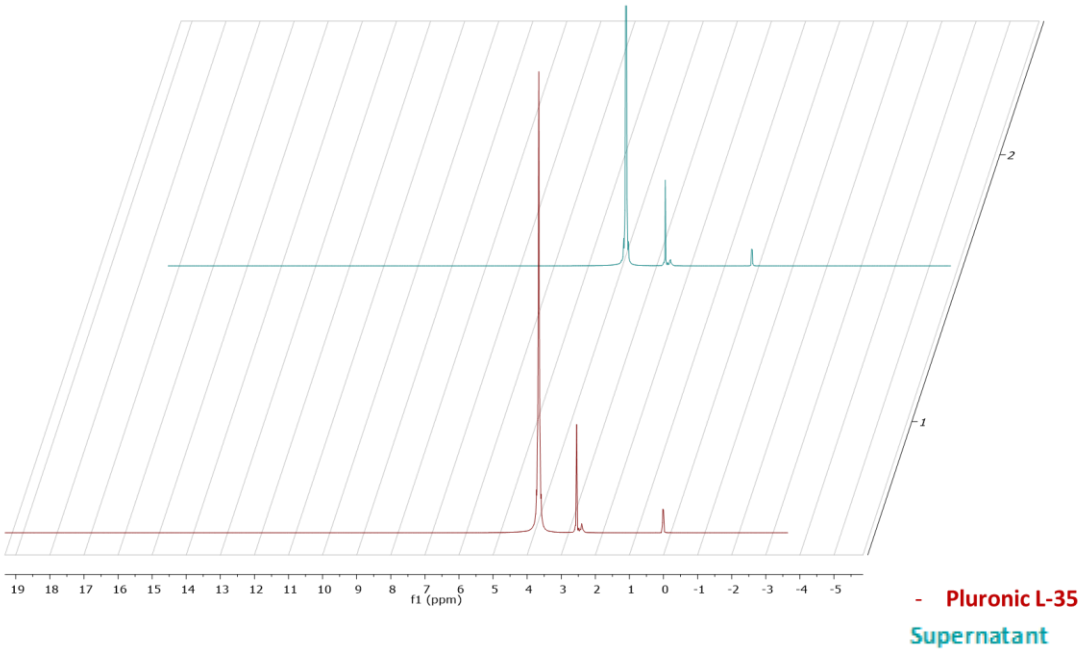

Fig. A.6. ^{1}H NMR of the supernatant proving the recovery of Pluronic through azocasein precipitation polishing step.

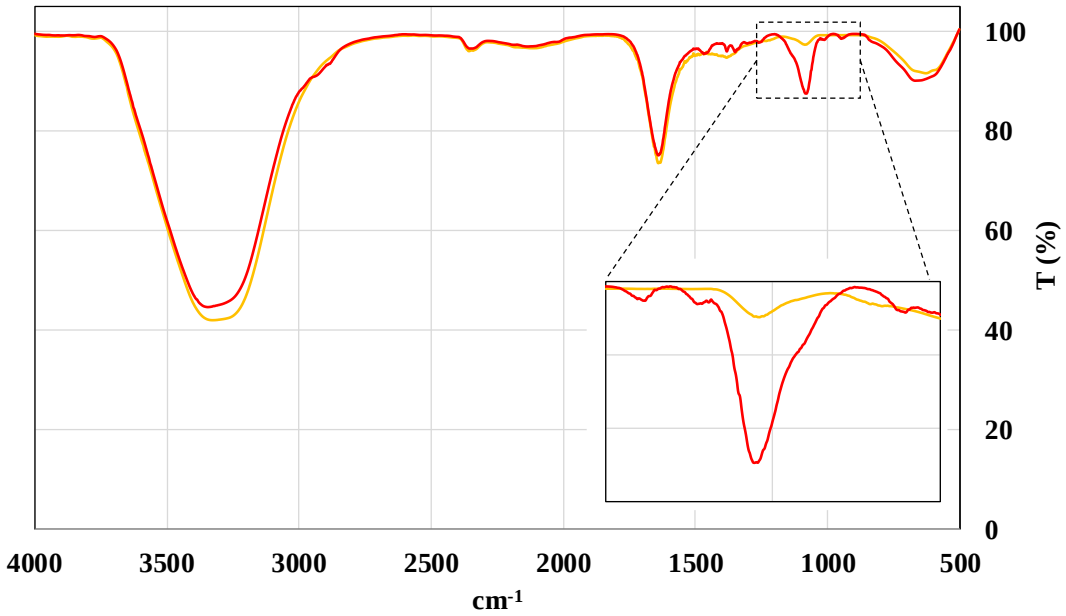

Fig. A.7. FTIR spectra of the supernatant (red) and the resuspended proteinic pellet (orange), proving the recovery of Pluronic through azocasein precipitation polishing step. Focus on the peak at 1085 cm^{-1}, characteristic of strong C-O stretching of primary alcohols.

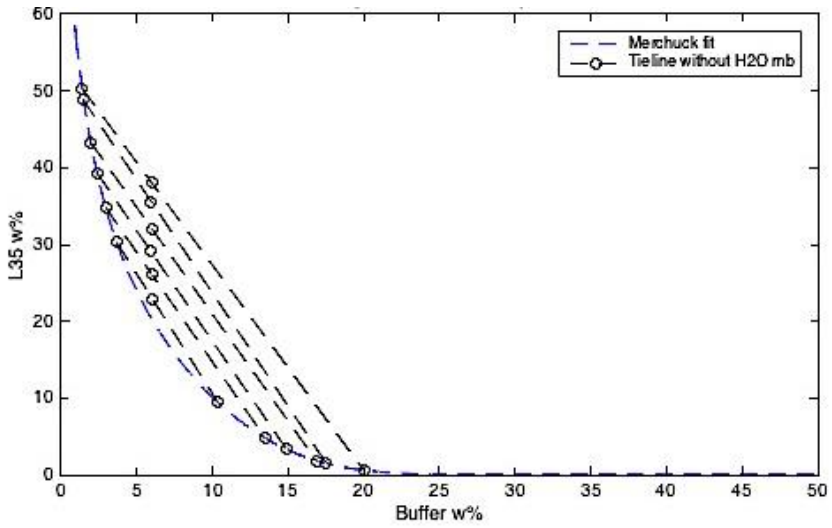

Fig. A.8. Example of the *TL*s calculated for the conventional ATPS (Pluronic L-35 + Phosphate buffer).

APPENDIX B

SUPPORTING INFORMATION OF CHAPTER 3

Table B.1. ASNase amine residues classification regarding the PEGylation probability as a function of pKa values.

PEGylation	Favorable (residue nº)[a]	Possible (residue nº)[b]	Difficult (residue nº)[c]
N-terminal Leucine (pKa ≈ 7.6)	1	-	-
Lysine pKa ≥ 10.5	29, 34, 43, 49, 79, 107, 139, 196, 207, 251, 288, 314	22, 262	71, 72, 104, 162, 172, 186, 213, 229, 301
TOTAL	12	2	9

[a]Partially protonated and located on the protein surface.
[b]Partially protonated and located on subunits interface.
[c]Fully protonated and/or in the protein inner region.

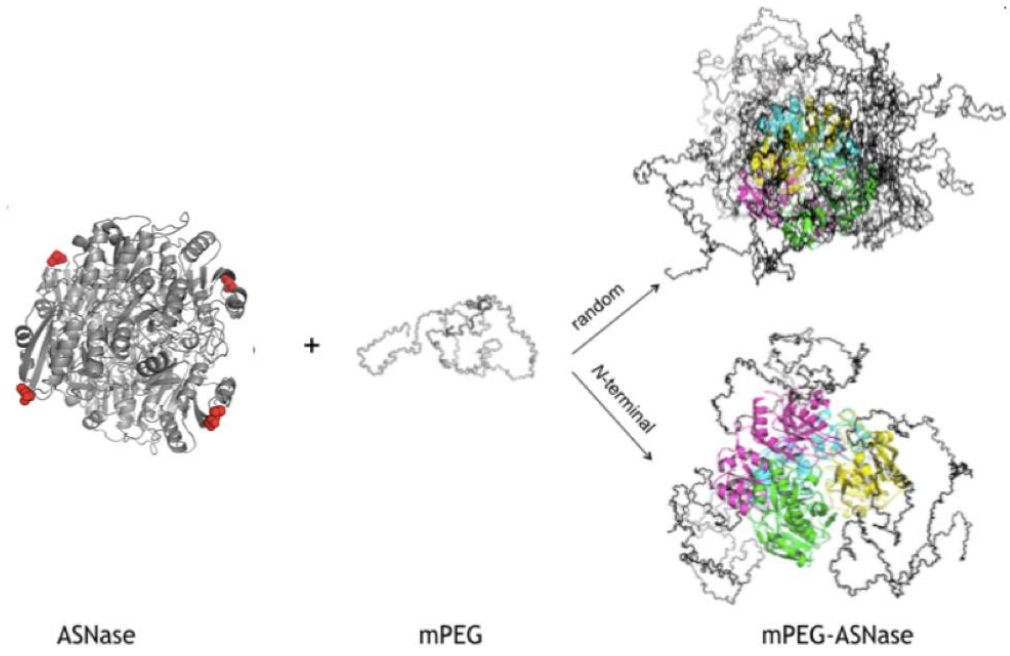

Fig. B.1. Schematic representation of L-asparaginase (PDB code 3ECA) PEGylation with mPEG-NHS (5kDa). Spheres represent N-terminal regions and PEGylation can occur randomly or site specifically depending on the amino acids protonation.

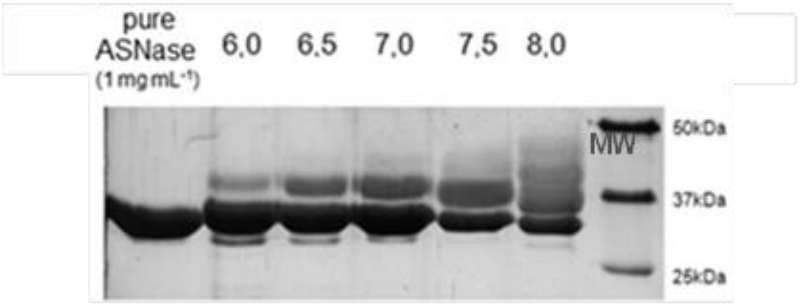

Fig. B.2. Electrophoresis (SDS-PAGE) in polyacrylamide gel stained with silver of L-asparaginase (ASNase) conjugation with PEG 2 kDa at 100 mM of PBS at different pH values. Column 1- pure ASNase (1 mg·mL^{-1}), column 2- pH 6.0, column 3- pH 6.5, column 4- pH 7.0, column 5- pH 7.5, column 6- pH 8.0 and column 7- Molecular weight standard (MW).

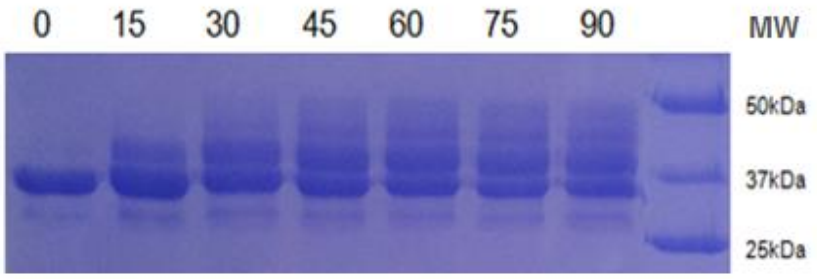

Fig. B.3. Electrophoresis (SDS-PAGE) in polyacrylamide gel stained with CBB of L-asparaginase conjugation with PEG 2 kDa in PBS 100 mM pH 7.5 at different reaction times. Column 1- 0 min, column 2- 15 min, column 3- 30 min, column 4- 45 min, column 5- 60 min, column 6- 75 min, column 7- 90 min and column 8- Molecular weight standard (MW).

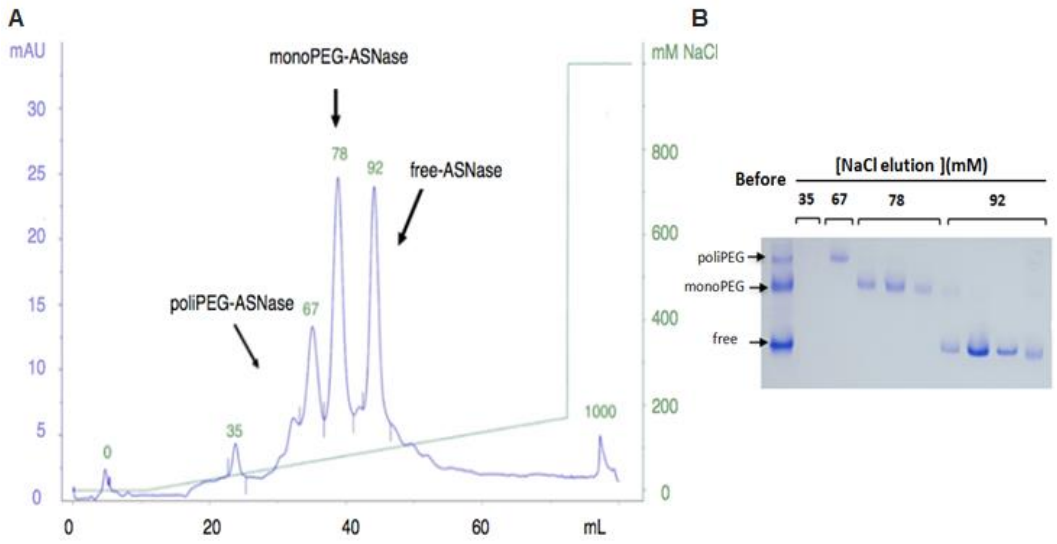

Fig. B.4. Purification of PEGylated L-asparaginase (ASNase) by anion exchange chromatography. **(A)** Chromatogram of the purification performed with a strong salt anion exchange column (Resource Q) with linear salt gradient, 12 column volumes, up to 170 mM of NaCl in Bis-Tris-HCl buffer, pH 7.0 1 M of NaCl. Gradient peaks are found in 35 mM, 67 mM, 78 mM and 92 mM NaCl. **(B)** Electrophoresis gel (Native-PAGE) stained with CBB. Column 1- PEGylation reaction before purification, column 2-elution fraction at 35 mM of NaCl, column 3- elution fraction at 67 mM of NaCl, columns 4 to 6- elution fractions at 78 mM of NaCl and columns 7 to 10: elution fractions at 92 mM of NaCl.

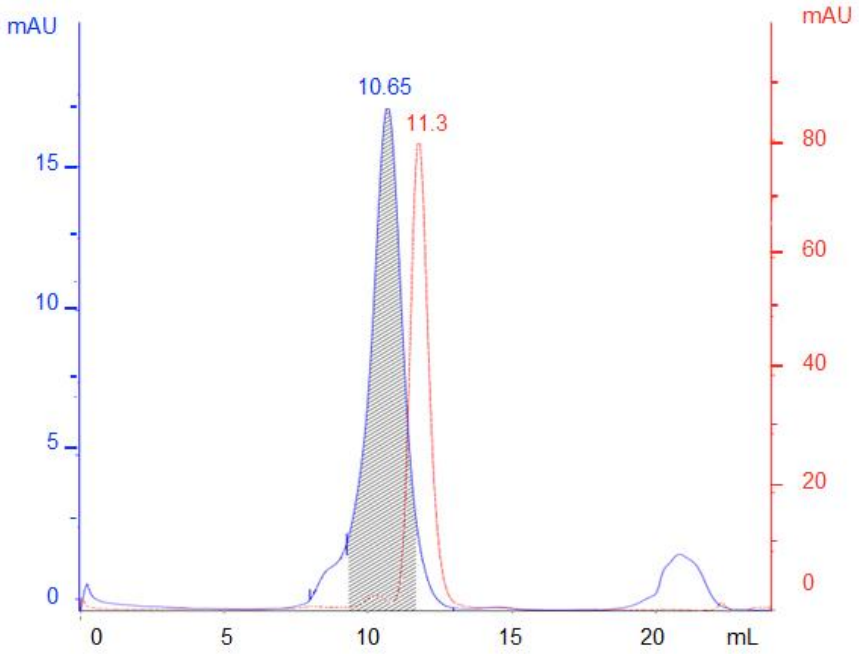

Fig. B.5. Purification by size exclusion chromatography (Superdex 200 10/300 GL column) of monoPEGylated L-asparaginase (from anion exchange chromatography). In hatched (70% area), monoPEG-ASNase eluted in 10.65 mL and in 11.39 mL, pure ASNase (control). Elution occurred isocratically, 1 mL·min^{-1}, with 50 mM of Tris-HCl buffer, at pH 8.6.

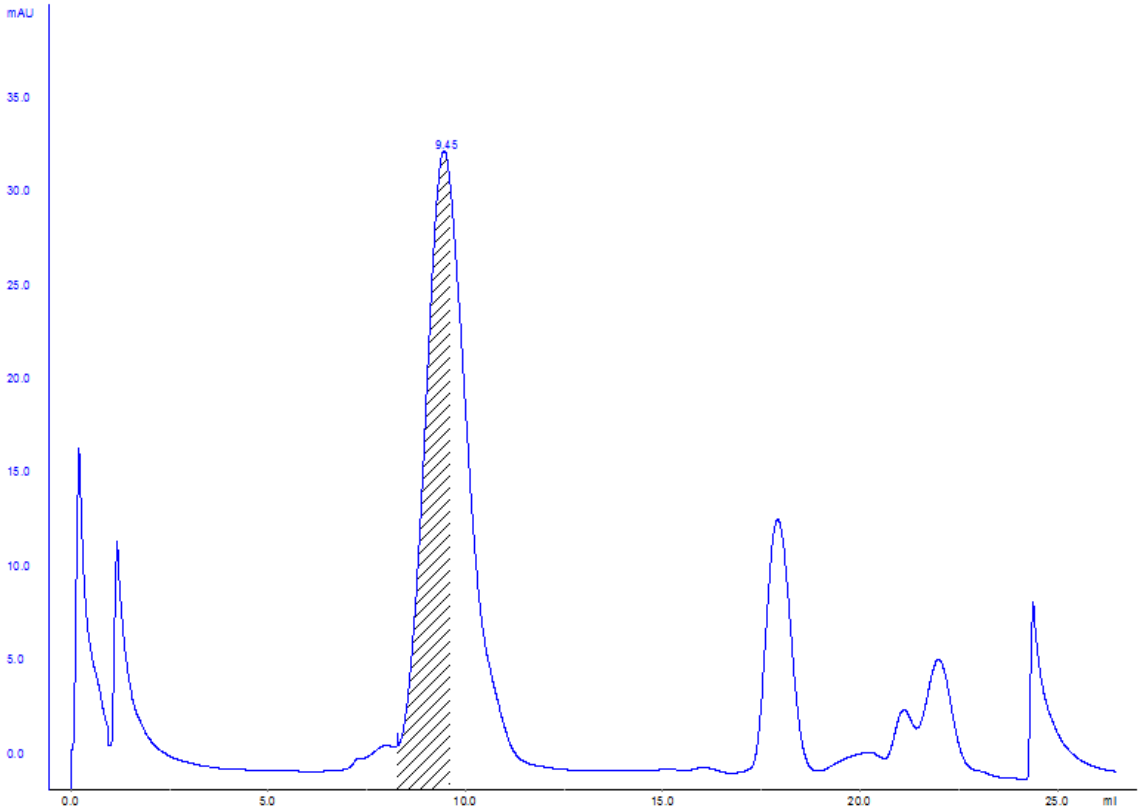

Fig. B.6. Purification by size exclusion chromatography (Superdex 200 10/300 GL column) of polyPEGylated L-asparaginase (ASNase). In hatched (58% peak area), polyPEG-ASNase eluted a range of 8.28 to 9.61 mL. Elution occurred isocratically, 1 mL·min^{-1}, with 50 mM of Tris-HCl buffer, at pH 8.6.

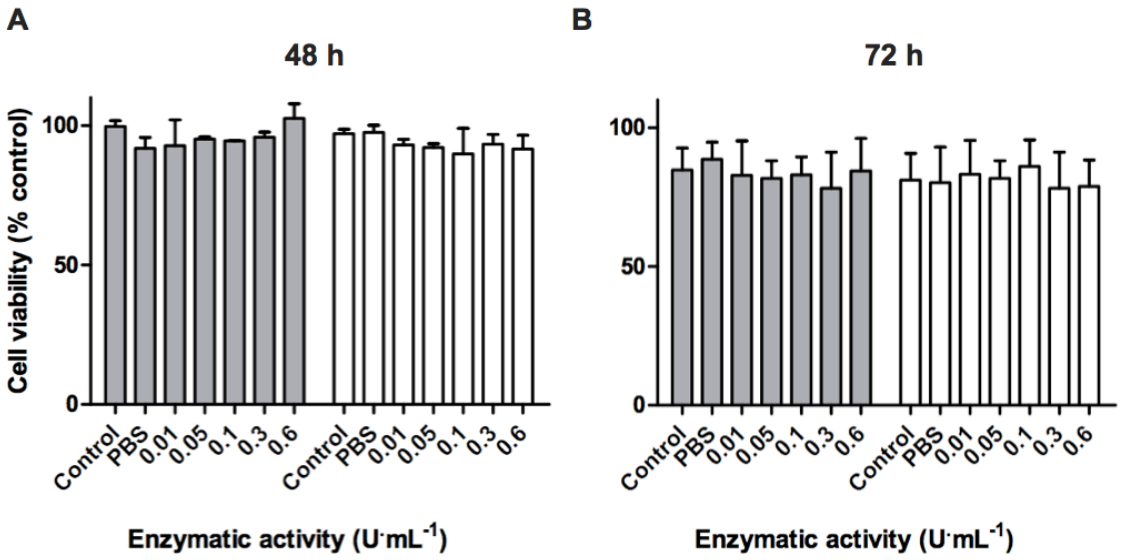

Fig. B.7. Cytotoxicity of monoPEG-ASNase in HUVEC cells. Assays performed at 48 and 72 h, with cells alone (control), without enzyme (PBS) and enzyme concentrations measured in activity (0.01, 0.05, 0.1, 0.3 and 0.6 U·mL^{-1}). Gray bars - free ASNase, white bars - monopegylated ASNase. Error bars represent the standard deviation.

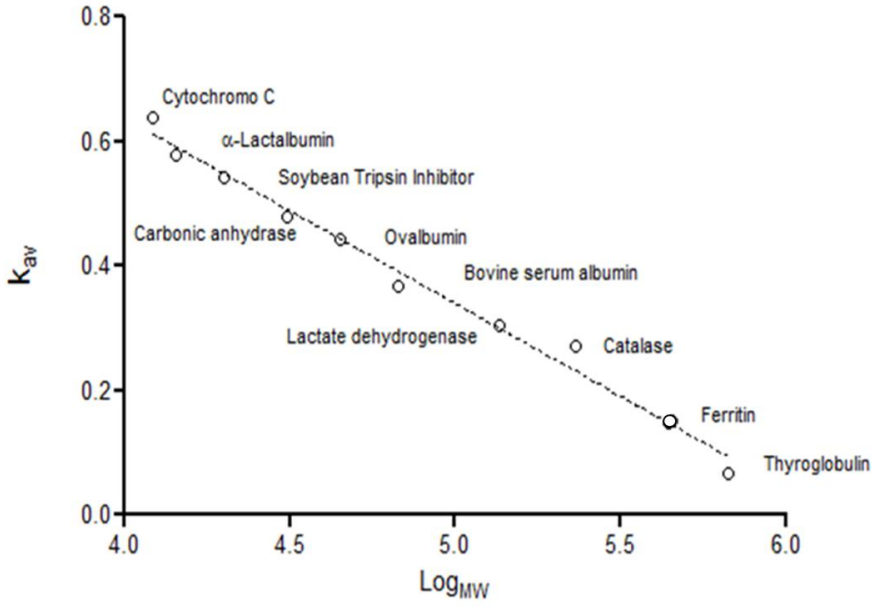

Fig. B.8. Calibration curve obtained by plotting the K_{av} value of each marker and the logarithms of their molecular weights (MW).

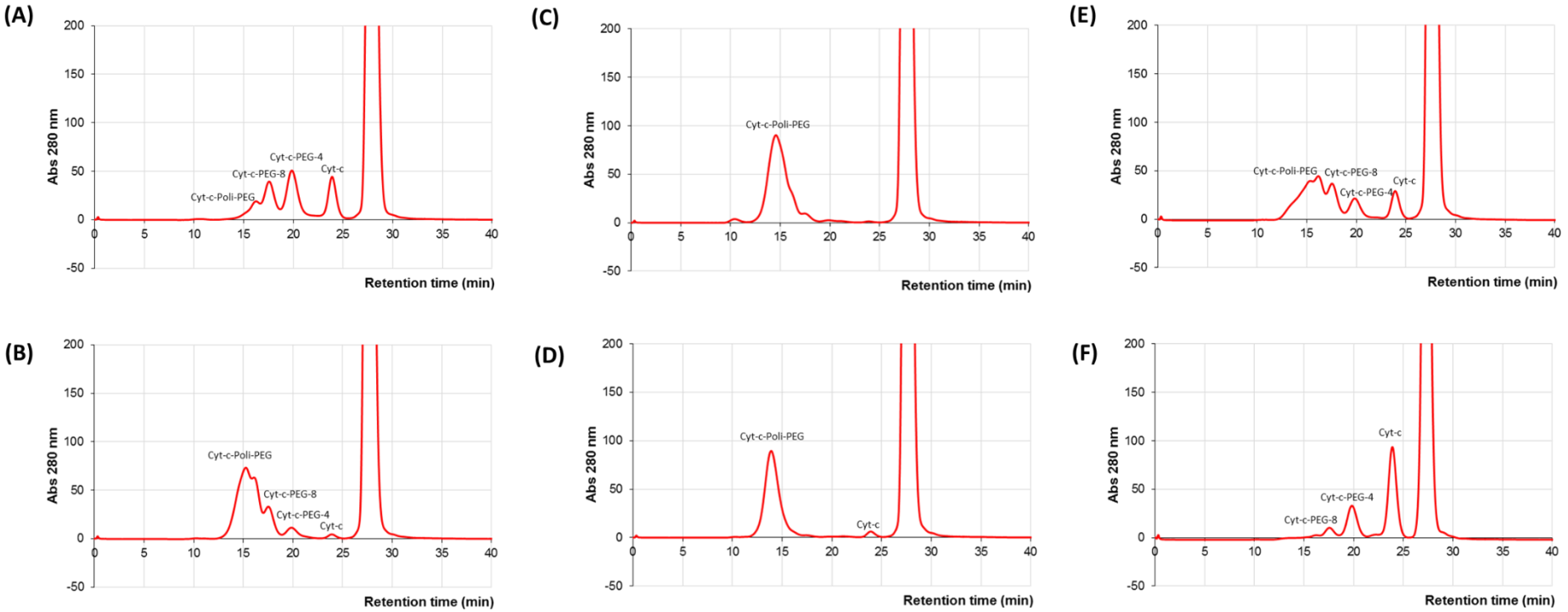

Fig. B.9. Chromatogram of the PEGylation reaction mixture obtained for the Cyt-c PEGylation in 0.1 M of potassium phosphate buffer at different pH values, 1:25 of molar proportion (protein:mPEG-NHS, 5 KDa), at room temperature and for 30 minutes. The peaks correspond to both Cyt-c PEGylated forms and unreacted protein. The studied pHs were: 7 (A), 8 (B), 9 (C), 10 (D), 11 (E), and 12 (F).

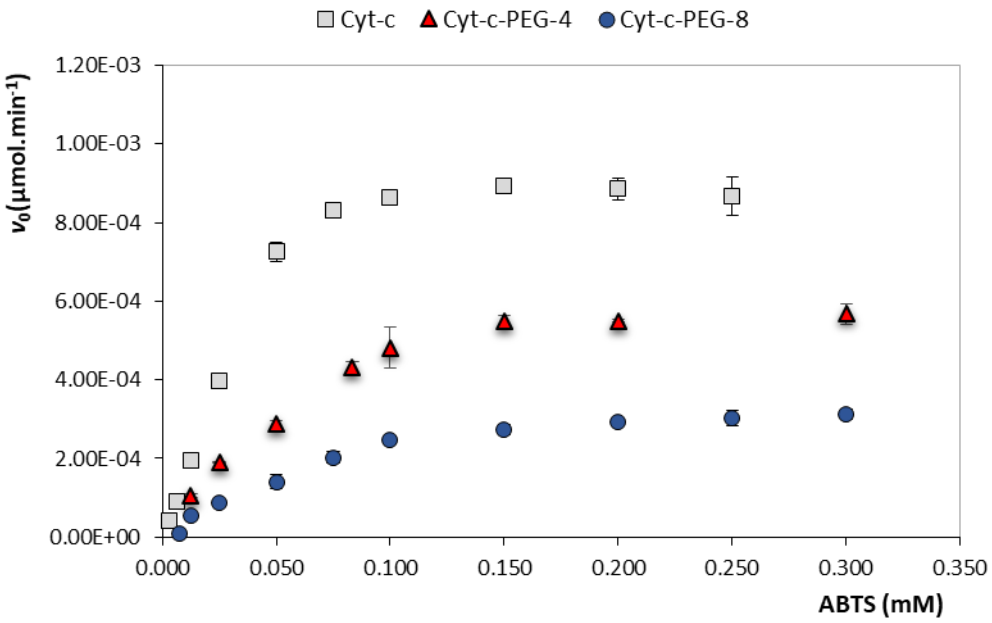

Fig. B.10. Oxidation kinetics for Cyt-c, Cyt-c-PEG-4 and Cyt-c-PEG-8, using ABTS as substrate (0.025-0.300 mM), with an initial concentration of Cyt-c of 0.6 mg.mL^{-1}, and in presence of 25 mM of H_2O_2.

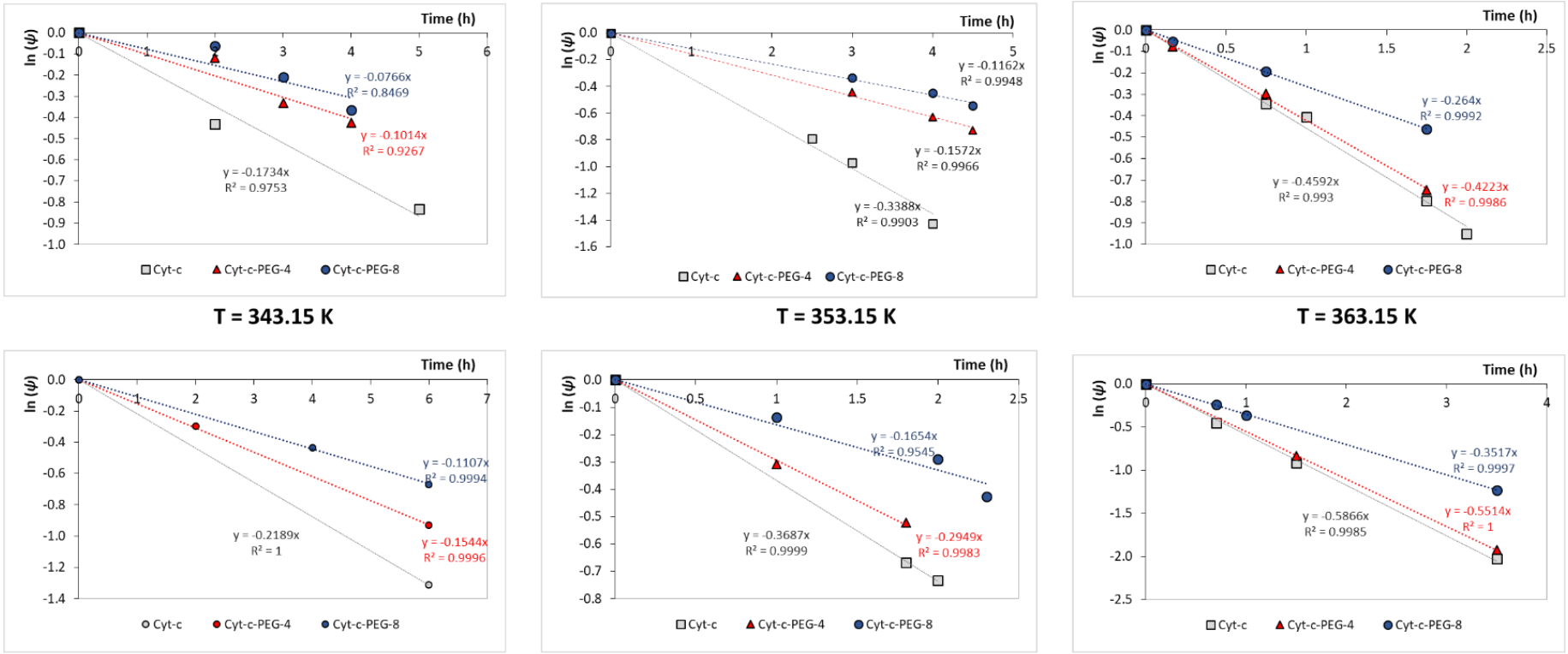

Cyt-c				Cyt-c-PEG-4				Cyt-c-PEG-8			
T (K)	$1/T$ (K^{-1})	k_d (h^{-1})	lnk_d	T (K)	$1/T$ (K^{-1})	k_d (h^{-1})	lnk_d	T (K)	$1/T$ (K^{-1})	k_d (h^{-1})	lnk_d
343.15	2.91E-03	0.173	-1.75	343.15	2.91E-03	0.101	-2.29	343.15	2.91E-03	0.077	-2.57
348.15	2.87E-03	0.219	-1.52	348.15	2.87E-03	0.154	-1.87	348.15	2.87E-03	0.111	-2.20
353.15	2.83E-03	0.339	-1.08	353.15	2.83E-03	0.157	-1.85	353.15	2.83E-03	0.116	-2.15
358.15	2.79E-03	0.369	-1.00	358.15	2.79E-03	0.295	-1.22	358.15	2.79E-03	0.165	-1.80
363.15	2.75E-03	0.459	-0.78	363.15	2.75E-03	0.422	-0.86	363.15	2.75E-03	0.264	-1.33
368.15	2.72E-03	0.587	-0.53	368.15	2.72E-03	0.551	-0.60	368.15	2.72E-03	0.352	-1.04

Fig. B.11. Semi-log plots of irreversible denaturation for Cyt-c, Cyt-c-PEG-4 and Cyt-c-PEG-8, at different temperatures (T = 343.15 K – 368.15 K). Experimental reaction conditions: 0.24 mL of Cyt-c (1.2×10^{-3} µM); 0.03 mL of ABTS (25 mM); and 0.03 mL of H_2O_2 (25 mM).

APPENDIX C

SUPPORTING INFORMATION OF CHAPTER 4

Table C.1. Recovery towards the top and bottom phases (in percentage) of the unreacted cytochrome c (Cyt-c) and the site-specific PEGylated forms (Cyt-c-PEG-4 and Cyt-c-PEG-8) in the ABS composed of 15 wt% of PEG + 20 wt% of potassium phosphate buffer (pH = 7).

	Cyt-c		Cyt-c-PEG-4		Cyt-c-PEG-8	
PEG MW ($g.mol^{-1}$)	**Rec Top (%)**	**Rec Bot (%)**	**Rec Top (%)**	**Rec Bot (%)**	**Rec Top (%)**	**Rec Bot (%)**
300	20. ± 3	80 ± 3	99.98 ± 0.01	0.02 ± 0.01	99.94 ± 0.01	0.06 ± 0.01
600	24.8 ± 0.2	75.2 ± 0.2	99.93 ± 0.01	0.07 ± 0.01	99.86 ± 0.01	0.14 ± 0.01
1000	0.3 ± 0.1	99.6 ± 0.1	99.5 ± 0.2	0.4 ± 0.2	99.9 ± 0.01	0.10 ± 0.01
1500	0.12 ± 0.05	99.88 ± 0.05	99.3 ± 0.6	0.7 ± 0.6	99.87 ± 0.01	0.13 ± 0.01
2000	0.11 ± 0.04	99.89 ± 0.04	92 ± 3	8 ± 3	98.5 ± 0.4	1.5 ± 0.4
4000	0.02 ± 0.01	99.98 ± 0.01	0.02 ± 0.01	99.98 ± 0.01	22 ± 2	78 ± 2
6000	0.02 ± 0.01	99.98 ± 0.01	0.02 ± 0.02	99.98 ± 0.02	45 ± 1	55 ± 1
8000	0.02 ± 0.01	99.98 ± 0.01	0.05 ± 0.05	99.95 ± 0.05	46 ± 1	54 ± 1

Table C.2. Recovery towards the top and bottom phases (in percentage) of the unreacted cytochrome c (Cyt-c) and site-specific PEGylated forms (Cyt-c-PEG-4 and Cyt-c-PEG-8) in the ABS composed of PEG 1500 + of potassium phosphate buffer (pH = 7) considering different mixture points.

	Cyt-c		Cyt-c-PEG-4		Cyt-c-PEG-8	
Mixture point	**Rec Top (%)**	**Rec Bot (%)**	**Rec Top (%)**	**Rec Bot (%)**	**Rec Top (%)**	**Rec Bot (%)**
(15; 15 wt%)	0.07 ± 0.01	99.93 ± 0.01	99.94 ± 0.01	0.06 ± 0.01	99.92 ± 0.03	0.08 ± 0.03
(17.5; 15 wt%)	0.10 ± 0.01	99.90 ± 0.01	99.90 ± 0.01	0.10 ± 0.01	99.89 ± 0.01	0.11 ± 0.01
(20; 15 wt%)	0.12 ± 0.01	99.88 ± 0.01	99.3 ± 0.6	0.7 ± 0.6	99.87 ± 0.01	0.13 ± 0.01
(22.5; 15 wt%)	0.12 ± 0.01	99.88 ± 0.01	97.1 ± 0.4	2.9 ± 0.4	99.83 ± 0.03	0.17 ± 0.03
(25; 15 wt%)	0.12 ± 0.02	99.88 ± 0.02	92.4 ± 0.1	7.6 ± 0.1	99.81 ± 0.01	0.19 ± 0.01

Table C.3. Weight fraction compositions for TLs and respective TLLs at the Top and Bottom (Bot) phases of the phase formers, namely the potassium phosphate buffer (PB), PEG (1500 and 8000) and water (W).

PEG 1500								
[PB] (wt%)	**[PEG] (wt%)**	**$[PB]_{Top}$ (wt%)**	**$[PEG]_{Top}$ (wt%)**	**$[W]_{Top}$ (wt%)**	**$[PB]_{Bot}$ (wt%)**	**$[PEG]_{Bot}$ (wt%)**	**$[W]_{Bot}$ (wt%)**	**TLL**
15	15	2.55	40.56	56.89	21.79	1.06	77.15	43.94
17.5	15	1.79	46.42	51.78	24.83	0.33	74.83	51.53
20	15	1.29	51.55	47.16	27.63	9.13×10^{-2}	72.28	57.81
22.5	15	0.89	56.97	42.14	30.21	2.21×10^{-2}	69.76	64.06
25	15	0.69	60.33	38.98	33.04	3.50×10^{-3}	66.95	68.45
PEG 8000								
[PB] (wt%)	**[PEG] (wt%)**	**$[PB]_{Top}$ (wt%)**	**$[PEG]_{Top}$ (wt%)**	**$[W]_{Top}$ (wt%)**	**$[PB]_{Bot}$ (wt%)**	**$[PEG]_{Bot}$ (wt%)**	**$[W]_{Bot}$ (wt%)**	**TLL**
20	15	1.12	57.49	41.39	26.67	4.95×10^{-6}	73.33	62.91

Table C.4. Composition of the streams of the single-step and multi-step processes using polymer-based ABS in terms of phase forming agents, namely phosphate buffer (PB), polyethylene glycol (PEG MW = 1500 and 8000) and water (W).

Single-step process				**Multi-step process**				
Stream	**[PB] (wt%)**	**[PEG 1500] (wt%)**	**[W] (wt%)**	**Stream**	**[PB] (wt%)**	**[PEG 1500] (wt%)**	**[PEG 8000] (wt%)**	**[W] (wt%)**
i	20	15	65	**i**	20	0	15	65
ii	1.29	51.55	47.16	**ii, iii**	26.67	0	4.95E-06	73.33
iii	27.63	9.13E-02	72.28	**iv, v**	1.12	0	57.49	41.39
				vi	27.63	9.13E-02	< 4.95E-06	72.28
				vii	1.29	51.55	< 4.95E-06	47.16

Table C.5. Parameters obtained through the Merchuk equation (Eq. 1) with the respective standard deviations (std) and correlation factors (R^2) along with the weight fraction data (wt%) for the systems composed of polyethylene glycol polymers (1) + $C_6H_5K_3O_7/C_6H_8O_7$ pH 7 (2) + H_2O systems determined in the present work.

mPEG 2 kDa		**PEG 2 kDa**	
A **± std = 87.44 ± 5.58** ***B*** **± std = -0.354 ± 0.029** ***C*** **± std = 2.3×10^{-4} ± 2.4×10^{-5}**		***A*** **± std = 83.18 ± 5.50** ***B*** **± std = -0.314 ± 0.030** ***C*** **± std = 2.0×10^{-4} ± 2.1×10^{-5}**	
R^2 = 0.9888		R^2 = 0.9855	
wt%(1)	**wt%(2)**	**wt%(1)**	**wt%(2)**
6.13	19.19	12.05	15.36
7.01	18.39	12.25	15.15
8.80	17.31	12.56	14.98
9.85	16.56	12.89	14.95
10.57	16.14	13.18	14.74
12.47	15.03	13.51	14.64
13.63	14.31	13.75	14.41
15.08	12.99	14.13	14.29
15.56	12.81	14.39	14.03
15.93	12.46	14.79	13.92
16.49	12.29	15.25	13.76
16.88	11.95	15.92	13.33
17.45	11.68	16.44	13.09
17.88	11.26	16.82	12.76
18.59	10.95	17.41	12.53
19.30	10.70	18.04	12.36
20.27	10.53	18.73	12.14
21.83	10.42	19.75	12.00
22.90	10.08	20.82	11.24
24.32	9.26	21.70	10.88
25.60	8.81	22.66	10.46
27.01	8.29	23.76	10.01
29.22	7.82	24.49	9.45
31.05	7.09	26.22	9.13
33.90	6.53	28.07	8.70
36.89	5.95	31.05	8.31
40.02	5.11	35.88	6.62
43.11	4.27	41.59	5.77
45.93	2.75	44.28	4.29
		47.05	2.69

Table C.6. Parameters obtained through the Merchuk equation (Eq. 1) with the respective standard deviations (std) and correlation factors (R^2) along with the weight fraction data (wt%) for the systems composed of polyethylene glycol (1) + $C_6H_5K_3O_7$/$C_6H_8O_7$ pH 7 (2) + H_2O systems determined in the present work.

PEG 6 kDa		**PEG 10 kDa**		**PEG 20 kDa**	
A **± std = 118.9 ± 6.2** ***B*** **± std = -0.501 ± 0.024** ***C*** **± std = 3.0×10^{-4} ± 2.3×10^{-5}** R^2 = 0.9966		***A*** **± std = 171 ± 21.8** ***B*** **± std = -0.665 ± 0.054** ***C*** **± std = 4.0×10^{-4} ± 4.3×10^{-5}** R^2 = 0.9937		***A*** **± std = 74.20 ± 2.62** ***B*** **± std = -0.526 ± 0.022** ***C*** **± std = 5.8×10^{-4} ± 8.2×10^{-5}** R^2 = 0.9941	
wt%(1)	**wt%(2)**	**wt%(1)**	**wt%(2)**	**wt%(1)**	**wt%(2)**
10.43	12.52	8.27	11.98	7.39	10.02
10.68	12.50	8.49	11.93	8.19	9.49
10.94	12.42	8.70	11.93	9.56	8.99
11.13	12.22	8.90	11.89	11.46	8.27
11.29	12.12	9.17	11.86	13.01	7.74
11.66	12.13	9.47	11.65	15.03	7.09
11.97	12.05	9.69	11.54	17.54	6.38
12.28	11.92	9.90	11.42	17.72	6.53
12.63	11.78	10.03	11.25	18.71	6.10
13.00	11.66	10.37	11.22	19.83	5.58
13.37	11.53	10.79	11.31	20.77	5.34
13.87	11.44	11.15	11.04	22.26	4.70
14.32	11.29	11.62	11.00	24.70	4.02
15.08	10.85	11.92	10.72	26.49	3.26
15.62	10.67	12.23	10.53	28.32	3.00
16.35	10.56	13.13	10.71	32.86	2.31
17.01	10.27	13.75	10.04	46.52	0.84
17.68	10.03	14.16	9.77		
18.69	9.94	14.79	9.59		
19.57	9.64	15.47	9.31		
20.50	9.30	16.35	9.27		
21.50	8.86	17.18	9.00		
23.42	8.00	17.94	8.65		
25.12	7.65	19.16	8.43		
27.11	7.21	20.30	8.09		
29.30	6.66	22.33	7.98		
32.24	6.00	24.14	7.43		
35.66	5.27	26.60	7.00		
41.46	4.57	35.64	5.11		
46.09	3.37				

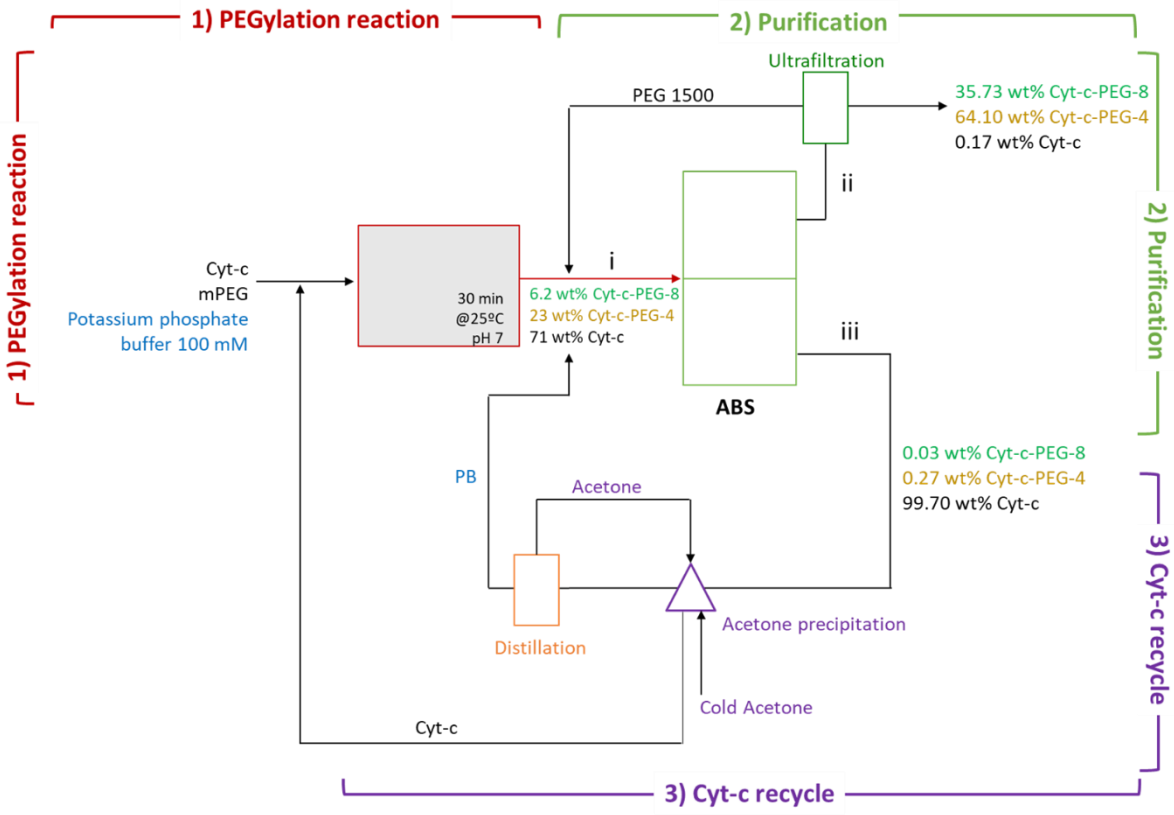

Fig C.1. Diagram of a single-step process to fractionate selectively the unreacted cytochrome c from their PEGylated conjugates (Cyt-c-PEG-4 and Cyt-c-PEG-8) using ABS. The proposed strategy indicates that after the PEGylation reaction the ABS composed of PEG 1500 + potassium phosphate buffer (pH = 7) is applied and able to separate the PEGylated conjugates (Cyt-c-PEG-4 and Cyt-c-PEG-8) from Cyt-c with the presented recovery yields. The recycling of Cyt-c for a novel PEGylation reaction is herein projected through a cold acetone precipitation step followed by the resuspension of the protein pellet in the conventional PEGylation buffer (100 mM potassium phosphate buffer, pH =7).

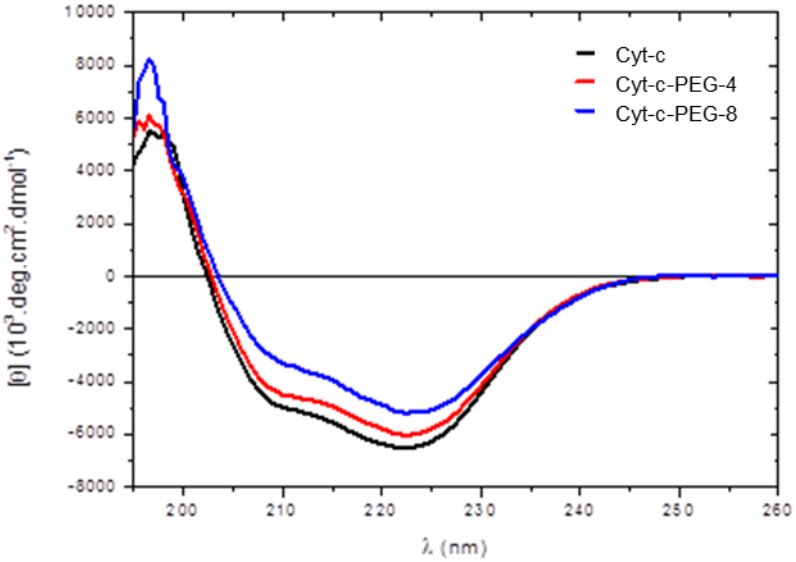

Fig C.2. Far-UV CD spectra of Cyt-c control (—), Cyt-c-PEG-4 (—), and Cyt-c-PEG-8 (—) purified through aqueous biphasic system.

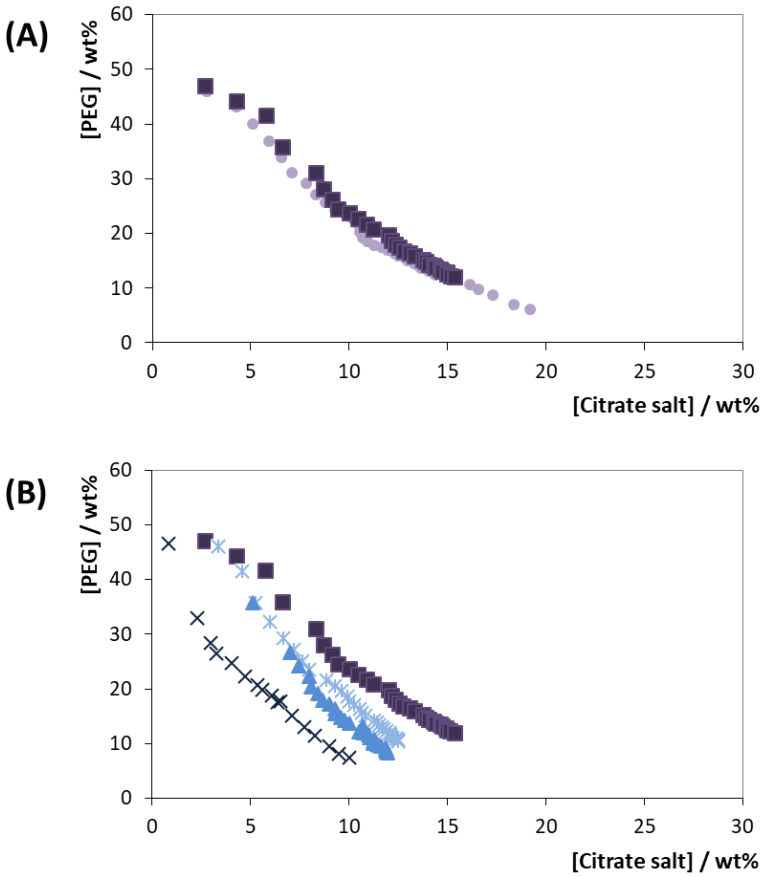

Fig. C.3. Ternary phase diagrams of the ABS composed of **(A)** mPEG 2kDa (●) and PEG 2 kDa (■) + $C_6H_5K_3O_7/C_6H_8O_7$ (pH = 7) **(B)** PEG 2 (■), 6 (✳), 10 (▲), and 20 (✕) kDa + $C_6H_5K_3O_7/C_6H_8O_7$ (pH = 7) at T = (298 ± 1) K and atmospheric pressure.

APPENDIX D

SUPPORTING INFORMATION OF CHAPTER 5

Table D.1. Partition coefficients (*K*) of Cyt-c and Cyt-c-PEG in PEG + potassium phosphate buffer in lab-scale ABS.

PEG + potassium phosphate buffer ABS	$K_{Cyt\text{-}c}$	$K_{Cyt\text{-}c\text{-}PEG}$
PEG 600	0.496	1114
PEG 1000	0.005	1548
PEG 1500	0.002	1128
PEG 2000	0.002	154
PEG 4000	0.001	5.24
Preferential Partition	Potassium phosphate buffer-rich phase	PEG-rich phase

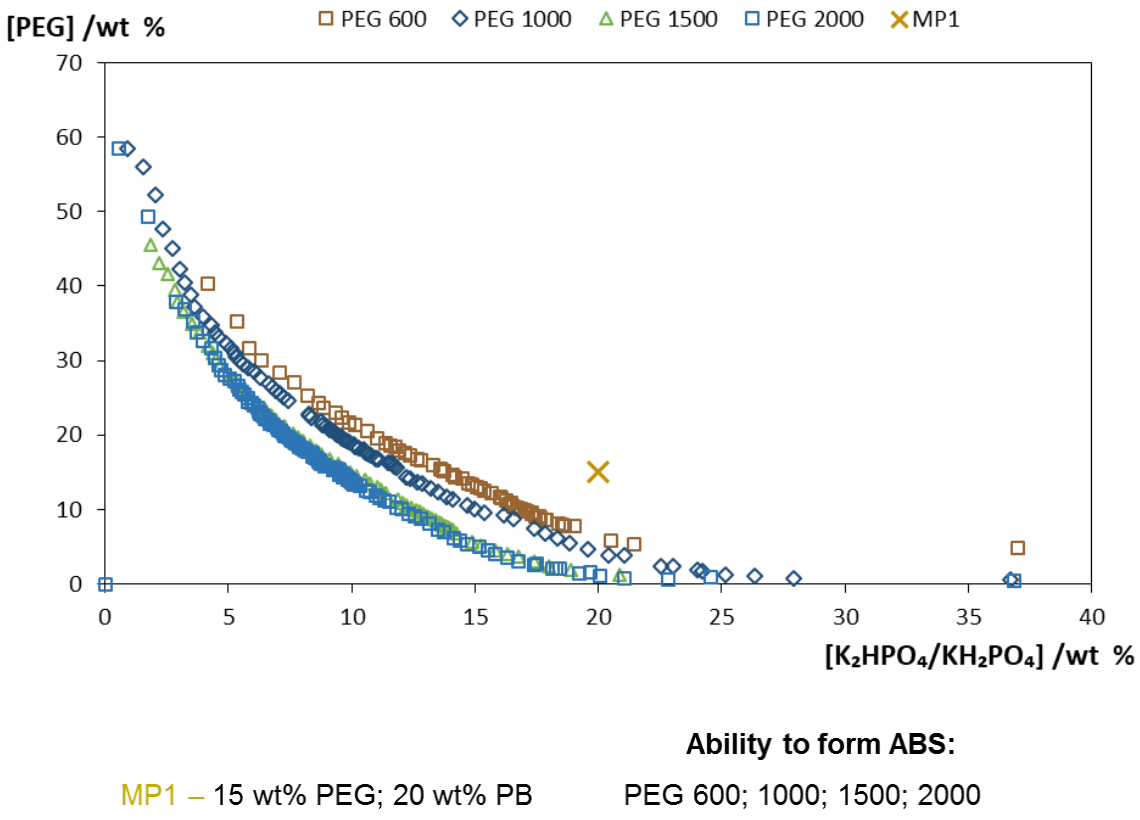

Fig. D.1. Phase diagrams of polyethylene glycol + potassium phosphate buffer and mixture point (MP) adopted to test the FCPC.